DEVELOPMENT OF A WET MUCK DATABASE AND DRAWPOINT SPILL HAZARD SUSCEPTIBILITY TOOL FOR AN OPERATING CAVE MINE

by

Jovian Varian

B.Eng., University of Exeter, 2017

M.Eng., The University of British Columbia, 2019

A THESIS SUBMITTED IN PARTIAL FULFILLMENT OF

THE REQUIREMENTS FOR THE DEGREE OF

MASTER OF APPLIED SCIENCE

in

THE FACULTY OF GRADUATE AND POSTDOCTORAL STUDIES

(Geological Engineering)

THE UNIVERSITY OF BRITISH COLUMBIA

(Vancouver)

March 2022

The following individuals certify that they have read, and recommend to the Faculty of Graduate and Postdoctoral Studies for acceptance, the thesis entitled:

Development of a Wet Muck Database and Drawpoint Spill Hazard Susceptible Tool for an Operating Cave Mine

submitted by Jovian Varian in partial fulfillment of the requirements for

the degree of Master of Applied Science

in Geological Engineering

Examining Committee:

Dr. Scott McDougall, Geological Engineering, UBC

Supervisor

Dr. Erik Eberhardt, Geological Engineering, UBC

Supervisory Committee Member

Allan Moss, Mining Engineering, UBC

Supervisory Committee Member

Dr. Roger Beckie, Geological Engineering, UBC

Supervisory Committee Member

Dr. Doug Stead, Department of Earth Sciences, SFU

Additional Examiner

Abstract

Wet muck (also known as mud rush) can be described as the sudden flow of fragmented rock into a drawpoint or other underground mine opening, exposing the mine to safety and operational risks. This hazard is analogous to an underground debris flow and is most commonly encountered in cave mines. Numerous fatalities, infrastructure damage, loss of reserves, and operational delays, have been reported in various caving operations.

To better understand and manage this hazard, this thesis uses data and experiences from the PT Freeport Indonesia, Deep Ore Zone (DOZ) block cave mine in Indonesia where the ground conditions and operational factors that both increase the susceptibility of a drawpoint and act to trigger a wet muck event. Spatio-temporal relationships are drawn from this data, recognizing that the probability of wet muck events tends to increase as a cave matures, with increasing draw column heights contributing to increase secondary fragmentation and the generation of fines. Other contributing factors included in the analysis are extraction rate, uniformity of draw, Height of Draw (HoD), and drawpoint condition.

Univariate and multivariate logistic regression models are developed, with the goal of improving prediction and mitigation of these events to improve safety and productivity in caving operations. Although the consequences of wet muck spill events are high, they are still relatively rare, resulting in an imbalanced dataset. Cost-sensitive learning is incorporated into the logistic regression models to address this technical challenge. These methods are used in this thesis to develop a spreadsheet-based wet muck susceptibility tool, which includes implementation guidelines and Python scripts. The concepts, methodologies and tools developed from this research are not restricted to the DOZ but can also be implemented in other caving operations that are susceptible to wet muck spills.

Lay Summary

Wet muck spill hazards involve the sudden inflow of a mixture of finely broken rock, similar to sand, and water into an underground mine, posing major safety and economic risks. This thesis focuses on identifying the causative and triggering factors for this type of hazard based on data from an operating block cave mine. The key factors that were identified include the amount of fines and water content of the material being mined, the maturity of the cave (i.e., age of the mine), and the degree of mining activity for a given area. The result is the development of a wet muck susceptibility tool that improves the evaluation of wet muck hazards in advance of mining to allow for risk-mitigation strategies to be implemented. Overall, this research provides a conceptual framework and workflow that can be applied to other cave mines that are susceptible to wet muck spills.

Preface

This thesis is original and independent work done by the author. I was responsible for the data processing, method development, data analysis, and writing of this thesis under the supervision of Dr. Scott McDougall. The proposal and initial scope of the project were developed by Dr. Scott McDougall, Dr. Erik Eberhardt, and Allan Moss. Collaboration and feedback on the approach, rationale, and deliverables were provided by Dr. Scott McDougall, Dr. Erik Eberhardt, and Allan Moss.

The data used in this thesis was provided by PT Freeport Indonesia from the Deep Ore Zone (DOZ) mine. Additional support and guidance with regards to the data context and industry knowledge were provided by Allan Moss and the PT Freeport Indonesia UG - Geoengineering team.

A version of Chapters 3 and 4 was submitted for abstract review at the time of thesis submission [Varian, J., McDougall, S., Ghadirianniari, S., Llewelyn, K., Campbell, R., Eberhardt., E., and Moss, A. (2022). Development of a Wet Muck Spill Susceptibility Tool for Short-term Prediction through a Logistic Regression Approach]. I was responsible for the majority of the manuscript composition with review and edits from the co-authors.

Table of Contents

List of Tables

List of Figures

List of Abbreviations

CU	Consolidated Undrained
DMLZ	Deep Mill Level Zone
DOM	District Ore Mine
DOZ	Deep Ore Zone
DP	Drawpoint
DPC	Drawpoint Classification
EDA	Exploratory Data Analysis
EESS	Ertsberg East Skarn System
ESZ	Ertsberg Stockwork Zone
GBC	Grasberg Block Cave
GBT	Gunung Bijih Timur
HoD	Height of Draw
ICaRN	International Caving Research Network
IOZ	Intermediate Ore Zone
ktpd	Kilo tonnes per day
LHD	Load Haul Dump
MLR	Multivariate Logistic Regression
PTFI	PT. Freeport Indonesia
RMR	Rock Mass Rating
RQD	Rock Quality Designation
SE	South East

SMOTE	Synthetic Minority Oversampling Technique
SPUI	Specific Index of Uniformity
SW	South West
UBC	University of British Columbia
UCS	Unconfined Compressive Strength
UI	Uniformity Index
ULR	Univariate Logistic Regression
UU	Unconsolidated Undrained

Acknowledgments

I would like to express my deepest and sincerest gratitude to my research supervisor, Dr. Scott McDougall, for his continuous support throughout my Master's, for his patience, and motivation. His guidance has helped me in many ways, shaping me to become a better engineer for the future.

I am very grateful to my supervising committee, Erik Eberhardt, Allan Moss, and Roger Beckie, for their valuable inputs throughout this research. Erik Eberhardt's direction for the initial research scope was critical to set up the benchmark of wet muck susceptibility study. In addition, his guidance on statistical and mechanistic understanding has helped me to improve my research. I am very grateful to have Allan Moss as a committee member; he introduced me to wet muck spill research, provided valuable insight on the operational perspective, and provided guidance on the applicability of the research to practical implementation. Special thanks to Roger Beckie for his guidance on managing a complex dataset.

I would like to thank the personnel at PT Freeport Indonesia for supporting the Wet Muck Susceptibility project, for the accommodation provided during the site visit, and for providing access to the data from the DOZ mine operation. Special thanks to Ryan Campbell and Karl Llewelyn, who have been the liaison between PT Freeport Indonesia and UBC, providing guidance, feedback, and practical insights into the implications of this research.

Many thanks to my fellow research students of the ICaRN Hazard Management Strategies research project for their effort in assisting the preliminary data transfer. Also, special thanks to the UBC Geohazard Research Team for their constructive feedback on database management, processing, and analysis throughout my research.

I am extremely grateful to my parents for their love, support, and sacrifices for educating and preparing me for my future in many ways. I am very thankful to my partner, Natalie Stanley, for her love and support throughout my academic studies. Also, my special thanks to my sisters for their support.

Chapter 1: Introduction

Declining ore grade near-surface has motivated many mines to go deeper underground while also maintaining the production (i.e., tonnages mined) achieved from open-pit mining. Block and panel caving is the lowest cost method of underground mass mining (Heslop, 2000), which relies on natural, gravity-induced ore fragmentation. These caving methods offer high production rates similar to an open-pit operation and have a lower cost per ton compared to other underground mining methods (Brown, 2002). Despite its advantages, cave mining has generally been understudied, which has led to various engineering challenges, including cave stalls, drawpoint hang-ups, rockburst, air blast, and inrush hazards (Laubscher, 2000).

Inrush hazards are known by several different names: wet muck spills, mud rushes, and running ground. They are defined as "sudden inflows of mud from drawpoints or other underground openings" (Butcher et al., 2000) and expose a mine to both safety and operational risks. Their occurrence increases as a cave matures, which has provoked many questions about the conditions that will lead to a spill. A better understanding of these conditions can provide insight for managing future events. This thesis examines wet muck spill conditions using detailed records and data provided by PT Freeport Indonesia's (PTFI) Deep Ore Zone (DOZ) mine at the Grasberg Mining Complex in Tembagapura, Indonesia.

1.1 Problem Statement

One of the major challenges encountered by block caving operations in wet climates is wet muck spill hazards. It is difficult to predict exactly when one of these unique events will occur due to the randomness of and difficulty ascertaining when certain conditions are met. The occurrence of a wet muck spill is a complex process requiring the simultaneous presence of four elements within the drawpoint vicinity (Butcher et al., 2000): (1) potential mud-forming materials (i.e., fines), (2) accumulation of water, (3) disturbance of the mud in the form of drawing or other mining activities, and (4) a discharge point. All of these elements are part of the nature of caving operations and are largely unavoidable.

The history of wet muck spills at the Grasberg mining complex, including the Deep Ore Zone (DOZ), has led to insights into the causative and triggering factors, including complex geological conditions, high annual rainfall, cave orientation, uneven draw, suspension of operation, and static and dynamic disturbance (Widijanto et al., 2012). Several cave mines around the world, such as the El Teniente Mining Complex, Cadia East Mine, Palabora Mine, and Kimberley Mine, have also been impacted by various forms of inrushes, including wet muck spills, dry muck spills, and water inrushes. The inrush characteristics, susceptibility, and severity are different depending on the hydrogeological conditions, cave geometry, operational history, and orebody geology of each mine. Current knowledge and mitigation strategies are largely anecdotal and rely on experience from historical inrushes. Several of the strategies, such as drawpoint closures and tonnage restrictions, are believed to help limit the number of high-risk drawpoints; however, the success rates are unknown, and these strategies negatively impact production rates while still being unable to resolve the progressive appearance of mud at a drawpoint.

The recently depleted DOZ mine recorded more than 1,900 spills since 2003. To proactively manage this hazard where future events are foreseeable at other cave mines, there has been extensive study of this data by PTFI personnel. The present work builds on this previous work using a complementary statistical analysis approach.

1.2 Research Objectives

The overall goal of this thesis is to help improve the safety and productivity of caving operations impacted by wet muck and inrush hazards by improving our understanding of the contributing causative and triggering factors. To achieve this goal, the following two main research objectives were defined:

1. *Compile, systematically review, and statistically analyze wet muck spill data from an operating mine (PTFI's DOZ).* The existing database of over 1,900 historical wet muck spills at the DOZ provides a unique opportunity to reduce the current knowledge gap, systematically identify the various causes and triggers of wet muck spills and quantify their relative influence.
2. *Develop a data-supported tool to aid operational decision-making.* Based on the results of the statistical analysis from Objective 1, new empirical relationships can be incorporated into a spreadsheet-based model to help improve existing wet muck prediction capabilities at the DOZ and, potentially, other caving operations (e.g., GBC and DMLZ).

This thesis is part of a larger multi-disciplinary collaboration under the International Caving Research Network (ICaRN), which aims to address a broad scope of research covering orebody knowledge, cave-to-mill processes, and ground-control hazard management strategies. This thesis fits under the latter general topic.

1.3 Research Approach and Thesis Structure

This research makes use of a large collection of data from the DOZ Mine provided by PTFI. It incorporates six key research steps that include: (1) a comprehensive review of the existing wet muck spill literature, (2) a compilation of the data provided by PTFI into a new database, (3) an exploratory analysis of the database, (4) a Univariate Logistic Regression (ULR) analysis, (5) a Multivariate Logistic Regression (MLR) analysis, and (6) the development of a spreadsheet tool based on the findings from steps 1 to 5. This research was carried out in close collaboration with personnel from PTFI and the DOZ.

Chapter 2 documents Step 1, a comprehensive literature review covering wet muck spill mechanisms and behavior, including historical observations from various caving operations. The Grasberg Mining Complex study area and early experiences and lessons learned are also summarized in this chapter. This literature review helped identify hypothetical causative and triggering factors that were used in subsequent steps of this research.

Chapter 3 documents Steps 2 and 3, the compilation and exploratory analysis of the new wet muck spill database. Data were collected in various forms at PTFI's DOZ Mine between 2008 and 2019. Patterns in the data were identified through an exploratory data analysis, which informed subsequent detailed statistical analyses.

Chapter 4 documents Steps 4 to 6, the statistical analyses performed using univariate and multivariate logistic regression, and subsequent development of a data-supported spreadsheet tool to aid operational decision-making.

Chapter 5 summarizes the main conclusions of this research and contributions made and presents recommendations for future wet muck spill research.

1.4 Study Site

1.4.1 Site Location and Mine Layout

The Grasberg Mining Complex is operated by PTFI, a joint venture between Freeport-McMoRan and PT Indonesia Asahan Aluminium (INALUM). It is located in the southern area of Jaya Wijaya Mountain, West Papua, Indonesia, and is considered to be one of the largest copper (Cu) and gold (Au) deposits in the world. Operations began in 1967 with the first production from the Ertsberg open pit in 1973, followed by the Gunung Bijih Timur (GBT) cave mine, the Grasberg open pit, the Intermediate Ore Zone (IOZ) cave mine, and the Deep Ore Zone (DOZ) cave mine. These five mines have been depleted while PTFI continuously expands its underground mining operations.

Three mines are currently operating: the GBC and DMLZ cave mines and the Big Gossan stoping mine (Casten et al., 2020). In addition, PTFI has several potential future operations, including the Kucing Liar and Gajah Tidur resources. Figure 1.1 illustrates the general layout of the different mines belonging to the Grasberg Mining Complex.

By 2019, the DOZ mine had produced 300 million tonnes of ore since it opened in 2000 (Casten et al., 2020). It is the third lift of the block cave mine in the East Ertsberg Skarn System (EESS), after the GBT and IOZ mines. The DMLZ mine underlies these orebodies as the fourth lift. There are three main operating levels at the DOZ block cave (Ramadhan et al., 2015): (1) the undercut level at elevation 3146 m, (2) the extraction level at elevation 3126 m, and (3) the haulage level at elevation 3076-3079 m (Ramadhan et al., 2015). The extraction level is at a depth of approximately 1200 m below the surface and includes 1347 drawpoints across 39 panels with column heights up to 750 m. The extraction level was constructed with an offset herringbone layout (Figure 1.2) to minimize wet muck flow distances (Botha et al., 2008). It can be accessed either from the North Fringe Drift (NFD) or South Fringe Drift (SFD.

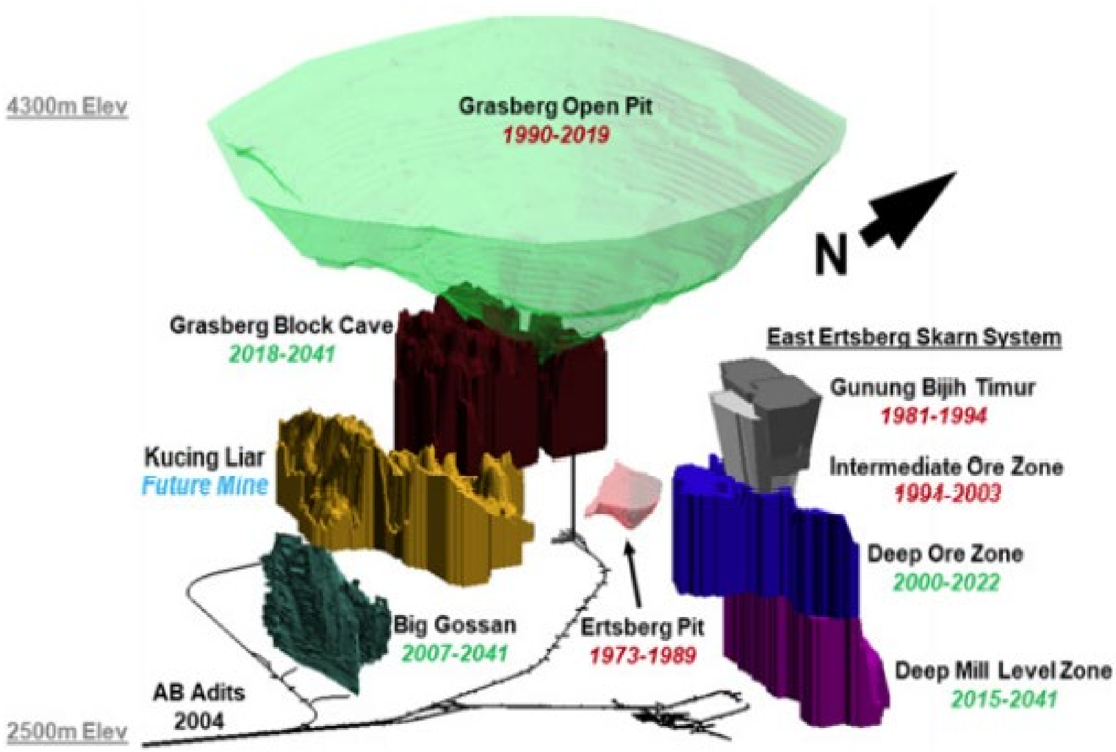

Figure 1.1. The general layout of the PTFI Grasberg Mining Complex. From (Casten et al., 2020)

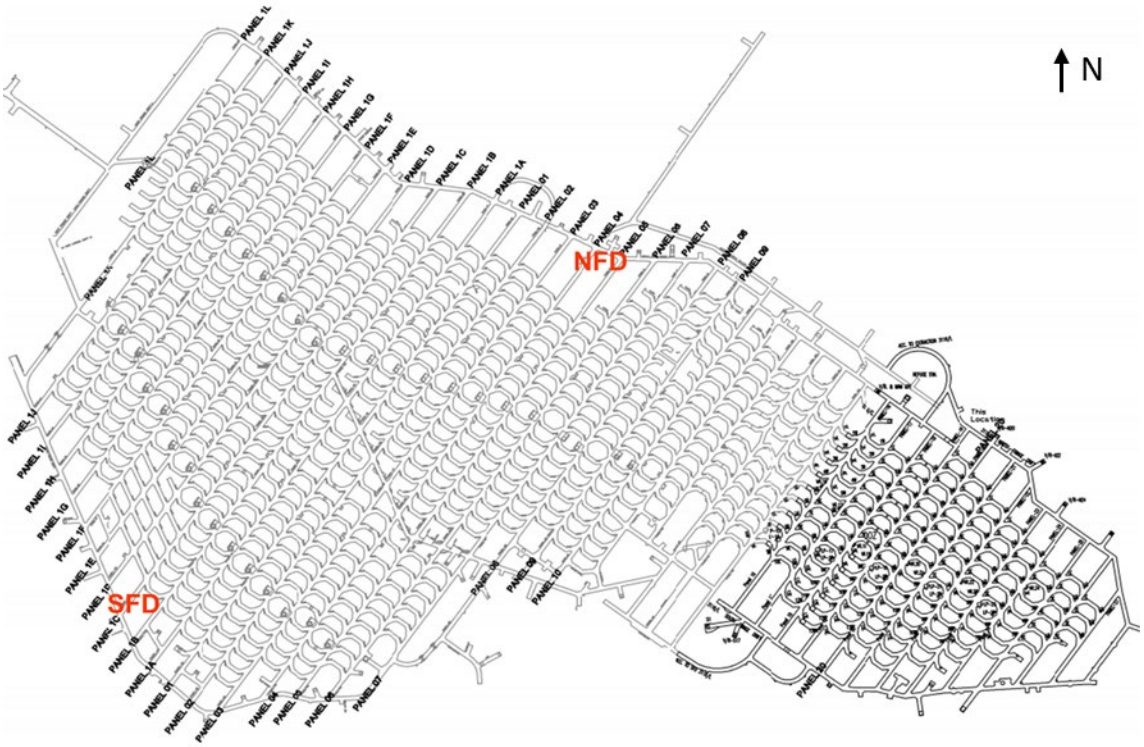

Figure 1.2. The layout of the DOZ extraction level. Image exported from DXF file provided by PT. Freeport Indonesia.

As shown in Figure 1.3, at the extraction level, panels are spaced 30 m apart, and drawpoints are spaced 18 m apart along each panel. Drawbells separated by major and minor pillars funnel fragmented ore to the drawpoints.

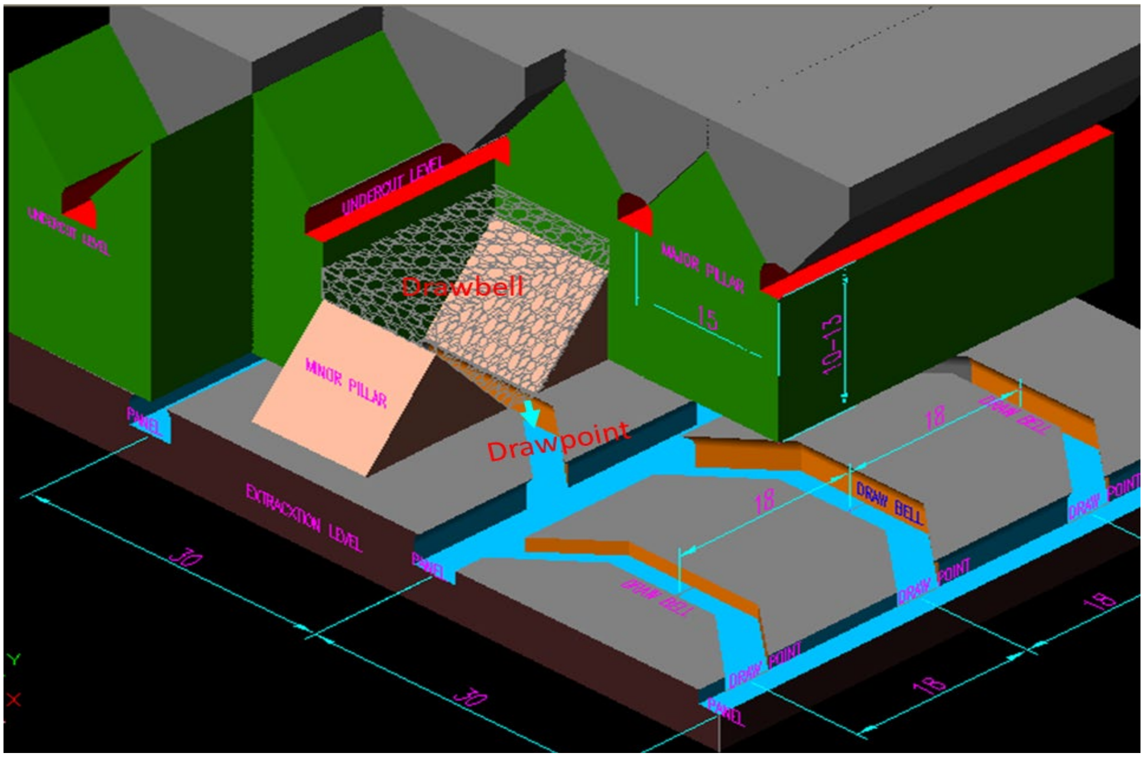

Figure 1.3. The DOZ mine drawpoint spacing layout between the extraction and undercut levels (PT. Freeport Indonesia, 2010a).

1.4.2 Geology

As shown in Figure 1.4, Figure 1.5 and Figure 1.6, the DOZ mine is comprised of two main deposits: the Ertsberg East Skarn System (EESS) and the Ertsberg Stockwork Zone (ESZ) (Haflil et al., 2014). Although both of these deposits have different geological characteristics and properties, they are physically contiguous (Casten et al., 2004).

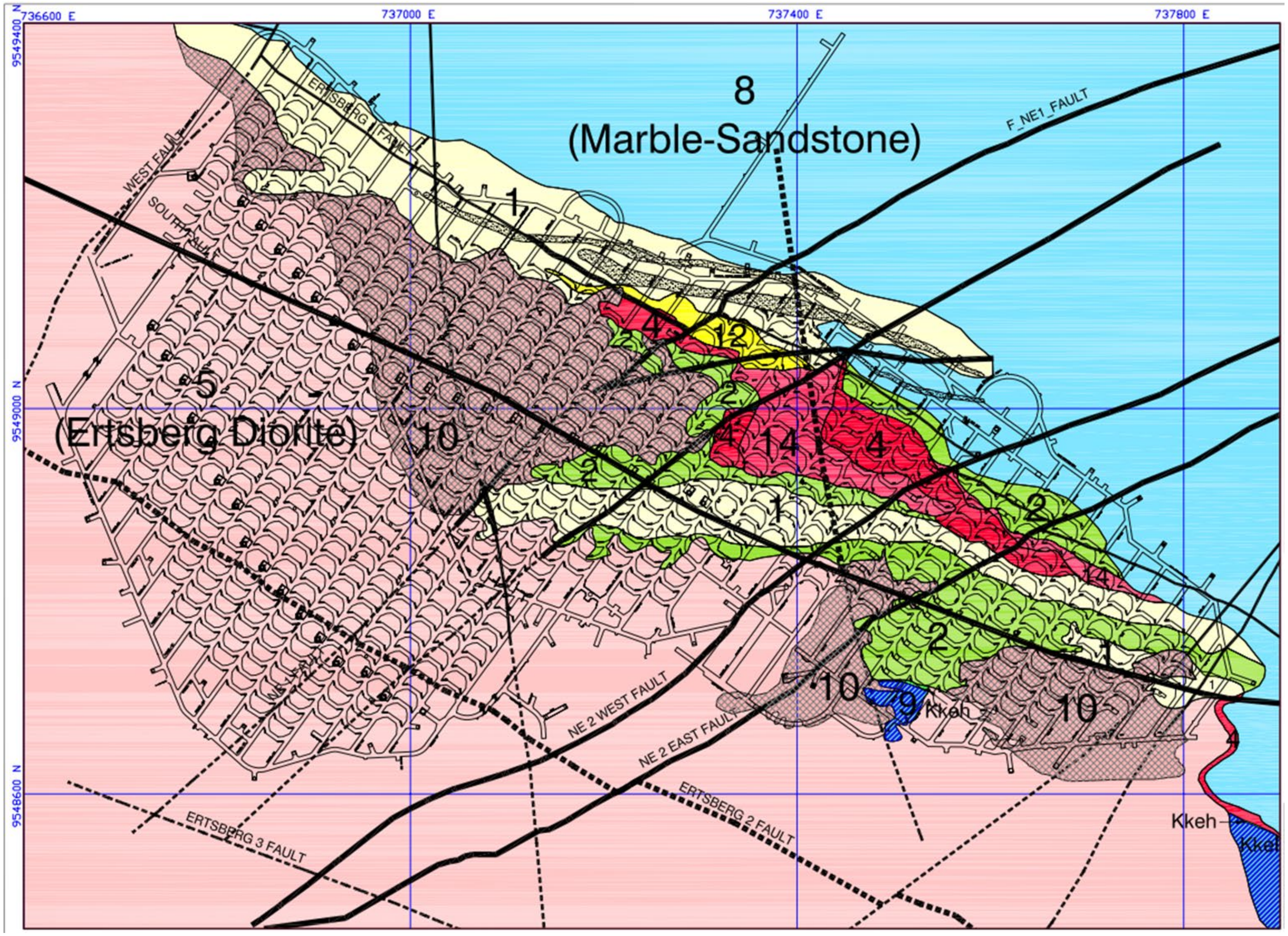

Geology of the DOZ Mine (PT. Freeport Indonesia, 2010b).

LEGEND OF ROCK CODE DOZ:

1 FORSTERITE SKARN
Diopside–locally pervasive/patchy/diffuse or as veinlets/fracture infill

2 FORSTERITE-MAGNETITE SKARN
10–40% magnetite as disseminated grains and / or x–cutting veinlets and stringers.

4 MAGNETITE SKARN
>50% magnetite; ± forsterite, garnet, serpentinite, tremolite/actinolite, calcite, chlorite, diopside, micas; locally brecciated

5 ERTSBERG DIORITE

8 MARBLE - SANDSTONE
Tw Waripi–Dolomitic Marble

9 Hornfels

10 Endoskarn

12 HALO 1
Forsterite breccia extensive carbonatization and oxidation. Retograde minerals include : talc, phlogopite, serpentine, minor chalcedony, clay, carbonate >15%

14 HALO 4
Magnetite forsterite breccia extensively carbonatization & oxidation. Retrograde minerals include : talc, phlogopite, serpentine, hematite, chalcedony, clay, carbonate > 15 %

FAULT CHARACTERISTICS	FAULT CONFIDENCE LEVEL
Broken Fault –Symbolized by distinct lines–	High Confidence Line with weight 5pt
Contain 5–20% broken, 5–20% crushed, 60–90% fractured, locally up to 5% clay gauge with RQD <50% Locally unconsolidated due to anhydrite cement leaching Joint spacing <0.5m	Already mapped (actual data from drift mapping) Fault, slicken slide, shear zone or related indication was observed in the field Observed intense of joint spacing and intersection
Reheal Fault –Symbolized by dot lines–	Low Confidence Line with weight 3pt
Contain >40% fractured, jointed–massive, RQD >50% Commonly tight filled by quartz filling, with minor sericite–bornite–chalcopyrite and some endoskarn Joint spacing <0.5m Reheal faults possible to re–activated due to mining activity and leaching process	Not yet mapped or no opening at current area Interpreted from geochemical trend or 3–D model Fault or slicken slide was not observed in the field Rare of joint spacing and intersection

.

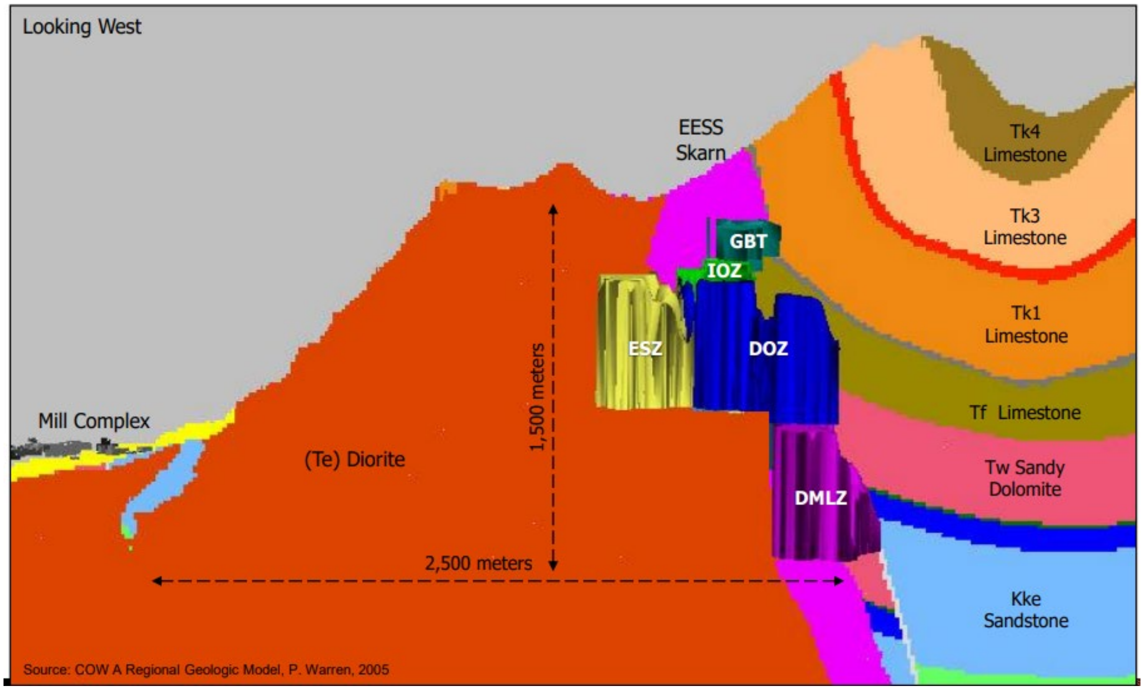

Figure 1.6. Geological cross-section through the GBT, IOZ, DOZ, and DMLZ mines. After Warren (2005).

Soebari et al., (2013) describe the geological formation of the ESZ orebody. It is hosted entirely within the Ertsberg Intrusion south of the EESS. The orebody is oriented northwest-southeast, with a strike length of over 650 m and a width of approximately 300 m. Mineralization of Cu and Au is associated with hydrothermal alteration centered in the late porphyry dikes enclosed by the Main Ertsberg Intrusion. Quartz-anhydrite-pyrite-chalcopyrite cuts across the entire system, which also introduced Cu-Au. During the final stage of ESZ hydrothermal system cooling, fluids along the contacts of the porphyry dikes caused propylitic alteration of the Main Ertsberg Intrusion and porphyry dikes.

The EESS is characterized by the presence of forsterite, diopside, forsterite-magnetite, marble, and endoskarn, which are generally fair to poor in rock quality with a Rock Mass Rating (RMR) ranging between 30 and 55. Caving was initiated at the DOZ Mine in this material. The ESZ is characterized by diorite and endoskarn with joint infill by quartz, chalcopyrite, pyrite, and anhydrite, which are generally good in rock quality with an RMR ranging between 70 and 75 (Widijanto et al., 2006). There is a high variability of rock types across the strike of the orebody, with ground conditions ranging from very poor at the hanging wall to very good at the footwall (Casten et al., 2004). The variability of each rock type is summarized in Table 1.1.

Table 1.1. Geotechnical classification of each rock type in the DOZ Mine (Modified after Sahupala & Srikant, 2007 and Widijanto, 2006).

Rock Type	UCS (MPa)	RQD (%)	RMR Class	Percentage (%)
DOZ Breccia	22	40	Very poor	9.6
Marble - Sandstone	22	65	Poor	1.2
Forsterite Skarn	127	84	Good	20.6
Forsterite - Magnetite Skarn	57	67	Fair	16.3
Magnetite Skarn	98	71	Good	1.9
Diorite	111	80	Good	50
Other	-	-	-	0.5

1.4.3 Climate

Papua province is one of the wettest regions in Indonesia, where it receives 2,500 to 4,500 mm of rainfall per year, with some areas, including Tembagapura can receive up to 7,000 mm per year (Prentice & Hope, 2007). Indonesia generally experiences two seasons, a dry season between April and October and a wet season between November and March. However, there is no seasonal pattern to the rainfall amounts in Papua; there is high variability in rain intensity that is received all year round (Figure 1.7). In 2020, the PTFI Grasberg operation recorded 5,000 mm of precipitation, and rainfall is considered one of the hazards at the operation (Freeport-McMoRan, 2020).

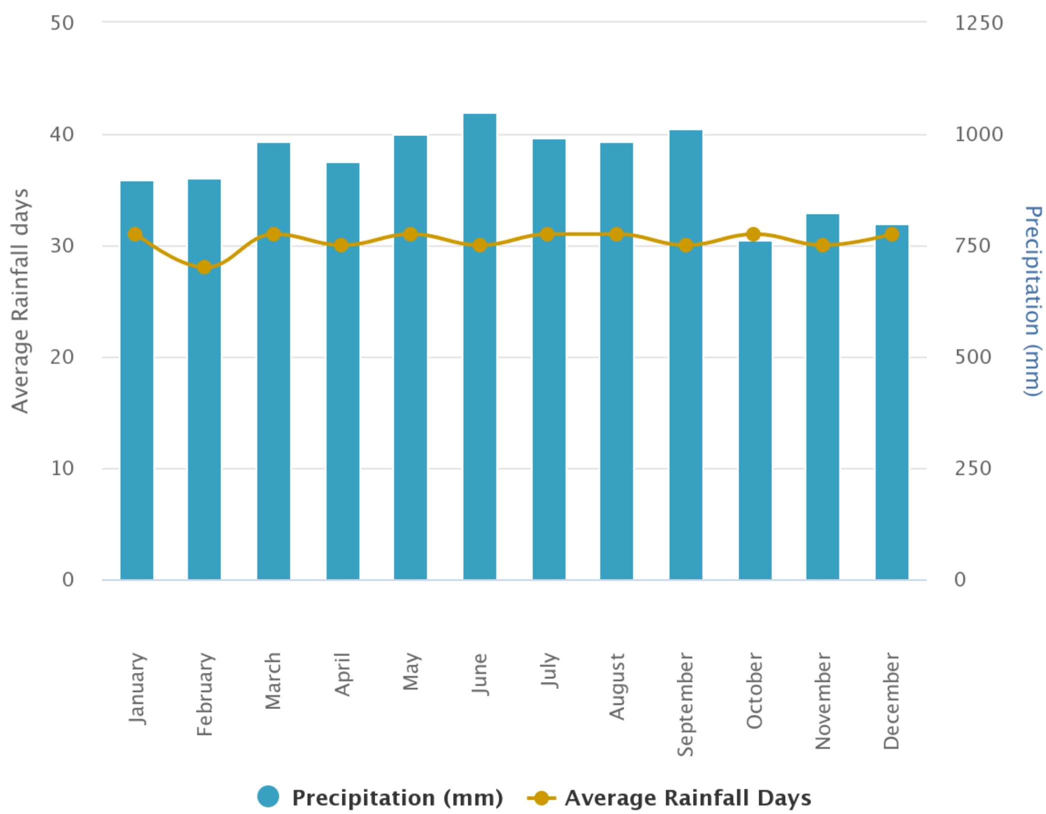

Figure 1.7. Tembagapura average monthly precipitation data (Retrieved from World Weather Online, 2022).

Chapter 2: Comprehensive Review of Wet Muck Spill Literature

2.1 Introduction to Block and Panel Caving Methods

The increasing depletion of near-surface resources mined by large open-pit operations has motivated mines to expand their operations deeper underground. Block and panel cave mining methods are underground mass mining methods that are predominantly favored for low-grade, weaker, massive, and steeply dipping orebodies. These methods have increasingly become preferred since they can achieve similar tonnages as an open pit operation and are lower cost-per-ton compared to other underground mining methods (Laubscher, 2000). Advancements in technology, for instance, the use of hydraulic fracturing to precondition an orebody and increase its fragmentation and caveability, have allowed these methods to be used in more competent orebodies (Eberhardt et al., 2015).

Caving relies on gravity- and stress-induced fracturing and fragmentation, where mining begins by progressively drilling and blasting below the base of the orebody, referred to as undercutting (Brown, 2002). Once undercut, the fractured rock collapses and caves into a series of bell-shaped ore passes, known as drawbells. The broken ore is extracted from drawpoints at the extraction or production level, which are developed underneath the drawbells. As the ore is removed by load-haul-dump (LHD) machines at the drawpoints, the cave propagates upwards, with the rock above the cave back continuing to fragment due to gravity and stress redistribution.

Block caving undercuts are done in a rectangular or square checkerboard pattern, where every block must be drawn evenly to maintain a near-horizontal cave back (Figure 2.1). Panel caving operates under the same principles as block caving. However, in panel caving, the orebody is partially undercut in several panels or strips, resulting in a cave front that moves across the orebody at a constant angle to the direction of undercut advancement (Brown, 2002) (Figure 2.2). Despite these differences, the term "block caving" is commonly used for all types of gravity-induced caving methods.

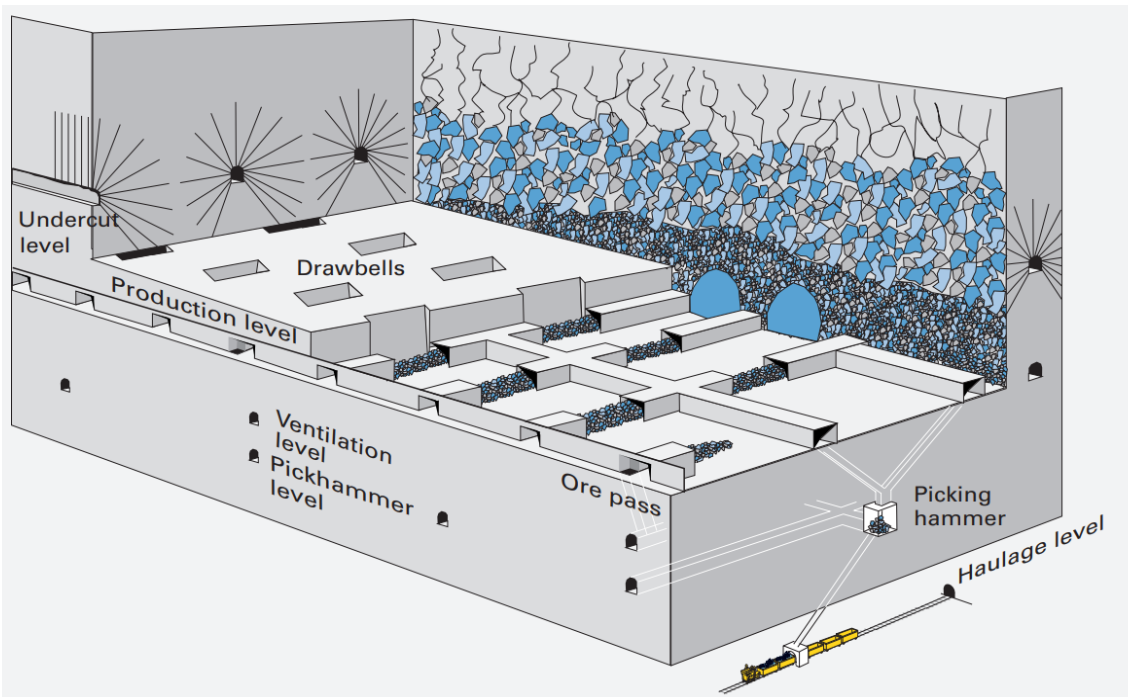

Figure 2.1. A typical block cave mine layout (Atlas Copco, 2007).

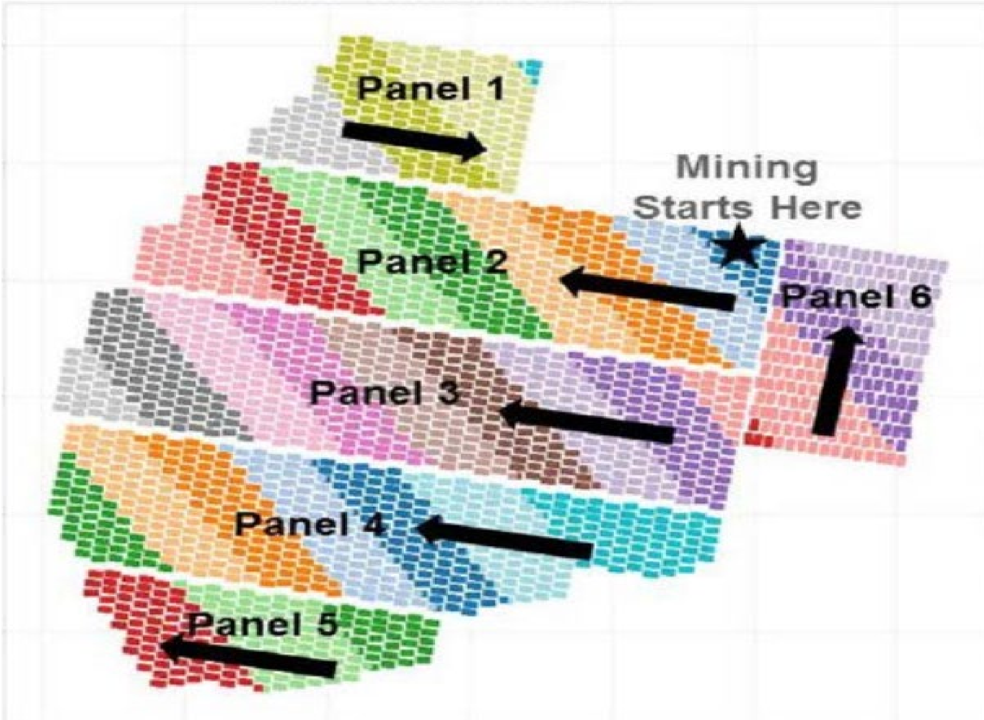

Figure 2.2. A typical panel cave mine layout; example from Resolution Copper Mine (Resolution Copper Mining, 2016).

2.2 Inrush Hazards in Cave Mining

Despite the economic advantages of cave mines, they are susceptible to operational hazards related to the geology and stress conditions, such as rockbursts, air blasts, and inrushes that can result in operational delays, economic losses, and/or fatalities. Butcher et al. (2000), Heslop (2000), Brown (2002), and Paetzold et al. (2020) classify inrush hazards in cave mining as follows:

1. Air inrush or air blast: a rapid flow of air through an underground opening by compression of the air in a confined space. This phenomenon is caused by a period of stalled cave propagation that results in a void developing between the top of the draw column and cave back, followed

by a sudden collapse of the cave back. It causes rock and dust to become airborne, exposing personnel and infrastructure to this hazard.

2. Wet muck spill or mud rush: sudden inflows of saturated fines from drawpoints or other underground openings. This phenomenon resembles a debris flow that occurs in an underground and confined environment. Wet muck spills can cause fatalities or infrastructure damage because the material travels at a high velocity.
3. Water and slurry inrush: phenomena that resemble mud rush, but with higher water contents and lower fines contents. The source of water may come from surface structures (i.e., water storage dam, tailings dam, cave break through to surface that connects to the underground workings) or underground structures (i.e., backfilled stope, overlying cave mines).
4. Dry inrush: an uncontrolled, free flow of dry, fine (sub-centimeter) caved material from a drawpoint. This phenomenon is similar to a wet muck spill but without a high water content in the flowing material. Although it has relatively low mobility, a dry inrush can still result in safety and operational issues.

As wet muck spills are the main subject of this research, most of the literature review that follows is based on this hazard. However, lessons learned from dry inrush and water inrush mechanisms were also considered in this study.

2.2.1 Fundamentals of Wet Muck Spills

A wet muck spill (Figure 2.3) is a complex process due to confinement, stress, mobility, and the uncontrolled nature of different materials and size ranges when mobilized (Jakubec et al., 2016). Many terms are used in the industry to describe the sudden ingress of wet material into drawpoints or other underground excavations, including wet muck spill, mud rush, mud push, inundation, and mudflow. This hazard is analogous to an underground debris flow. (Jakubec et al., 2016) describe the following terms:

- Wet muck: a mixture of unsorted fine particles and water, which are mixed in proportions that can potentially flow by gravity if undermined or disturbed.
- Wet muck spill: an uncontrollable or sudden ingress of wet muck into the underground workings (e.g., via the drawpoints).

In other words, wet muck is a condition that can potentially lead to a mud rush or wet muck spill.

Figure 2.3. An example of a wet muck spill, which buried an LHD at the DOZ Mine, Indonesia (Widijanto et al., 2012).

The phenomenon of a wet muck spill is a complex process requiring the simultaneous presence of four elements within the drawpoint vicinity (Butcher et al., 2000):

- A source and accumulation of water from surface water-inflow and groundwater.
- An accumulation of mud-forming material (fines), both internally (within cave zone) and / or externally (at the surface).
- A disturbance that causes the mud to flow towards the drawpoints.
- Freedom for the mud to discharge into the underground workings.

All of these elements are part of the nature of caving operations and are largely unavoidable. The ingress and accumulation of water entering the cave from an overlying open pit or subsidence crater around a cave that has broken through to the surface, along with the fines generated during the extraction process, will form wet muck. Depending on the conditions of the operating mine, an absence of water or fines can still result in inrushes, as described in the introduction to Section 2.2.

Once the fines and water conditions are fulfilled, Call & Nicholas Inc et al., (1998) described two triggers that can initiate wet muck spills:

- Static (self-initiated): increase in pore pressure due to rising water level in a drawbell, static liquefaction, consolidation within the drawbell, or a combination of these processes.

- Dynamic (external stimulus): secondary fragmentation, cave back collapse, seismic event, or mucking.

Butcher et al., (2000) classified wet muck entry modes into three categories:

- External Wet Muck: generated externally to the underground physical environment by the inrush of caved material or stope backfill if a cave intersects an overlying cave/stope; or similarly, the inrush of tailings or slope failure debris if a cave breaches the surface or the bottom of an open pit.

- Internal Wet Muck: mud formed internally within the cave draw column (muckpile) through secondary fragmentation or in clay-forming country rocks and clay mineral-rich ores, resulting in the accumulation of water, fine particles, and compaction.

- Mixed Wet Muck: a mixture of both external and internal wet muck.

Based on their flow characteristics and mobility, (Jakubec et al., 2016a) grouped wet muck spills into two categories:

- Fluid muck: the debris tends to be shallow with uniformly graded mud resembling a thin slurry or water discharge; this has a higher moisture content (up to 50%).
- Viscous muck: generally exhibits thixotropic properties and tends to be stiffer; this type of muck has a lower moisture content (17 - 23%), does not tend to flow as freely under gravity, and might extrude at the drawpoint.

2.2.2 Conditions Influencing Wet Muck Spill Susceptibility

The presence of fine grain-sized material is the first condition of wet muck spills and is a function of geology and comminution through the caved zone. The further the material travels down through the cave, the finer the particle size due to mechanical breakage (Butcher et al., 2000). This cannot be controlled, and therefore the presence of fines must be recorded to identify wet muck risk areas. Water acts as the second condition and mainly comes from precipitation and/or groundwater entering into the cave. Through proper drainage, water entering the caved zone can be controlled.

Jakubec et al., (2016) argued that the rainfall and wet muck spill relationship could be neglected in mature mines. It is still possible to change several drawpoints directly underneath the surface catchment during high rainfall or snow melt seasons. Water does not need to be excessive; if it can accumulate and flow through the caved zone, it will gradually increase the probability of mud formation. The gradual accumulation of groundwater in a mine is arguably more important to consider than a sudden inrush of groundwater or rainwater (Castro et al., 2018). Observations from several caving operations indicate that 100% of the water from rainfall and other surface run-off does not necessarily enter into the caved zone due to evaporation, water movement, and absorption into cave material; some estimates suggest only 30-50% of the water from the surface directly infiltrates and flows down through the cave (Laubscher, 2000).

Wet muck spills can occur when a drawpoint is disturbed through mucking activities or secondary breakage. Mucking creates voids and changes material porosity, allowing water and fines to migrate. If a wet drawbell is not being pulled and the muck has been saturated, water levels can rise and migrate to the surrounding adjacent drawbells (Olua et al., 2015). No mucking activity can also lead to muck consolidation if the surrounding drawbells are in the wet area footprint. Depending on the location of mud pockets, over-extraction and isolated/uneven draw may also lead to spills (Holder et al., 2013). Therefore, the probability of a wet muck spill may be related to the probability of drawing these mud pockets towards a drawpoint.

Butcher et al., (2000) explained that isolated or uneven draw begins with ground control issues that require maintenance or secondary fragmentation. This encourages the operation to introduce unplanned draws to achieve the production target. If these processes are repeated over time, it may lead to drawpoint closure due to the presence of wet muck, which in turn leads to reserve loss. Drawpoints that remain in good condition and are thus drawn over their planned capacity may create an increase in the porosity inside the drawbell, allowing wet muck to form and flow to those drawpoints. Even when best practices are applied, it is difficult to achieve a perfectly even draw. Furthermore, it may only delay the inevitable occurrence of future wet muck spills due to the nature of cave mines (Rachmad et al., 2011).

There are three categories described by Widijanto et al. (2012) that result in an increased susceptibility to wet muck spills:

- Ground conditions (hang-up, packed, or sticky materials).
- Operational constraints (repair activity, political risks, or panel/drawpoint closure).
- Poor mining practices (poor draw control or unrealistic production targets).

2.3 Experiences of Wet Muck Spills at the Grasberg Mining Complex

The Grasberg Mining Complex underground operation has a long history of wet muck spills since the GBT operation (Hubert et al., 2000). The GBT represents the first cave (or lift) in the series with the IOZ beneath it and the DOZ beneath the IOZ (Figure 1.1). The wet muck was generally understood to originate from comminution within the draw column combined with high rainfall (Edgar et al., 2020). The second lift IOZ mine was also impacted by wet muck spills leading to the implementation of the first remote loader technologies aimed at reducing employee exposure to these hazards (Hubert et al., 2000). The DOZ mine experienced its first spill in 2003 (Ginting & Pascoe., 2020) and had recorded more than 1,900 spills as of July 5, 2019 (Figure 2.4 and Figure 2.5).

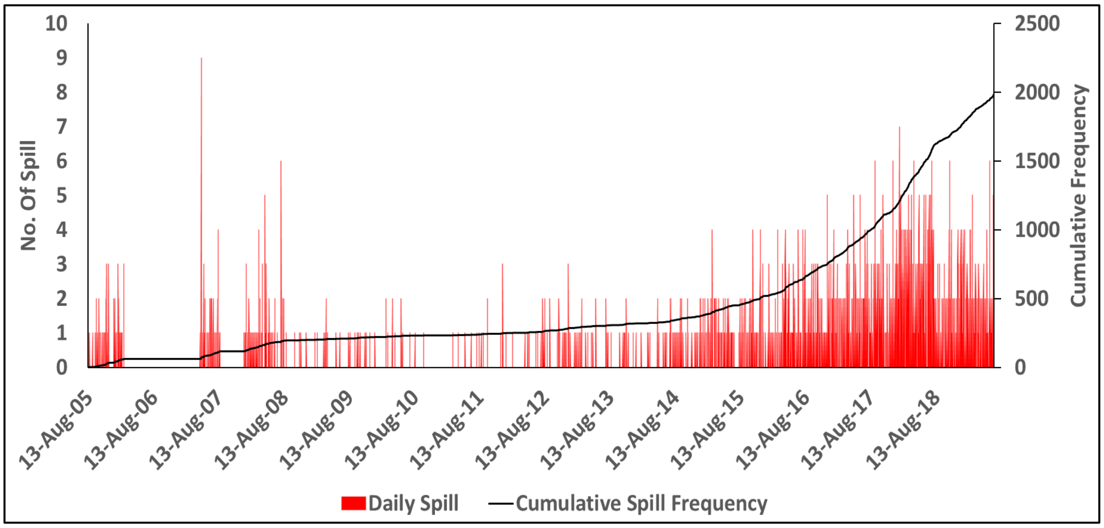

Figure 2.4. Historical wet muck spills at the DOZ mine, up to July 5, 2019.

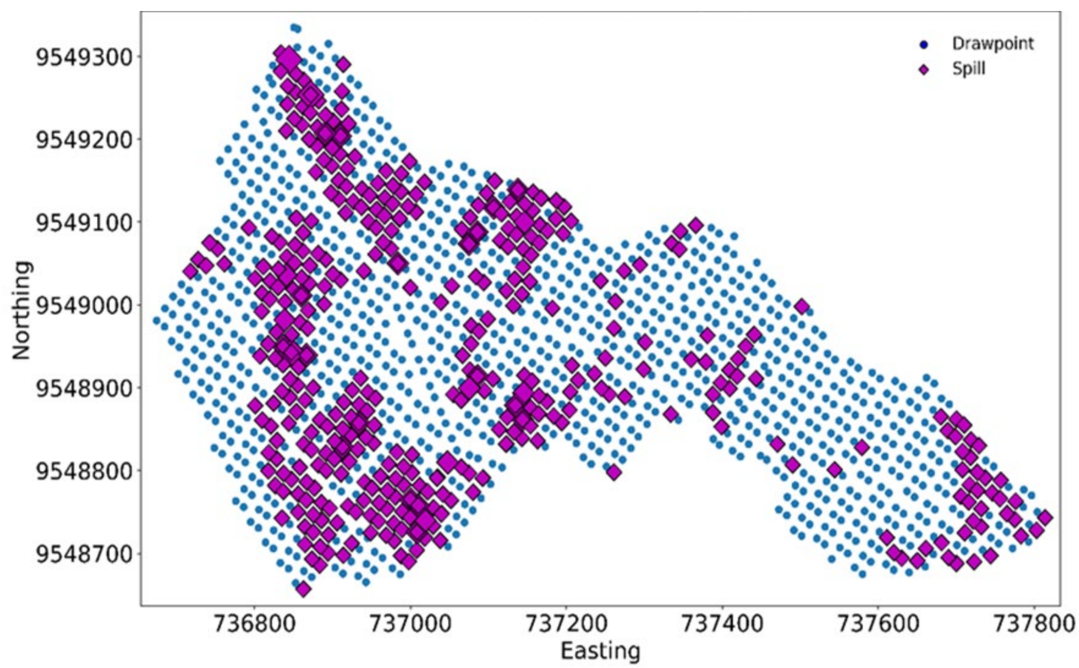

Figure 2.5. Historical wet muck spill drawpoint location at the DOZ mine, up to July 5, 2019.

2.3.1 IOZ Wet Muck Study

One of the first PTFI wet muck studies was documented by Call & Nicholas Inc et al., (1998), who evaluated the structural geology, hydrology, water chemistry, and material properties at the IOZ. They concluded that the material grain size and saturation (a function of dry density and moisture content) are the predominant factors for wet muck spills. Material grain size and its degree of sorting and packing cannot be controlled but can be understood through geotechnical properties and their sensitivity to water content. Water content can be controlled by continuous water drainage and interception before it enters the caved zone. The main water sources were either surface water entering the cave, groundwater, or a mixture of both. Rainwater entering from the surface enters the cave when the caved zone intersects with the surface catchment and subsidence zone; locally, the flow of this water generally follows the draw pattern. Groundwater entering the cave can originate from the surrounding rock, especially if permeable (e.g., the limestone unit in the hanging wall of the IOZ), or if the cave intersects conductive geological structures such as faults.

Geotechnical testing by Call & Nicholas Inc et al., (1998) identified a correlation between wet muck spills and the grain size distribution, density, void ratio, and moisture content of the drawpoint materials. These materials were sampled from the skarn domain, GBT material, and fine-grained in-situ material. Moisture content was used to determine the degree of saturation and mobility of the material.

The Call & Nicholas Inc et al., (1998) study also considered a failure mechanism using a brittleness index derived from triaxial test data. The brittleness index indicates the loss in strength due to collapse when loose material is sheared. A significant change in the void ratio via consolidation indicates the material is collapsible. When the material is less than 80% saturated, significant undrained pore pressure is unlikely to be sustained. At saturation greater than 80%, the excess pore pressure could result in mobile flows. In other words, the first condition of wet muck spills is the material grain size distribution, which is a function of geology and distance traveled through the cave. The material becomes finer the further it travels through the cave due to mechanical breakage (point loading, abrasion, comminution, etc.). Water is the second requirement to change the material behavior to be more fluid and easier to mobilize. Material with 8% moisture content will generate moderate mobility, while 10% moisture content corresponds to high mobility. However, this is not applicable for coarser materials, which were shown by the test results to be significantly less affected by similar moisture contents.

Combining their findings, Call & Nicholas Inc et al., (1998) classified a drawpoint as having the potential to generate a wet muck spill where the following criteria are met:

1. Unsorted material with greater than 20% sand-sized particles (grain size < 2mm).
2. Material must be at least 80% saturated or greater than 8.5% water content.
3. Drawpoint toe must be loosely packed (less than 90% relative density).

2.3.2 DOZ Wet Muck Studies

As described by Casten et al. (2020), the DOZ mine was originally designed for a maximum production rate of 25 ktpd, but was gradually increased up to 80 ktpd between 2000 and 2010 (Figure 2.6). Between 2011 and 2014, the mine experienced a series of strikes and government restrictions that resulted in production delays. This significantly reduced the production to 50 ktpd.

Throughout this period, the delays in production caused extraction and undercut level damage, which allowed the build-up and migration of wet muck within the caved zone.

Spill frequency significantly increased from 2015 onwards due to the cave experiencing more saturation, which in turn led to an increasing drawpoint closure rate to maintain safety. Very large spills have also occurred with up to 6000 m^3 total volume; these spills flowed beyond the exclusion gate with a total distance of up to 150 m (Edgar et al., 2020). For reference, these large spill volumes are comparable to the volume of the drawbells, which are approximately 6350 m^3 (Widijanto et al., 2012).

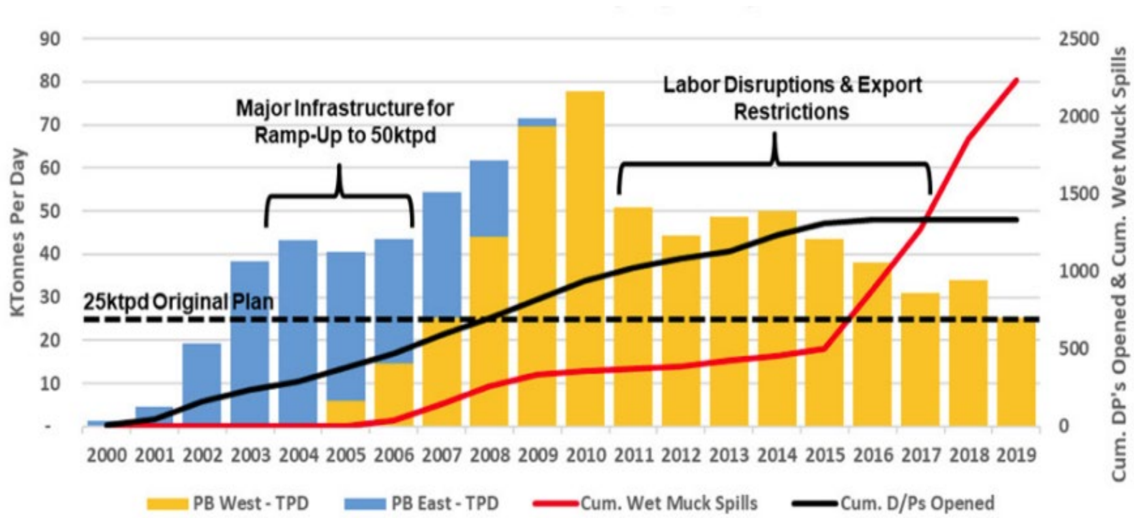

Figure 2.6. Historical production between 2000 and 2019 vs. cumulative wet muck spills (Casten et al., 2020).

Widijanto et al., (2012) classified DOZ sources of fragmentation into three types:

1. Original fine or clayey material – Dominated by DOZ breccia rock types (HALO), marble or dolomite, and IOZ fine material.

2. Fine material from comminution processes – Coarse forsterite skarn, magnetite skarn, and forsterite-magnetite skarn are comminuted into fines after traveling 125 m through the cave and draw column.
3. Coarse material – More competent rock such as diorite and endoskarn are comparatively more difficult to comminute, which requires a longer travel distance at approximately 225 m for endoskarn and 325 m for diorite.

Water sources mixing with these materials in the DOZ reflect those of the Grasberg Mining Complex, which is heavily affected by high rainfall with approximately 5,500 mm per annum (Putra, 2016; Ramadhan et al., 2015; Widijanto et al., 2012). There has been various evidence of surface catchments trapping water, which then flows down through the GBT cave that breaches the surface, into the IOZ cave underneath it, and then into the DOZ cave underneath the IOZ (see Figure 1.1). The water infiltrating the DOZ has been observed to increase over time as the DOZ cave breaches and expands into the bottom of the IOZ cave. This water also includes any groundwater entering the GBT and IOZ, in addition to the groundwater that directly infiltrates into the DOZ mine.

2.3.3 DOZ Water Source Studies

Rachmad et al. (2011) suggest that rainfall alone is not able to saturate the DOZ drawpoints. There is at least 30 to 50% water loss due to evaporation and surface run-off. Combining rainfall with a larger groundwater catchment area can accumulate water, which then might infiltrate and saturate a drawpoint directly underneath it within a few days. There have been observations during heavy rainfall periods of dry drawpoints changing to moist or wet drawpoints.

There are five major bedrock units and fault systems that can serve as groundwater sources potentially entering the DOZ mine: (1) diorite to the SW-SE of the EESS, (2) the West Fault Zone to the west of the EESS, (3) limestone on the northern side of the EESS, (4) the East Fault Zone along the east side of the EESS, and (5) the diorite/skarn/marble contact to the SE of the EESS (PT. Freeport Indonesia, 2017).

Various tracer tests have been conducted using tracer dyes released from the surface at key areas around and within the overlying GBT-IOZ-DOZ subsidence zone. These show that the rate of rainwater percolation down to the DOZ extraction level has increased over time, changing from 14 days in 2000, to 4 days in 2005 and 2007, and to 24 hours in 2011 (Widijanto et al., 2012). In 2017, another tracer test was conducted at the DOM (District Ore Mine) valley targeting the fractured diorite block where ponding and infiltration of water were observed. It took 72 to 96 hours for the dye to be detected at the DOZ drawpoints. The difference between the travel time is caused by the high variability of permeability of the caved material. Surface water is not only flowing vertically but also sub-laterally through the fractured diorite, which discharges at both drawpoints and dewatering holes. It was concluded that there is a hydraulic connection between the DOM area and the southern panel of the DOZ, which increases the wet conditions experienced at the drawpoints (PT. Freeport Indonesia, 2017).

2.3.4 DOZ Fines Migration Studies

In time, the mixture of water and broken rock tends to mix and form mud. Depending on the density and permeability of the mud, these zones can concentrate and form layers of mud in the middle of the caved zone. This phenomenon is called pack-muck, frozen muck, or stuck muck (Olua et al., 2015) and is sensitive to stops in mining. The longer operations are stopped and mucking at the drawpoints delayed, the higher the possibility of pack muck developing in response to no movement inside the caved zone. Various mitigation techniques, such as minor blasting and using a water cannon, have been applied to remove pack-muck, but were unsuccessful and have reduced the DOZ total ore reserve over time.

Geological mapping is conducted at individual drawpoints to track and record mined rock type, grain size, changes of rock type, wetness, and clay content. The DOZ northern area (i.e., EESS) is dominated by forsterite skarn, whereas the southern area (i.e., ESZ) is dominated by diorite and endoskarn (Olua et al., 2015). Between 2012 and 2015, there was a gradual increase in endoskarn (Esk) percentage in the southern diorite area, as well as marble (Mbl) in the northern area (Figure 2.7). The EESS forsterite (Fo) is a white fine-grain-sized granular mineral (<5cm) and can easily be distinguished from the coarser (>5cm) diorite and endoskarn material. Assuming the material in the cave and draw columns moves vertically, the EESS material would be expected to only appear at the drawpoints underlying the EESS area, not the adjacent ESZ area. However, data from DOZ Panel 3 (Figure 2.8) shows that the forsterite (Fo) laterally migrated to the southwest and was recorded at the diorite dominant ESZ drawpoints (Haflil et al., 2014). Material migration can be defined as rilling, where material tends to migrate laterally along the gap between the cave back and the top of the broken ore draw column, with flow following the direction of cave advancement and mucking.

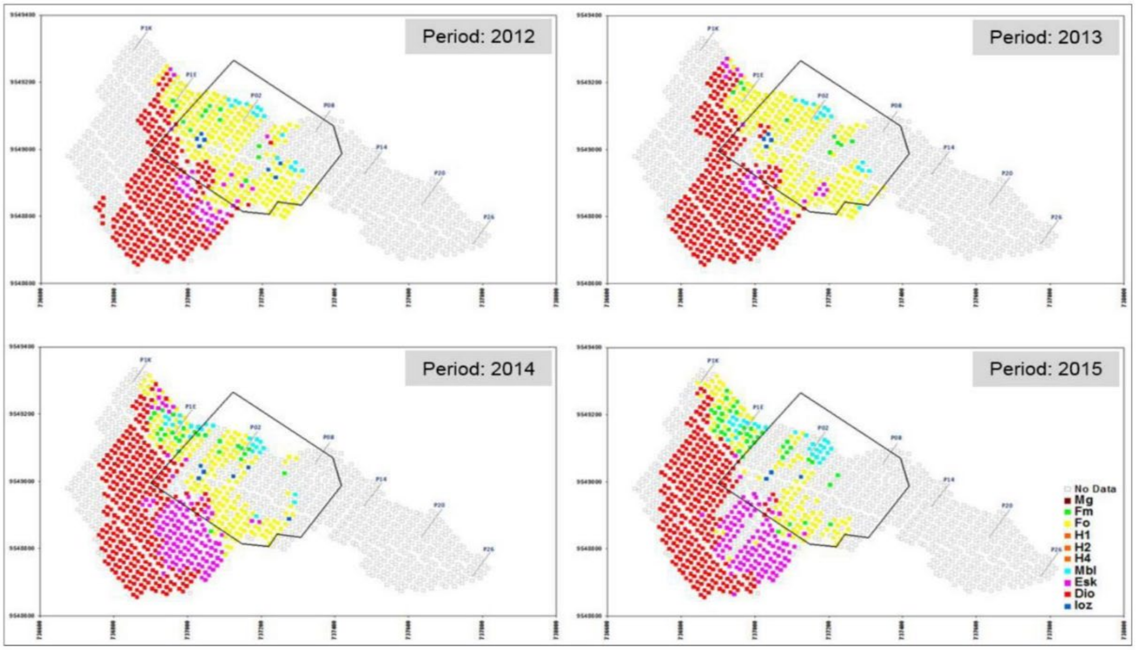

Figure 2.7. The dominant rock types mapped during the period 2012 – 2015 (Olua et al., 2015).

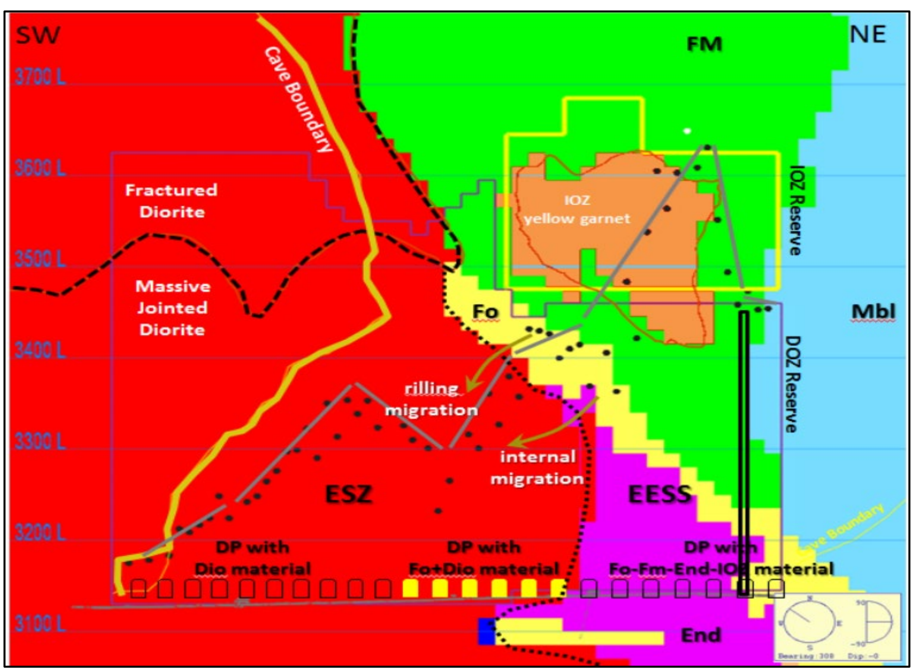

Figure 2.8. Example of the EESS forsterite (Fo) migrating laterally and appearing at the Diorite (Dio) dominant drawpoints under the ESZ in DOZ Panel 3 (Haflil et al., 2014).

Slow cave propagation and larger fragmentation of the diorite in the southwest area of the DOZ contribute to slower vertical movement of diorite blocks. In contrast, the finer forsterite can move faster than the coarser diorite (Haflil et al., 2014; Soebari et al., 2013). With respect to draw management, previous wet and dry muck mixing protocols for material handling at 1:3 for moist drawpoints and 1:6 for wet drawpoints (PT. Freeport Indonesia, 2015) has resulted in a higher extraction rate (tonnage drawn per day) at newer drawpoints in the coarser diorite area. In addition, various panel or drawpoint maintenance activities (e.g., spill cleanup, repair) and secondary fragmentation have forced operations to increase the mining rate in the southern drawpoint area in order to achieve production targets. These factors have resulted in the forsterite material migrating laterally towards the higher concentration of mucking at the southern drawpoints (Olua et al., 2015; Soebari et al., 2013).

Water can also migrate laterally. Numerous wet drawpoints were mapped in the more mature and higher height of draw (HoD) drawpoints, which mostly consist of fine-grained clays. The evidence of clays in the northern area mixing with the uneven mining pattern has created pack-muck, blocking water flow towards the underlying drawpoints and accumulating and migrating towards the southern drawpoints (Olua et al., 2015). Wet muck conditions have required the southern drawpoints to be changed to remote loader operation to safely manage wet muck spill hazards. The first visual evidence of a spill event in the southern part of the DOZ mine that was recorded in 2013 and involved 10-15% EESS forsterite skarn material (Haflil et al., 2014) (Figure 2.8). Since then, numerous spill events have occurred in the vicinity, which continuously spread throughout the southern DOZ.

Furthermore, Ramadhan et al. (2015) considered the Fractured Diorite Zone (FDZ), which is located above the DOZ, capable of trapping and accumulating large amounts of water. When combined with Rock Quality Designation (RQD) values of less than 30% - 50%, and therefore potential to generate fines, these characteristics can act to trigger massive water and wet muck inrush into the DOZ.

2.3.5 DOZ Drawpoint Response Studies

A study by Rachmad et al. (2011) analyzed a spill event from a drawpoint that had last been classified as being fine and dry; the adjacent drawpoint from the same drawbell was mapped as coarse and wet (Figure 2.10). The sudden change of the drawpoint moisture content leading to the spill event was attributed to the near 100% depletion of the overlying DOZ draw column, with material from the IOZ and GBT appearing at the drawpoint toe. Given the high HoD this represents, the draw column was assumed to connect to the surface. Water might directly infiltrate from the surface to the drawbell within a few days, but not immediately, especially considering the preferred flow path would be through the coarser material of its adjacent drawpoint, which was wet. The spill drawpoint had no recorded mining activities for the previous 19 days, which would serve to consolidate the material above the drawpoint and possibly alter the flow paths, changing pockets of dry material to moist or wet. This introduces the possibility that the spill event was caused by static liquefaction due to pore pressure change, where liquefaction is a failure mechanism that can occur when saturated soils are subjected to static or dynamic loading (Taiebat et al., 2007). The buildup of pore pressure would result in material softening and sudden loss of effective shear strength, transforming the material to a viscous liquid and mobilizing it as a spill event.

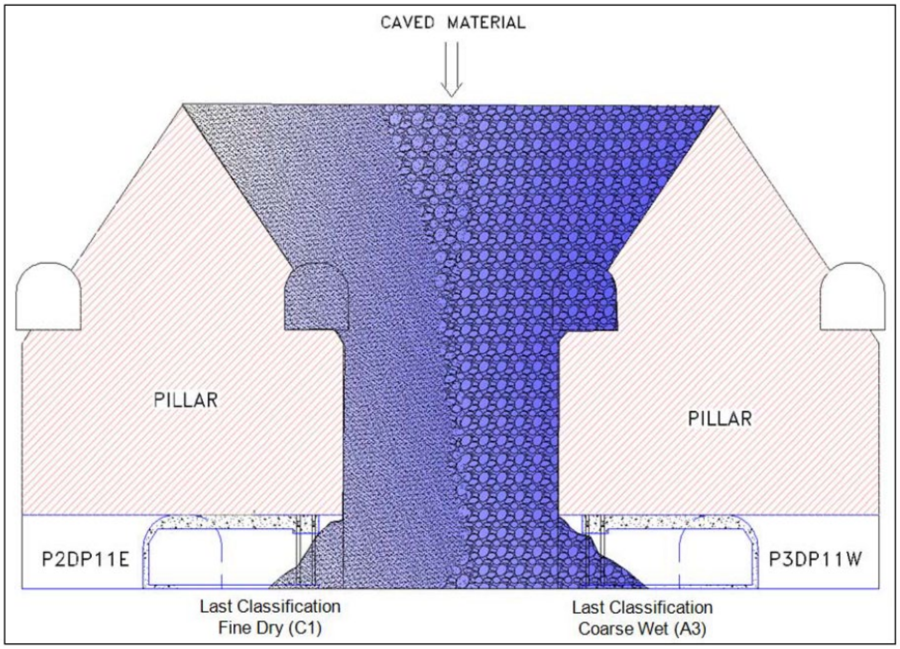

Figure 2.9. Example of a wet muck spill with the unique condition of coarse and wet and fine and dry adjacent drawpoints belonging to the same drawbell (Rachmad et al., 2011).

2.3.6 DOZ Uniformity Index Studies

Uneven or isolated draw, defined as mucking activities concentrated at a drawpoint with limited or no mucking at the adjacent drawpoints, is a challenge at many cave mines (Butcher et al.,2000). This is especially true for the DOZ mine due to the heterogeneous rock mass conditions and different cave-ability rates between the skarn and diorite areas, which can lead to an isolated draw condition (Haflil et al., 2014; Olua et al., 2015; Soebari et al., 2013). An isolated draw will create a funnel for fines to migrate to the drawpoint. In doing so, it will create differential porosity and preferential water migration towards the adjacent least mucked drawpoints (Figure 2.11).

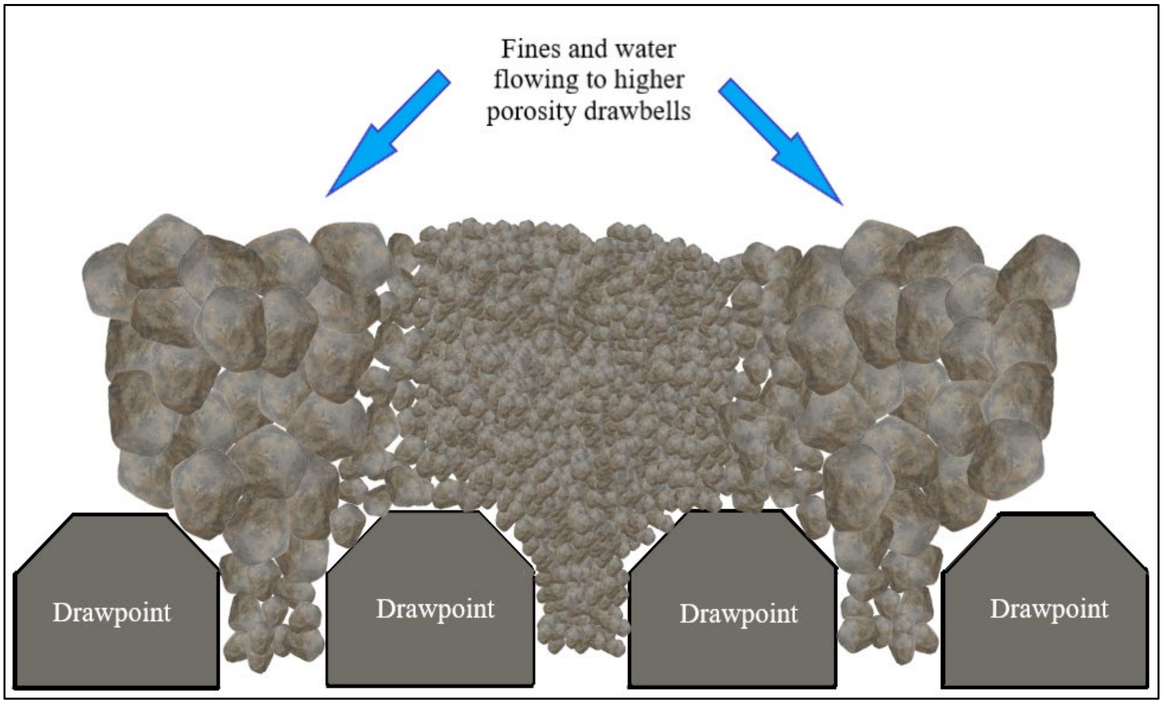

Figure 2.10. Example of isolated draw at the center drawbell causing water to migrate to the coarser drawpoint.

The significant difference in tonnages drawn from drawpoints in the vicinity of one another over a given time period can be quantified using the Uniformity Index (UI), which was first developed by Susaeta (2004) to control dilution at the El Teniente mine in Chile and was based on a layout with six neighboring drawpoints. It was trialed at the DOZ mine to monitor draw uniformity. Several drawbacks were observed by Rachmad (2016), who proposed using a Specific Index of Uniformity (SPUI), where a completely uniform draw has a value of 0 and a completely isolated draw has a value of 1. The formula developed is summarized in Equation 2.1.

Equation 2.1. Uniformity Index Formula (Susaeta, 2004)

$$I.U = \Delta + \underbrace{\boxed{r \cdot \frac{(t_p - t_{min})}{t^2{}_{max} \cdot n} \cdot \sum (t_{max} - t_i)}}_{\text{Specific index of uniformity}} ;$$

Δ: number of inactive draw points in the drawpoint vicinity

r: factor of normalization, equal to 99/89

t_p tonnage extracted from drawpoint *p* under analysis, in a specific period of time

t_i: tonnage extracted from drawpoint *i* belonging to the drawpoints inside the radius of influence in the same period of time

t_{max}: maximum tonnage extracted inside the radius of influence in the same period of time

t_{min}: minimum tonnage extracted inside the radius of influence in the same period of time

n: number of drawpoints inside the radius of influence

2.3.7 DOZ Drawpoint Classification Studies

Call & Nicholas Inc et al., (1998) found that loose packed, unsorted material with 20% sand-size particles and saturation at 80% is the predominant cause of wet muck spills. This led to the development of a wet muck drawpoint classification system based on grain size and moisture content at the loose toe of the drawpoint. This classification was categorized into six different classes from A to F (coarse dry to fine wet) and formed the basis for the classification system implemented by PTFI for the DOZ in 2000 (Table 2.1).

Between 2008 and mid-2018, PTFI added three middle wet muck classifications considering medium size material. The classification system categorized each drawpoint by visual observation and sampling on grain size and water content (Widijanto et al., 2012). Illustrations of each drawpoint classification are shown in Figure 2.12. This system determined the risk, loader type, and level of supervision necessary, as shown in Table 2.2. By the end of 2018, there were no drier drawpoints available at the DOZ mine, and this caused the operation to switch to mining all panels using remote LHDs (Edgar et al., 2020).

Table 2.1. Wet muck drawpoint classification developed for the IOZ and early DOZ (Modified from Samosir et al., 2008).

Engineering Class	Operational Class
A: Coarse Dry 70% or higher coarse fragmentation (>50mm) and moisture content less than 8.5%	**AL: Any Loader** No supervision, even draw and check twice a week for a change
B: Fine Dry 30% or higher fine fragmentation (<50mm) and moisture content less than 8.5%	
C: Coarse Wet 70% or higher coarse fragmentation (>50mm) and moisture content between 8.5% - 11%	**RL: Remote Loader** Required supervision to set up loader, draw at least six buckets per shift, and check each shift
D: Coarse Very Wet 70% or higher coarse fragmentation (>50mm) and moisture content greater than 11%	
E: Fine Wet 30% or higher fine fragmentation (<50mm) and moisture content between 8.5% - 11%	
F: Fine Very Wet 30% or higher fine fragmentation (<50mm) and moisture content greater than 11%	

Figure 2.11. Photo examples of each drawpoint classification at the DOZ mine (modified from PT. Freeport Indonesia, 2014).

Table 2.2. PTFI drawpoint wet muck classification system (Modified from Widijanto et al., 2012).

Wetness / Water Content	Grain Size (M) > 5 cm		
	M ≥ 70% (Coarser Grain)	70% ≥ M ≥ 30% (Medium Grain)	M ≤ 30% (Finer Grain)
Dry (< 8.5%)	A1	B1	C1
Moist (8.5% - 11.0%)	A2	B2	C2
Wet (> 11%)	A3	B3	C3

Green	: Any Loader
Yellow	: Any Loader with Close Supervision
Red	: Remote Loader

The above classification led to the empirical wet muck risk scoring system that is currently used at the DOZ operation (Table 2.3). Through experience and historical data, the six contributing factors shown in Table 2.3 were identified as contributing to wet muck risk for each individual drawpoint. The isolated drawpoints factor, refers to as inactive or not mucked drawpoint within 24 hours, considers up to nine drawpoints near the drawpoint in question, as shown in Figure 2.13. The sum of neighbouring drawpoints that are considered isolated is then categorized as minor, moderate or significant, as shown in Table 2.3. The total risk score is based on a weighted sum, as shown in Equation 2.2 The results of the calculation are categorized as low, medium or high risk, and colour-coded accordingly to aid visualization using a daily wet muck risk map. The weighting factors are based on DOZ wet muck experience. The wet muck risk matrix enables the operation to estimate the likelihood of large spills from a drawpoint (Edgar et al., 2020). Other factors, such as rainfall, seismicity, and tonnages, are not considered in this system, but are still continuously monitored.

Table 2.3. Wet muck risk matrix currently used at the DOZ Mine (Modified from Edgar et al., 2020).

Contributing Factor (CF)	Range (R) Minor (1)	Moderate (2)	Significant (3)	Weighting Factor (WF)
Drawpoint Class	A1, B2, B1, C1	A3	B2, B3, C2, C3	30%
Total Spill Frequency (Since Drawpoint Opened)	< 10	11 - 20	> 20	20%
Isolated Drawpoints (DP)	< 1	2 - 5	6 - 9	20%
Biggest Spill Volume (m^3)	< 500	500 - 100	> 1000	10%
Longest Spill Distance (m)	< 75	75 - 150	> 150	10%
HoD (m)	< 100	100 - 200	> 200	10%

Category	Total Risk Score
Low Risk	0 - 1.5
Medium Risk	1.6 - 2.0
High Risk	2.1 - 3.0

Equation 2.2. The DOZ Mine total risk score

$$\text{Total Risk Score} = [R_{(CF1)} \times WF_{(CF1)}] + [R_{(CF2)} \times WF_{(CF2)}] + [R_{(CF3)} \times WF_{(CF3)}] + [R_{(CF3)} \times WF_{(CF4)}] + [R_{(CF4)} \times WF_{(CF4)}] + [R_{(CF5)} \times WF_{(CF5)}] + [R_{(CF6)} \times WF_{(CF6)}]$$

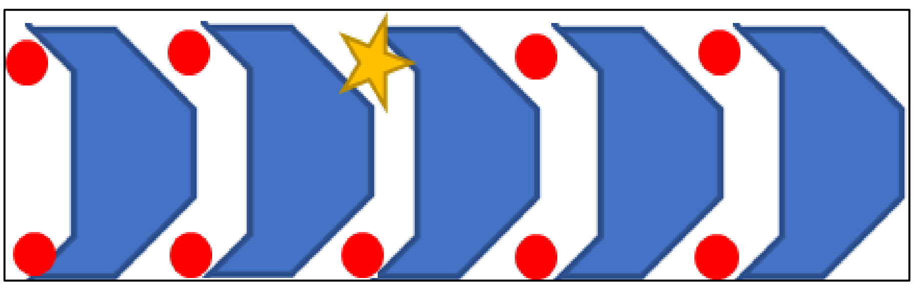

Figure 2.12. The current DOZ mine influential drawpoints (red dots) for wet muck spill observation from the observed drawpoint (yellow star).

In addition to the wet muck risk matrix, various mitigation strategies to reduce wet muck spills have been implemented throughout the DOZ operation (Edgar et al., 2020; Putra, 2016; Widijanto et al., 2012). These strategies include:

1. Wet muck drawpoints are mucked with remote loader to minimize personnel exposure.
2. Permanently closed wet muck drawpoints are sealed with a concrete wall to withstand long-term loading. Temporarily closed drawpoints are secured with 100 m of fibrecrete on the drawpoint toe. Plastic drain pipes are installed to minimize water accumulation.
3. After a spill has occurred, a 24-hour exclusion zone is employed within the influence area (the nine adjacent drawpoints, as per the wet muck risk matrix) until inspection and the drawpoints are declared safe to continue mining activities.
4. Wet muck drawpoints require a 170 m stand-off distance for personnel after mucking for a minimum of 24 hours.
5. Restrictions on mined tonnages are applied based on the level of drawpoint risk. High-risk drawpoints are only allowed to have a maximum of 9 buckets per shift, increasing to 17 buckets per shift for medium-risk drawpoints and 27 buckets per shift for low-risk drawpoints.
6. Mining activities such as mucking and secondary blasting for drawpoints closed because of high risk must use remote and automated equipment.
7. Continuous dewatering is used within the periphery of the DOZ cave, with more than 300 drainage holes intercepting groundwater and reducing water pressures.
8. Rainfall monitoring with a 20mm/day threshold is used for early detection of water entering the caved zone, potentially changing the drawpoint class.

2.4 Experiences of Wet Muck Spills at Other Block and Panel Cave Mines

2.4.1 El Teniente Mine, Chile

The El Teniente Mine, located in the Andes of central Chile, is the world's largest copper-molybdenum mine and one of the largest underground mines in the world. There are several operating sectors within the El Teniente mining complex (Figure 2.14): Diablo Regimiento Mine, Reservas Norte Mine, Block-1 Esmeralda Mine, Pipa Norte Mine and Sur Andes Pipa Mine. These operations have been impacted by wet muck spills over the past two decades (Castro et al., 2018).

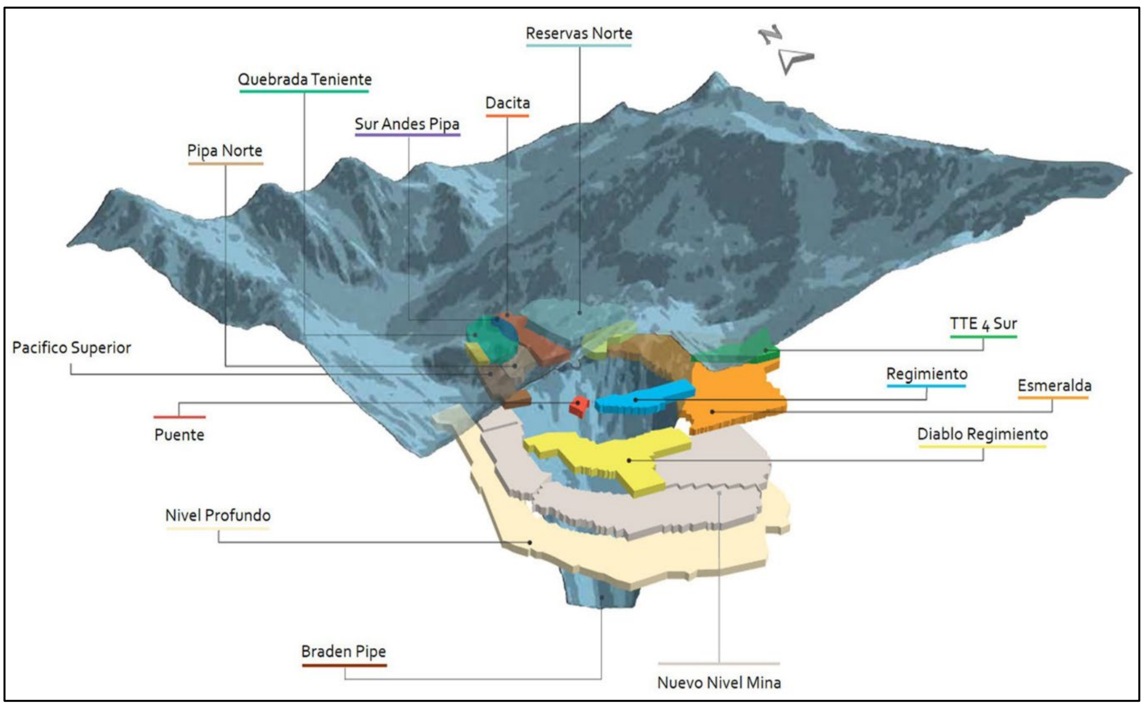

Figure 2.13. The El Teniente mining complex (Castro et al., 2018).

The success rate of the current mitigation strategies for wet muck spills at El Teniente is still unknown. Draw control restrictions and drawpoint closure due to wet muck conditions have severely impacted the operations while progressively spreading wet muck into neighboring drawpoints (Castro et al., 2018; Navia et al., 2014). It is known that the accumulation of water and stress conditions can increase pore pressure and cause mud material to fluidize. Three triggering mechanisms can be summarized as follows (Valencia et al., 2016):

- Static mechanisms: increase in pore pressure and/or sudden increase of stress due to collapse of arches above or within a drawbell.
- Dynamic mechanisms: mostly caused by disturbance, for example, secondary fragmentation efforts (blasting) and/or seismic activity.
- Water as a movement force: increase in water content will change mud properties, resulting in a more fluid-like material.

Various research has been conducted to systematically understand wet muck entry modes and ore geomechanical and geotechnical properties. The first attempted wet muck entry research was carried out by Navia et al. (2014) using a historical extraction database at the Diablo Regimiento Mine. They concluded that height and uniformity of draw are the main variables controlling wet muck entry. Castro et al. (2018) identified two wet muck entry modes at drawpoints: vertical entry and lateral entry (Figure 2.15). In the vertical entry mode, as cave material is extracted, the cave back continuously propagates to the surface, creating a channel for potential mud forming material and water to flow vertically to the ore column and appear at the drawpoint. In the lateral entry mode, extraction of ore in the vicinity of wet muck drawpoints allows wet muck to spread horizontally into the neighbouring drawpoint. Multivariate logistic regression approaches were used by Castro et al. (2018) to estimate the presence or absence likelihood of wet muck entry based on a series of risk variables, including: extraction rate, the presence of a topographic gutter, and neighbouring drawpoint wet muck conditions. Wet muck entry generally occurs when a drawpoint is located underneath a topographic gutter, is over-drawn, and located in a wet muck area.

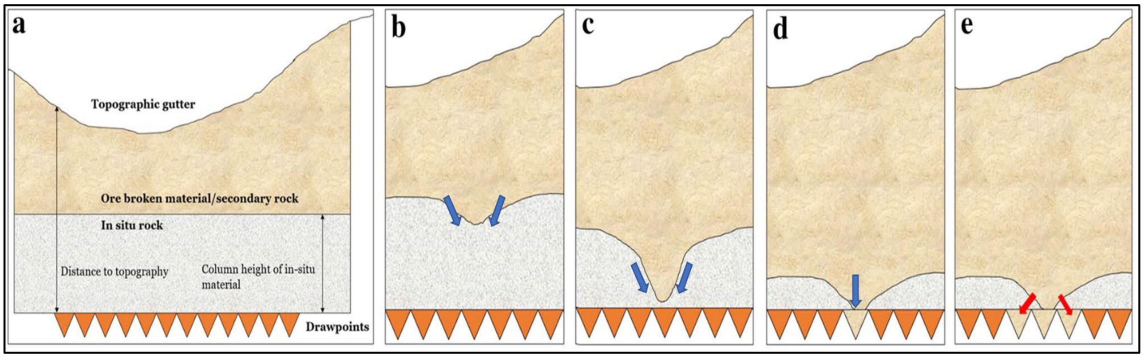

Figure 2.14. Schematic cross-section showing wet muck entry modes at Diablo Regimiento Mine. Blue arrow shows a vertical entry and red arrow shows a lateral entry (modified from Castro et al., 2018).

To define ore geotechnical characteristics and geomechanical behavior, three types of mud ore samples are taken from "critical risk" drawpoints in the Diablo Regimiento Mine. Mud ore is a semi-saturated fine-grained material, where its void ratio and porosity are uncertain due to the constant density changes caused by ore flowing inside the caved zone until it reaches the drawpoint (Castro et al., 2017). The mud ore is sampled based on its color, where grey mud is associated with sulphide ores, and yellow mud is associated with oxide ores (Vallejos et al., 2017). Consolidated Undrained (CU) and Unconsolidated Undrained (UU) triaxial tests were conducted by Vallejos et al. (2017) at the Universidad de Chile laboratory with two extreme cases of wet muck consolidation before failure. The CU tests simulated a low extraction rate, where ore can consolidate and dissipate excess pore pressure. The UU tests simulated a high extraction rate, where the rapid loss of confinement can result in undrained failure. The mud ore types from the Diablo Regimiento Mine only liquefied in UU conditions, meaning wet muck spills are more likely to occur under high drawing rates that loosen the drawpoint material and result in low stress and consolidation.

Also, the porosity of ore will increase, increasing pore pressure due to water accumulation (Vallejos et al., 2017). Comparing the three mud ore geomechanical properties, sulphide mud ore is more prone to flow with lower water content, at 11%, compared to other mud ore. Therefore, a critical risk drawpoint occurs when the drawpoint toe water content exceeds 11% (Table 2.4).

Table 2.4. Drawpoint classification matrix at El Teniente cave mines (Modified from Becerra, 2011).

Moisture Content	Material Size (M ≤ 25 cm)		
	M < 30% (Coarse Material)	30% ≤ M < 70% (Medium Material)	M ≥ 70% (Fine Material)
< 4%			
4% - 7%			
7% - 10%			
≥ 10%			

Normal Condition
Mud Observation
Critical Risk

2.4.2 Palabora Mine, South Africa

The Palabora Mine, located in South Africa, is a deep, hard rock block cave copper mine that is an extension of a depleted open pit operation above it. The first block cave lift (Lift 1) was the first block cave expansion at 400 m below the bottom of the open pit. Lift 2, located 450 m below Lift 1, is in its ramp-up stage (Paetzold et al., 2020). Both lifts utilize the same underground conveyor infrastructure, linked by an inclined conveyor system for material handling to the surface. The main conveyor connecting to four underground crushers was heavily damaged in a fire incident in July 2018, which caused fatalities and completely stopped the operation for ten months. Potential inrush risks were identified, where dry and wet muck spills might occur once mining in Lift 1 is recommenced (Paetzold et al., 2020).

An increased rate of dry and wet inrushes was identified during the nine-month restart period and reduced the production tonnage, where Lift 1 produced a monthly average of 800,000 tonnes before the incident and 460,000 tonnes after the incident. It is hypothesized by Paetzold et al., (2020) that operation suspension allowed water to accumulate in the cave, which mixed with fine material during cave restart. However, this hypothesis cannot be proven due to the limited available data in the caved zone.

2.4.3 Kimberley Mine, South Africa

The Kimberley Underground Mine, located in South Africa, consists of three cave mines: Dutoitspan, Bultfontein, and Wesselton. Unlike the previous case studies, the Kimberley underground cave mine is a diamond mine operation where the kimberlite host rock is weak and generates more fines. Holder et al. (2013) investigated a mud push at the Dutoitspan mine in November 2011 (Figure 2.16). It was fortunate that a mud push occurred instead of a mud rush, which travels at higher velocities. Well-trained personnel also reacted fast to the event, resulting in no fatalities. Several key contributing factors were identified, including poor drainage control, accumulation of water at a surface catchment, waste and/or dilution entry at a nearly depleted drawpoint, and the drawpoint condition.

Figure 2.15. Mud push event at the Dutoitspan Mine (Holder et al., 2013).

The Kimberley Underground Mine implemented a mud rush risk scoring system for each drawpoint, consisting of the following factors: surface water ingress into the cave, underground water ingress into the cave, drawpoint moisture condition, drawpoint waste percentage, drawpoint depletion, three-month moving average draw control, drawpoint damage status, drawpoint condition, and hang-up status. Each risk score was empirically derived using engineering judgment to assign values to each variable based on the observed conditions. The outcome of the model classified drawpoints into low, moderate, high, and very high risk and has shown good correlations based on ten years of data. Further detail on Kimberley Underground Mine mud rush scoring system can be found in Holder et al., (2013)

2.5 Summary of Literature Review

A review of documented experiences at several operating cave mines was carried out to identify the potential causes and triggers of wet muck spills. Key findings, which informed the subsequent work described in Chapters 3 and 4, are summarized in this section.

The majority of cave operations have identified that wet muck (i.e., loosely packed, fine grained and highly saturated material) is a key factor leading to spill events. The wet muck condition of adjacent drawpoints is also an important factor to be considered. Where low porosity material prevents water from flowing out from a drawpoint, accumulated water in the drawbell can discharge to a drawpoint with a higher void ratio or porosity.

The presence of fine grain-sized material is a function of geology and comminution through the caved zone. Increasing draw column height influences secondary fragmentation, resulting in finer material at the drawpoint toe. Furthermore, higher fine materials and water inflow are to be expected once the draw column connects to the surface or overlying caves. Various evidence of dilution entry also can be observed at nearly depleted and over-extracted drawpoints.

Accumulation of rainwater in the surface catchment, operating in high rainfall areas, trapped water in the overlying caves, and groundwater has been identified as the main water source entering the caved zone. Rainwater run-off may or may not enter the caved zone due to evaporation, water movement, and absorption into cave material. Breakthrough to overlying caves or the surface increases cave saturation through the infiltration of trapped water and can create a channel for future water inflow.

Non-uniform draw is largely unavoidable because of temporary mucking suspensions caused by various operational challenges. Although the timeframe of non-uniform draw consequences is unknown, a non-uniform draw can accelerate the wet muck formation through changes in the cave stress. In addition, early dilution entry can also be seen at uneven draw drawpoints.

Drawpoint mucking activity is a critical parameter that disturbs the drawpoint condition, loosens the drawpoint material, and causes dynamic liquefaction of material, transforming it into a viscous liquid and mobilizing it as a spill event. The porosity of the drawbell is also increased, creating a void inside the drawbells and preferential flow paths for wet muck material to migrate. Wet muck can migrate either laterally, vertically, or a combination of both. In addition, material migration can cause wet muck pockets to fluidize and flow to nearby actively mucked drawbells. However, mucking suspension in the wet area footprint can also lead to muck consolidation and migration to the surrounding adjacent drawbells.

Chapter 3: Wet Muck Database Compilation and Exploratory Analysis

A wet muck database was compiled consisting of a historical archive of PTFI DOZ wet muck data, including spill locations and operational activities that are associated with potential wet muck causative and triggering factors. This chapter details the process of creating the wet muck database, including the workflow, filtering of useable variables, exploratory analysis, and data pre-processing. Limitations of the dataset are also discussed. The different factors and variables considered important to wet muck spill susceptibility are presented. Definitions of the selected variables are provided in Appendix A. Detailed results of the exploratory analysis are provided in Appendix B.

3.1 Database Development

3.1.1 Data Sources

The wet muck database was developed based on daily data recorded by PTFI for all 1,347 drawpoints at the DOZ mine between January 2008 and June 2019. An early version of the database was initiated in 2018 as part of my M.Eng. project, which included a preliminary summary of lessons learned from wet muck spills at the DOZ mine and a preliminary analysis of potential correlations between spills and rainfall, tonnages, and drawpoint conditions (Varian, 2019). This database was extended to include new data related to wet muck spill causative and triggering factors.

Raw data to build the new database were provided by PTFI representatives; because the data requests evolved as new knowledge and understanding were gained, these requests were recorded in a spreadsheet for tracking purposes. These data were transferred through a secure PTFI-UBC Sharepoint online portal to protect data confidentiality. If any data or reports received were corrupted, included errors, or did not match the request description, these data were re-requested from PTFI. Additional data were obtained from a site visit conducted in October 2019. The final database covers the period between 2008 January and 2019 June and consists of 5,656,053 daily drawpoint records, including 1,853 total spills that occurred from 374 drawpoints. A summary of the data is provided in Table 3.1.

Table 3.1. Datasets and supporting documents received from PTFI.

Received Dataset	Supporting Documents
Wet Muck Spill (2005 – 2019)	Wet muck spill reports (2016 – 2019)
Monthly height of draw (2000 – 2019)	Weekly geoengineering reports
Monthly extraction ratio (2005 – 2019)	PTFI internal reports and presentation on wet muck spills at DOZ and GBC
Daily tonnages (2000 – 2019)	Previous research on wet muck spills
Daily rainfall (2005 – 2020)	Sample of DOZ daily draw order
Daily drawpoint classification	n/a
DOZ and IOZ cave footprint	n/a
Surface topography (2017 - 2019)	n/a
Water discharge from drawpoint (2012 - 2020)	n/a
DOZ drawpoint material hydraulic conductivity (2012 – 2020)	n/a
DOZ seismic database	n/a
DOZ drawpoint hang-up status (2016 – 2019)	n/a
DOZ drawpoint geology mapping (2001 – 2020)	n/a

3.1.2 Data Quality Check

For each drawpoint spill incident, PTFI produces a wet muck spill report that includes the spill location, time, total number of buckets drawn during the shift, spill class, and drawpoint class. These reports were used to carry out a quality check of the wet muck spill data by manually comparing the data records to the corresponding 2016 to 2019 wet muck spill reports to ensure consistency. In addition, missing drawpoint classification records were assumed to have similar conditions from the previous day. Wet muck spill records with errors or missing key identifiers were removed from the study database. For example, a spill event recorded as "multiple spills" triggered at a set of surrounding drawpoints was removed because its origin was not identified. Once the data quality check was completed, it was assumed that the dataset was sufficiently accurate for the purposes of statistical analysis.

Mapped data on water flow, drawpoint rock distribution, and rock fragmentation size were not included in the present study database because these datasets were incomplete (e.g. due to the inability of personnel to access wet muck panels). However, these variables are likely important factors related to wet muck susceptibility and could be considered in future work.

3.1.3 Data Challenges and Limitations

The observational datasets, such as those derived from drawpoint mapping, are often prone to human biases (e.g., subjectivity) or limited by the impracticality of collecting data on a daily basis. The drawpoint mapping dataset consists of wet muck classification, mineral distribution, rock fragmentation, and water discharge. Drawpoint mapping activities are often conducted on a weekly basis and up to monthly, depending on the drawpoint availability for inspection. For example, due to safety risks, personnel are not allowed to enter areas that are susceptible to a wet muck spill. Since most of the DOZ footprint is saturated and susceptible to wet muck spills, delays in drawpoint mapping led to inconsistencies and repetition in the datasets where previously mapped values are carried forward in the data record.

Other key challenges that affect the data quality include:

- Continuous mucking activity can cause the drawpoint classification to change to a worse class, but it is not always feasible to keep track of these changes due to operational constraints in the mapping frequency.
- Historical wet muck spills prior to 2016 have no supporting documents (e.g., spill reports, weekly geoengineering reports) for quality checking. In addition, in the absence of specific information, wet muck spills were assumed to originate only from single drawpoints.
- The spill class can differ from the drawpoint class, as run-out material can originate above the drawpoint toe (i.e., from areas that cannot be observed). The wet muck classification in the present study was based on the mapped drawpoint class unless other information was provided.
- Most of the inaccuracies in the pre-2016 data were caused by infrequent and non-systematic database updates.

3.2 Data Pre-processing

Once inconsistencies in the raw data were filtered, potential wet muck susceptibility variables were identified for further exploratory and detailed analysis. In total, 177 variables were identified. All of the variables are described in Appendix A.

3.2.1 Spatio-Temporal Data Manipulations

3.2.1.1 Spatial Data Manipulation

Wet muck formation in response to the cave development is largely influenced by the spatial movements of fines and water inside the cave. These cannot be observed directly, and instead, the corresponding spatial responses and interactions between neighboring drawpoints are analyzed using a radius of influence relative to each drawpoint. It is noted that the DOZ footprint is not symmetrical, as the spacing between minor pillars is approximately 18 m, the spacing between major pillars is approximately 20 m, and the spacing between drawpoints within the same drawbell is approximately 12 m. To capture this potential range, a multiplier of 12 m was used up to a maximum radius of 48 m around each drawpoint. Scenarios involving the nearest five and nearest seven drawpoints were also considered. Testing of radii greater than 48 m introduced too much noise into the spatial data.

3.2.1.2 Temporal Data Manipulation

The analysis of wet muck accumulation in the caved zone requires the identification of temporal patterns. Variables derived from tonnages (adjacent tonnages, differential tonnages, uniformity of draw, drawpoint mucking activities, adjacent drawpoint mucking activities, consecutive drawpoint mucking activities) and rainfall were temporally manipulated with lagging periods including one day, two days, three days, seven days, 14 days, 21 days, and 28 days. "Current day" data were excluded for the following main reasons:

1. When a spill occurs, the drawpoint mucking tonnage and clean-up spill tonnage are not always separated.

2. Daily data are not always readily available.

3.2.2 3D Mine Geometry Data

The Mira Geoscience software package (GoCAD and Geoscience Analyst), Maptek, and AutoCAD were used to process the LiDAR and DXF data for the mine footprint geometry. Added to this information were the IOZ wireframe and yearly subsidence profiles above the DOZ mine between 2017 and 2019. The distance from each drawpoint to the IOZ horizon and surface was also processed using these software packages.

3.2.3 Data Transformation

Prior to data transformation, the database was split into a training and testing dataset. Details of the training-testing split are described in detail in Chapter 4. The split followed an 86:14 ratio of training to testing data, respectively. The training dataset covers the period 2008 to 2015, while the testing dataset covers the period between 2016 and June 2019. Three distinct data types are included in the wet muck database: numerical, categorical, and ordinal data types. Each of the data types was processed differently prior to the analysis presented in Chapter 4, as described below.

3.2.3.1 Numerical Data

Numerical data is measured/recorded either as a continuous variable through time or as a discrete value at a given point in time. The value of each numerical variable was standardized to prevent biases that would otherwise be introduced when using variables with different units and/or scales (Scikit Learn, 2021a). Standardizing the numerical variables results in the data mean (μ) being equal to 0, with a standard deviation from the mean (σ) of 1. The standardization score, or z score, can be calculated with Equation 3.1, where x is the original value.

Equation 3.1. Standardization z score formula

$$z = \frac{x - \mu}{\sigma}$$

The standardization process utilized training data to calculate each numerical dataset mean and standard deviation. The testing datasets were also standardized based on the mean and standard deviation calculated from the training data.

3.2.3.2 Categorical Data

Categorical data is often represented in words or non-ordinal numerical values containing multiple classes. Each class is required to be converted into a machine-learning readable format. The presence or absence of wet muck spill (response variable) was indicated using a binary code, where presence is indicated by a value of 1 and absence is indicated by a value of 0. A similar approach was adopted for predictor variables that are represented by two classes. Multiple class predictor variables that have no ordinal relationship were encoded using "one-hot encoding", in which a binary column is created to represent each class (Scikit Learn, 2021b). One-hot encoding removed the categorical variable and transformed it into one new binary variable for each unique category in the variable.

3.2.3.3 Ordinal Data

Ordinal data is a type of data that has a natural rank order with an unknown distance between each rank. A number is assigned to each class based on its rank. The ordinal dataset is not standardized as it will not affect the statistical model due to its low-value range (e.g., the total number of wet muck drawpoints range between 0 and 24 drawpoints at a 48m sampling radius).

3.3 Data Exploration and Descriptive Statistics

3.3.1 Overview

The statistical model development is an iterative process that begins with Exploratory Data Analysis (EDA). The EDA aims to screen, identify, and select relevant variables to be used in the statistical models. The HoD, extraction ratio, tonnages, and UI were initially plotted over time using an animation format to visually identify patterns of these variables with historical wet muck spills. Then, the distribution of wet muck spills corresponding to each variable in the study database was plotted (e.g., Figure 3.1 shows the distribution of wet muck spills corresponding to each drawpoint class). Although initially developed, the severity of each spill was not included in the EDA or statistical model, as it was not the focus of this study.

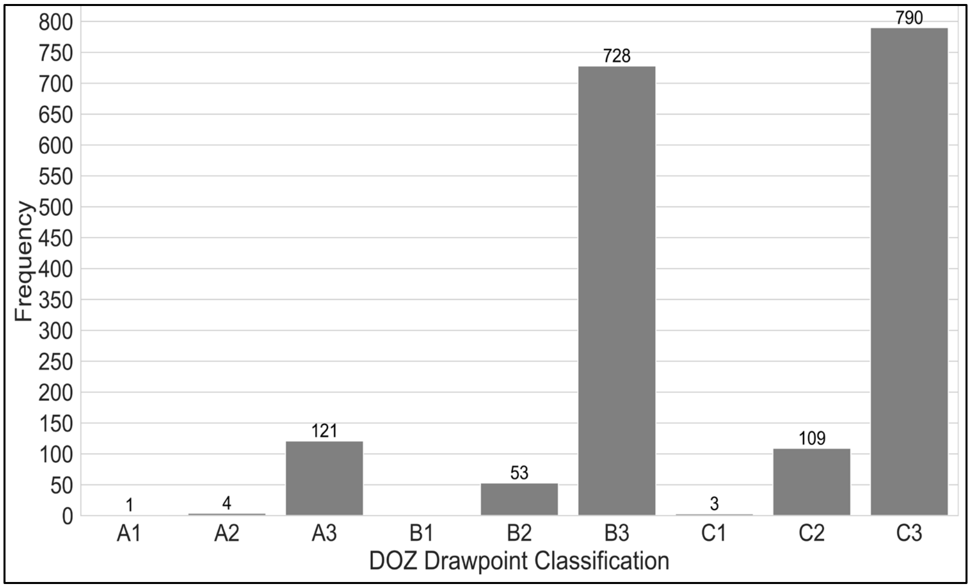

Figure 3.1. Distribution of wet muck spill events corresponding to each drawpoint class for the period January 2008 to June 2019.

3.3.2 Results

The results of the EDA are provided in Appendix B. The following sections summarize the main findings from the EDA.

3.3.2.1 Wet Muck Spill Frequency

The frequency of wet muck spills was observed to increase as the DOZ mine and cave matured. This increase in frequency corresponds with the increasing presence of fines and wet materials detected at the drawpoints. An increase in significant spill events started between the 2015 and 2016 period, in parallel with the increased reporting of wet muck drawpoints (Figure 3.2). There were 402 spills between 2008 and 2015, compared to 1,451 spills between 2016 and June 2019. This increase also resulted in more than 100 drawpoints being closed since 2016.

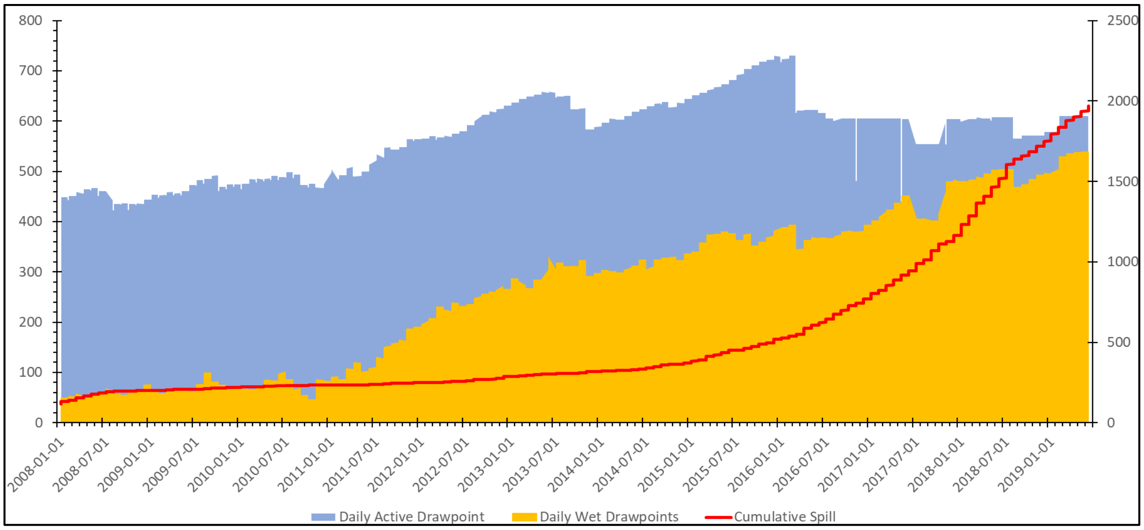

Figure 3.2. Monthly wet muck spills at DOZ vs. total number of active drawpoints.

3.3.2.2 Drawpoint Classification

The drawpoint mapping data considers nine drawpoint classes for active drawpoints and ten drawpoint classes for adjacent drawpoints. For drawpoints that experience a spill event, the drawpoint class used in the database was the mapped drawpoint class prior to the spill. This means a spill classification can be different from the drawpoint classification. The data exploration shows that a majority of wet muck spills occurred at wet muck drawpoints, mostly drawpoint classes B3 and C3 (Figure 3.1). Observing the adjacent drawpoints, spills often occurred when the adjacent drawpoints experienced wet muck (mostly B3 and C3) or were closed (Figure 3.3). Therefore, both variables (drawpoint class and adjacent drawpoint class) are considered to be significant explanatory variables.

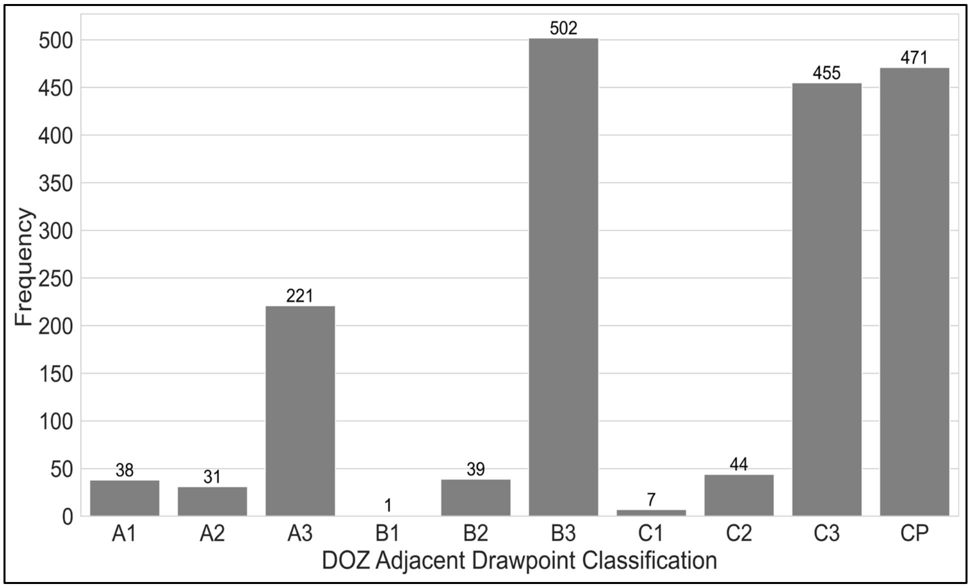

Figure 3.3. Distribution of DOZ wet muck spill events corresponding to adjacent drawpoint class for the period January 2008 to June 2019.

3.3.2.3 Total Number of Wet Muck Neighbors

The occurrence of wet muck spill events was observed to correlate with neighboring drawpoints reporting wet muck, regardless of using a 24 m, 36 m, or 48 m radius zone of influence (Figure 3.4, Figure 3.5, and Figure 3.6). There is an upward trend with these radii, where wet muck spills tend to increase with an increasing number of wet muck neighbors. These variables are hypothesized to be strong explanatory variables in the statistical models.

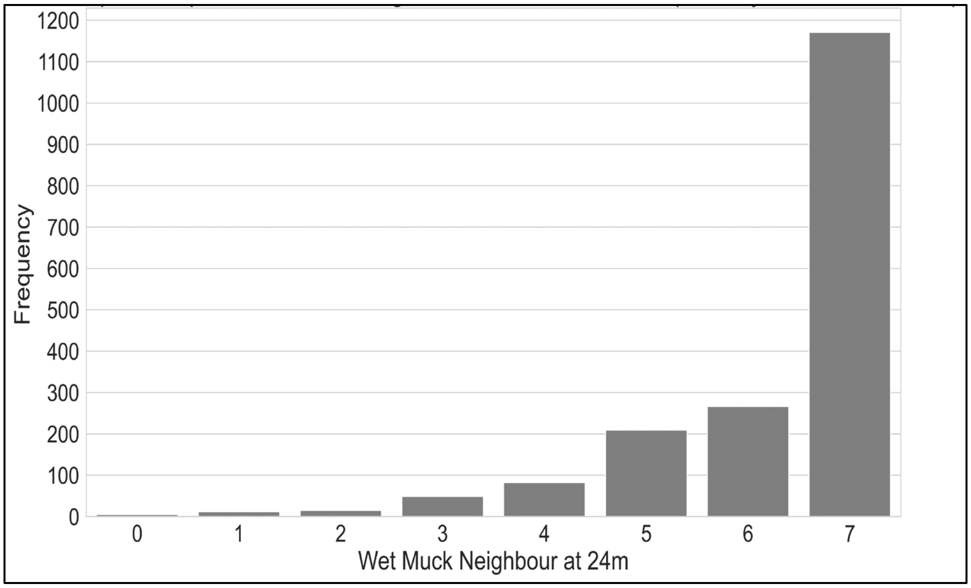

Figure 3.4. The DOZ mine spill frequency between January 2008 and June 2019 based on the total number of wet muck neighboring drawpoints within a 24-meter radius.

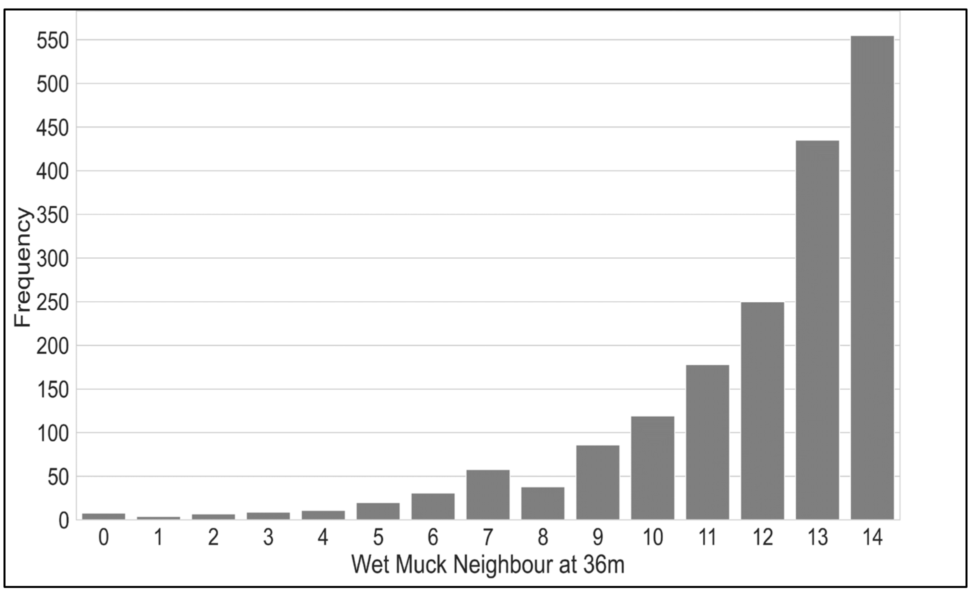

Figure 3.5. The DOZ mine spill frequency between January 2008 and June 2019 based on the total number of wet muck neighboring drawpoints within a 36-meter radius.

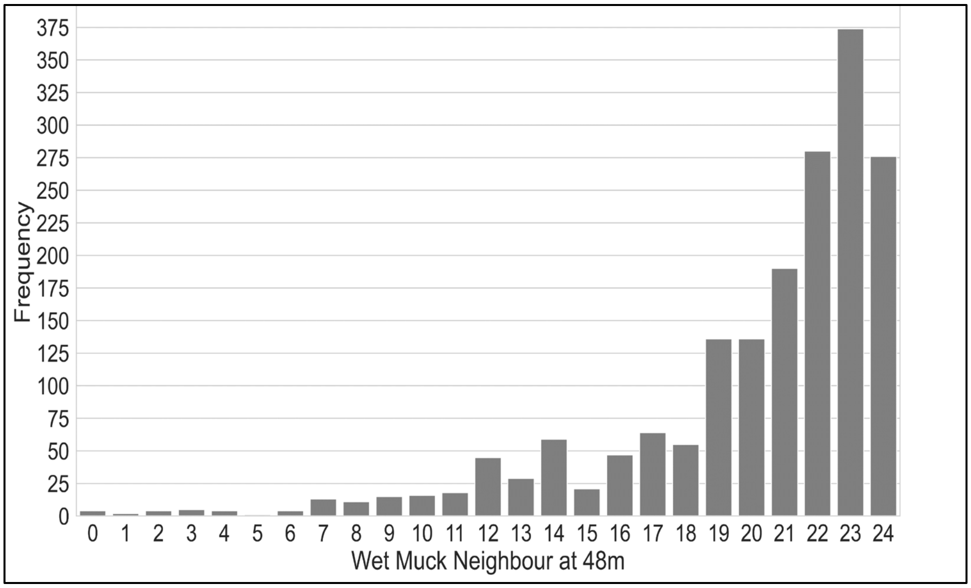

Figure 3.6. The DOZ mine spill frequency between January 2008 and June 2019 based on the total number of wet muck neighboring drawpoints within a 48 meter radius.

3.3.2.4 Height of Draw and Extraction Ratio

The distribution of HoD data generally ranges between 170 m and 350 m (Figure 3.7). Breakthrough of the DOZ mine to the overlying IOZ restricted most of the draw column heights to approximately between 225 m to 300 m (Figure 3.7), although drawpoints within the IOZ boundary reached between 350 – 750 m. The DOZ drawpoints outside of the IOZ cave footprint reached more than 350 m and up to 750 m. Although this causes a skewed dataset that does not show a linear trend for the logistic regression input, HoD is still a significant variable, showing a trend between 170 m – 350 m, and therefore it was tested in the statistical analysis. The adjacent HoD shows similar trends, with drawpoint HoD data ranging between 125 m and 300 m (Figure 3.8). The extraction ratios for both the individual drawpoints (Figure 3.9) and adjacent drawpoints (Figure 3.10) show a linear relationship with spills, where most spills tend to occur as drawpoints reach depletion. Differences between drawpoints sharing the same drawbell were also developed, but no correlation could be identified, with spills mostly occurring between ± 25 m to ± 50 m for differential HoD (Figure 3.11) and -0.2 to 0 for differential extraction ratio (Figure 3.12). The DOZ HoD values as of June 2019 are shown in Figure 3.13.

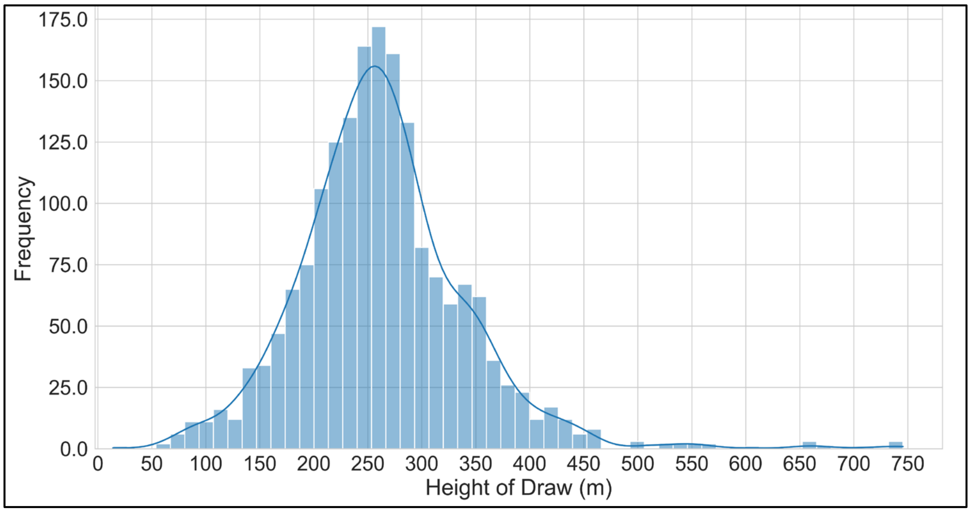

Figure 3.7. The DOZ mine HoD distribution at spill drawpoints between January 2008 and June 2019.

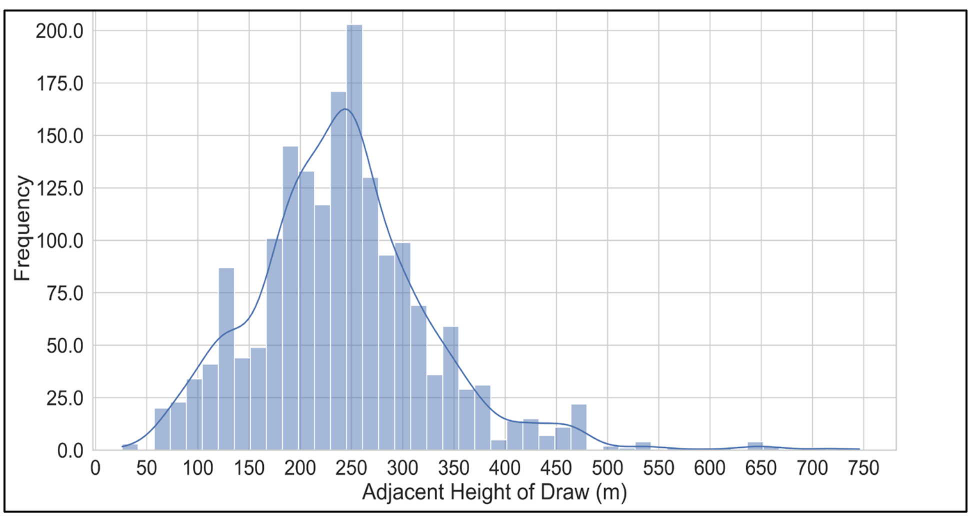

Figure 3.8. The DOZ mine Adjacent HoD distribution at spill drawpoints between January 2008 and June 2019.

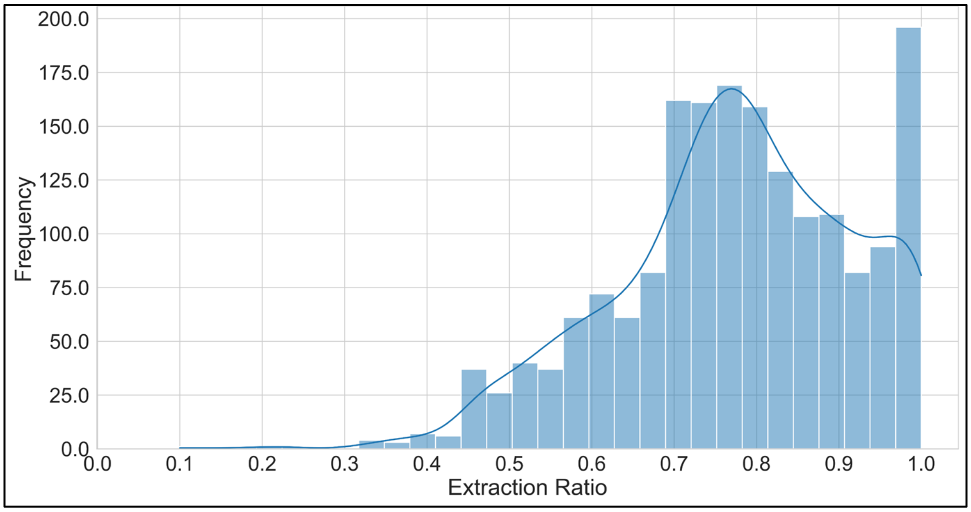

Figure 3.9. The DOZ mine Extraction Ratio distribution at spill drawpoints between January 2008 and June 2019.

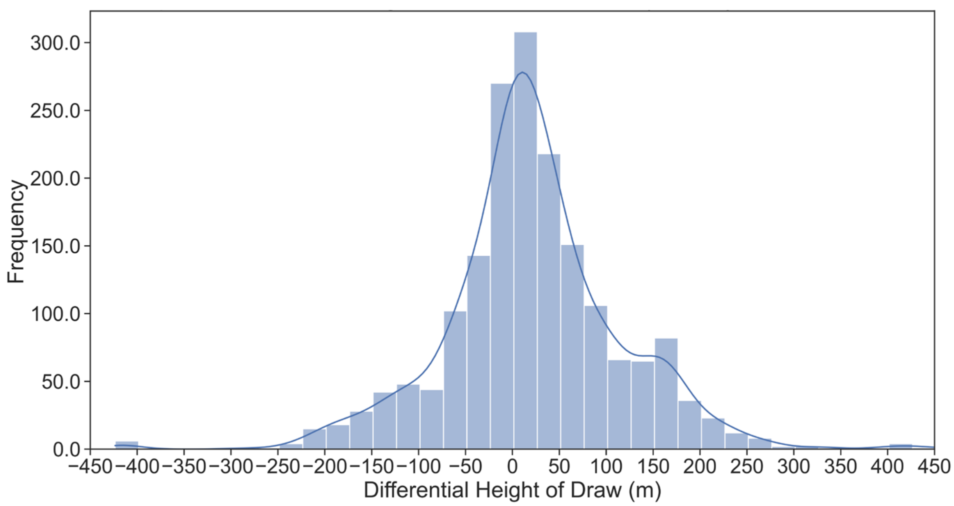

Figure 3.10. The DOZ mine Differential HoD distribution at spill drawpoints between January 2008 and June 2019.

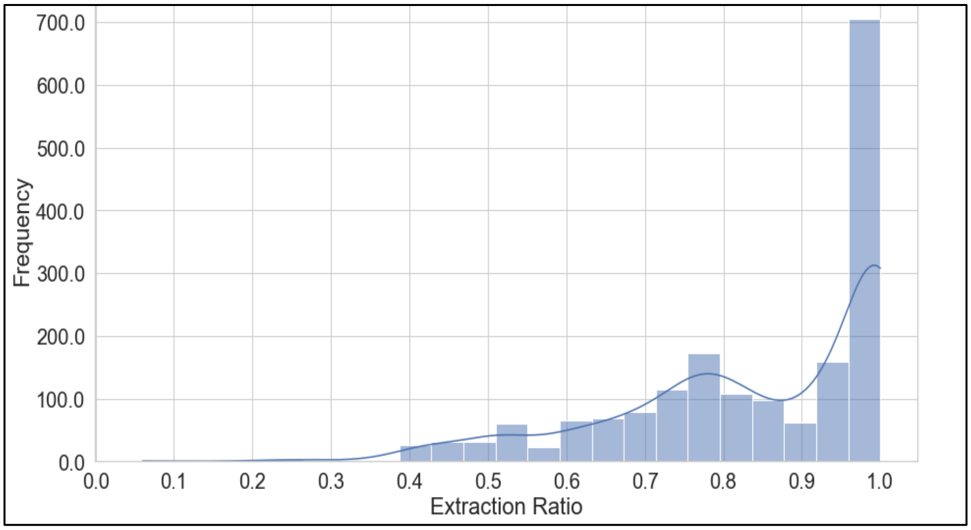

Figure 3.11. The DOZ mine Adjacent Extraction Ratio distribution at spill drawpoints between January 2008 and June 2019.

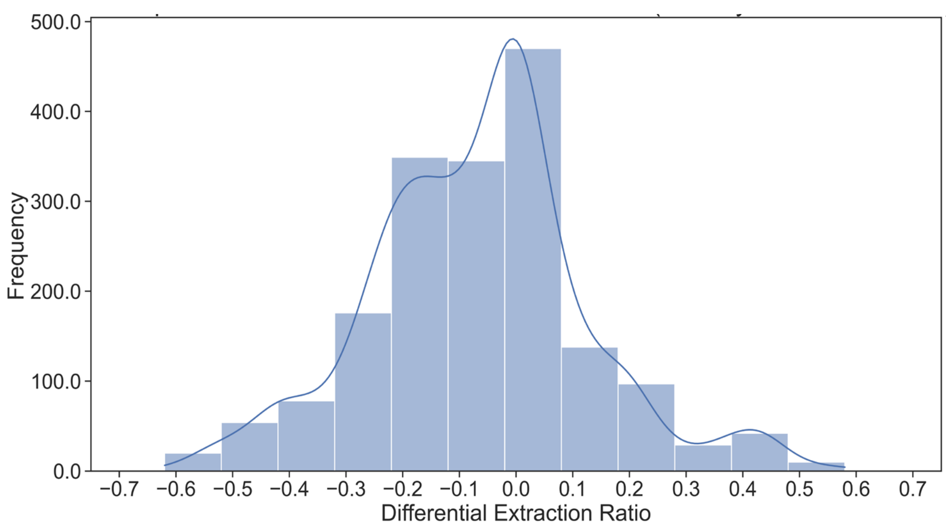

Figure 3.12. The DOZ mine Differential Extraction Ratio distribution at spill drawpoints between January 2008 and June 2019.

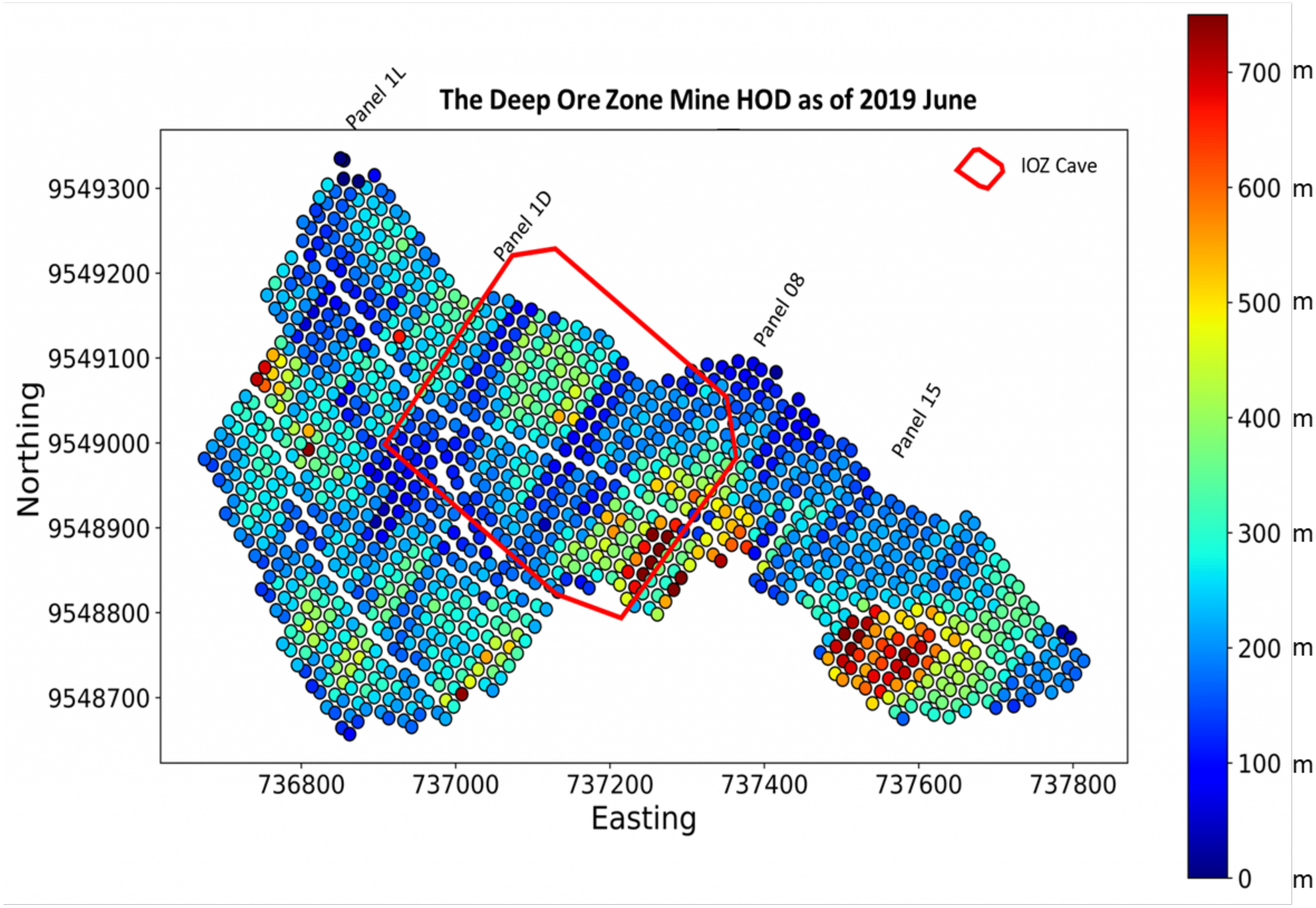

Figure 3.13. The Height of Draw (HoD) at the DOZ Mine as of June 2019.

3.3.2.5 Tonnage

The daily tonnage datasets are often combined with spill clean-up, where clean-up activities can be started as soon as it is safe for the LHD to enter the panel. Depending on the spill volume, clean-up can be completed within the same day. This will likely dilute the dataset, as tonnage drawn on spill days includes the clean-up tonnage. Therefore, the temporal manipulation of the drawpoint data considered data from the previous day.

The distribution of tonnages shows a non-relationship with wet muck spill occurrences (Appendix B). Increasing draw rates at any given period did not show an uptrend relationship with wet muck spills. However, if tonnage data were converted into a categorical format, a clear relationship can be seen between 0 and 50 tonnes and greater than 250 tonnes per 2 days (eg., Figure 3.14, or refer to Appendix B for detailed results). This might indicate that wet muck spills can occur at any active drawpoint that is over- or under-drawn. Although operational experience indicates that spills occurred when adjacent drawpoints were drawn, the draw rates at adjacent drawpoints did not show a relationship with wet muck spills. In addition, no correlation could be identified when analyzing differences between tonnages drawn from the two drawpoints that share the same drawbell.

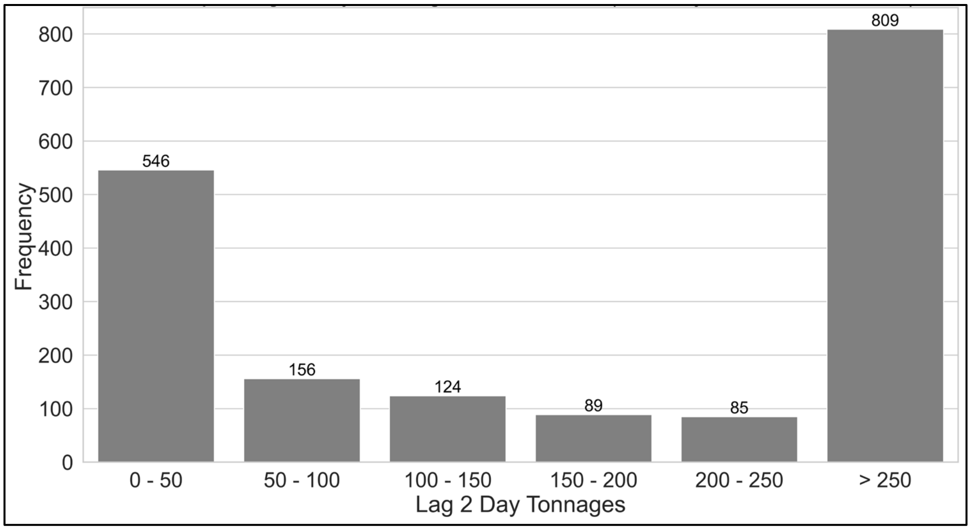

Figure 3.14. The DOZ Mine two days cumulative tonnages distribution at spill drawpoints between January 2008 and June 2019.

3.3.2.6 Mucking

A mucking dataset, with a value of 1 representing a draw of over 10 tonnes (approximately 1 bucket) per day and a value of 0 representing a draw of less than 10 tonnes per day, was generated for both drawpoints and adjacent drawpoints. It was observed that wet muck spills often occurred at drawpoints that were actively drawn during any given period. The higher the temporal period, the higher the number of spills recorded at the mucked drawpoints (e.g., Figure 3.15 and Figure 3.16, or refer to Appendix B for detailed results). However, this correlation can be misleading because the drawpoint might not be mucked consecutively over the given period. In compiling the dataset, mucking was designated as being present if the drawpoint was mucked at least one time during the specified period. This results in a higher presence of mucking when longer periods are considered. To address this deficiency, a consecutive mucking term was developed, defined as two consecutive days with mucking; this term shows a correlation with wet muck spills (e.g., Figure

3.17 or refer to Appendix B for detailed results). Further analysis on the mucking threshold is presented with the ULR results presented in Chapter 4, although it is noted here that definitions using more than two consecutive days of mucking do not show any correlations with wet muck spills.

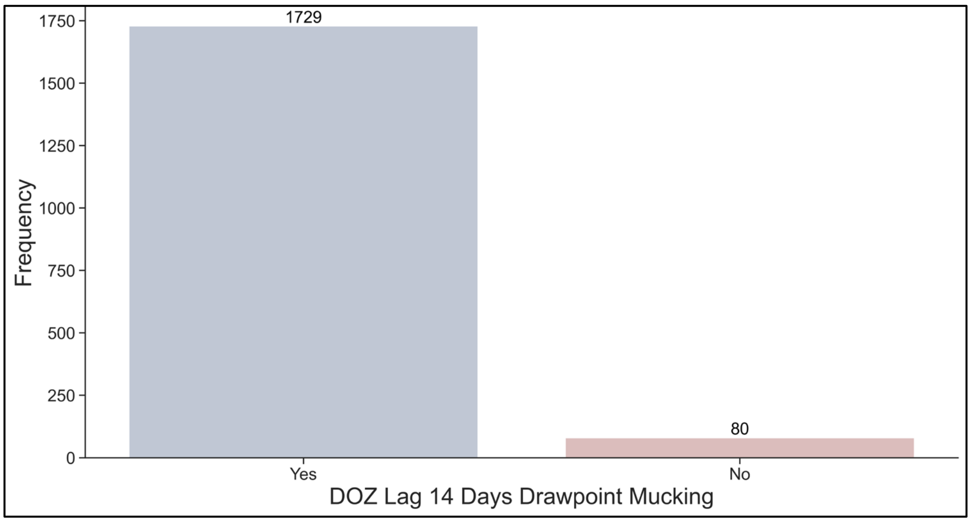

Figure 3.15. Wet muck spill distribution at the DOZ mine during 14 days of drawpoint mucking activities between January 2008 and June 2019.

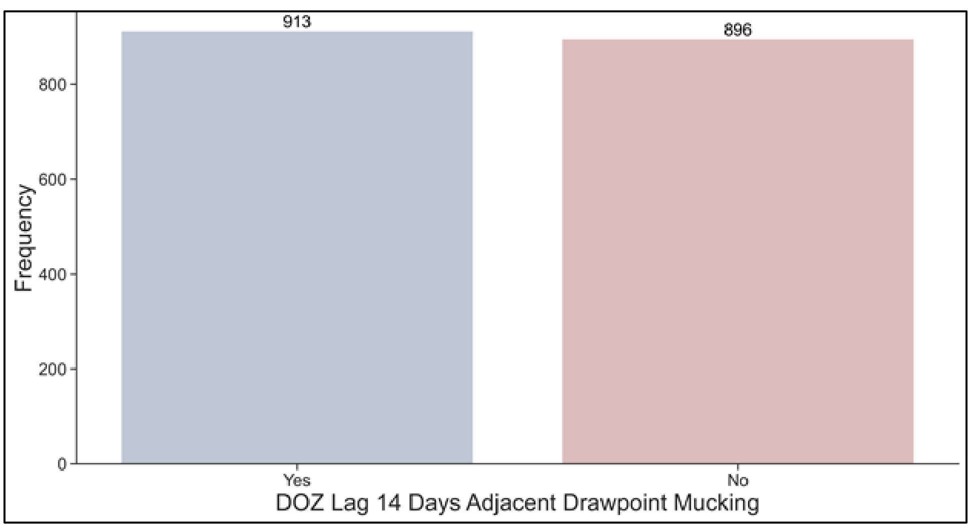

Figure 3.16. Wet muck spill distribution at the DOZ mine during 14 days of adjacent drawpoint mucking activities between January 2008 and June 2019.

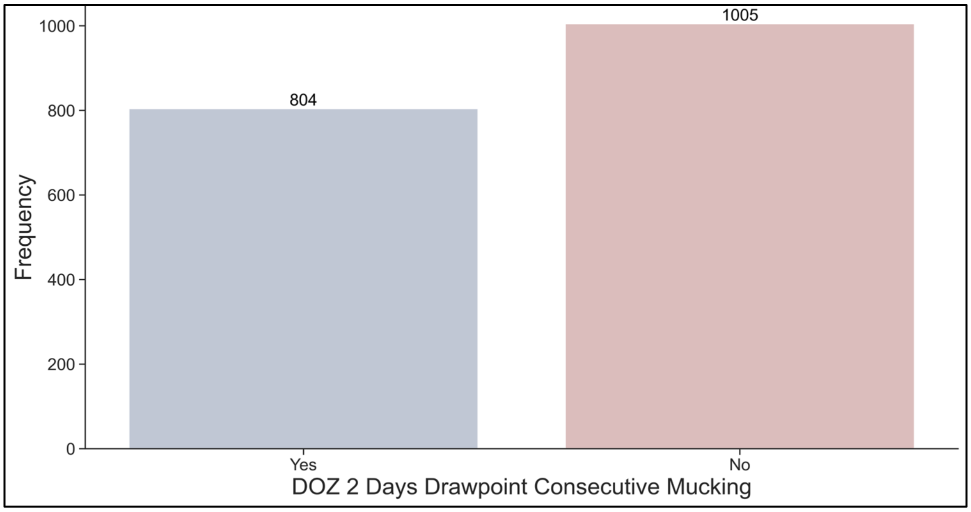

Figure 3.17. Wet muck spill distribution at the DOZ Mine during two days of consecutive drawpoint mucking activities between January 2008 and June 2019.

3.3.2.7 Total Number of No Mucking Days

Although it was first hypothesized that wet muck spills are correlated with longer periods of no mucking, when mucking of a drawpoint has been suspended, the distribution of the total number of no mucking days shows no correlation with wet muck spills (Figure 3.18).

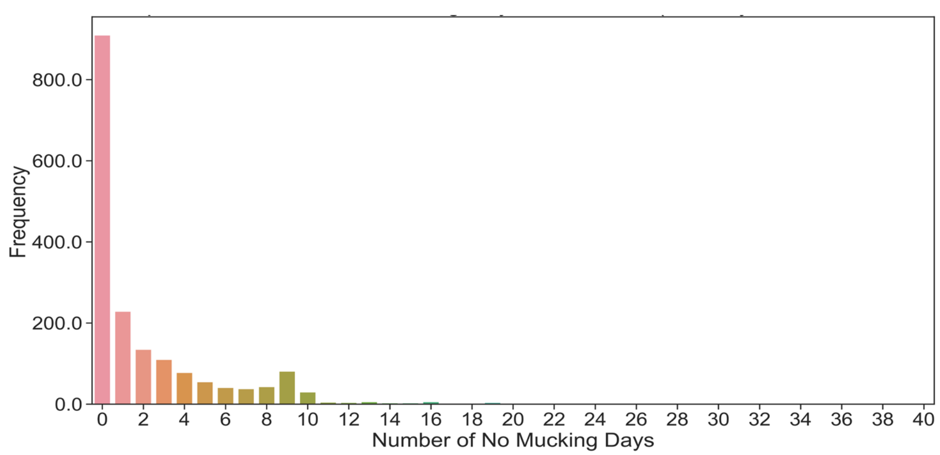

Figure 3.18. The DOZ mine number of no mucking days distribution at spill drawpoints between January 2008 and June 2019.

3.3.2.8 Uniformity Index, Specific Index of Uniformity, and Number of Inactive Drawpoints

The UI and SPUI are calculated as a function of the total number of inactive drawpoints. As summarized in Appendix B, SPUI and the number of inactive drawpoints were tested in the EDA. However, there are no significant patterns that can be observed in both the number of inactive drawpoints (eg., Figure 3.19) and SPUI (eg., Figure 3.20). Using the seven nearest drawpoints, between a 1 day and 3-day lag, the results show a UI of 2 or higher is associated with the majority of wet muck spills under any drawpoint classification (Figure 3.21).

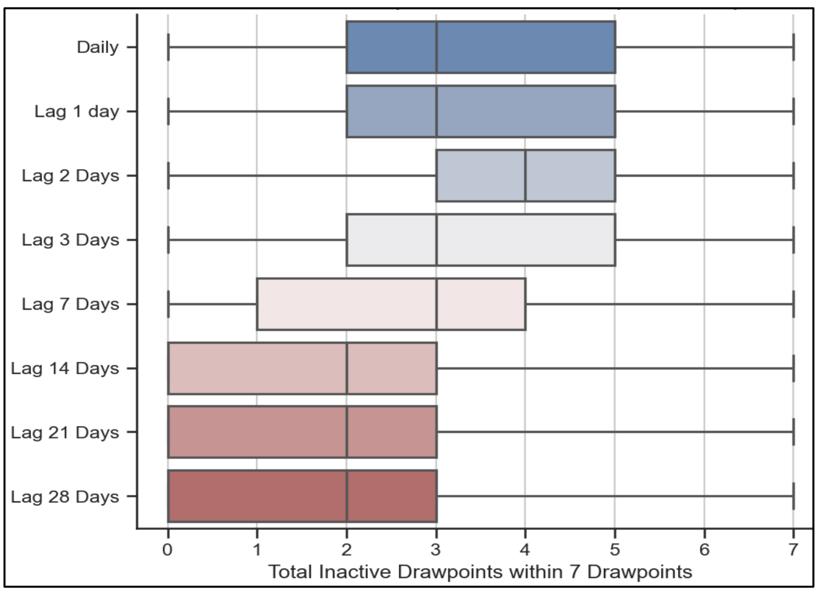

Figure 3.19. Total number of inactive drawpoints within seven nearest drawpoints distribution at spill drawpoints between January 2008 and June 2019.

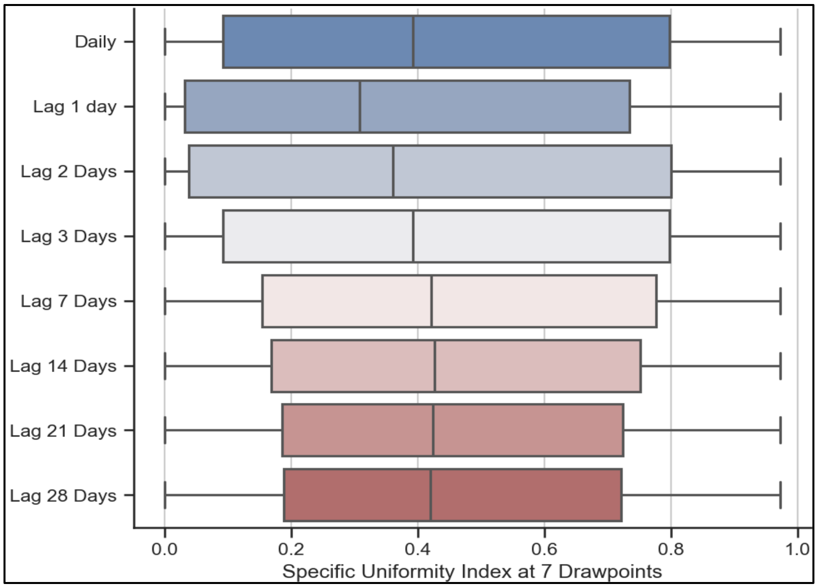

Figure 3.20. Specific Index of uniformity within seven nearest drawpoints distribution at spill drawpoints between January 2008 and June 2019.

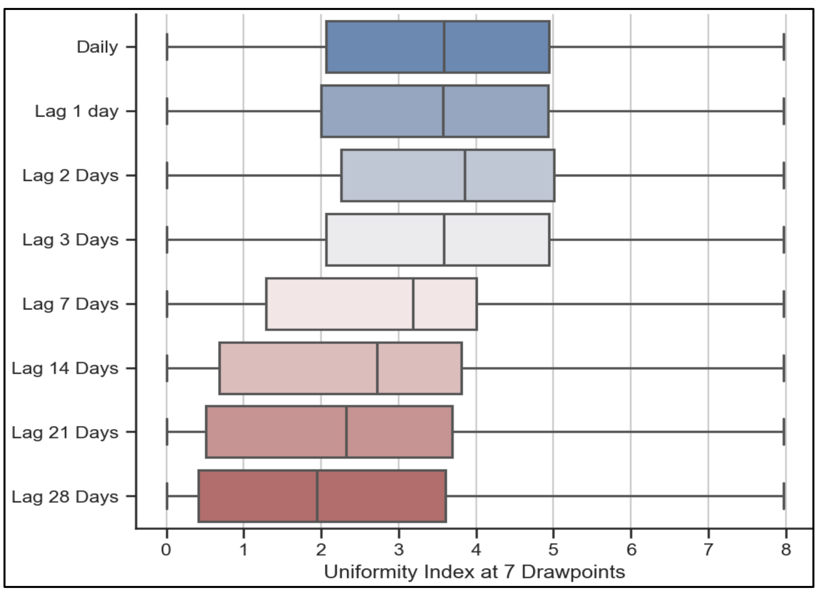

Figure 3.21. Uniformity Index within seven nearest drawpoints distribution at spill drawpoints between January 2008 and June 2019.

3.3.2.9 Rainfall

Since rainfall is recorded from surface rainfall monitoring stations, the rainfall value is assumed to have the same value for all drawpoints. The data exploration shows that spills often occurred when rainfall was more than 10 mm to 15 mm per day (eg., Figure 3.22, or refer to Appendix B for detailed results). Although rainfall is one of the major sources of water entering the caved zone, it is difficult to analyze further because drawpoint mapping is conducted on a weekly to bi-weekly basis and specific data is not recorded at each drawpoint when high or low rainfall occurs. In addition, the percentage of rainwater entering the cave zone is unknown due to dewatering, evaporation or unknown water flow paths. Due to these uncertainties, rainfall data were not considered in the statistical model.

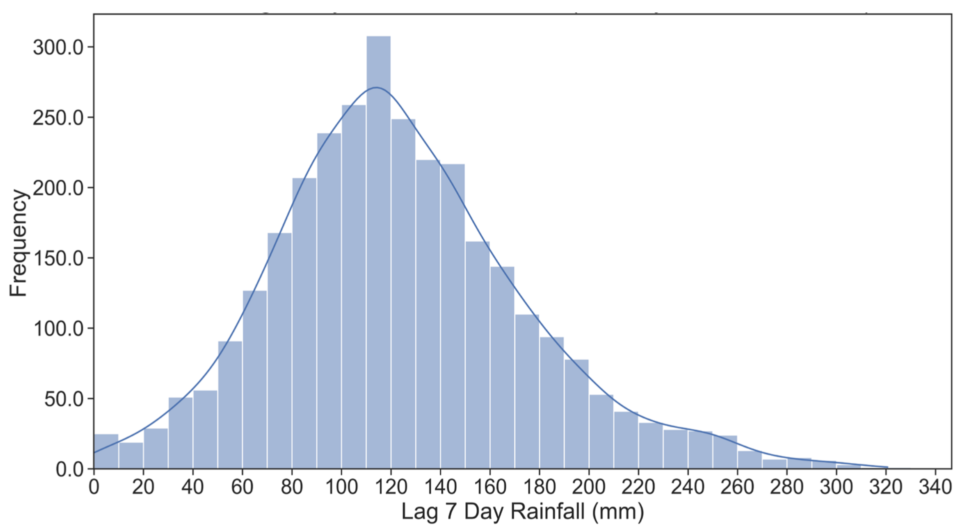

Figure 3.22. The Grasberg Mining Complex cumulative seven days rainfall distribution at spill events between January 2008 and June 2019.

3.3.2.10 Distribution of Material Types at the Drawpoint Toe

Due to the wet muck risks at the DOZ mine (e.g. inability for personnel to access wet muck drawpoints), the drawpoint material types were not mapped as frequently as other datasets, resulting in incomplete data. Therefore, information related to geological distribution was not included in the statistical model.

3.3.2.11 Geological Domain and Vertical Distance to IOZ and Surface

The geological domain of the DOZ mine is divided into the skarn area (east) and the diorite area (west). The data exploration shows an approximately equal spill distribution in these two areas (Figure 3.23). In addition, the classification of the geological domain at spill drawpoints did not consider wet muck migration mechanisms and, therefore, was not included in the subsequent statistical analysis.

Three-dimensional mine geometry data, including the IOZ wireframe and yearly subsidence data, were transformed into numerical and categorical formats. Categorical topographic data is represented by the presence of drawpoint locations vertically underneath the IOZ and subsidence zones. Numerical data is based on the closest distance from each drawpoint to the subsidence zone and IOZ. The data exploration shows that wet muck spills are not related to the location of the drawpoints relative to the IOZ (Figure 3.24). In contrast, wet muck spills do tend to occur vertically below the subsidence zone (Figure 3.25). However, this dataset was developed using the 2017 to 2019 subsidence LiDAR data and previous periods were not available. Therefore, the locations of drawpoints relative to the IOZ and subsidence zone were not included in the subsequent statistical analysis.

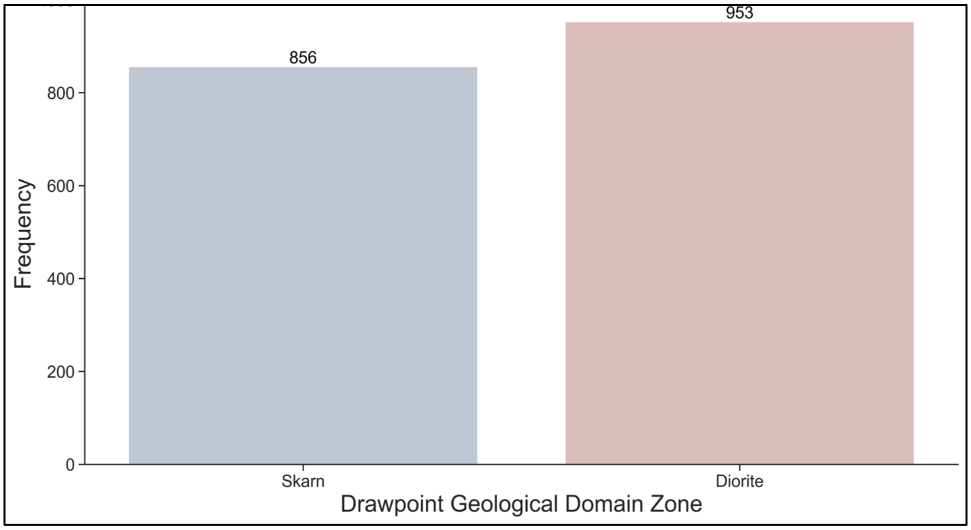

Figure 3.23. The DOZ mine spill frequency distribution in the skarn and diorite areas between January 2008 and June 2019.

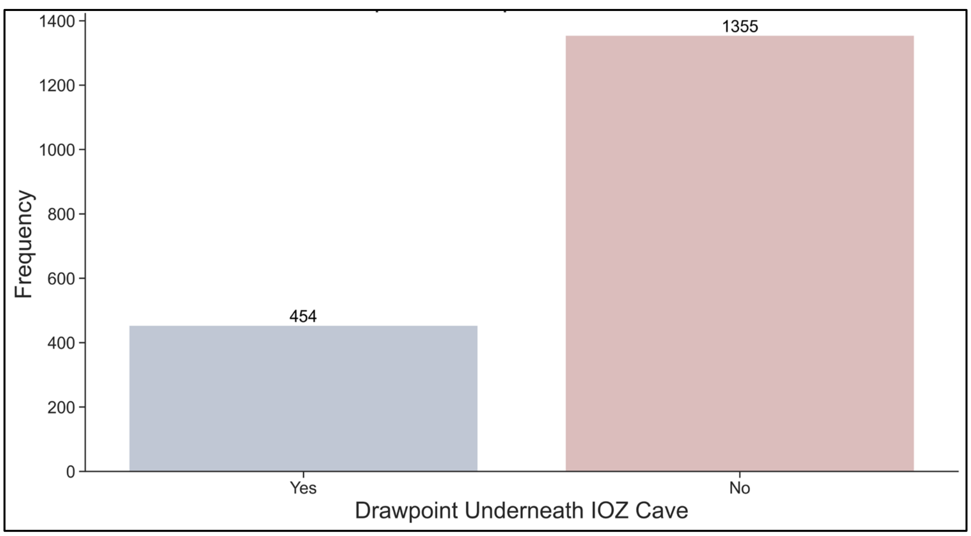

Figure 3.24. The DOZ mine spill frequency distribution for drawpoint location relative to the IOZ cave between January 2008 and June 2019.

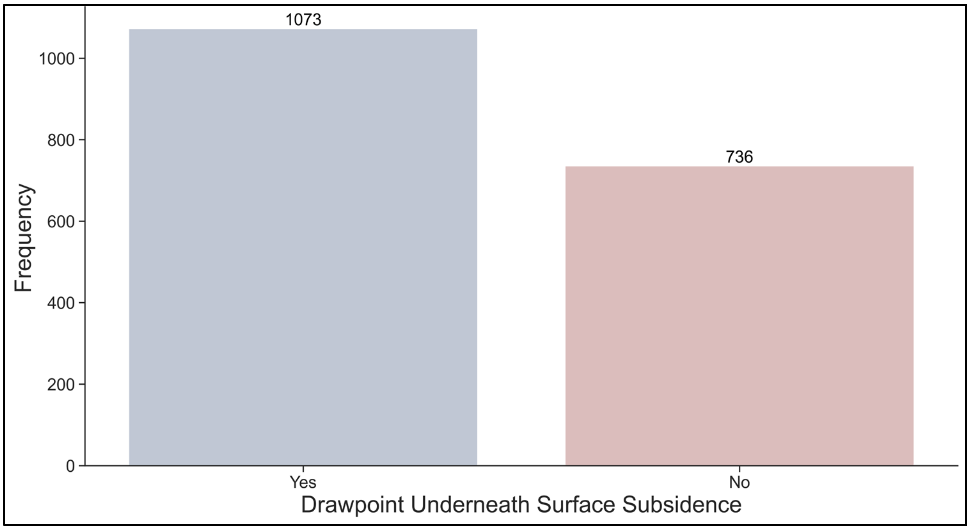

Figure 3.25. The DOZ mine spill frequency distribution for drawpoint location relative to the surface subsidence between January 2008 and June 2019.

3.4 Discussion

Exploratory data analysis has shown patterns in the hypothetical variables, which inform the consideration of the input variables for the logistic regression analysis in Chapter 4. A summary of key findings is included in this section.

The developed drawpoint classification at the DOZ mine was effective in predicting wet muck spill events, where the majority of spills originated from wet muck class drawpoints (mainly B3 and C3). However, B2 and C2 classifications were originally considered worse than the A3 classification, yet more spills actually originated from the A3 class. This can be caused when drawpoints were previously mapped as A3, but conditions change before they can be remapped prior to a spill. The adjacent drawpoint classification is also an important variable to be included in the statistical model. There have been numerous events where the spill drawpoint was classified as coarse material and moist/wet conditions, while the adjacent drawpoint was classified as a wet muck drawpoint, with finer-grained, lower permeability, and wetter material. Water from these low permeability drawpoints cannot drain properly from the drawpoint, which leads to the accumulation of water inside the drawbell. Once triggered, a spill can occur from a coarser drawpoint, with material originating from its adjacent water-saturated drawpoint.

Drawpoints designated as being wet muck have increased at a steady rate since late 2011, contributing to drawpoint closures. An uneven draw pattern was then largely unavoidable, allowing wet muck materials to migrate to actively drawn drawpoints, which increased the number of wet muck class drawpoints in the active mining area. Finer and saturated material forms a wet muck material resembling a clay-like texture, which has created challenges in material handling and processing. This required the DOZ operation to start dry-wet material mixing (with one wet bucket to 3-6 dry buckets, depending on the material wetness). To comply with this mixing protocol, production has resulted in an uneven draw that has further exacerbated the increase in the number of wet muck drawpoints. This condition is hypothesized to be one of the causative factors for spill susceptibility leading to a non-uniform draw.

Wet muck spills tend to occur when there is a high concentration of wet muck neighboring drawpoints in the vicinity. This also indicated that the area is highly saturated. It is hypothesized that the wet muck condition at the drawpoint has a similar condition above the drawbell, with material able to flow following the preferential path created by mucking activities following the mining direction.

Various cave draw strategies have been implemented at the DOZ mine since the beginning of the operation. The increase of wet muck spills has forced the operation to adapt to the wet muck condition. The EDA shows that spills occurred at various draw rates, which suggests that mucking activity acts as a triggering factor for wet muck spills. The majority of spills occurred when there were drawpoint mucking activities. Active mucking loosens the drawpoint toe material and can result in liquefaction due to pore pressure changes. However, there were no significant patterns identified between spill events and adjacent drawpoint mucking or consecutive mucking.

The operation has shown that increases of the HoD and extraction ratio have an upward trend alongside spill occurrences. Although the majority of the HoD ranges between 150 and 350 m at spill drawpoints, this corresponds with the limiting vertical distance between the DOZ mine and the overlying IOZ cave (approximately at 300 m). Breakthrough to the IOZ cave may have introduced additional fines and water trapped in the overlying caves. These wet muck materials can directly flow vertically to the DOZ drawpoints located within the IOZ footprint. However, there were insufficient data to identify migration patterns from IOZ to DOZ drawpoints. Therefore the potential correlation is not considered further in this research.

Although rainfall is one of the major sources of water entering the caved zone, it is difficult to calculate the percentage of rainwater entering the caved zone. Therefore, only water contents indicated by the numeric attributes of the drawpoint classification were used as the water input variable for the logistic regression analysis.

These findings were valuable in providing ideas for the downstream statistical analysis. However, it is important to note that the exploratory data analyses only considered variables in up to three-dimensions. Wet muck spills are a complex engineering challenge that requires a more sophisticated method to analyze the inter-relationships for each variable.

Chapter 4: Logistic Regression Analyses and Tool Development

4.1 Overview

This chapter provides a comprehensive description of the procedures and analyses carried out in the development of an empirical wet muck spill predictive tool. The susceptibility of a wet muck spill at a drawpoint on a daily basis can be posed as a binary classification problem represented as class 0 or class 1. In this study, class 0 refers to a drawpoint that has not experienced a wet muck spill (also referred to as 'negative' with respect to an event occurring; i.e., not occurring), while class 1 indicates a drawpoint that has experienced a spill (i.e., 'positive' with respect to an event occurring). Logistic regression analysis is appropriate to use for these problems since their objective is to predict the probability of a binary outcome based on several explanatory variables (causative and triggering factors, covariates, independent variables) that can be either continuous or categorical. In addition, logistic regression results are easier to interpret, straightforward to develop and improve, and able to identify patterns in a large dataset. Interpretation of each independent variable and their coefficient can be directly utilized to determine important variables along with the magnitude and direction of association between independent and dependent variables (Höppner et al., 2021).

The susceptibility model for wet muck spills at the DOZ was developed using the Python programming language. The MLR module in the machine learning software uses sklearn, which is available from the Python library (Scikit Learn, 2021c). The selection of the explanatory variables was based on the hypothetical variables summarized in Appendix C, where each variable was first tested through ULR before being selected for the MLR probabilistic model. The initial study database was divided into training and testing datasets, with consideration given to the temporal nature of the data. The models were assessed using a confusion matrix (classification or contingency table) and precision-recall scores. Model parameters were fit to the data using a cross-validation package from sklearn, and balancing of the dataset was carried out using oversampling or by adjusting the class weight of the binary outcome. The illustration of the MLR concept in this study is illustrated in Figure 4.1. A comprehensive description of the process used to develop the empirical wet muck predictive tool is provided in the sub-sections below.

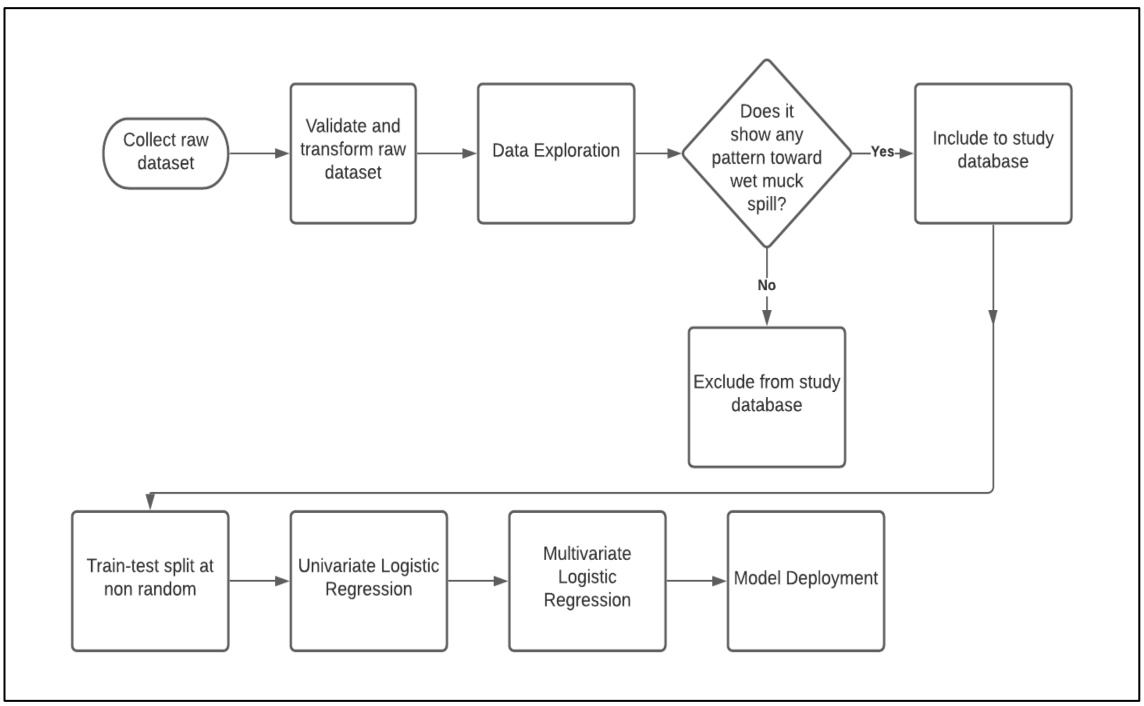

Figure 4.1. Adopting the multivariate logistic regression concept for wet muck spill susceptibility analysis.

4.2 Data Sampling

4.2.1 Training-Testing Data Split

Logistic regression is a supervised machine learning technique that requires two sets of data: a training set and a testing set (Kuhn & Johnson, 2013; Pawluszek-Filipiak & Borkowski, 2020). The training set is used for the learning process and estimates the relationships between the seen input and output data, while the testing set evaluates the relationships derived by measuring the success of the predictions using unseen data (Liu & Wu, 2012). Both are derived from the same database, with the training set split being larger to achieve a higher classifier performance. During the learning process, the training dataset is further divided to split off a small validation dataset, which is used to optimize the input parameters for the logistic regression. This process is called hyper-parameter tuning.

Since the wet muck spill database has a temporal nature, the train-test datasets must be divided based on the same time periods instead of being random. This approach provides an unbiased classifier result. The train-validation dataset was processed using the *TimeSeriesSplit* function from Python sklearn library (Scikit Learn, 2021d), which divides the dataset into defined iterations, referred to as folds, for validation (Figure 4.2).

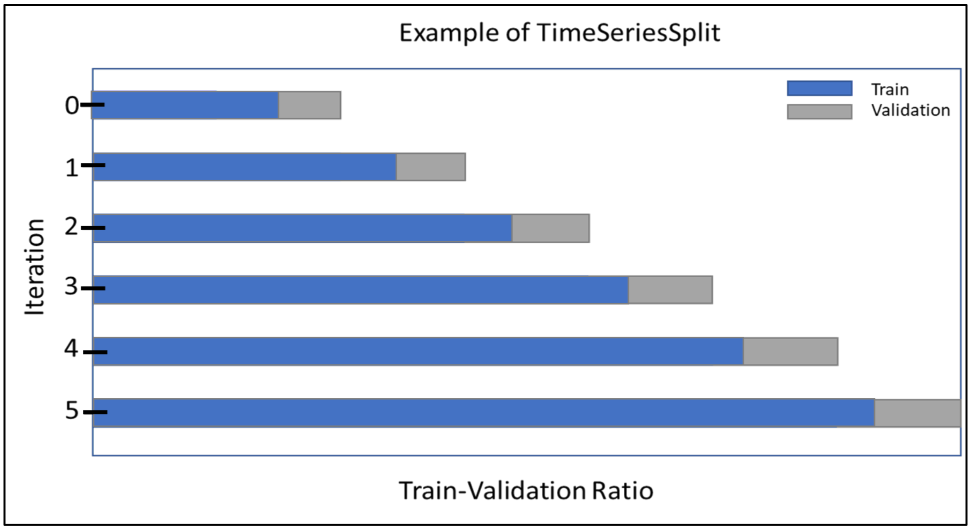

Figure 4.2.TimeSeriesSplit example with 5 iteration at 86% : 14% train-test split.

The training dataset consists of 1033 spill events from 2,074,145 observations between January 2008 and December 2017. This comprises approximately 86% of the overall study database. The testing dataset samples the subsequent period from January 2018 to June 2019 and contains 776 spill events from 325,171 observations (approximately 14% of the study database). For the training split, the validation set was processed using five iterations/folds, with the size of the validation set being kept constant for each iteration based on an 86% to 14% split between the training and validation sets. Using a longer period for the training dataset (extending beyond December 2017) did not have a significant influence on the model results. Therefore, the training dataset for the stated period was considered to have sufficient data for downstream correlation processes.

4.2.2 Imbalanced Dataset

Although wet muck spills are a relatively frequent occurrence, they did not occur on a daily basis. For instance, only one spill occurred for every 385 observations in 2018. In total, there were 1809 spills (minority class) and 2,399,316 no-spills (majority class) over the 11.5 years of operational history covered by the database. This is considered to be an imbalanced dataset, where the proportion of occurring (positive) spill events is very low compared to the proportion of non-occurring (negative) no-spill events. The main challenges with an imbalanced dataset are poor model performance and a tendency for the results tend to be biased toward the majority class (Akosa, 2017; Jeni et al., 2013; Spelmen & Porkodi, 2018)

There are two ways to address the issue of an imbalanced dataset: by assigning cost or weight to both the minority and majority classes, or by resampling the data using undersampling or oversampling (Akosa, 2017; Chawla et al., 2002). For the first approach, a cost-sensitive algorithm was used to assign different costs or penalties, where higher cost is assigned to misclassification of the minority class (false negatives) than misclassification of the majority class (false positives). Consequently, the training model is biased towards the minority class, thereby affecting the model parameters and performance (Akosa, 2017). In this study, the class weight is set to balance the minority class weight, which is calculated using Equation 4.1, where w_i is the minority class weight, n is the number of observations, k is the total number of classes, and n_i is the number of observations in the minority class (King & Zeng, 2001).

Equation 4.1. Minority class weight

$$w_i = \frac{n}{k \cdot n_i}$$

The logistic regression analysis using the sklearn package provides class weight specified as a model hyper parameter. A *class_weight* function is a dictionary that defines each class label (0 and 1) and weight to be applied in the calculation of negative log-likelihood when fitting the model. Although it is possible to search for a variation of weight for 0 and 1, it is recommended to keep the class weight as balanced as possible (King & Zeng, 2001). The best practice is to use the class weight that is the inverse of the class distribution proportional to their respective frequency present in the dataset (King & Zeng, 2001). A "balanced" class weight provides a higher cost to the minority class by increasing the weight so that it has a higher penalty of misclassification and, at the same time, reduces the weight of the majority class. Therefore, the algorithm error can be reduced when predicting the minority class. The open-source imbalanced learn library Imblearn (Imbalanced Learn, 2021) was used for both under- and over-sampling, where the dataset is set to have equal distribution for class 0 and class 1.

The use of undersampling aims to balance the class distribution with roughly equal classes through the reduction or elimination of majority classes (Kotsiantis et al., 2006). However, undersampling can discard important data, specifically in severely imbalanced cases. The *NearMiss* and *Condensed Nearest Neighbor* algorithms in Imblearn were trialed to balance the dataset, but resulted in poor performance in the logistic regression stage. More than 2 million observations were removed, which left the model unable to differentiate between spill and no-spill. Given that one of the objectives of this study is to understand the causative and triggering factors associated with wet muck spills, removing any real data from the study database is not recommended.

The use of oversampling methods creates extra training data from the minority class at a set percentage depending on the imbalanced ratio. For this, the Synthetic Minority OverSampling (SMOTE) technique can be utilized and has proven to be successful at the ULR stage. It aims to balance the class distribution by oversampling the minority class through the generation of synthetic data along with the feature space within the k-nearest neighbors (Chawla et al., 2002; Fernández et al., 2018). Depending upon the amount of oversampling required, neighbors from the k nearest neighbors are randomly chosen. Further discussion on the SMOTE oversampling technique can be found in Chawla et al. (2002).

The application of SMOTE is only applicable when the dataset is nominal. Therefore SMOTE-NC (Synthetic Minority Oversampling Technique - Nominal Continuous) was used instead to oversample both nominal and categorical attributes from the minority data. The categorical dataset was oversampled following the feature space of the nominal dataset applying similar principles from SMOTE.

4.3 Logistic Regression Analysis

4.3.1 Overview

Logistic regression analyses are discussed in detail by Hosmer et al. (2013) and King & Zeng (2001) with respect to cost-sensitive methods. Predicting the presence or absence of a wet muck spill constitutes a classification problem where the outcome is binary encoded, with presence indicated by a value of 1 and absence indicated by a value of 0. Linear regression cannot be utilized to model wet muck susceptibility in this binary context, since it requires a continuous response variable. Instead, logistic regression is appropriate for binary response problems with multiple explanatory variables.

Logistic regression (logistic or logit model) is a regression technique that analyzes the relationship between one or more independent variables and a binary or dichotomous outcome, and estimates the probability of occurrence by fitting the data with a logistic curve (Park, 2013). Similar to the fitted line in a linear regression model, the logit link function or logistic transformation (Equation 4.2) is used to calculate the probability (P) of the binary outcome (Y) by taking the natural logarithm of the odds of the event relative to one or more explanatory variables (x); the odds being the ratio of the probability of an event occurring to the probability of an event not occurring. Using only one variable (univariate), the continuous linear model ($\beta_0 + \beta x$) can be applied in logistic regression, where the binary outcome is the sum of the intercept (β_0) and slope or coefficient of a variable (β) multiplied by the value of variable x. Therefore, the probability of an event occurring ($P|Y = 1$) can be calculated by taking an inverse of Equation 4.3. Since the wet muck susceptibility model requires a MLR analysis, the logit link function can be extended into Equation 4.4; hence the probability of a wet muck spill occurring can be extended into Equation 4.5.

Equation 4.2. Univariate logit link function

$$logit\ (Y) = \ln(\frac{P}{1-P}) = \beta_0 + \beta_X$$

Equation 4.3. Univariate Logistic regression

$$P(Y=1) = \frac{e^{\beta_0+\beta_1 x_1}}{1+e^{\beta_0+\beta_1 x_1}}$$

Equation 4.4. Multivariate logit link function

$$logit\ (Y) = \ln(\frac{p}{1-p}) = \beta_0 + \beta_1 x_1 + \beta_2 x_2 + \cdots + \beta_n x_n$$

Equation 4.5. Multivariate Logistic regression

$$P(Y=1) = \frac{e^{\beta_0+\beta_1 x_1+\beta_2 x_2+\cdots+\beta_n x_n}}{1+e^{\beta_0+\beta_1 x_1+\beta_2 x_2+\cdots+\beta_n x_n}}$$

The coefficient of logistic regression is associated with the change in logit corresponding to the change of value in the explanatory variable. For example, increasing an explanatory variable value of 1 multiplies the odds of having the outcome by e^{β}. A coefficient can be either positive or negative, where a positive coefficient reflects a higher probability of an event occurring and a negative coefficient reflects a lower probability of an event occurring. The significance of the logistic regression coefficient is represented by its magnitude; the further from zero, the more significant the variable is. The explanatory variable can either be categorical, continuous, or ordinal. A continuous variable coefficient represents the relative increase or decrease of the odds as the variable moves away from the mean by one standard deviation. It is scaled relative to the mean and standard deviation used in the training dataset. A coefficient for an ordinal variable represents the relative increase or decrease of the odds as the variable increases or decreases one order. A coefficient for a categorical variable uses one member of the category as a reference level.

The ULR started by analyzing the 177 explanatory variables developed in the study database. Each of the explanatory variables is analyzed individually with the occurrence of a wet muck spill to identify its relationship. Any non-significant variables, indicated by poor performance metrics (low precision, low recall, and high false positives and false negatives), were not included in the downstream process. When two or more variables were derived from one primary dataset, only one variable was selected for the MLR to avoid multi-collinearity. For example, HoD is the column height of a drawpoint with respect to the equivalent volume mined from the drawpoint, and the extraction ratio is the percentage of the extracted column over the planned column height. These two variables are directly related and therefore follow the same trends. Accordingly, the ULR shows both HoD and extraction ratio as being statistically significant. At the multivariate stage, HoD and extraction ratio were tested individually with other significant variables to identify which variable was more significant than the other. If both resulted in similar model performance, the selection was based on which variable is easier for the operation to monitor and control in the future. This approach was also applied to temporal variables that were derived from one primary dataset, where only one temporal period that had the highest performance was selected for downstream processes.

The MLR approach is similar to the ULR, but with more than one independent variable included at this stage. Each of the explanatory variables was sequentially added, starting from a ULR model. The objective of using a MLR is to estimate the variable coefficient, its significance, and interrelationship with other variables. The inclusion or exclusion of an explanatory variable in the MLR model was determined through the model performance metrics. If the model performance was improved with the addition of the variable compared to its exclusion, it was considered to be significant and was included in the MLR (Hosmer et al., 2013).

To achieve an optimum outcome, the logistic regression requires the model to be fitted correctly (not under- or over-fitted) and little to no multicollinearity between independent variables. Although multicollinearity will not affect the model prediction capability, it will result in difficulty in identifying and interpreting significant variables, unstable coefficients, and overfitting (Shrestha, 2020). The Pearson correlation coefficient was plotted to show the collinearity between independent variables at the MLR stage. Several studies on the Pearson correlation coefficient cut-off are summarized in Schober & Schwarte (2018), who classified the correlation strength category based on the correlation coefficient (Table 4.1). Depending on the dataset, it is recommended to use the variable when the correlation coefficient is less than 0.7 (Dormann et al., 2012)

Table 4.1. Pearson correlation matrix

Correlation Coefficient	Indication
0 - 0.1	Very weak correlation
0.1 - 0.39	Weak correlation
0.4 - 0.69	Moderate correlation
0.7 - 0.89	Strong correlation
0.9 - 1	Very strong correlation

Overfitting means the model has a very high complexity, but with large errors, unstable prediction, and unrealistic coefficients (Hosmer et al., 2013). This is shown when the training set score is higher than the test set score, and the model performs well at the training stage but poorly against realistic data (e.g., the test set). Underfitting is the opposite of overfitting, where the model has low complexity with no meaningful variables identified (Bilmes, 2020). This is shown by a high error rate on both the training and testing data. A model is optimum when it has a low training and a low testing error, or similar training to testing scores (Mani et al., 2019). The sklearn program provides model optimization through regularization to avoid overfitting (Scikit Learn, 2021c). Regularization reduces the insignificant coefficients close to zero, hence reducing the variance in the model. Cross-validation is conducted to find the best inverse of the regularization strength (C) and then select the C value that satisfies the optimum model.

4.3.2 Performance Metrics

A binary classifier labels the samples as either a positive occurrence (spill) or a negative occurrence (no-spill). Results from the classifier can be represented in a confusion matrix, also known as an error matrix or contingency table. The confusion matrix (Table 4.2) was used to measure the classifier performance, which represents the counts of actual and predicted values from the test dataset (Kuhn & Johnson, 2013). The confusion matrix consists of:

- True Positives (TP) – Model correctly predicts a positive outcome.
- False Positives (FP) – Model incorrectly predicts a positive outcome.
- True Negatives (TN) – Model correctly predicts a negative outcome.
- False Negatives (FN) – Model incorrectly predicts a negative outcome.

Table 4.2. A 2 × 2 Confusion Matrix

Positive = 1	Actual Negative (y = 0)	Actual Positive (y = 1)
Predicted Negative (c = 0)	True Negative (TN)	False Positive (FP) Error Type 1
Predicted Positive (c = 1)	False Negative (FN) Error Type 2	True Positive (TP)

Various performance metrics exist, but there are no perfect metrics. Appropriate metrics need to be chosen according to the data, classification context, and objectives (Labatut & Cherifi, 2011). This study uses several common performance metrics for model evaluation, including accuracy, precision, recall, and the AUC-ROC curve (area under the receiver operator characteristic curve). The equations for these metrics are summarized below, as reported in Kulkarni et al. (2020). Accuracy measures the proportion of true instances from both positive and negative model outcomes (Equation 4.6) and is commonly used as a performance metric for machine learning. Precision measures the ratio of correct positive predictions made over all positive predictions

(Equation 4.7). Recall (also Sensitivity or True Positive Rate) measures the strength of a model to predict positive outcomes (Equation 4.8). The F1-score measures the weighted harmonic mean between the precision and recall outcomes (Equation 4.9). The receiver operator characteristic (ROC) curve evaluates the performance of the classifier by plotting the false positive rate (FPR) (Equation 4.10) on the x axis and the true positive rate (TPR) on the y axis. The Area Under the Curve (AUC) is calculated with a range from 0 to 1, with an ideal result having a value of 1 with the ROC curve located in the upper left corner. An AUC-ROC score below 0.5 represents a model that is performing poorer than random guessing, which is not desirable from a binary classifier model.

Equation 4.6. Accuracy Formula

$$Accuracy = \frac{True\ Positive + True\ Negative}{True\ Positive\ + True\ Negative + False\ Positive + False\ Negative}$$

Equation 4.7. Precision Formula

$$Precision = \frac{True\ Positive}{True\ Positive\ + False\ Positive}$$

Equation 4.8. Recall Formula

$$Recall = \frac{True\ Positive}{True\ Positive\ + False\ Negative}$$

Equation 4.9. F1-Score Formula

$$F1 - Score = 2\ \times \frac{Precision\ \times Recall}{Precision\ + Recall}$$

Equation 4.10. False Positive Rate Formula

$$False\ Positive\ Rate = \frac{False\ Positive}{False\ Positive\ + True\ Negative}$$

Several studies (Chawla, 2009; Fernández et al., 2019; He & Garcia, 2009; Juba & Le, 2019) have suggested that precision and recall are more appropriate for evaluating model performance when dealing with an imbalanced dataset. Accuracy is often misleading in imbalanced analyses because it assumes an equal weight between positive and negative classes and is more sensitive to detecting the majority class. In addition, accuracy treats all error costs equally, which is not applicable in imbalanced dataset analysis. A model can have high accuracy but still predict model outcomes comparable to a random guess or worse. Furthermore, although ROC-AUC curves are commonly used in binary classifier analysis, they cannot represent the true performance in an imbalanced dataset. Since the wet muck model tolerates high false positives, this will not affect the FPR in the AUC-ROC calculation. Therefore, the selection of variables in the wet muck spill susceptibility analysis was ultimately based on the precision, recall, and confusion matrix results. The spill threshold for the confusion matrix is set at 0.5, where a probability below 0.5 indicates a no-spill potential and a probability above 0.5 indicates a spill potential.

4.3.3 Precision vs. Recall Score Selection

Ideally, it is preferable to have a model with high precision and recall. However, the trade-off between precision and recall importance needs to be considered based on the misclassification cost during model parameter tuning for optimization purposes. If the model tolerates a high false positive, then recall is prioritized over precision and vice versa. A model with high recall – low precision provides a good overall positive prediction but includes many incorrect negative outcomes (False Positives). For example, a drawpoint may be classified as being susceptible to wet muck spills, and if most of the contributing conditions are met but a spill does not occur on any given day, this results in a high number of false alarms. However, if a spill occurs, the drawpoint is most likely to be classified as wet muck spill susceptible. On the contrary, a model with high precision – low recall provides a higher number of correct positive predictions for a given period but poor overall positive prediction (FN). For example, a drawpoint is only classified as spill susceptible if certain conditions are met that result in a spill. However, a spill can also occur at a drawpoint that is not classified as being wet muck spill susceptible.

The essence of the misclassification cost in this study considers that, even when a wet muck spill might not occur at a high spill-susceptible drawpoint, the operation can minimize operational, economic, and safety risks by classifying a drawpoint as spill susceptible when all factors are present. Wet muck spills have a severe impact that can lead to fatalities, operational delays, and economic losses, which require an early detection tool. In this context, it is more important to alert the operator of a potential wet muck spill rather than predict exactly when and where it will happen. Since a high number of false negatives are less tolerable, the model prioritizes a high recall score. Furthermore, the imbalanced database has a very low spill observation rate. Any hypothesized causative and triggering factors of wet muck spills can be present, but with the result of no-spill, which provides a high false-positive rate even if the model is set to achieve high precision. Historically, the DOZ has been operating under a high rate of false positives, with various mitigation strategies for wet muck spills enacted. Therefore, a low precision is acceptable for this study.

4.4 Logistic Regression Results

4.4.1 Univariate Logistic Regression

A total of 177 variables were initially assessed individually against the DOZ historical wet muck spill occurrences using the ULR analysis. Statistically significant variables were selected based on the performance metrics (precision and recall via the confusion matrix) and their capability to predict spill and no-spill conditions. All of the variables tested had a very low precision score, between 0 and 0.03, while the recall scores varied between 0.34 and 1. Although it is important for the model to precisely predict future wet muck spills, from a hazard and safety perspective, it is more important for the model to alert the operation to all potential wet muck spills, with the trade-off of a high number of false alarms. A missed prediction of a wet muck spill can result in fatalities, but a false alarm simply alerts the operation to a drawpoint condition that is susceptible to a spill. Therefore, the recall score and confusion matrix were prioritized for this initial stage of variable selection. In addition, selected variables for the MLR cannot have a similar nature in the data to avoid multicollinearity. From each spatial and temporal manipulated dataset, only one variable can be selected based on its confusion matrix results.

Detailed results, including the variable coefficient and performance metrics from the ULR variable selection, are tabulated in Appendix C. The following points highlight the findings from the ULR and are summarized at the end of this section in Table 4.3:

1. Both extraction ratio and HoD provided similar results (Figure 4.3), as did their corresponding values for the adjacent drawpoints (e.g., adjacent extraction ratio). Since the extraction ratio is a function of the height of the draw, only one of these variables should

be selected for the final prediction model. However, both were further tested separately in the MLR stage to help with this selection. Differential HoD did not perform as strongly, while and differential extraction ratio showed a negative correlation. These variables were therefore not tested further.

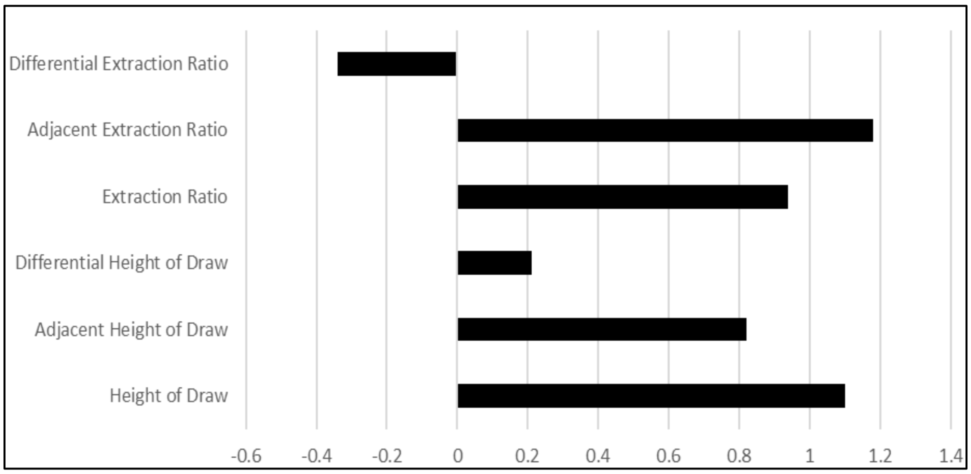

Figure 4.3. Univariate logistic regression coefficients for draw column variables.

2. Drawpoint class showed a strong correlation with wet muck spills, where wet muck drawpoints have a high positive coefficient and non-wet muck drawpoints have a high negative coefficient (Figure 4.4). Drawpoint class is, therefore, one of the significant variables that was carried forward to the MLR stage.

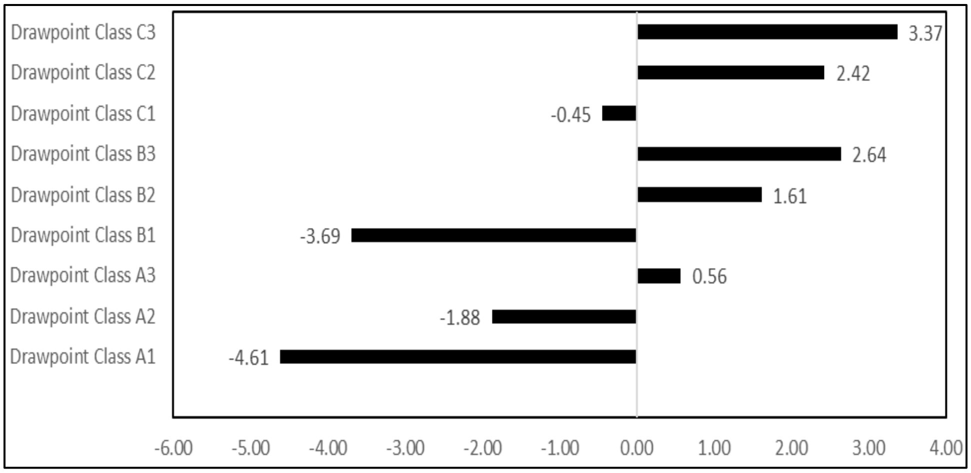

Figure 4.4. Univariate logistic regression coefficients for drawpoint classification variables.

3. Similar to the drawpoint class, the adjacent drawpoint class showed a strong positive correlation to wet muck spills, with high positive coefficients except for adjacent drawpoint classes A1 and B1 (Figure 4.5). Adjacent drawpoint class is therefore one of the significant variables that was included at the MLR stage.

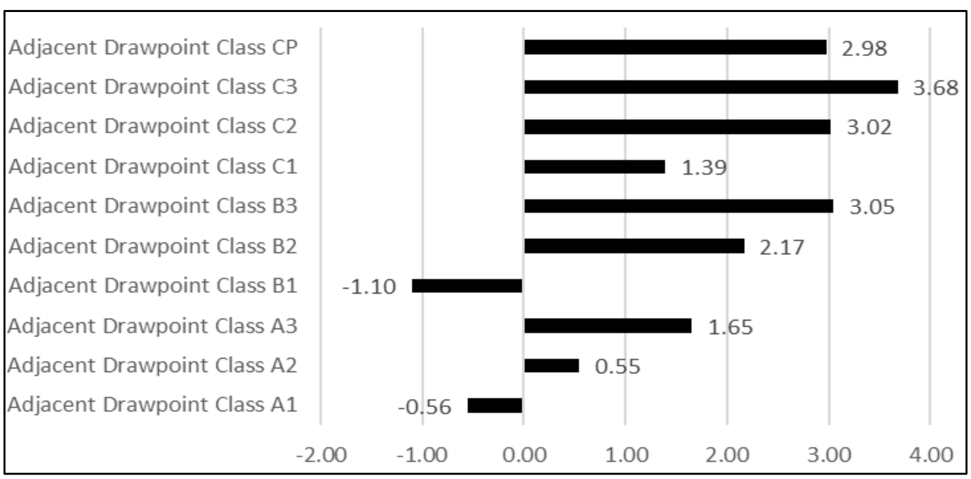

Figure 4.5. Univariate logistic regression coefficients for adjacent drawpoint classification variables.

4. Wet muck neighboring drawpoint at any radius showed similar performance, with a positive correlation to wet muck spills (Figure 4.6) and high true positives. However, no spatially manipulated variables were able to predict no-spill events effectively, resulting in high false positive numbers.

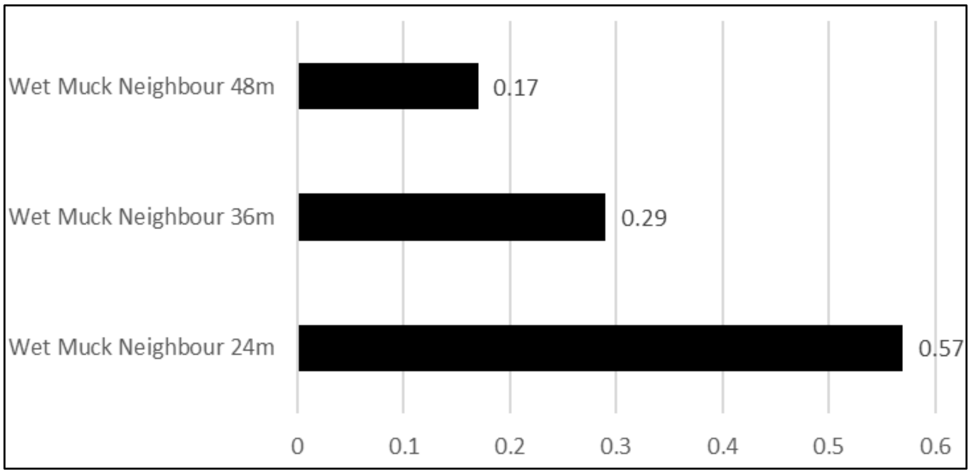

Figure 4.6. Univariate logistic regression coefficients for the total number of wet muck neighboring drawpoint variables.

5. Tonnage variables showed a positive correlation (Figure 4.7) with high recall scores, true positives, and true negatives. Comparing adjacent drawpoint tonnages, all variables showed negative correlations to wet muck spills (Figure 4.8), as the model cannot predict no-spill events effectively. Differential tonnage variables at any temporally manipulated period showed a positive correlation, with similar trends observed in drawpoint tonnage variables (Figure 4.9). However, performance metrics for the differential tonnage variables were poorer than those for drawpoint tonnage. Therefore, drawpoint tonnage datasets with periods between 7 and 28 days were tested at the MLR stage.

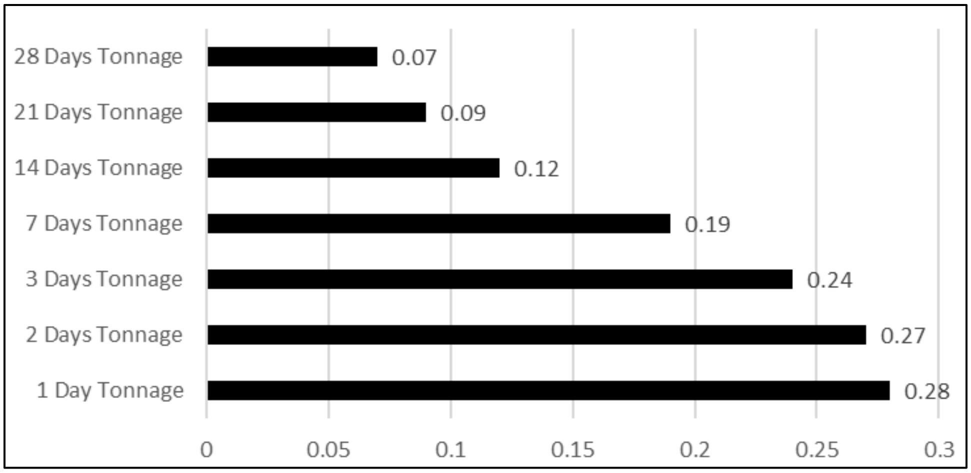

Figure 4.7. Univariate logistic regression coefficients for drawpoint tonnage variables.

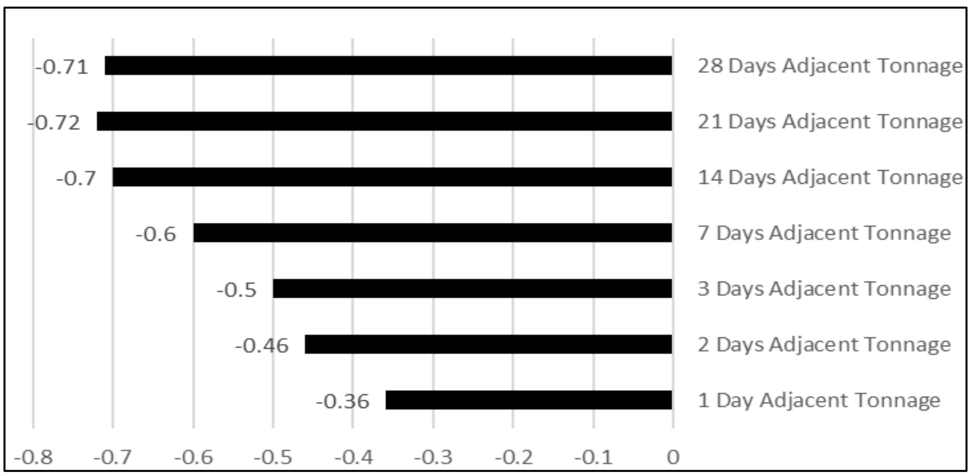

Figure 4.8. Univariate logistic regression coefficients for adjacent drawpoint tonnage variables.

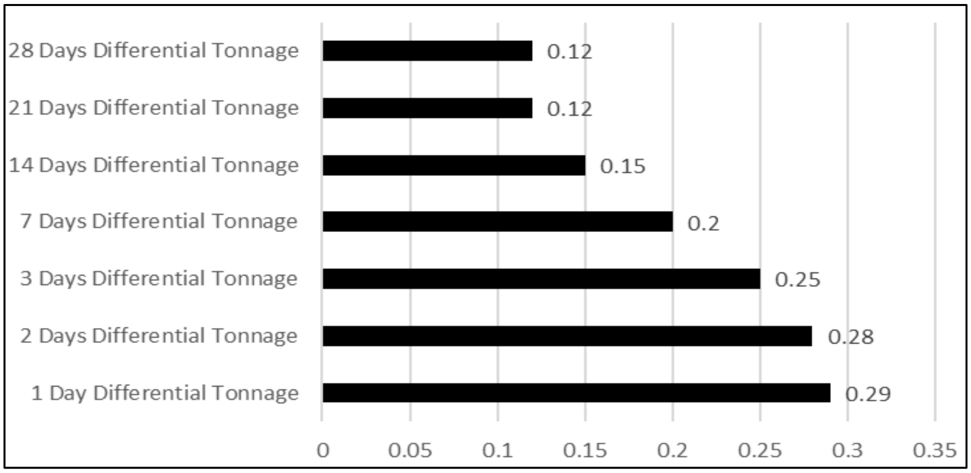

Figure 4.9. Univariate logistic regression coefficients for drawpoint differential tonnage variables.

6. The UI, SPUI, and the number of inactive drawpoints were tested at various radii of influence. The number of inactive drawpoints at any radius and the corresponding period did not show a correlation with spills (Appendix C) and therefore were not considered for downstream analysis. The MLR analysis considered a 2-to-7-day range. Although showing a higher positive correlation, it is not operationally feasible to control uniform draw within a short time period at a radius of influence of 24 m, 36 m, or 48 m, since every drawpoint is then associated with a different number of surrounding drawpoints. Therefore, only the 5 and 7 nearest drawpoints were considered for the MLR stage, as it showed a positive correlation (Figure 4.10 and Figure 4.11). Since the UI considers both SPUI and the number of inactive drawpoints, only UI was selected as one of the controllable variables for downstream analysis.

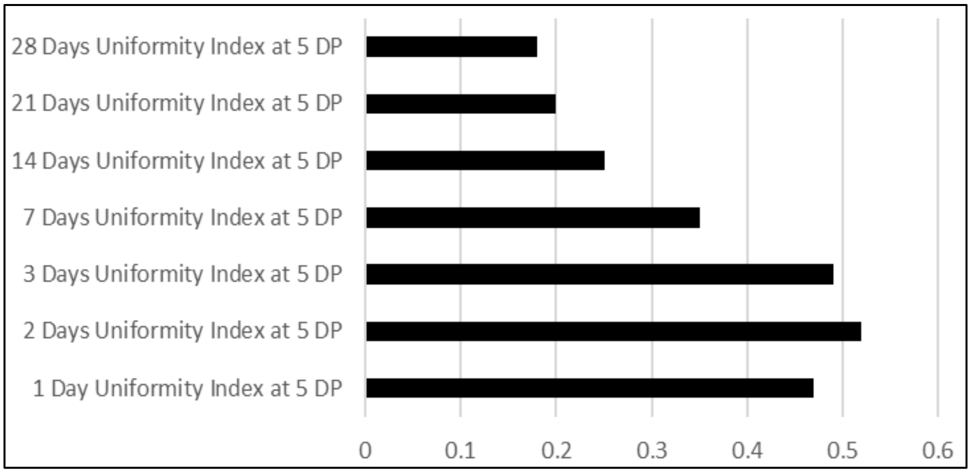

Figure 4.10. Univariate logistic regression coefficients for Uniformity Index within five nearest drawpoint variables.

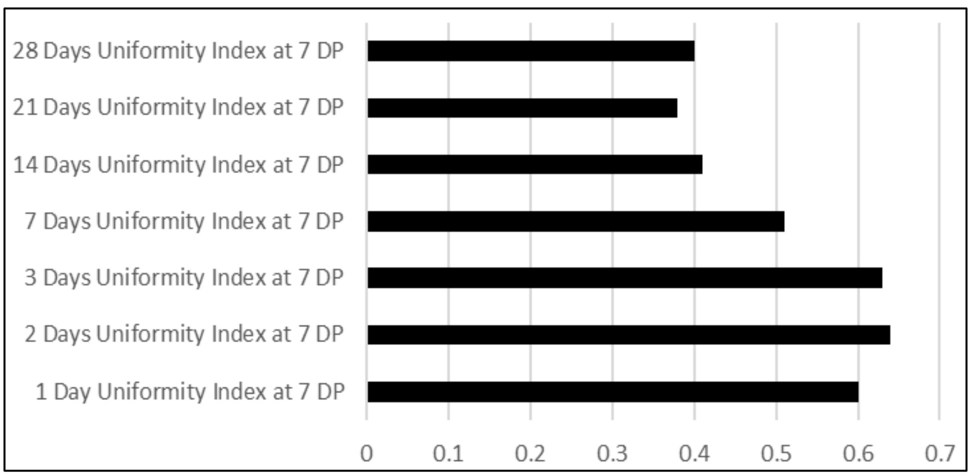

Figure 4.11. Univariate logistic regression coefficients for Uniformity Index within seven nearest drawpoint variables.

7. All mucking variables showed strong positive correlations to wet muck spills (Figure 4.12), with longer periods resulting in higher true positives but lower true negatives. With regard to adjacent drawpoint mucking activities, the ULR showed negative correlations to all adjacent mucking variables (Figure 4.13), with shorter periods resulting in higher true

positives but lower true negatives. Since there is a significant difference in the confusion matrix between 3 and 7 days and a minimal difference between 21 and 28 days (Appendix C1), the drawpoint mucking and adjacent drawpoint mucking variables between 7 and 21 days were tested to identify the optimum period. To be consistent, both the period for drawpoint and adjacent drawpoint mucking needs to be the same (i.e., seven days drawpoint mucking and seven days adjacent drawpoint mucking) when brought into the MLR model. Furthermore, only two days of consecutive mucking showed a positive correlation (Figure 4.14), with high true negatives compared to the other consecutive mucking periods.

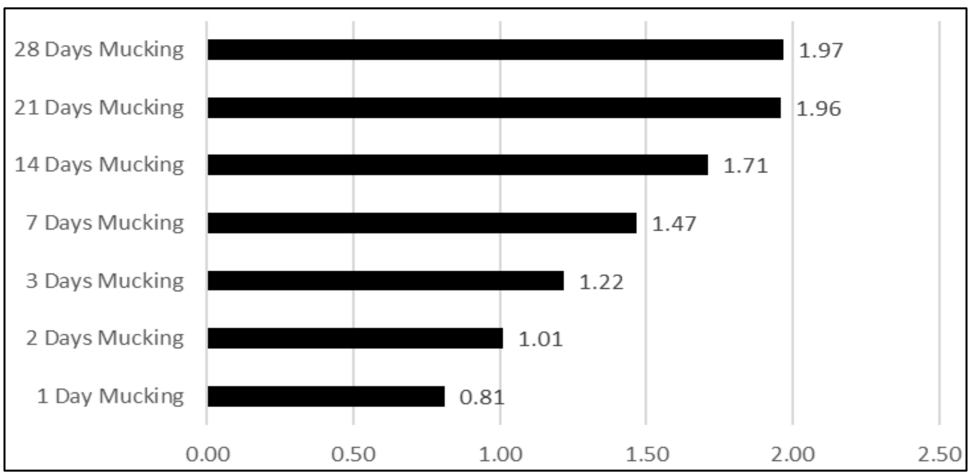

Figure 4.12. Univariate logistic regression coefficients for drawpoint mucking variables.

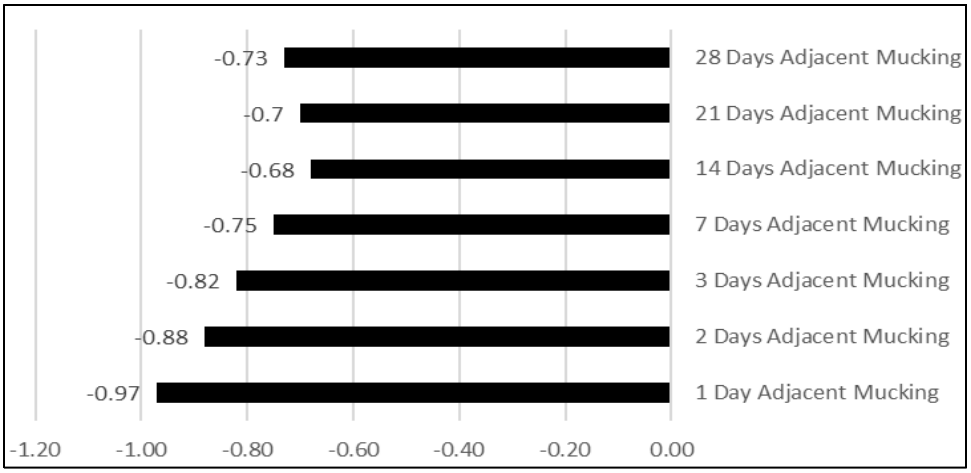

Figure 4.13. Univariate logistic regression coefficients for adjacent drawpoint mucking variables.

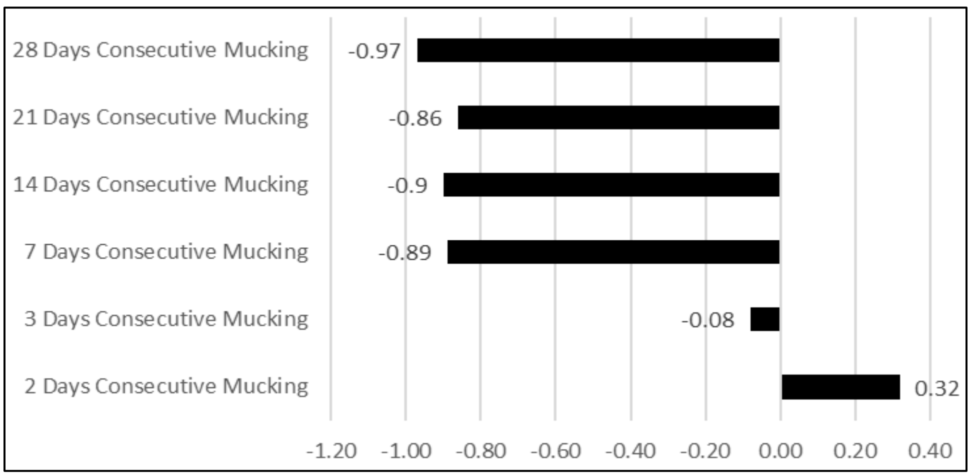

Figure 4.14. Univariate logistic regression coefficients for drawpoint consecutive mucking variables.

Table 4.3. Summary of the univariate logistic regression results

No	Variable	Coefficient	Precision	Recall	True Positive	True Negative	False Positive	False Negative
1	Height of Draw	1.1	0	0.44	345	227,049	97,346	431
2	Adjacent Height of Draw	0.82	0	0.43	330	212,105	112,290	446
3	Differential Height of Draw	0.21	0	0.45	349	190,568	133,827	427
4	Extraction Ratio	0.94	0	0.44	338	194,754	129,641	438
5	Adjacent Extraction Ratio	1.18	0	0.47	414	196,456	127,939	414
6	Differential Extraction Ratio	-0.34	0	0.46	354	195,861	128,534	422
7	Drawpoint Class	Varies	0	0.97	752	127,062	197,333	24
8	Adjacent Drawpoint Class	Varies	0	0.87	678	109,397	214,998	98
9	Wet Muck Neighbour 24m	0.57	0	0.94	732	83,699	240,696	44
10	Wet Muck Neighbour 36m	0.29	0	0.91	706	89,020	235,375	70
11	Wet Muck Neighbour 48m	0.17	0	0.9	701	86,494	237,901	75
12	7 Days Tonnage	0.19	0.01	0.73	567	278,619	45,776	209
13	14 Days Tonnage	0.12	0.01	0.78	605	271,231	53,164	171
14	21 Days Tonnage	0.09	0.01	0.78	609	267,192	57,203	167
15	28 Days Tonnage	0.07	0.01	0.79	610	264,472	59,923	166
16	2 Days UI at 5 DP	0.52	0	0.73	570	196,846	127,549	206
17	3 Days UI at 5 DP	0.49	0	0.72	556	186,688	137,707	220
18	7 Days UI at 5 DP	0.35	0	0.67	517	173,602	150,793	259
19	2 Days UI at 7 DP	0.64	0	0.76	587	182,591	141,804	189
20	3 Days UI at 7 DP	0.63	0	0.74	573	171,747	152,648	203
21	7 Days UI at 7 DP	0.51	0	0.66	511	156,465	167,930	265
22	3 Days Mucking	1.22	0.01	0.88	682	234,754	89,641	94
23	7 Days Mucking	1.465	0.005	0.93	720	199,924	124,472	56
24	14 Days Mucking	1.71	0	0.98	758	165,093	159,302	18
25	7 Days Adjacent Mucking	-0.75	0	0.58	449	103,319	221,077	327
26	14 Days Adjacent Mucking	-0.68	0	0.49	381	130,563	193,832	395
27	21 Days Adjacent Mucking	-0.7	0	0.44	339	147,560	176,835	437

4.4.2 Multivariate Logistic Regression

Since the DOZ mine has been using drawpoint classification to indicate the drawpoint wet muck susceptibility condition, the MLR reveals the susceptibility model improvement from a one-dimensional matrix into multi-dimensional matrices. A decision framework for variable addition or exclusion at this stage is illustrated in Figure 4.15. Each of the significant explanatory variables identified in Section 4.4.1 was gradually added into the MLR model, starting with the drawpoint classification.

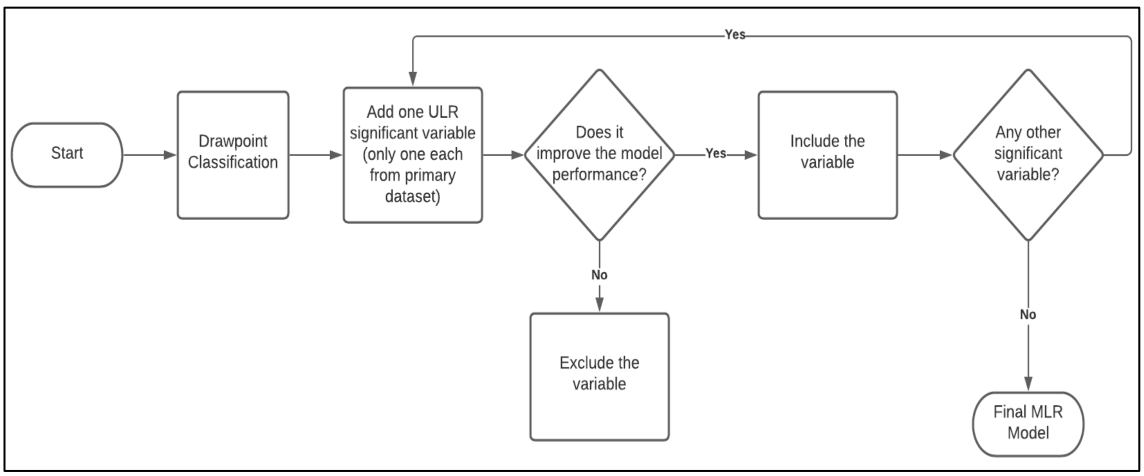

Figure 4.15. Variable inclusion/exclusion flow chart in the multivariate logistic regression process.

Multiple models were developed to compare other significant variables (i.e., HoD vs. extraction ratio) to identify the optimum variable inclusion for the MLR analysis (Table 4.4). The following points summarize the model comparisons and the selection of optimum variables.

1. **Height of draw and adjacent height of draw:** In order to be consistent, Model 1 was developed using HoD and adjacent HoD, while Model 2 was developed using extraction ratio and adjacent extraction ratio. Comparison of these two models showed that HoD and extraction ratio produced similar results. Model 1 had a higher true positive, while Model 2 had a higher true negative. Since it is more important to alert the operation to wet muck spill events, HoD and adjacent HoD were selected as the more appropriate draw column variables. These datasets can also be easily obtained by caving operations on a monthly basis.
2. **Total number of wet muck drawpoint neighbors:** Sensitivity analyses between 24 m (Model 3), 36 m (Model 4), and 48 m (Model 5) were carried out to identify the optimum radius of influence for predicting a wet muck spill. Each of these models had a similar performance with high recall and low precision. However, Model 4 had the highest true positives compared to the other models, and hence 36 m was selected for the optimum radius of wet muck drawpoint neighbors.
3. **Drawpoint and Adjacent Mucking Activity:** The period for drawpoint mucking and adjacent drawpoint mucking activity needed to be the same for consistency, where Model 6 considers seven days, Model 7 considers 14 days, and Model 8 considers 21 days. Models 6 and 7 performed similarly, while Model 8 performed poorly. With Model 7 having the highest true positives, the 14 day period was included in the final MLR model. In addition, increasing the mucking activity period would only restrict mine operations further from mucking activity needed to meet production targets.
4. **Uniformity Index:** Although the MLR model with a UI within 36 m had good performance metrics, discussions with PTFI indicated that a 36 m radius contains a high number of

drawpoints needing to be controlled/managed within a short period of time. Both the five nearest drawpoints and seven nearest drawpoints were tested instead. Model 9 considered 2Days-5DP, Model 10 considered 3Days-5DP, Model 11 considered 7Days-5DP, Model 12 considered 2Days-7DP, Model 13 considered 3Days-7DP, and Model 14 considered 7Days-7DP. Models 10, 12, and 13 were very similar, with Model 13 having the highest number of true positives. Discussions with PTFI indicated that three days is optimum for the operation to control uniform draw, and therefore, three days uniformity index with the seven nearest drawpoints was used as the controllable factor.

5. **Tonnages:** Periods of 7-, 14-, 21- and 28-days cumulative tonnage were tested during the MLR stage in Model 15, Model 16, Model 17, and Model 18, respectively. Each of these models reduced the number of true negatives in the MLR model when combined with the other variables mentioned above (Models 9 to 14). Therefore, the tonnage dataset was excluded in the final MLR analyses.

Table 4.4. Sensitivity analysis of each model prior to optimum variable selection.

Model	Precision	Recall	True Positive	True Negative	False Positive	False Negative
Model 1	0.99	0.01	769	188,186	136,209	7
Model 2	0.99	0.01	766	189,090	135,305	10
Model 3	0.99	0.01	766	191,080	133,314	10
Model 4	0.99	0.01	769	188,186	136,209	7
Model 5	0.99	0.01	767	187,290	137,105	9
Model 6	0.98	0.01	761	169,681	154,714	15
Model 7	0.99	0.01	769	188,186	136,209	7
Model 8	0.98	0.01	764	190,218	134,177	12
Model 9	0.99	0.01	767	187,668	136,727	9
Model 10	0.99	0.01	766	186,889	137,506	10
Model 11	0.99	0.01	767	185,930	138,465	9
Model 12	0.99	0.01	767	188,635	135,760	9
Model 13	0.99	0.01	769	188,186	136,209	7
Model 14	0.99	0.01	767	185,930	138,465	9
Model 15	0.99	0.01	769	187,234	137,161	7
Model 16	0.99	0.01	769	187,138	137,257	7
Model 17	0.99	0.01	769	187,384	137,011	7
Model 18	0.99	0.01	768	187,623	136,772	8

The development of the MLR model is started with drawpoint classification where the DOZ mine is currently using as their primary drawpoint susceptibility assessment. Thus, through the sensitivity analyses of variable inclusion or exclusion carried out during the MLR stage, the initial model consists of: (A-1) daily drawpoint classification, (B-1) daily adjacent drawpoint classification, (C-1) the daily total number of wet muck drawpoints within a 36 m radius, (D-1) daily HoD, (E-1) daily adjacent HoD, (F-1) 3 days UI within seven nearest drawpoints, (G-1) 14 days drawpoint mucking activity, (H-1) 14 days adjacent drawpoint mucking activity, and (I-1) 2 days consecutive mucking. Each of these nine variables was added sequentially to show the improvement of the susceptibility model (Table 4.5). There is a gradual increase in true positives by adding more variables, while true negatives start to increase when mucking variables are added from models G-1, H-1, and I-1. The initial Model I-1 coefficients are shown in Figure 4.16.

Table 4.5. Gradual improvement of the wet muck spill susceptibility model by adding significant variables.

MLR Model	Recall	Precision	True Positive	True Negative	False Positive	False Negative
Model A-1	0.97	0	752	127,062	197,333	24
Model B-1	0.97	0	753	128,740	195,655	23
Model C-1	0.98	0	757	121,458	202,937	19
Model D-1	0.98	0	760	120,901	203,494	16
Model E-1	0.98	0	760	120,995	203,400	16
Model F-1	0.98	0	763	120,942	203,453	13
Model G-1	0.99	0.01	767	186,201	138,194	9
Model H-1	0.99	0.01	769	186,286	138,109	7
Model I-1	0.99	0.01	769	188,186	136,209	7

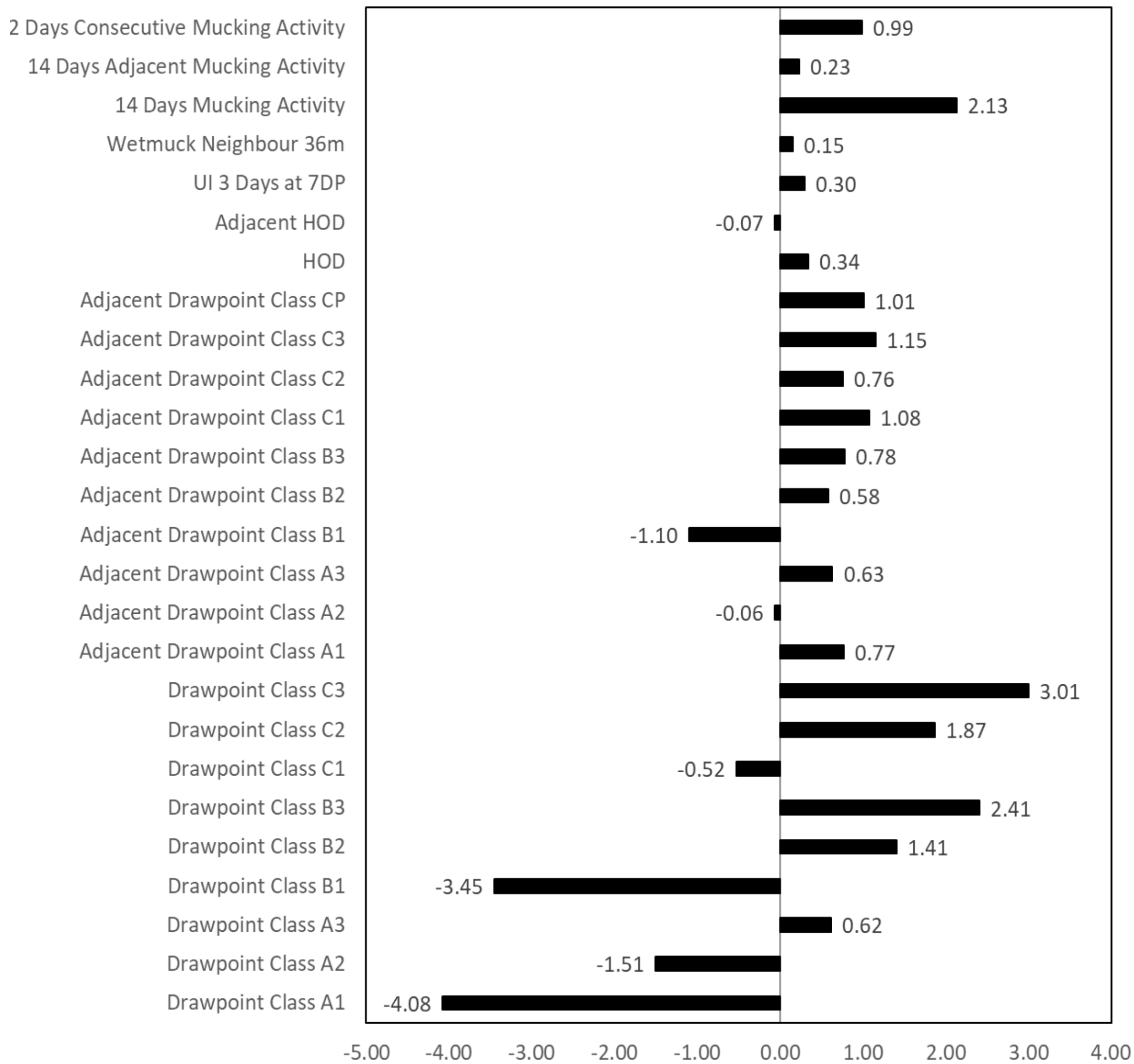

Figure 4.16. Multivariate logistic regression initial model coefficients Model I-1.

To analyze the multicollinearity in this initial proposed model, a Pearson correlation coefficient heat map was plotted to identify each independent variable's correlation strength (Figure 4.17). All of the variables showed low correlation strength, except HoD with Adj HoD, with a correlation strength of 0.76. This causes the adjacent HoD to have a negative correlation. Since it is necessary to remove highly correlated variables to minimize overfitting, adjacent HoD was not included in the final proposed model. Exclusion of adjacent HoD reduces the true positives to 768 and true negatives to 187,264 when comparing Model I-1 to Model H-2, but does not significantly change the other variables' coefficients (Figure 4.18).

With the exclusion of adjacent HoD, each variable from the initial model was gradually re-added to show the incremental model improvements (Table 4.6). The updated model consists of: (A-2) daily drawpoint classification, (B-2) daily adjacent drawpoint classification, (C-2) daily total number of wet muck drawpoints within 36 m radius, (D-2) daily HoD, (E-2) 3 days UI within seven nearest drawpoints, (F-2) 14 days drawpoint mucking activity, (G-2) 14 days adjacent drawpoint mucking activity, and (H-2) 2 days consecutive mucking. The updated model still had a good fit, with a low training score and a low test score with similar values. No high correlations between variables were observed in the Pearson correlation coefficient heat map, as shown in Figure 4.19. Therefore, it can be concluded that the MLR model that was developed achieved an optimum result.

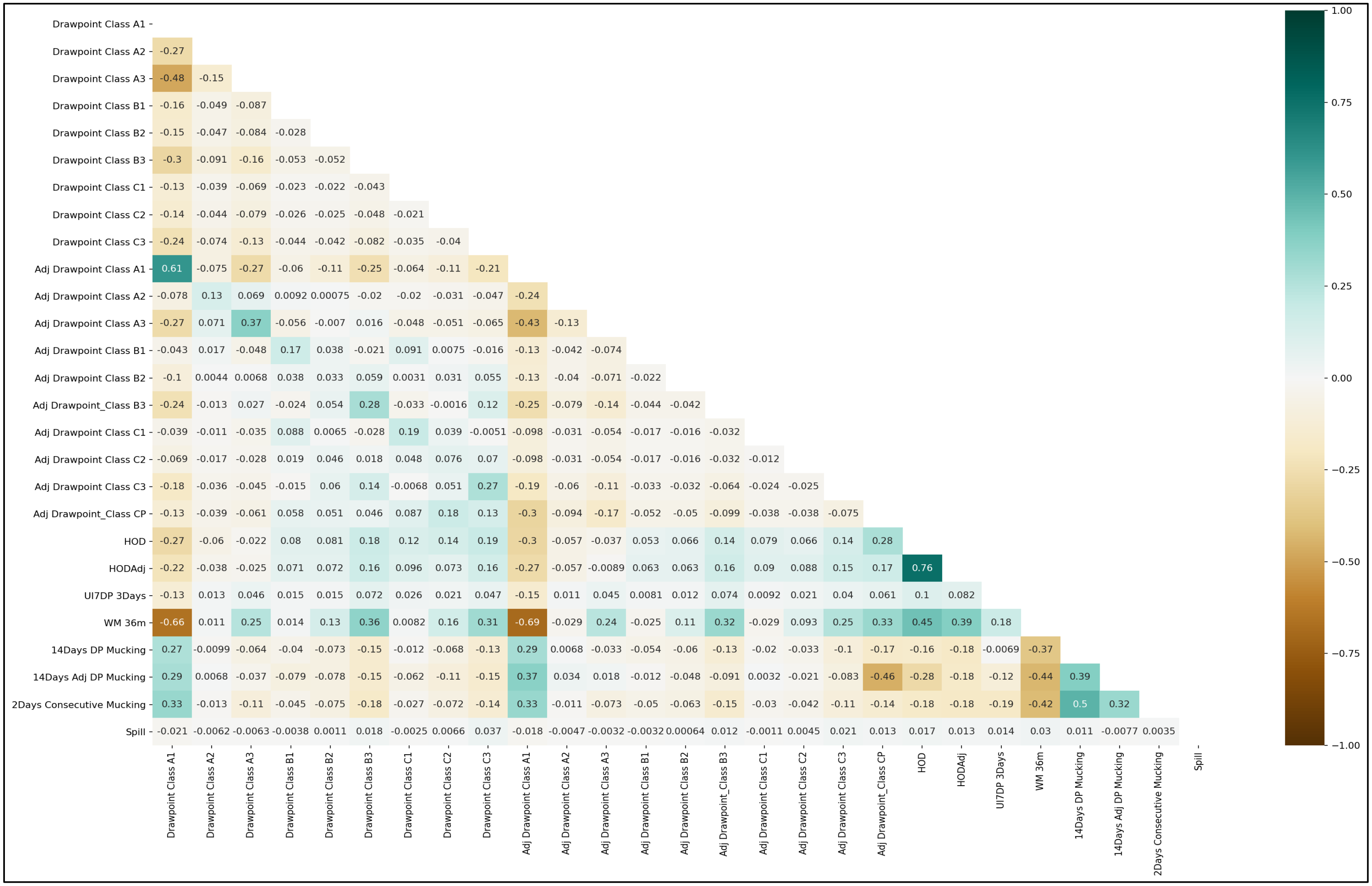

Figure 4.17. Model I-1 correlation heatmap based on the Pearson Correlation Matrix.

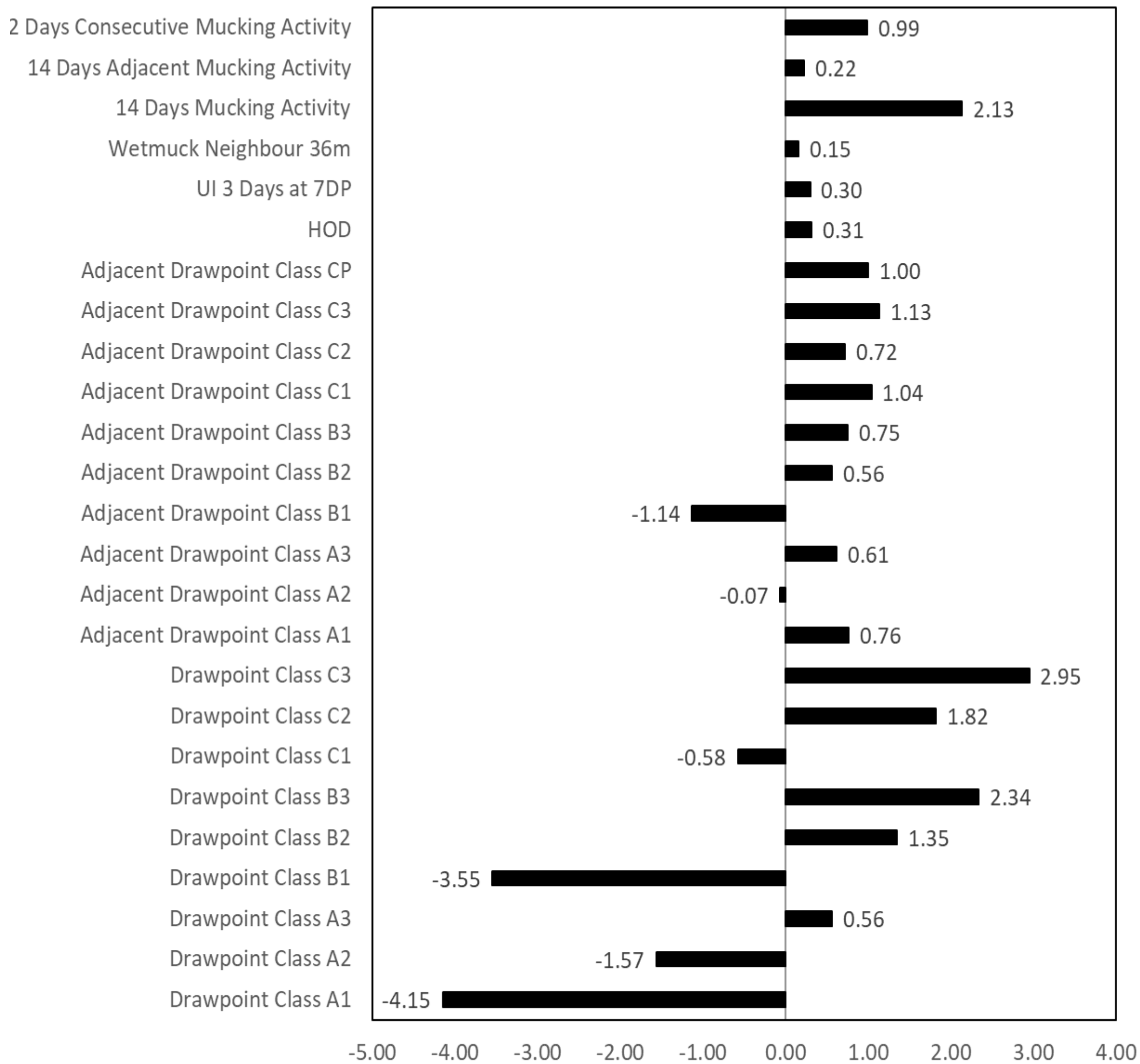

Figure 4.18. Multivariate logistic regression coefficients for Model H-2.

Table 4.6. The gradual improvement of wet muck model susceptibility by adding significant variables.

MLR Model	Recall	Precision	True Positive	True Negative	False Positive	False Negative
Model A-2	0.97	0	752	127,062	197,333	24
Model B-2	0.97	0	753	128,740	195,655	23
Model C-2	0.98	0	757	121,458	202,937	19
Model D-2	0.98	0	760	120,901	203,494	16
Model E-2	0.98	0	763	120,892	203,503	13
Model F-2	0.99	0.01	767	185,272	139,123	9
Model G-2	0.99	0.01	768	186,261	138,134	8
Model H-2 (Final Model)	0.99	0.01	768	187,264	137,131	8

.

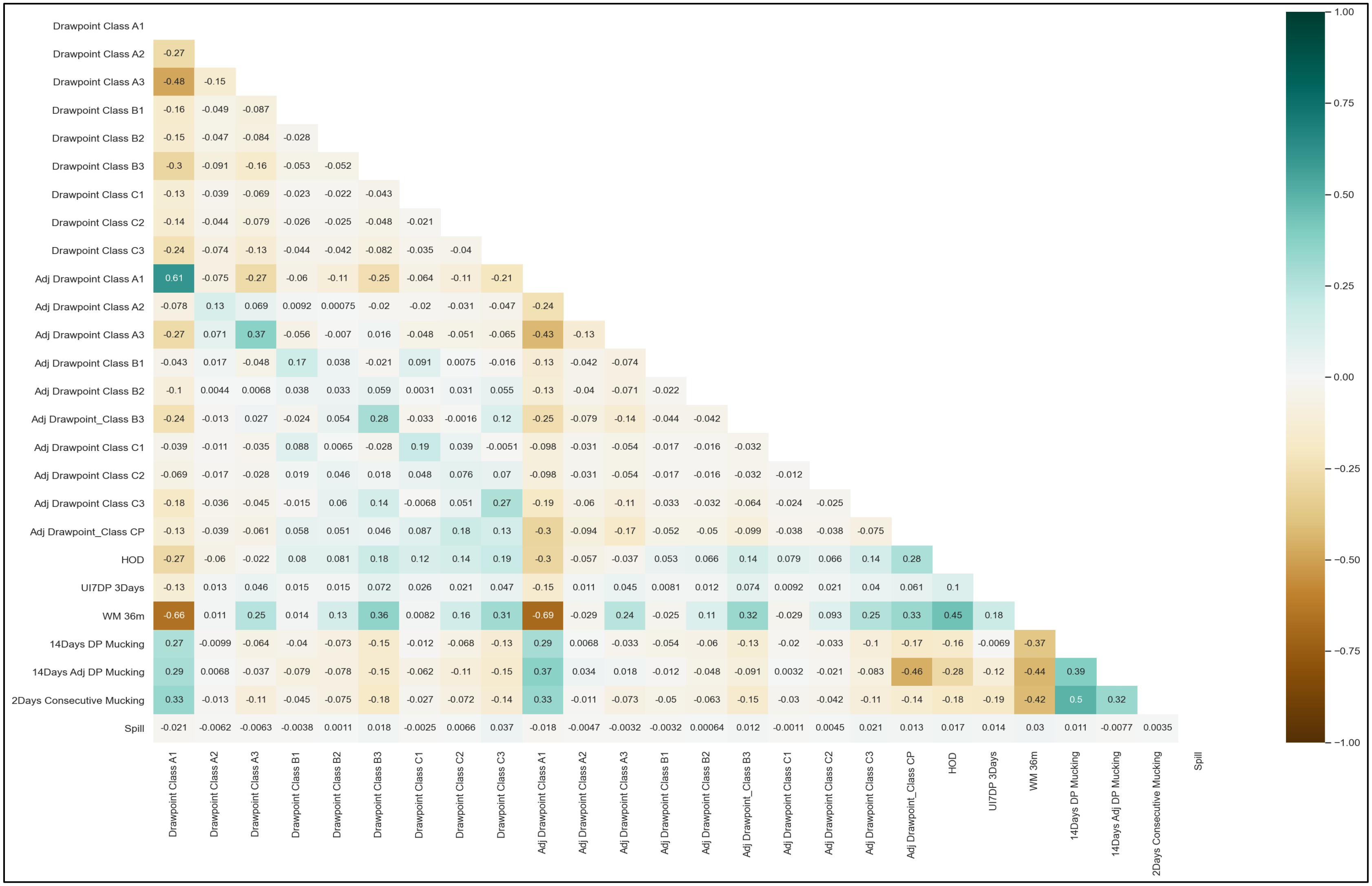

Figure 4.19. Model H-2 correlation heatmap based on the Pearson Correlation Matrix.

A comparison was made between the cost-sensitive (weighted) and SMOTE balancing techniques based on Model H-2 (Table 4.7). The SMOTE technique resulted in lower performance metrics compared to the weighted technique, although its coefficients showed a similar pattern (Figure 4.20). The SMOTE model obtained two more true positives at the cost of 14,085 false positives. Therefore, the weighted logistic regression model was selected for deployment.

Table 4.7. Confusion matrix comparison between cost-sensitive (weighted) and SMOTE balancing techniques based on Model H-2.

Balancing Technique	Cost-Sensitive (Weighted)	SMOTE
TP	768	770
TN	187,264	173,179
FP	137,131	151,216
FN	8	6

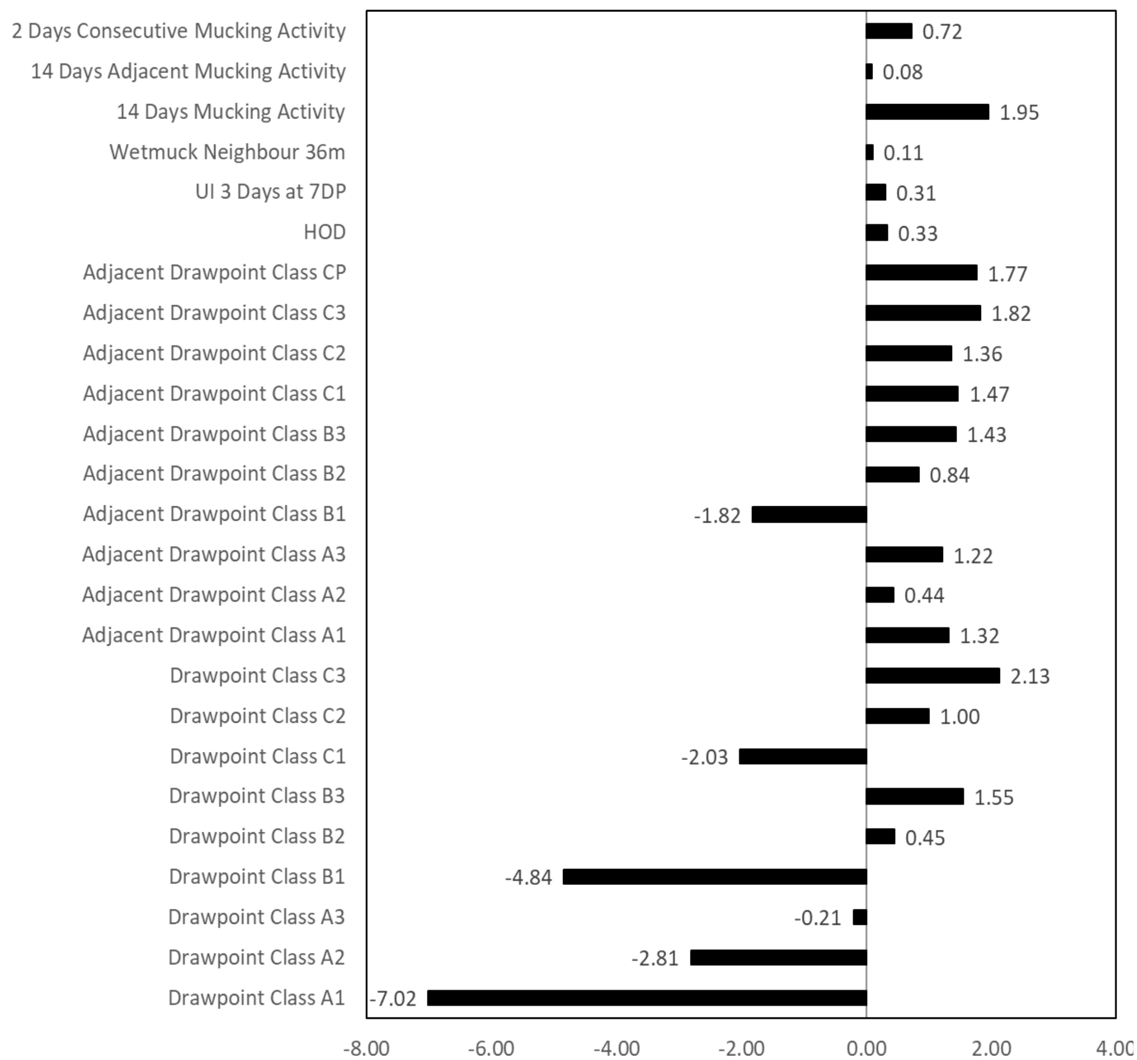

Figure 4.20. Multivariate logistic regression coefficients for Model H-2 using SMOTE.

4.4.3 MLR Model Deployment

The final model, based on Model H-2, was deployed using 100% of the available data as the training set (Figure 4.21). This final model was not tested using more recent data (i.e., post-June 2019). Further testing and re-training using recent data may improve the model performance, but is beyond the scope of this thesis. The statistical and mechanistic understanding of the deployed model is discussed in Section 4.6.

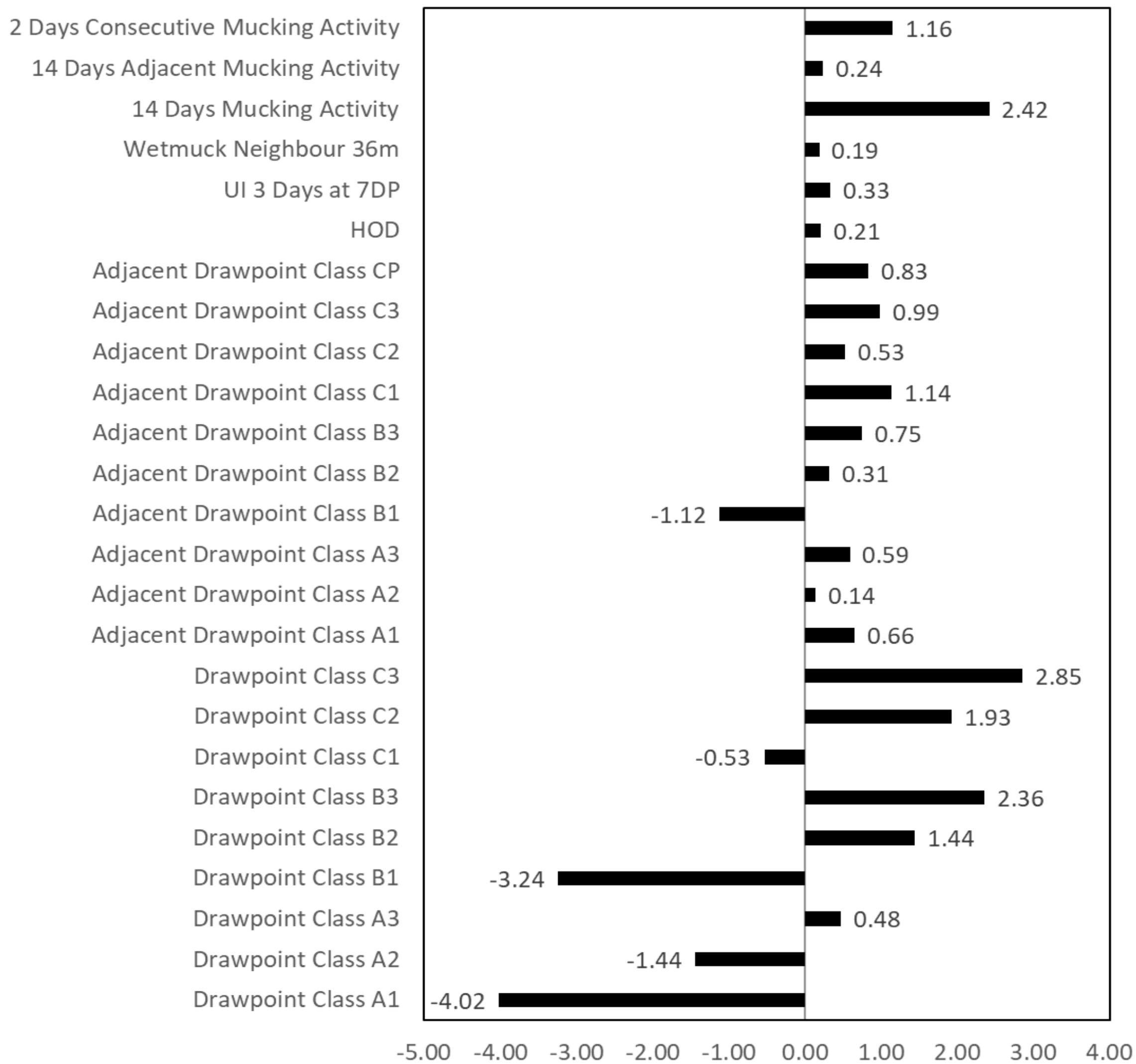

Figure 4.21. Multivariate logistic regression coefficients based on Model H-2 using 100% of the data as the training set (final deployed model).

4.5 Development of Data-Supported Tool for Wet Muck Spill Prediction

4.5.1 Suggested Grasberg Mining Complex Uniformity Index Matrix

Through discussion with the PTFI site team, an updated UI matrix, building on the original work by Susaeta (2004), is suggested for the PTFI operation based on the seven nearest drawpoints. The original UI was initially developed for the layout at the El Teniente mine in Chile (see Section 2.3.6 for UI development and Section 2.4.1 for El-Teniente Mine studies), which is based on six neighboring drawpoints (4 between the minor apex and two between the major apex). The El Teniente mine also operates in mostly dry conditions. In contrast, the DOZ drawpoint layout is constructed with an offset herringbone pattern, for which most drawpoints have seven nearest neighbors (5 along the minor apex and two along the major apex). In addition, site experience indicates that Susaeta's UI might not be applicable under wet conditions and needs to be modified for semi-uniform to isolated draw. Therefore, an updated UI matrix was developed for this study, as shown in Table 4.8.

The UI values below 2 were observed to have a low impact on the predictive model, although 0.6 to 1 and 1.4 to 2 are annotated as a non-uniform draw. Since the logit link function is a linear model that fits the logistic regression, it assumes a linear increase of a value will increase the log-odds of an event occurring. This is one of the limitations of the model. To overcome this limitation, the UI is suggested to be within the uniform draw range even though the logistic regression provides a negative correlation when the value is between 0.6 to 1 and 1.4 to 2.

Table 4.8. Proposed UBC Uniformity Index Matrix for the DOZ Mine.

Number of Inactive Drawpoints	Specific Index of Uniformity				
	0 - 0.2	0.2 - 0.4	0.4 - 0.6	0.6 - 0.8	0.8 - 1.0
0	Uniform	Uniform	Uniform	Non-Uniform	Non-Uniform
1	Uniform	Uniform	Non-Uniform	Non-Uniform	Non-Uniform
2	Uniform	Non-Uniform	Non-Uniform	Non-Uniform	Non-Uniform
3	Non-Uniform	Non-Uniform	Non-Uniform	Non-Uniform	Non-Uniform
4	Non-Uniform	Non-Uniform	Non-Uniform	Non-Uniform	Non-Uniform
5	Non-Uniform	Non-Uniform	Non-Uniform	Non-Uniform	Non-Uniform
6	Non-Uniform	Non-Uniform	Non-Uniform	Non-Uniform	Non-Uniform
7	Non-Uniform	Non-Uniform	Non-Uniform	Non-Uniform	Non-Uniform

4.5.2 UBC-ICaRN Wet Muck Spill Susceptibility Tool Development

A spreadsheet-based wet muck spill susceptibility prediction tool, named the UBC-ICaRN Wet Muck Spill Susceptibility Tool, was developed based on the eight most significant variables identified in the MLR model analyses. The aim of this tool is to provide the daily probability of a wet muck occurrence for every drawpoint, calculated using the MLR equation (Equation 4.5). The spill probability for each drawpoint is then updated relative to the frequency that the input parameters are updated. If a drawpoint is closed permanently, which might involve building a barricade in front of the drawpoint, the probability of a wet muck spill is zero, as there are no discharge point available for a wet muck spill to occur.

The spreadsheet also includes an adjustable worksheet that can be used as a drawpoint-specific forecast planning tool . An example of a probability calculation is shown in Table 4.9 for a drawpoint classified as C3, actively being mucked, and located in the wet area. This results in a probability of a spill event occurring of 0.71. Assuming the spill threshold is set to 0.5, this drawpoint is predicted to have a relatively high likelihood of experiencing a spill for each day the conditions remain and do not subside. A second example is shown in Table 4.10 for drawpoint with similar conditions, except it is in a drier area, resulting in a probability of a spill event of 0.45. Assuming a similar spill threshold at 0.5, this drawpoint is predicted to have a relatively low likelihood of experiencing a spill for each day the conditions remain.

Table 4.9. Example 1 of the UBC-ICaRN Wet Muck Susceptibility forecasting tool.

Variable	Condition (x)	Coefficient (β)	β* x
Intercept		-6.83	
Drawpoint Class	C3	2.85	2.85
Adjacent Drawpoint Class	B2	0.31	0.31
Number Wet Muck Drawpoints at 36m	10	0.19	1.90
Height of Draw (m)	250	0.24	0.13
3 Days Uniformity Index 7DP	3.00	0.32	0.15
14 Days Mucking Activities	1	2.42	2.42
14 Days Adjacent Mucking Activities	0	0.24	0.00
2 Days Consecutive Mucking	0	1.16	0.00
Prediction			0.71

$$P(Y=1) = \frac{e^{-6.83+2.85\cdot 1+0.31\cdot 1+0.19\cdot 10+0.24\cdot\frac{250-179}{133}+0.32\cdot\frac{3-2}{2.2}+2.42\cdot 1+0.24\cdot 0+1.16\cdot 0}}{1+e^{-6.83+2.85\cdot 1+0.31\cdot 1+0.19\cdot 10+0.24\cdot\frac{250-179}{133}+0.32\cdot\frac{3-2}{2.2}+2.42\cdot 1+0.24\cdot 0+1.16\cdot 0}} = 0.71$$

Table 4.10. Example 2 of the UBC-ICaRN Wet Muck Susceptibility forecasting tool.

Variable	Condition (x)	Coefficient (β)	β* x
Intercept		-6.83	
Drawpoint Class	C3	2.85	2.85
Adjacent Drawpoint Class	B2	0.31	0.31
Number Wet Muck Drawpoints at 36m	4	0.19	0.76
Height of Draw (m)	250	0.24	0.13
3 Days Uniformity Index 7DP	3.00	0.32	0.15
14 Days Mucking Activities	1	2.42	2.42
14 Days Adjacent Mucking Activities	0	0.24	0.00
2 Days Consecutive Mucking	0	1.16	0.00
Prediction			0.45

$$P(Y=1) = \frac{e^{-6.83+2.85\cdot 1+0.31\cdot 1+0.19\cdot 4+0.24\cdot\frac{250-179}{133}+0.32\cdot\frac{3-2}{2.2}+2.42\cdot 1+0.24\cdot 0+1.16\cdot 0}}{1+e^{-6.83+2.85\cdot 1+0.31\cdot 1+0.19\cdot 4+0.24\cdot\frac{250-179}{133}+0.32\cdot\frac{3-2}{2.2}+2.42\cdot 1+0.24\cdot 0+1.16\cdot 0}} = 0.45$$

Since there is uncertainty in the model, specifying only one spill susceptibility cut-off threshold (e.g., 0.5) may not be effective in assisting operational planning. Different strategies and mitigation procedures can be applied to different susceptibility thresholds. The following interim thresholds for wet muck susceptibility are suggested following a traffic light protocol (green, yellow, red):

1. Low Susceptibility: spill probabilities between 0 and 0.4, color-coded green.
2. Medium Susceptibility: spill probabilities between 0.4 and 0.75, color-coded yellow.
3. High Susceptibility: spill probabilities between 0.75 and 1, color-coded red.

These susceptibility threshold cut-offs are based on the model H-2 test set results (Figure 4.22). Out of 776 wet muck spills between 2018 and June 2019, the model was able to predict the majority of these events, with 723 (93.2%) being classified as high susceptibility and 49 (6.3%) being classified as medium susceptibility. Only 4 (0.5%) were misclassified as having a low susceptibility to a wet muck spill. Since this study encountered an imbalanced dataset in wet muck spill distribution, a high false positive (false alarm) rate cannot be avoided. There were 86,183 false alarms, where drawpoints experienced no-spill but were classified as high susceptibility.

As shown in Figure 4.23, if the threshold is lowered by 0.1 at each susceptibility level (i.e., low susceptibility up to 0.3, medium susceptibility between 0.3 and 0.65, and high susceptibility greater than 0.65), the model only misclassified two spills within the low susceptibility class, but with the trade-off of a higher false alarm rate. There were 100,350 cases where drawpoints experienced no-spill but were classified as high susceptibility. On the contrary, if the spill threshold is increased by 0.1 at each susceptibility level (Figure 4.24) (i.e., low susceptibility up to 0.5, medium susceptibility between 0.5 and 0.85, and high susceptibility greater than 0.85), the model misclassified eight spills within the low susceptibility class. However, it reduces the false alarms to 64,629 cases.

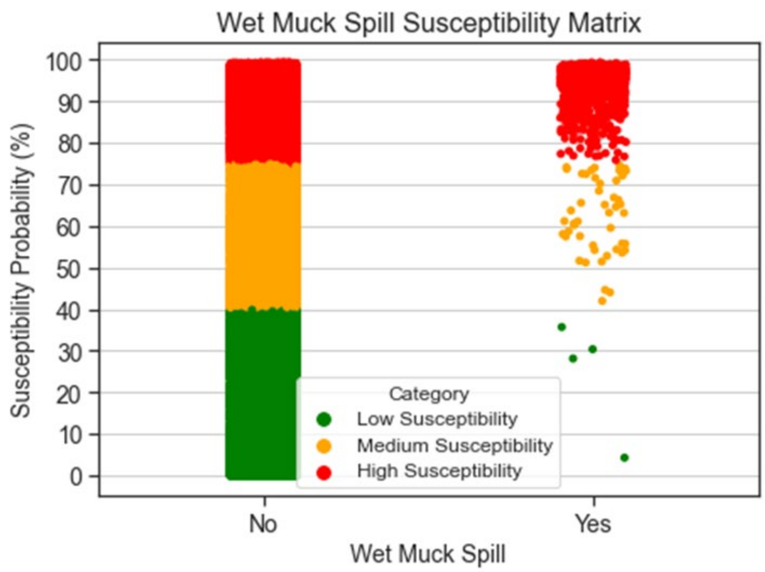

Figure 4.22. Proposed model (Model H-2) performance on the test set with interim susceptibility thresholds.

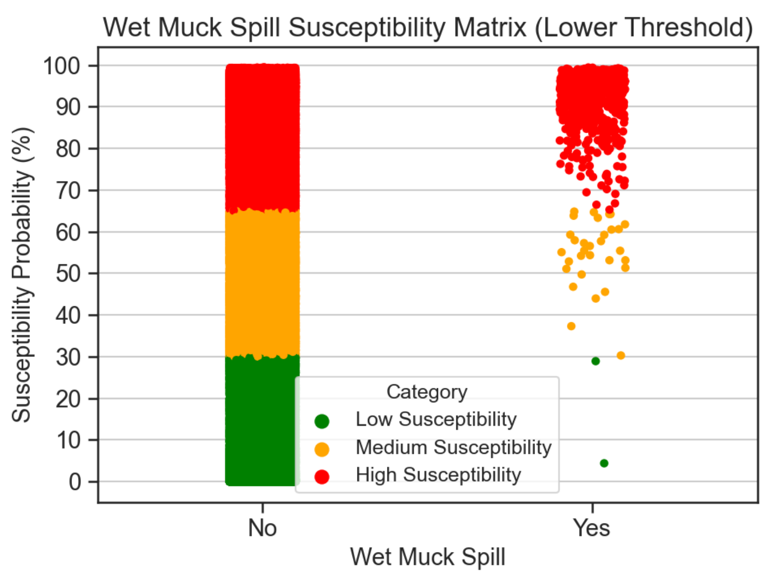

Figure 4.23. Proposed model (Model H-2) performance on the test set with lower susceptibility thresholds.

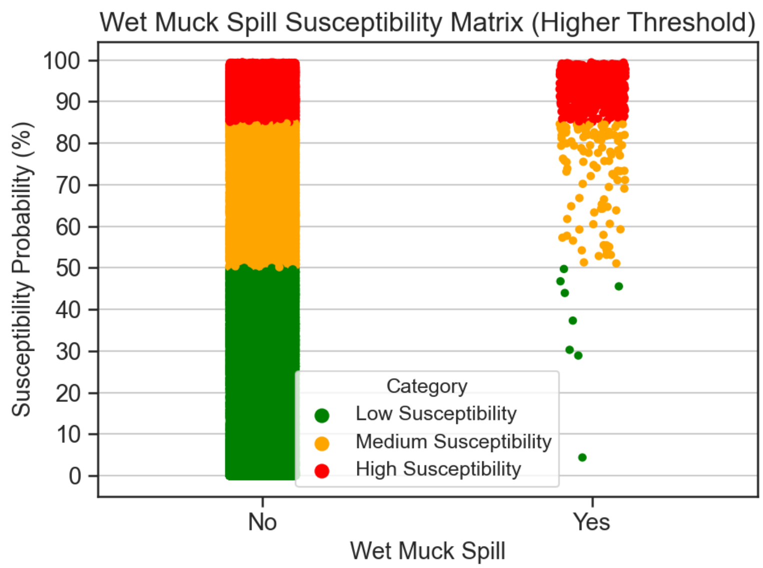

Figure 4.24. Proposed model (Model H-2) performance on the test set with higher susceptibility thresholds.

It is important that the interim thresholds suggested above be reviewed and modified to suit the operation's risk tolerance and associated wet muck spill mitigation strategies (e.g., limiting the number of buckets per shift that can be drawn at drawpoints in each susceptibility range). For example, raising the threshold between low and medium susceptibility ranges could ease operational strategies on mucking, but result in higher false negatives that may lead to infrastructure damage and production interruptions. For communication purposes, the calculated spill susceptibility for every open drawpoint can be plotted using the traffic light protocol; an example for the DOZ operation is shown as a susceptibility map for the extraction level footprint (Figure 4.25) and as a gridded engineering map (Figure 4.26).

Details for the four false negatives based on the interim thresholds, where the model incorrectly missed predicting a spill event, are shown in Table 4.11. The spill event that occurred in drawpoint P1A-17E appears to be an anomaly. The spill class was recorded as A2 (coarse, moist), but there were no supporting documents to confirm this. Drawpoint P01-01E experienced a spill even though the drawpoint had not been mucked over the previous 14 days. However, on the day of the spill, mucking started, which triggered the spill. The other two spills were classified as A3 yet were misclassified by the model, or the drawpoint material may have changed before it could be remapped. If the low susceptibility threshold is lowered to 0.3, the spills at P01-01E and P1F-10W would be better classified as medium susceptibility. But again, there is a trade-off between reducing the false negatives at the cost of higher false alarms, as well as potential lower production rates due to additional safety measures that may be implemented at medium to high susceptibility drawpoints.

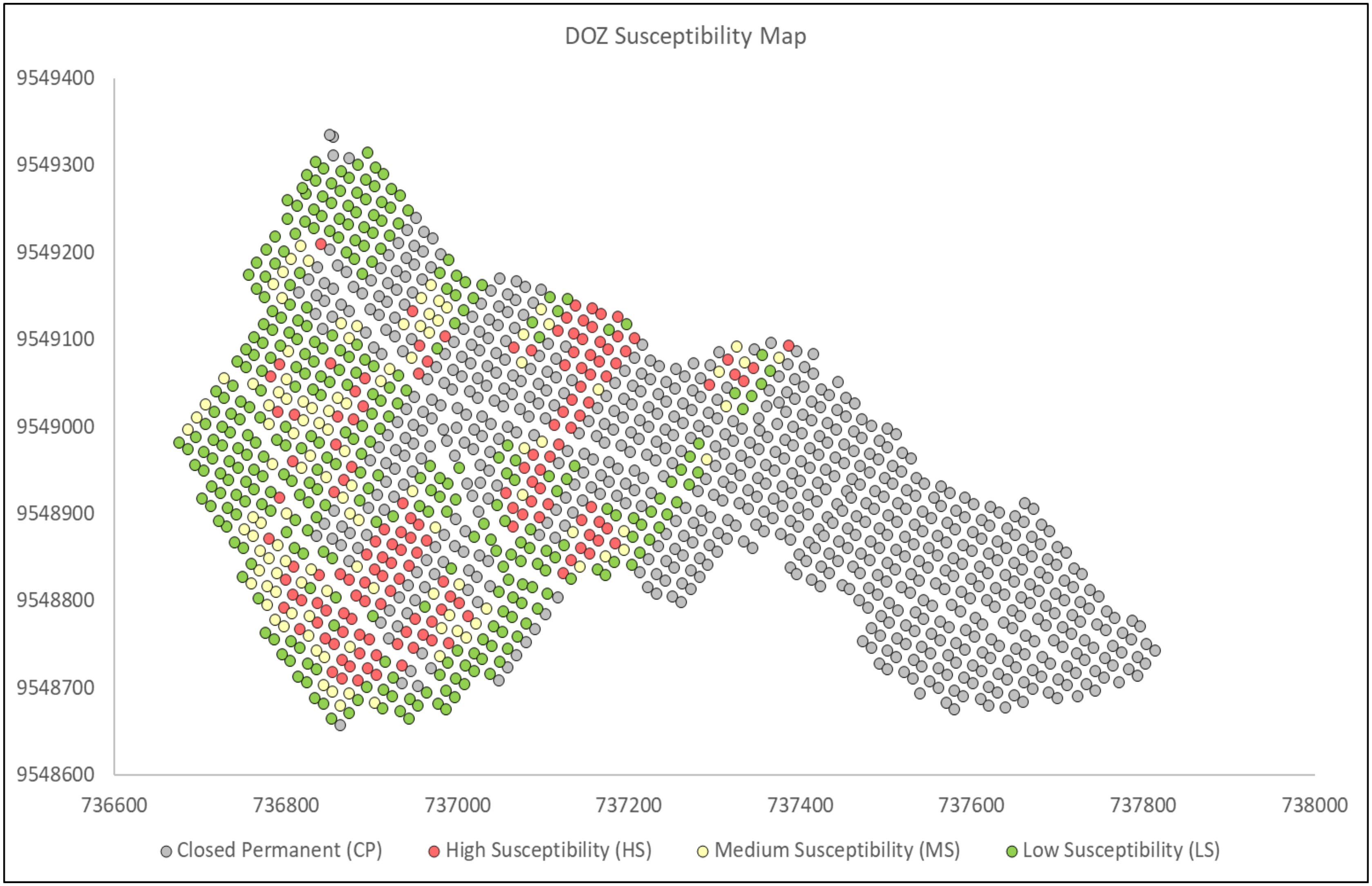

Figure 4.25. Example of DOZ cave footprint susceptibility traffic light protocol map.

Panel	P1L		P1K		P1J		P1I		P1H		P1G		P1F		P1E		P1D	
D/P	W	E	W	E	W	E	W	E	W	E	W	E	W	E	W	E	W	E
00		CP				0.09	0.09	0.03	0.03	0.02	CP	CP	CP	CP	0.17			
01		CP	CP		0.01	0.22	0.19	0.24	0.20	0.28	CP	CP	CP	CP	0.17	0.06	0.05	0.00
02		0.38	0.22	CP	0.16	0.04	0.04	0.05	0.25	0.30	CP	CP	CP	CP	0.41	0.40	0.36	0.14
03		0.26	0.38	0.14	0.26	0.26	0.26	0.13	0.11	0.36	CP	CP	CP	CP	0.43	0.42	0.45	0.35
04		0.14	0.06	0.19	0.25	0.24	0.24	0.21	0.30	0.34	CP	CP	CP	CP	0.89	0.42	0.42	0.39
05		0.05	0.03	0.30	0.20	0.21	0.09	0.06	0.10	0.12	CP	CP	CP	CP	0.52	0.41	0.43	0.88
06			0.00	0.14	0.23	0.78	CP	CP	CP	CP	CP	CP	CP	CP	CP	CP	0.86	0.39
07			0.18	0.00	0.32	0.68	CP	CP	CP	CP	CP	0.68	CP	CP	CP	CP	0.71	0.85
08			0.00	0.09	0.47	0.40	CP	CP	CP	CP	0.74	0.73	0.05	0.05	0.22	0.62	0.00	0.84
09			0.02	0.01	0.48	0.04	CP	0.00	CP	CP	0.24	0.33	0.06	0.35	0.88	0.65	0.07	0.24
10			0.04	0.03	0.42	0.48	0.01	0.00	0.00	0.28	0.32	0.83	0.23	0.28	0.76	0.21	0.21	0.19
11				0.12	0.51	0.03	0.03	0.02	0.22	0.20	0.25	0.27	0.20	0.58	0.62	0.81	0.37	0.01
12				0.21	0.13	0.36	0.13	0.34	0.74	0.12	0.19	0.27	0.25	0.70	0.97	0.84	0.09	0.08
13						0.03	0.21	0.39	0.80	0.59	0.23	0.46	0.49	0.46	0.46	0.33	0.10	0.08
14						0.17	0.21	0.33	0.79	0.48	0.45	0.93	0.50	0.27	0.28	0.76	0.48	0.00
15						0.16	0.21	0.75	0.30	0.47	0.88	0.30	0.57	0.10	0.43	0.31	0.36	0.86
16						0.50	0.21	0.03	0.18	0.07	0.66	0.36	0.37	0.81	0.49	0.36	0.53	0.92
17						0.14	0.23	0.00	0.07	0.02	0.02	0.00	0.62	0.29	0.34	0.21	0.21	0.90
18						0.49	0.06	0.02	0.11	0.03	0.00	0.00	0.15	0.36	0.82	0.17	0.21	0.20
19						0.47	0.04	0.01	0.02	0.00	0.00	0.00	0.18	0.33	0.31	0.65	0.17	0.19
20						0.50	0.04	0.02	0.10	0.00	0.00	0.04	0.00	0.48	0.45		0.03	0.12
21						0.35	0.03	0.02	0.01	0.16	0.19	0.25	0.35	0.41	0.40	0.87	0.50	0.32
22										0.11	0.17	0.23	0.19	0.23	0.31	0.42	0.45	0.62
23																0.25	0.41	0.61
24																0.15	0.65	0.40
25																		0.29

Figure 4.26. Example of DOZ engineering map between Panel L and Panel D. Each susceptibility value and color-code is based on Figure 4.22.

Table 4.11. Details of four false negatives that were identified based on the Model H-2 test set.

Drawpoint	Date	Drawpoint Class	Adjacent Drawpoint Class	HoD	UI 3 Days at 7DP	Wet muck Neighbour 36m	14 Days Mucking Activity	14 Days Adjacent Mucking Activity	2 Days Consecutive Mucking Activity	Spill Probability
P01-01E	25-04-18	C2	C3	253.6	4	9	0	1	0	0.30
P1A-17E	25-04-18	A2	A2	183.6	4.66	11	1	1	0	0.043
P1F-10W	01-01-19	A3	B3	84.5	0.58	14	1	1	0	0.36
P03-29W	02-01-19	A3	A3	202	3.58	9	1	0	0	0.28

4.6 Discussion

4.6.1 Statistical Understanding (Correlation)

Explanatory variables in the proposed model, as summarized below, were assessed based on their statistical correlations to wet muck spills at the DOZ mine. The sensitivity of input changes at each explanatory variable is illustrated in Appendix D.

Drawpoint Classification: DOZ drawpoints classified as wet muck (A3, B2, C2, and C3; refer to Table 2.2 for drawpoint class descriptions) represent the strongest predictors of wet muck spills (refer to Figure 4.21 for the MLR coefficients), with 99.6% of wet muck spills originating from wet muck class drawpoints (refer to Figure 3.1 for spill class illustration), including 83.9% originating from B3 and C3 drawpoints (i.e., wet and fine to medium grain). However, only 9% of spills originated from B2 and C2 drawpoints and 6.7% of spills originated from A3 drawpoints, although classified as wet muck class. This shows that the combination of high water content with the reduction in fragmentation size contributes to higher spill susceptibility. In contrast, non-wet muck class drawpoints experienced a total of only eight spill events (0.4%), indicating a strong negative relationship to wet muck spills. However, the conditions at these drawpoints may have changed since they were last mapped.

Adjacent Drawpoint Classification: The adjacent drawpoint class similarly represents one of the strongest predictors of wet muck spills, including when classified as wet or closed permanently (refer to Figure 3.3 for adjacent drawpoint wet muck classes) with 95.7% of wet muck spills originating from adjacent wet muck class and closed drawpoints. Notably, adjacent drawpoints classified as A1 and C1 (i.e., dry) also showed positive relationships, although not as strong as those classified as wet muck class. A similar pattern as drawpoint classification was observed, where a low percentage of B2 and C2 adjacent drawpoint classes (16.5%) had wet muck spills.

Total Number of Wet Muck Drawpoints within 36 m: The MLR identified a positive relationship between an increased total number of wet muck drawpoints within 36 m and wet muck spills. Every increase of one wet muck drawpoint within the 36 m radius increases the coefficient by 0.19 (Figure 4.21). This result also supports the EDA results (Figure 3.4, Figure 3.5, and Figure 3.6), which suggested spill occurrences increase with an increasing number of wet muck drawpoints.

Height of Draw: Although HoD shows a positive correlation, it was not a strong predictor of wet muck spills (Figure 4.21). The model predicts that HoD starts to become significant at the DOZ once the draw column exceeds 170 meters. At HoD values below 170 m, a negative correlation was observed.

3 Days Uniformity Index at 7 Drawpoints: As one of the controllable variables, operationally, the UI shows a positive correlation with wet muck spills. UI values greater than 2 result in a positive coefficient. Compared to drawpoint classification and adjacent drawpoint classification, UI is not a strong predictor of wet muck spills since a maximum UI value of 8 only produces a coefficient of 0.91. This shows that a wet muck spill is likely to occur even though a uniform draw is applied to a wet muck drawpoint. Based on the proposed UI matrix, there is a non-linearly increasing probability of wet muck spills when the UI value is in the ranges of 0.6 to 1 and 1.4 to 2, which are considered non-uniform or isolated draw (Table 4.8). UI values in these ranges provide negative coefficients, which indicates a reduction in the spill probability.

14 Days Mucking Activity: Mucking activity represents the strongest controllable predictor of wet muck spills, acting as a triggering mechanism; most of the drawpoints that experienced spills were actively being mucked. The presence of mucking is associated with a coefficient of 2.42 (Figure 4.21), which increases the wet muck spill susceptibility prediction. The proposed model contained one missed prediction of wet muck spill, where no mucking activities were observed within 14 days at the drawpoint (Table 4.11). However, there was mucking activity at the drawpoint on the day of the spill. Therefore, it is suggested to change the value from 0 (absence) to 1 (presence) when the operation is planning to muck a drawpoint on the analysis date, in order to obtain a more realistic spill susceptibility calculation.

14 Days Adjacent Mucking Activity: Although discussions with PTFI suggested that adjacent mucking activity is an important predictor of wet muck spills, the model did not show a strong positive correlation to this variable (Figure 4.21). The presence of 14 days of adjacent drawpoint mucking activity only increases the wet muck spill susceptibility calculation by a coefficient of 0.24. However, exclusion of this variable reduces the model performance by one true positive and 989 true negatives, when comparing model F-2 (without 14 days adjacent drawpoint mucking) to model G-2 (with 14 days adjacent drawpoint mucking). This shows that adjacent drawpoint mucking activity contribute to wet muck spills, although its influence is minimal.

2 Days Consecutive Mucking Activity: Consecutive days mucking at a drawpoint showed a positive relationship to wet muck spills (Figure 4.21). The presence of two days of consecutive mucking is associated with a coefficient of 1.16, which increases the wet muck spill susceptibility. Although the EDA did not reveal the impact of consecutive days mucking (Figure 3.16), its combination with other variables shows that such activity influences spills.

4.6.2 Mechanistic Inferences and Understanding (Causation)

Explanatory variables in the proposed model, as summarized below, were assessed based on their possible mechanistic influence on drawpoint behavior and wet muck spills at the DOZ mine.

Drawpoint Classification: Drawpoint classes A3, B3, and C3 were observed to have the strongest influence on wet muck spill susceptibility. This result agrees with PTFI's experiences and the wet muck classification system they have developed, where A3, B2, B3, C2, and C3 drawpoints are designated as being medium to high risk (see Table 2.2 and Table 2.3). These classes include those with fines, high water content, or both. This aligns with the key elements of wet muck spills (fine material and water) as outlined by Butcher et al. (2000) based on findings from South African mines. The mobility of broken rock, debris, etc., is known to increase with an increasing percentage of fines and water (Jakubec et al., 2016). Therefore, the drawpoint class is an important indicator of wet muck spill potential.

Adjacent Drawpoint Classification: Various spill events have occurred in the DOZ record from drawpoints classified as coarse, but where the adjacent drawpoint is fine and/or wet. As reported by Rachmad et al. (2011), a small number of spills have occurred from A3 drawpoints, which are coarse (and wet), but where the adjacent drawpoint is classified as C3 fine (and wet). If water from the C3 drawpoint is trapped in the drawbell above due to low permeability fines below and cannot discharge through the drawpoint opening, the water can accumulate, building up pore pressures and causing a reduction of shear strength, leading to a spill from the adjacent drawpoint sharing the same drawbell, even if it is coarser and/or drier. It is most likely that the water is backing up above the drawbell and spilling over into the adjacent drawbell.

Therefore, it is necessary to consider the adjacent drawpoint classification and monitor any changes in its fragmentation and saturation when it is classified as a wet drawpoint or permanently closed.

Total Number of Wet Muck Drawpoints within 36 m: The clustering of wet muck drawpoints within the radius of influence indicates a concentration of fines and water across a larger area. It is assumed that wet muck drawpoints reflect the condition in the drawbell, but also above the drawbell, with the latter enabling a migration of wet muck that follows the mining direction (i.e., drawpoints being mined more aggressively than others). In other words, if the increase of fines and water is contained inside the drawbell, the adjacent drawpoint sharing the same drawbell is similarly at risk. If an accumulation of fines and water builds up above the drawbell, then the wet muck material can migrate to the surrounding drawbells, resulting in an increased likelihood of spills triggered by mining activities at drawpoints within the radius of influence (Castro et al., 2018). For this situation, a 36 m radius was observed to have higher performance metrics related to the total number of wet muck drawpoints, but also encompasses the drawbell interaction between its minor and major apexes. Since the origin of wet muck migration is unknown inside the cave, different radii were tested for their sensitivity. Using a 24 m radius was seen to be too restrictive, as it only allows the model to capture material migration for up to 7 adjacent drawpoints, while a 48 m radius considers too many neighbors, which introduces noise into the analysis.

Height of Draw: Finer fragmentation is often associated with higher heights of draw due to the higher cave loads and longer distances the material travels through the cave until it reaches a drawpoint (Dorador, 2016). Thus, the higher the HoD, the more comminution the material expereinces, and the more likely the drawpoint will change to a class indicating fines, resulting in a long-term susceptibility to fines. A linear increase of HoD with wet muck spills is consistent with the findings of this study summarized in Section 4.6.1.

3 Days Uniformity Index at 7 Drawpoints: Non-uniform draw is generally not recommended for caving operations, as it often results in negative impacts, such as early dilution entry, changes in cave load, and changes in cave porosity, which can lead to preferential flow for wet muck material to flow into an isolated drawpoint (Butcher et al., 2000; Castro et al., 2018; Holder et al., 2013; Widijanto et al., 2012). The UI is one of the controllable factors that needs to be monitored closely; the PTFI historical operation UI has a high average value of 3.5 at wet muck drawpoints (Figure 4.27). Although the UI is not a strong explanatory variable, it needs to be controlled, as low as operationally possible, to reduce the wet muck susceptibility based on the findings in Section 4.6.1.

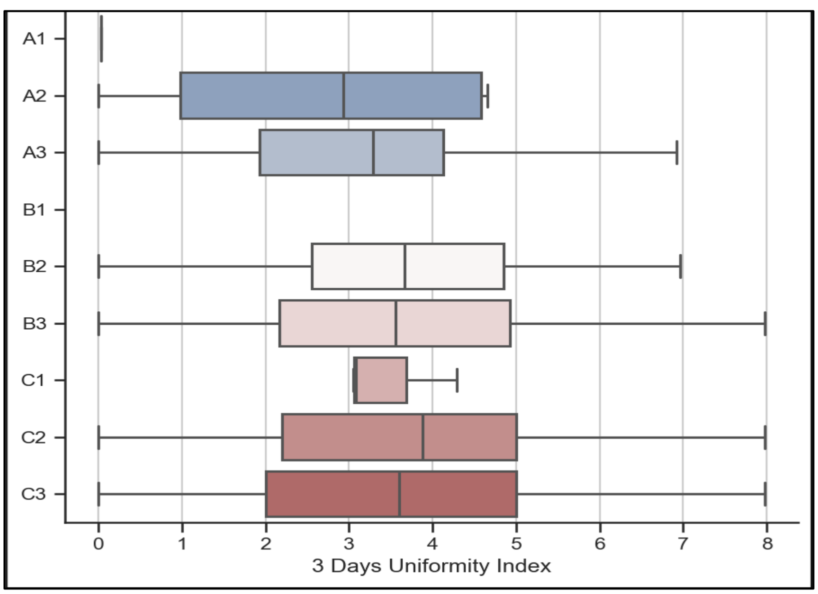

Figure 4.27. Distribution of 3-days uniformity index at seven nearest drawpoint at each drawpoint class.

14 Days Mucking Activity: Mucking activity was observed to be the key, if not only, triggering factor. As illustrated in Figure 4.28, the combination of mucking activities within a 14 day period led to the majority of spills at the DOZ mine. Mucking serves to loosen the drawpoint material at its toe, material that serves as a buttress supporting the material in the drawpoint above. Destabilizing this buttress can trigger the mobilization of accumulated water and fines through liquefaction inside the drawbell, and can also progressively draw mud pockets inside the caved zone into the drawbell.

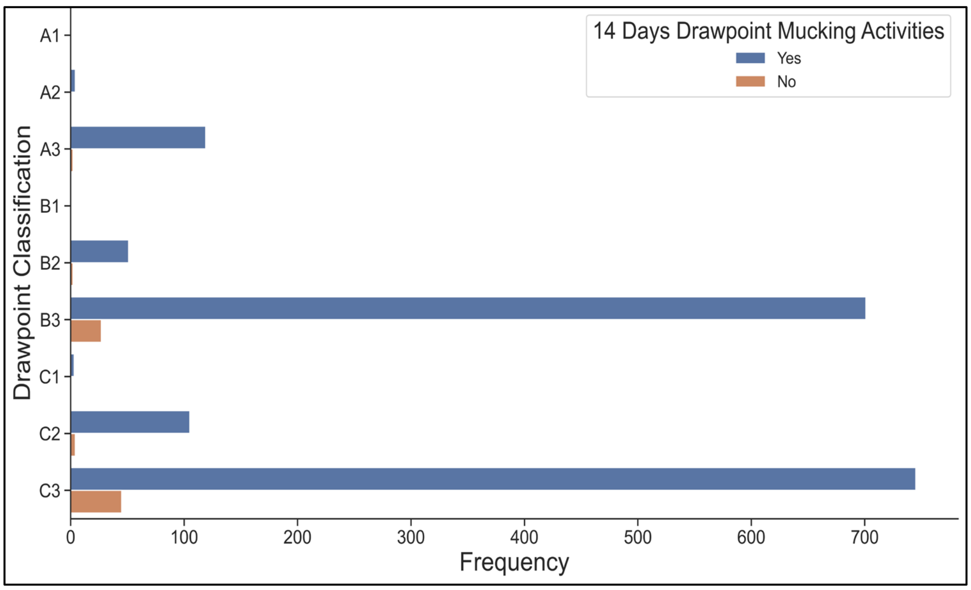

Figure 4.28. Distribution of wet muck spill occurrences at the DOZ mine with the presence or absence of 14 days of drawpoint mucking activities at each drawpoint classification.

14 Days Adjacent Mucking Activity: Although adjacent mucking can disturb a wet muck drawpoint and trigger a wet muck spill, the model shows that mucking activities at a given drawpoint are more significant than those at an adjacent drawpoint. As illustrated in Figure 4.29, not all adjacent drawpoint mucking activities led to wet muck spills. At high susceptibility conditions, it is preferred to minimize mucking activity at adjacent drawpoints to reduce the spill susceptibility. Adjacent drawpoint mucking can disturb the material inside the drawbell, but can also loosen the drawpoint material at its toe. However, mucking at adjacent wet muck class drawpoints can increase the material porosity, allowing water to flow out and reducing the accumulation of water inside the drawbell. These study findings cannot completely conclude the positive influence of adjacent drawpoint mucking on wet muck spills, and therefore need to be analyzed further.

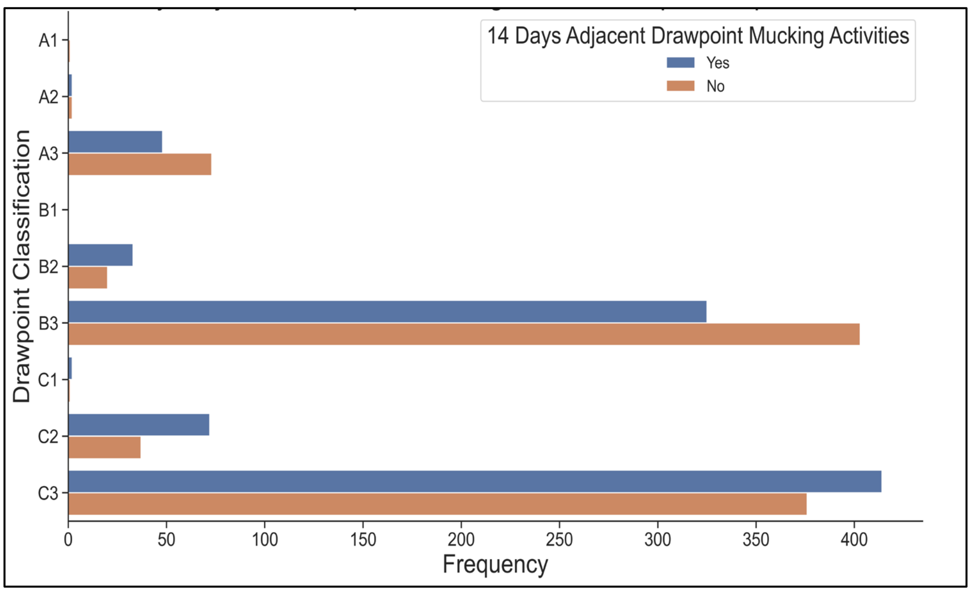

Figure 4.29. Distribution of wet muck spills occurrences at the DOZ mine with the presence or absence of 14 days adjacent drawpoint mucking activities at each drawpoint classification.

2 Days Consecutive Mucking Activity: If a wet muck drawpoint is constantly disturbed, there is a high probability of a spill being triggered from that drawpoint. The presence of two days of consecutive mucking activity at wet muck drawpoints shows correspondingly high spill occurrences (Figure 4.30). However, there were also high spill occurrences where the absence of two days of consecutive mucking was observed. This correlates with the findings from Section 4.6.1, as this variable is also a wet muck spill predictor but not as strong as 14 days mucking activities.

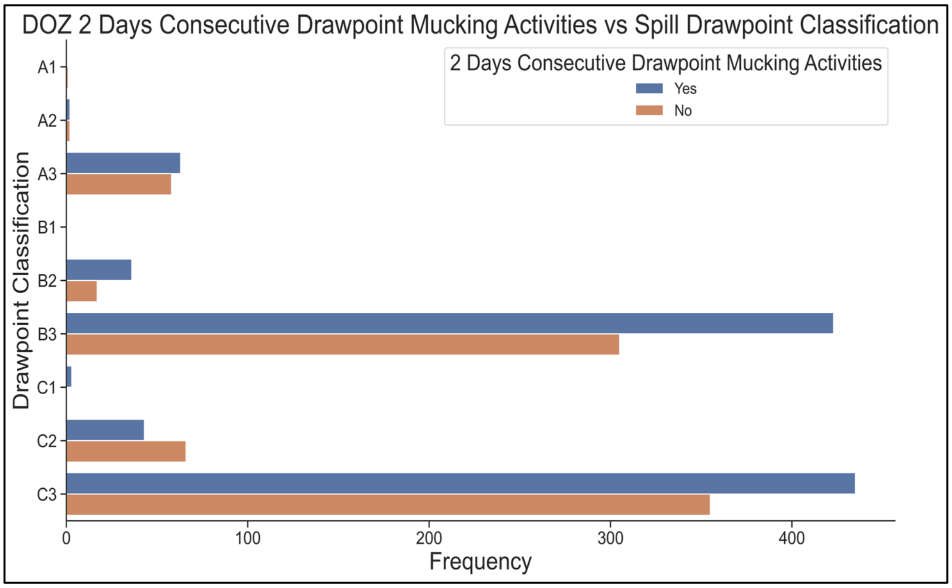

Figure 4.30. Distribution of wet muck spill occurrences at the DOZ mine with the presence or absence of 2 days consecutive mucking activities at each drawpoint classification.

Chapter 5: Conclusions and Recommendations for Future Work

To date, research on wet muck spill causative and triggering factors has been mostly based on operational experiences and engineering judgment, with limited published results. This study provides an opportunity to improve the statistical understanding of wet muck spill occurrences at the DOZ mine and develop a tool that can improve safety and operation productivity. The research includes the development of the DOZ database, data exploration, descriptive analysis, and the development of statistical models to predict and explain the presence or absence of a wet muck spill occurrence at the DOZ mine. A cost-sensitive logistic regression model was used to evaluate each explanatory variable and its statistical relationship with wet muck spills. This approach allowed the model to reduce the effects of the severely imbalanced nature of the dataset, applying equal weight to spill and no-spill data. The work represents a significant advancement beyond Castro et al.'s (2018) multivariate logistic regression approach to identify wet muck entry or non-entry at a drawpoint.

A key deliverable of this study is a wet muck database (UBC-ICaRN Wet Muck Database) and spreadsheet-based tool (UBC-ICaRN Wet Muck Susceptibility Tool), which includes implementation guidelines and Python scripts so that it can be adapted to other caving operations and build upon current prediction methods used by PTFI. Furthermore, this research delivers a concept of wet muck susceptibility tool development using a cost-sensitive multivariate logistic regression, which can be applicable to other caving operations around the world that experience wet muck spill hazards.

5.1 Summary of Findings

The main results of this research are summarized below:

1. The UBC wet muck database was compiled from the PTFI raw data and used to identify 177 hypothetical variables that can correlate with wet muck spills. The research covered the DOZ mine database between the period 2008 January to 2019 June, which consisted of more than 5 million observations. The data confidence was improved through the validation of each spill observation with the associated attributes through available supporting documents.
2. Exploratory data analysis revealed that wet muck spills were correlated with mucking activities, and the combination of high-water content and finer fragmentation size, as shown by B3 and C3 classifications. Although B2 and C2 classifications are considered wet muck, only a small percentage of spill events originated from these classes. The wet muck condition at the adjacent drawpoint also confirmed the hypothesis summarized in Section 2.5. Water from the low permeability drawpoints cannot be appropriately drained and migrated to the higher permeability drawpoints.
3. A sensitivity analysis of drawpoint radius of influence concluded that 36 m is the optimum distance when considering wet muck neighboring drawpoints. A drawpoint will have a higher likelihood of wet muck spills when the surrounding drawpoints are identified as wet muck drawpoints. The UI radii were optimum when including the seven nearest drawpoints, adopting similar considerations from Susaeta (2004) UI based on the El Teniente layout.

4. The DOZ geological domain and distance to the surface or IOZ mine were not compatible with short-term wet muck susceptibility predictions. Similarly, rainfall data were recorded from a rainfall station at the surface, but the proportion of surface water entering the cave zone and distributing to each drawpoint is unknown. In addition, the influence of high or low rainfall cannot be immediately mapped at each drawpoint because the mapping is carried out weekly to bi-weekly.
5. The imbalanced distribution of a binary outcome creates challenges for the model fitting. A cost-sensitive multivariate logistic regression is an effective machine learning tool to analyze binary classifier problems involving a large and severely imbalanced dataset. It can provide a statistical understanding of the magnitude and interrelationship of multiple explanatory variables to the binary outcome. The statistical model, based on 776 known drawpoint wet muck spills from month 2018 to June 2019, identified 723 of these as high susceptibility drawpoints and 49 as medium susceptibility drawpoints. The model had a high recall score (99%) but a low precision score (1%). This means that the proposed model cannot provide a precise prediction (in the temporal sense of when a wet muck spill might occur at a specific drawpoint), but can be used as a spatial forecasting tool to alert the operation to drawpoints where spills are more likely to occur, and mitigation strategies may be most effective.
6. The HoD showed a positive correlation above 170 m, indicating where and when finer fragmentation is more likely to be generated. Furthermore, the UI shows a positive correlation to wet muck spills above a UI value of 2. This result matched with the proposed UI matrix (Table 4.8), where isolated draw is indicated by a UI value of 2.2.

7. The statistical model confirmed that PTFI's existing drawpoint classification system is a good predictor of wet muck spills. The 14-days mucking activity was also identified as a triggering factor. This study improves the susceptibility analysis by adding dimensionality from a two-parameter drawpoint classification matrix to an eight-parameter matrix, which is able to improve current spill and no-spill outcomes. Following is the order of significant variables, from highest to lowest: (1) drawpoint classification, (2) 14-day drawpoint mucking activity, (3) total wet muck neighbors within 36 m, (4) 2-day consecutive mucking activity, (5) adjacent drawpoint classification, (6) 3-day UI within the seven nearest drawpoints, (7) HoD, and (8) 14-day adjacent drawpoint mucking. Although the UI is not one of the strongest explanatory variables, it is still an important factor that can be controlled, with the goal of achieving uniform draw, when all of the uncontrollable contributing factors are present.
8. Significant variables were classified as controllable or uncontrollable based on the operational capability to control the variable. Controllable variables consist of 14-day drawpoint mucking activity, 14-day adjacent drawpoint mucking, 2-day consecutive mucking, and 3-Day UI within the seven nearest drawpoints. Uncontrollable variables include drawpoint classification, adjacent drawpoint classification, total wet muck neighbors within 36 m, drawpoint HoD, and adjacent drawpoint HoD.
9. A spreadsheet-based wet muck susceptibility tool was developed using the eight most significant variables identified from this research. This tool can provide daily drawpoint susceptibility, annotated through a traffic light system, with interim thresholds for low susceptibility (< 0.4), medium susceptibility (0.4 – 0.75) and high susceptibility (> 0.75). Based on the test dataset between 2018 January and 2019 June, the susceptibility threshold

shows a good performance. However, due to the imbalanced dataset, there were still false alarms.

10. The outcome of this research provides a concept of using a logistic regression approach to calculate drawpoint spill susceptibility that can be applied to other caving operations susceptible to wet muck spills. The developed UBC-ICaRN wet muck susceptibility tool can also provide an empirical guideline to other operations. In addition, an updated UBC Uniformity Index for the offset herringbone drawpoint layout was developed based on Susaeta's (2004) Uniformity Index matrix for the El Teniente drawpoint layout.

5.2 Challenges and Limitations

1. Analysis of the observational datasets, such as drawpoint classification and wet muck neighboring drawpoints within 36m is challenging because observations can be subjective and vary between different mine workers mapping and recording the data at different times. The susceptibility model strongly correlates with these observational variables. A wet muck class drawpoint might not be mapped as frequently as a non-wet muck class drawpoint due to safety risks limiting access for mapping. Consequently, information on drawpoint class and its associated variables do not necessarily reflect reality.
2. The collection of data related to wet muck spills has improved over time, particularly since 2016. The study database is assumed to be accurate, with significant outliers removed. However, some potentially important factors, including drawpoint water discharge, hydraulic conductivity, and rock type distributions, were not considered in this study due to incompleteness of the datasets. In addition, the tonnage dataset is skewed because

various strategies (wet-dry tons mixing ratio, unrecorded tonnage combined with spill cleanup) were implemented throughout the history of the operation.

3. Only significant variables were selected for use in the susceptibility model. However, these explanatory variables have their limitations. For example, differential HoD did not reveal its correlation to wet muck spills. However, a high difference between HoD in a drawbell can result in a shear failure that can lead to a wet muck spill. Other variables include UI, where the tonnage threshold for the total number of inactive drawpoints (Δ) is unknown. Uneven draw can occur even with a low UI value. For example, a drawpoint being mucked 400 tons per three days while each surrounding drawpoint is mucked 100 tons per three days results in a UI of 0.55, while an inactive drawpoint counts as zero. However, over an extended period, the drawpoint will experience isolated draw, causing uneven cave shape.
4. A logistic regression model is a generalized linear model that assumes a linear relationship between the logit link function and explanatory variables (Dobson & Barnett, 2018). However, wet muck spills are a complex problem that may involve non-linear relationships. For example, the UI is a nonlinear variable where UI values between 0.6 and 1 and 1.4 and 2 are considered uniform draw, but the susceptibility model negatively correlates these values to wet muck spills. Therefore, it is still recommended to maintain a uniform draw following the developed UI matrix (Table 4.8).
5. The susceptibility model predicts a short-term drawpoint susceptibility to wet muck spills. Calculations with higher temporal inputs might not result in higher accuracy. The explanatory variables selected were primarily operational factors. The consequences of poor draw strategies were not statistically feasible to analyze due to data record limitations.

In addition, further research is required to validate the results of this statistical model to identify the mechanistic links between the significant variables and wet muck spills.

5.3 Model Implementation and Recommendations for the Grasberg Mining Complex

5.3.1 Implementation at DOZ

Even though the DOZ susceptibility model produces a high false alarm rate, it can be utilized as a forecasting tool to alert the operation to drawpoints that have relatively high susceptibility to spills. Instead of classifying the model outcomes into spill or no-spill categories using a single threshold, spill susceptibility is suggested to be classified into three categories (refer to section 4.5.2). The proposed susceptibility categories were obtained from the testing process using data between 2018 and June 2019. This model should be tested again with newer data to validate its ongoing performance and retrained if necessary. Similarly, the susceptibility class thresholds should be reviewed in the context of PTFI's risk tolerance and evolving risk management strategies.

Updating the DOZ mine susceptibility map daily is recommended to reflect near real-time operational conditions. Although not all data are readily available on a daily basis, updating the variables as soon as they are reported strengthens the model predictive capability. The calculation of drawpoint susceptibility needs to consider the planned date of mucking activity at drawpoints and adjacent drawpoints. If a drawpoint experienced no mucking activity over the past 14 days (0) and is planned to be mucked on the day of the susceptibility calculation, the drawpoint 14 days mucking activity should be manually adjusted to active mucking (1).

5.3.2 Implementation at GBC and DMLZ

The DOZ model can provide an empirical guideline for the GBC and DMLZ mine, but the explanatory variables might be different since the mine is not operating under the exact same conditions. For example, the proposed model considers HoD to be significant above 170 m. However, this reflects the specific geology and conditions at the DOZ, where the average distance to the IOZ is approximately 250 m. The GBC mine might have a lower planned HoD since the existing Grasberg Open Pit is directly above it, and fines and water may flow directly into the cave after it breaks through the surface. Furthermore, the GBC and DMLZ mine has adopted the El Teniente drawpoint layout, which is different from the offset herringbone layout used at the DOZ. The radius of influence should therefore be re-analyzed to obtain the optimum value for the GBC. This research delivers a concept, using cost-sensitive multivariate logistic regression, which can be applied to develop a similar wet muck susceptibility tool for these mines. Newly recorded data, such as water discharge and hydraulic conductivity, should be tested in each respective mine model. Finally, the GBC and DMLZ mine is a newer operation for which the database is not as extensive as that of the DOZ mine. As more data becomes available at the GBC, the model should be updated.

5.3.3 Additional Variables and Updating Susceptibility Model

Since the operation is continuously improving their database, previous manually recorded data were updated into a cloud database. However, not all of the manually recorded data could be used. For example, water discharge, hydraulic conductivity, and drawpoint rock type distributions were not considered in this study, as noted above. These variables should be tested as more data become available, and added to the model if they are determined to be significant. Other new variables should also be considered, such as drawpoint fragmentation. The influence of large-scale geological structures and domains could also be analyzed to identify potential large-scale spatial and/or long-term temporal correlations with wet muck conditions at drawbells or clusters of drawpoints.

5.3.4 Physical and Numerical Modelling

This study provides a statistical understanding of causative and triggering factors for wet muck spills at the DOZ mine. Limited information was available on long-term factors related to historical wet muck spills at the DOZ. Consequently, these factors were not considered in this analysis. Long-term spatial-temporal influences, such as the formation of wet muck, geological conditions, secondary cave fragmentation, wet muck preferential flow paths, and muckpile shear failure at drawpoints or drawbells are potential topics for future research, through numerical modeling and/or physical tests.

5.3.5 Influence of draw-related strategies

Hypothetically, wet muck spills are correlated with high draw rates and isolated/uneven draw, which can create preferential flow paths for wet muck materials to migrate. However, the model did not reveal that higher draw rates result in high spill susceptibility. As the explanatory variables for this study were selected based on the model performance metrics, insignificant hypothetical variables were not included in the final model. It may be possible to further define the influence of draw strategies on wet muck spills through additional research focused on medium to high susceptibility drawpoints. Furthermore, the UI has its own limitations, and should be updated further. Spatial clustering, drawbell interactions through various draw strategies, global cave footprint draw patterns, and differential movement between draw columns may provide insights into the causation of wet muck spills due to poor draw strategies.

References

Akosa, J. (2017). Predictive accuracy: A misleading performance measure for highly imbalanced data. Proceedings of the SAS Global Forum 2017 Conference. Cary, North Carolina: SAS Institute Inc.

Atlas Copco. (2007). Mining Methods in Underground Mining. Second Edition.

Becerra, C. (2011). Controlling drawpoints prone to pumping—El Teniente mine. In: Geomin 2011: Proceedings of the Second International Seminar on Geology for the Mining Industry, Antofagasta, Chile

Bilmes, J. (2020). Underfitting and Overfitting in Machine Learning. DataScience Foundation. https://www.kaggle.com/dansbecker/underfitting-and-overfitting

Botha, J., Watson, S., Arkadius, T., Samosir, E., (2008). Simulation applications at PT Freeport Indonesia's DOZ / ESZ block cave mine. Massmin 2008: Proceedings of The Sixth International Conference & Exhibition on Mass Mining, Canadian Institute of Mining, Metallurgy and Petroleum, Ontario, Canada. pp 237 – 246.

Brown, E. T. (2002). Block Caving Geomechanics (2nd Edition). Julius Kruttschnitt Mineral Research Centre, The University of Queensland.

Butcher, R., Joughin, W., & Stacey, T. (2000). A Booklet on Methods of Combating Mudrushes in Diamond and Base Metal Mines. In Safety in Mines Research Advisory Committee.

Call & Nicholas Inc, Co., Freeport-McMoRan Copper and Gold & Hydrology Consultants Inc. (1998). IOZ Wet Muck Study. Internal Report.

Casten, T., Johnson, M., Zimmer, C., & Mahayasa, M. (2020). PT Freeport Indonesia – The transition to underground production. MassMin 2020: Proceedings of the Eighth International Conference & Exhibition on Mass Mining, 23–38. https://doi.org/10.36487/acg_repo/2063_0.03

Casten, T., Clark, B., Ganesia, B., Barber, J., & Thomas, L. (2004). The DOZ Mine – A Case History of a mine startup. In A. Karzulovic, M. Alfaro, & Instituto de Ingenieros de Chile (Eds.), MassMin 2004 proceedings : 22-25 August 2004. Instituto de Ingenieros de Chile.

Castro, R., Garcés, D., Brzovic, A., & Armijo, F. (2018). Quantifying Wet Muck Entry Risk for Long-term Planning in Block Caving. Rock Mechanics and Rock Engineering. https://doi.org/10.1007/s00603-018-1512-3

Castro, R., Basaure, K., Palma, S., & Vallejos, J. (2017). Geotechnical characterization of ore related to mudrushes in block caving mining. Journal of the Southern African Institute of Mining and Metallurgy. https://doi.org/10.17159/2411-9717/2017/v117n3a9

Chawla, N. (2009). Data Mining for Imbalanced Datasets: An Overview. Data Mining and Knowledge Discovery Handbook, January 2005, 875–886. https://doi.org/10.1007/978-0-387-09823-4_45

Chawla, N., Bowyer, K, Hall, L., & Kegelmeyer, W. (2002). SMOTE: Synthetic minority over-sampling technique. Journal of Artificial Intelligence Research. https://doi.org/10.1613/jair.953

Coutts, B., Flint, D., Belluz, N., Susanto, H., Edwards, A., 1999. Geology of the Deep Ore Zone Ertsberg East Skarn System Irian Jaya, Indonesia, pp. 2-8 (Papua, Indonesia).

Dobson, A., & Barnett, A. (2018). An Introduction to Generalized Linear Models (4th Edition). Boca Raton. https://doi.org/10.1201/9781315182780

Dorador, L. (2016). Experimental investigation of the effect of broken ore properties on secondary fragmentation during block caving.

Dormann, C., Schymanski, S., Cabral, J., Chuine, I., Graham, C., Hartig, F., Kearney, M., Morin, X., Römermann, C., Schröder, B., & Singer, A. (2012). Correlation and process in species distribution models: Bridging a dichotomy. Journal of Biogeography. https://doi.org/10.1111/j.1365-2699.2011.02659.x

Eberhardt, E., Woo, K., Stead, D., & Elmo, D. (2015). Transition from surface to underground mining : Integrated mapping , monitoring and modeling data to better understand complex rock mass interaction. ISRM Congress 2015 Proceedings - Int'ernational Symposium on Rock Mechanics.

Edgar, I., Prasetyo, R., & Wilkinson, M. (2020). Deep Ore Zone mine wet ore mining empirical learnings, mining process evolution and development pathway. MassMin 2020: Proceedings of the Eighth International Conference & Exhibition on Mass Mining, 385–393. https://doi.org/10.36487/acg_repo/2063_24

Fernández, A., García, S., Galar, M., & Prati, R. (2019). Learning from Imbalanced Data Sets. Springer. https://doi.org/10.1007/978-3-319-98074-4

Fernández, A., García, S., Herrera, F., & Chawla, N. (2018). SMOTE for Learning from Imbalanced Data: Progress and Challenges, Marking the 15-year Anniversary. Journal of Artificial Intelligence Research, 61, 863–905. https://doi.org/10.1613/jair.1.11192

Freeport-McMoran. (2020). 2020 Climate Report. https://doi.org/10.1088/2058-7058/33/8/24

Ginting, A., & Pascoe, N. (2020). Grasberg open pit to Grasberg block cave transition wetmuck and mine design. MassMin 2020: Proceedings of the Eighth International Conference & Exhibition on Mass Mining, 357–369.

Haflil, D., De Jong, G., Wicaksono, D., & Soebari, L. (2014). Evidence of Lateral Movement-Rilling and Mining Implications at the DOZ (Deep Ore Zone) Block Cave Mine, Papua, Indonesia. Unpublished.

He, H., & Garcia, E. (2009). Learning from imbalanced data. IEEE Transsactions on Knowledge and Data Engineering. https://doi.org/10.1007/978-3-030-04663-7_4

Heslop, T G, 2000. Block caving-controllable risks and fatal flaws, in Proceedings MassMin 2000, pp 437-454 (The Australasian Institute of Mining and Metallurgy: Melbourne.)

Holder, A., Rogers, A., Bartlett, P., & Keytert, G. (2013). Review of mud rush mitigation on kimberley's old scraper drift block caves. Journal of the Southern African Institute of Mining and Metallurgy, 113(7), 529–537.

Höppner, S., Baesens, B., Verbeke, W., & Verdonck, T. (2021). Instance-dependent cost-sensitive learning for detecting transfer fraud. European Journal of Operational Research, 297(1), 291–300. https://doi.org/10.1016/j.ejor.2021.05.028

Hosmer, D., Lemeshow, S., & Sturdivant, R. (2013). Applied Logistic Regression. (3rd ed.). John Wiley & Sons, Inc., Hoboken. https://doi.org/10.2307/2532419

Hubert, G., Dirdjosuwondo, S., Plaisance, R., and Thomas, L. (2000). Tele-Operation at Freeport to Reduce Wet Muck Hazards. Proceedings of Massmin 2000, Brisbane, Australia, 29 October–2 November. Australasian Institute of Mining and Metallurgy, Melbourne.

Imbalanced Learn. (2021). Imbalanced-Learn Documentation. Available from https://imbalanced-learn.org/stable/

Jakubec, J., Clayton, R., & Guest, A. (2016a). Mudrush risk evaluation. CIM Journal, 7(1). https://doi.org/http://dx.doi.org/10.15834/cimj.2016.1

Jeni, L., Cohn, J., & De La Torre, F. (2013). Facing imbalanced data - Recommendations for the use of performance metrics. Proceedings - 2013 Humaine Association Conference on Affective Computing and Intelligent Interaction, ACII 2013, 245–251. https://doi.org/10.1109/ACII.2013.47

Juba, B., & Le, H. S. (2019). Precision-Recall versus accuracy and the role of large data sets. The Thirty-Third AAAI Conference on Artificial Intelligence (AAAI-19), 4039–4048. https://doi.org/10.1609/aaai.v33i01.33014039

King, G., & Zeng, L. (2001). Logistic regression in rare events data. Journal of Statistical Software. https://doi.org/10.18637/jss.v008.i02

Kotsiantis, S., Kanellopoulos, D., & Pintelas, P. (2006). Handling imbalanced datasets : A review. GESTS International Transactions on Computer Science and Engineering. http://citeseerx.ist.psu.edu/viewdoc/download?doi=10.1.1.96.9248&rep=rep1&type=pdf

Kuhn, M., & Johnson, K. (2013). Applied Predictive Modeling. Springer Nature. https://doi.org/10.1007/978-1-4614-6849-3

Kulkarni, A., Chong, D., & Batarseh, F. A. (2020). Foundations of data imbalance and solutions for a data democracy. In Data Democracy: At the Nexus of Artificial Intelligence, Software Development, and Knowledge Engineering. Elsevier Inc. https://doi.org/10.1016/B978-0-12-818366-3.00005-8

Labatut, V., & Cherifi, H. (2011). Evaluation of Performance Measures for Classifiers Comparison. Ubiquitous Computing and Communication Journal, 6:21-34, 2011. http://arxiv.org/abs/1112.4133

Laubscher, D. (2000). A Practical Manual On Block Caving - International Caving Study (1997 - 2000).

Liu, Q., & Wu, Y. (2012). Supervised Learning. Encyclopedia of the Sciences of Learning. https://doi.org/10.1007/978-1-4419-1428-6

Mani, S., Sankaran, A., Tamilselvam, S., & Sethi, A. (2019). Coverage Testing of Deep Learning Models using Dataset Characterization. http://arxiv.org/abs/1911.07309

Navia I, Castro R, Valencia M (2014) Statistical analyses of mud entry at Diablo Regimiento sector—El Teniente's Mine. In: Castro R (ed) Caving 2014: Proceedings of the third international symposium on block and sublevel caving, University of Chile, Santiago, Chile, pp. 372–378

Olua, D., Antoro, B., & Jong, G. De. (2015). Predicting Wetmuck Spills Based on Packmuck Distribution in DOZ Block Cave Mine, Papua. Prosiding TPT XXIV Dan Kongres IX PERHAPI.

Paetzold, H., Lourens, P., & Brazier, R. (2020). Reopening and closure of a block cave. MassMin 2020: Proceedings of the Eighth International Conference & Exhibition on Mass Mining, 103–114. https://doi.org/10.36487/acg_repo/2063_02

Park, H. A. (2013). An introduction to logistic regression: From basic concepts to interpretation with particular attention to nursing domain. Journal of Korean Academy of Nursing. https://doi.org/10.4040/jkan.2013.43.2.154

Pawluszek-Filipiak, K., & Borkowski, A. (2020). On the importance of train-test split ratio of datasets in automatic landslide detection by supervised classification. Remote Sensing. https://doi.org/10.3390/rs12183054

Prentice, M. L., & Hope, G. S. (2007). Climate of Papua. In A. Marshall & B. Beehler (Eds.), The Ecology of Papua: Part one. Periplus Editions.

PT. Freeport Indonesia. (2010a). UG Mine Division DOZ Engineering. Internal Document.

PT. Freeport Indonesia. (2010b). 3116 - 3126 Level Geology (DOZ Extraction). Internal Document.

PT. Freeport Indonesia. (2014). Pelatihan Wet Muck Assessor. Internal Document.

PT. Freeport Indonesia. (2015). Standard Operating Procedure (SOP) Underground Mine Division - General Procedure Wet Muck Handling. Internal Document.

PT. Freeport Indonesia. (2017). Interoffice Memo - DOZ 2017 Tracer Test Report. Internal Report.

PT. Freeport Indonesia. (2020). Standard Operating Procedure (SOP) Underground Mine Division - Wet Muck Inspection in Underground Mine Area DOZ and GBC. Internal Document.

Putra, F. (2016). East DOZ Dewatering Program in DOZ Underground Mine, PT. Freeport Indonesia, Papua, Indonesia.

Rachmad, L. (2016). Update Review Wetmuck and Wetmuck Analysis. Internal Report

Rachmad, L., Nicholas, D., & Standridge, L. (2011). Technical Assessment of Wetmuck Spill on 18 April 2011 and Proposed Modifications to the Wetmuck Operating Procedure at P.T Freeport Indonesia's DOZ/ESZ Mine. Internal Report

Ramadhan, M. R., Wicaksono, D., Haflil, D., & Antoro, B. (2015). New Perspective of Wetmuck Risk Map : Lesson Learned From Wet Muck Spill in Coarse Fragmentation at Deep Ore Zone (DOZ) Block Caving Mine, Papua, Indonesia. Prosiding TPT XXIV Dan Kongres IX PERHAPI.

Resolution Copper Mining. (2016). General Plan of Operations: Resolution Copper Mining.

Rubin, J., & Kyle, J. (1997). Precious metal mineralogy in porphyry-, skarn-, and replacement-type ore deposits of the ertsberg (Gunung Bijih) district, Irian Jaya, Indonesia. Economic Geology. https://doi.org/10.2113/gsecongeo.92.5.535

Sahupala, H., & Srikant, A. (2007). Geotechnical inputs for cave management in the DOZ block cave. 1st Canada - U.S. Rock Mechanics Symposium, Vancouver, Canada, May 2007. https://doi.org/10.1201/noe0415444019-c163

Samosir, E., Basuni , J., Widijanto, E., Syaifullah, T. (2008) The manage- ment of wet muck at PT Freeport Indonesia's Deep Ore Zone Mine. Massmin 2008: Proceedings of The Sixth International Conference & Exhibition on Mass Mining, Canadian Institute of Mining, Metallurgy and Petroleum, Ontario, Canada, pp. 323–332

Schober, P., & Schwarte, L. (2018). Correlation coefficients: Appropriate use and interpretation. Anesthesia and Analgesia, 126(5), 1763–1768. https://doi.org/10.1213/ANE.0000000000002864

Scikit Learn. (2021a). Sklearn.preprocessing.StandardScaler¶. Available from https://scikit-learn.org/stable/modules/generated/sklearn.preprocessing.StandardScaler.html#sklearn.preprocessing.StandardScaler.

Scikit Learn. (2021b). Sklearn.preprocessing.OneHotEncoder. Available from https://scikit-learn.org/stable/modules/generated/sklearn.preprocessing.OneHotEncoder.html

Scikit Learn. (2021c). Sklearn.linear_model.LogisticRegression¶. Available from https://scikit-learn.org/stable/modules/generated/sklearn.linear_model.LogisticRegression.html

Scikit Learn. (2021d). Sklearn. model_selection.TimeSeriesSplit. Available from https://scikit-learn.org/stable/modules/generated/sklearn.model_selection.TimeSeriesSplit.html

Shrestha, N. (2020). Detecting Multicollinearity in Regression Analysis. American Journal of Applied Mathematics and Statistics, 8(2), 39–42. https://doi.org/10.12691/ajams-8-2-1

Soebari, L., Sriyanto, I., Haflil, D., & Wicaksono, D. (2013). Study of Forsterite Skarn Movement in DOZ (Deep Ore Zone) Block Caving Underground Mine, Papua, Indonesia. MGEI PMR BALI 2013.

Spelmen, V., & Porkodi, R. (2018). A Review on Handling Imbalanced Data. Proceedings of the 2018 International Conference on Current Trends towards Converging Technologies, ICCTCT 2018. https://doi.org/10.1109/ICCTCT.2018.8551020

Susaeta, A. (2004). Theory of Gravity Flow (Part 2). In A. Karzulovic, M. Alfaro, & I. de I. de Chile (Eds.), MassMin 2004 proceedings : 22-25 August 2004. Instituto de Ingenieros de Chile.

Taiebat, M., Shahir, H., & Pak, A. (2007). Study of pore pressure variation during liquefaction using two constitutive models for sand. Soil Dynamics and Earthquake Engineering, 27, 60–72. https://doi.org/10.1016/j.soildyn.2006.03.004

Valencia, M. E., Basaure, K., Castro, R., & Vallejos, J. (2016). Towards and Understanding of Mud Rush Behaviour in Block-Panel Caving Mines.

Vallejos, J., Basaure, K., Palma, S., & Castro, R. (2017). Methodology for evaluation of mud rush risk in block caving mining. Journal of the Southern African Institute of Mining and Metallurgy, 117. https://doi.org/http://dx.doi.org/10.17159/2411-9717/2017/v117n5a7

Varian J (2019) Understanding the Trigger Mechanism of Mudrush Occurrence at PT Freeport Indonesia – Deep Ore Zone Panel Cave Mine. UBC MEng Project. Unpublished

Warren, A. (2005). COW A Geological Model. Internal Document.

Widijanto, E. (2006). Geotechnical challenges in the DOZ block cave mine. CF Leung & YX Zhou (eds), Proceedings of the 4th Asian Rock Mechanics Symposium: Rock Mechanic in Underground Construction, World Scientific Publishing Co. Pte. Ltd., Singapore, pp. 210–216.

Widijanto, E., Sunyoto, W. S., Wilson, A. D., Yudanto, W., & Soebari, L. (2012). Lessons Learned in Wet Muck Management in Ertsberg East Skarn System of PT Freeport Indonesia. Massmin 2012: Proceedings of The Sixth International Conference & Exhibition on Mass Mining.

World Weather Online. (2022). Tembagapura Climate Weather Averages. Available from https://www.worldweatheronline.com/tembagapura-weather-averages/papua/id.aspx

Appendices

Appendix A - Variable Development, Descriptions, and Assumptions

The analysis was completed for each drawpoint, where each drawpoint coordinate and elevation was provided by PTFI and used to develop each drawpoint distance for spatially manipulated variables. The study database was developed based on daily drawpoint observations ranging from January 2008 to June 2019. Each drawpoint has multiple attributes associated with hypothetical wet muck spill causative and triggering factors experienced from various caving operations totaling 177 variables. Publicly available software, Python, was used for data processing and statistical analysis. The Mira Geoscience software package was used to convert LiDAR data into the CSV format. A description of each variable development, the spatio-temporal manipulation, and associated assumptions are described below:

A.1 Wet Muck Spill

A list of confirmed wet muck spills at the DOZ mine, including the run-out characteristics, seismic events, mining activities, and severity, was provided by PTFI. At the DOZ mine, an uncontrollable muck discharge is considered a wet muck spill when the muck outflow surpasses the opposite panel rib. For every drawpoint in the study database, events were recorded as spill (1) or no-spill (0) on a daily basis, with the assumption of the absence of wet muck spill when there were no reported spills. Daily repetitive spills from a drawpoint were recorded as one event ignoring the frequency.

A.2 Drawpoint Wet Muck Classification

All permanently closed drawpoints were removed from the study database, as the drawpoints were no longer operational. Actively drawn drawpoints with wet muck spills recorded at closed drawpoints were checked and adjusted based on the supporting documents. The drawpoint classification describes the fragmentation size and water content of a drawpoint. Each drawpoint is mapped through an Android table, capturing the material fragmentation and water content, water discharge, and rock types. At PTFI caving operations, fragmentation size is recorded in alphabet convention, while water content is recorded in numbering convention (Figure X). PT. Freeport Indonesia (2020) defines each convention as follows:

- A – Dominant coarse material(>5cm) with a percentage of above 70%.
- B – Mixture of coarse and fines (< 5cm) with the percentage between 30% to 70%
- C – Dominant fine muck (< 5cm) with a percentage of above 70%
- 1 – Dry condition muck
- 2 – Moist condition muck with 8.5% to 11% water content
- 3 – Wet condition with water content greater than 11%

The A3, B2, B3, C2, and C3 classifications are considered as wet muck drawpoints. A drawpoint is reported as Closed Temporary (CT) when there is drawpoint maintenance, spill clean-up, hang-up, or high spill susceptibility, while a drawpoint is reported as Closed Permanently (CP) when it is no longer operational. The CP drawpoints were removed from the study database, while the CT drawpoints were manually adjusted following the previous class. Although it is important to continuously update drawpoint class, it is not feasible to map all potential wet muck drawpoints due to the safety risks. To reduce this data gap, it was assumed that wet muck drawpoints do not change classification until they are mapped again. An adjacent drawpoint is created based on the drawpoint coordinate, which is filled with the drawpoint class. In this study database, an adjacent drawpoint refers to a neighboring drawpoint within the same drawbell.

A.3 Total Number of Wet Muck Neighboring Drawpoints

The total number of wet muck neighboring drawpoints was calculated by summing the total number of wet muck class drawpoints within a specified radius of influence on each day. The radius of influence was set at 24 m, 36 m, and 48 m with a circular layout. This variable represents the general wet muck condition of each drawpoint within the specified radius of influence. It is hypothesized that wet muck material can migrate to surrounding drawpoints, changing the drawpoint classification to a worse classification.

A.4 Height of Draw and Extraction Ratio

The HoD is a vertical distance of a drawpoint draw column, while extraction ratio is the ratio of actual HoD over the planned HoD. At the DOZ mine, HoD and extraction ratio are measured on a monthly basis. Adjacent HoD and adjacent extraction ratio were also developed to analyze the influence of differential HoD and differential extraction ratio at the drawbell.

The wet muck susceptibility analysis requires these datasets to be converted on a daily basis with the exact value from the first day to the last day of the month. Interpolation of the data on a daily basis had very minimal influence as the changes from month to month are small and did not have any effect on the data distribution.

A.5 Tonnages

The tonnage dataset, which represents the amount of material drawn for production from each drawpoint, was recorded on a daily basis. Several temporal periods were developed for the tonnage dataset at lags of 1 day, 2 days, 3 days, 7 days, 14 days, 21 days, and 28 days to understand the cumulative influence of tonnage on wet muck spills. It is hypothesized that the higher the tonnage drawn from a drawpoint, the higher the probability of a wet muck spill occurrence. At a spill drawpoint, the recorded tonnages may be combined with the production tonnages and spill clean-up tonnages. It is unknown whether a spill clean-up is conducted within the same day as the spill. Therefore, the temporal period considered cumulative lagging of the specified period, starting from one day before. A similar principle was applied to the development of the adjacent tonnage dataset. Differential tonnage for each temporal period was calculated by deducting the drawpoint tonnage from the adjacent drawpoint tonnage within the same drawbell.

A.6 Mucking Activity.

The presence of mucking activity (1) in the drawpoint was set when the drawpoint was drawn over 10 tonnes (1 bucket) per day, while mucking lower than 10 tonnes was recorded as absent (0). This threshold was set to minimize bias in the tonnage dataset caused by the tonnage drawn and clean-up of spills. In this study database, mucking activity was transformed from lags of 1 day, 2 days, 3 days, 7 days, 14 days, 21 days and 28 days to analyze the impact of mucking on spill susceptibility. A similar approach was applied to the adjacent drawpoint mucking activity.

A.7 Cumulative Days of No Mucking.

The cumulative days of no mucking activity were developed using the daily mucking activity dataset. If a drawpoint was consecutively mucked over 10 tonnes per day over the specified period, it was considered as presence (1) and absence (0) when no consecutive mucking activities were observed.

A.8 Vertical Distance from Drawpoint to IOZ and Surface Subsidence

The nearest distance between the IOZ cave footprint and yearly surface subsidence was measured from each DOZ drawpoint in meters. In addition, the presence (1) or absence (0) of the overlying IOZ and surface subsidence above each drawpoint was assigned to each drawpoint.

A.9 Uniformity of Draw (UI, SPUI, and number of inactive drawpoints)

The UI is a function of tonnage, which adds the value of the specific index of uniformity and the total of inactive drawpoinst within the radius of influence and time period (Equation 2.1). The SPUI is measured from the difference in tonnages drawn from drawpoints in the vicinity of one another over a given time period. At PTFI, UI input data is calculated through the sum of tonnage over "n" days. The calculation of average "n" days UI provides calculation bias, as it is not operationally feasible to muck all drawpoints and have a low average UI value. SPUI and the number of inactive drawpoint datasets were also developed to analyze their correlation with wet muck spills. Various radii of influence were developed based on the five nearest drawpoints, seven nearest drawpoints, drawpoints within 24 m, drawpoints within 36 m, and drawpoints within 48 m. In addition, each of the radii was extended for each temporal period from lags of 1 day, 2 days, 3 days, 7 days, 14 days, 21 days, and 28 days.

A.10 Rainfall

Rainfall data is recorded at the nearby station on the surface. Since it is unknown how much precipitation entering the cave flows to each drawpoint, it was assumed that every drawpoint experienced the same rainfall intensity throughout the footprint on any given day, temporally manipulated from daily to a cumulative lag of 28 previous days.

A.11 Geological Domain

The DOZ mine consists of two different geological domains: the EESS (mainly skarn) and ESZ (mainly diorite). Drawpoints located in the EESS domain were specified with a value of 1, while drawpoints located in the ESZ domain were specified with a value of 2.

Appendix B - Exploratory Data Analysis

B.1 Draw Column Distributions

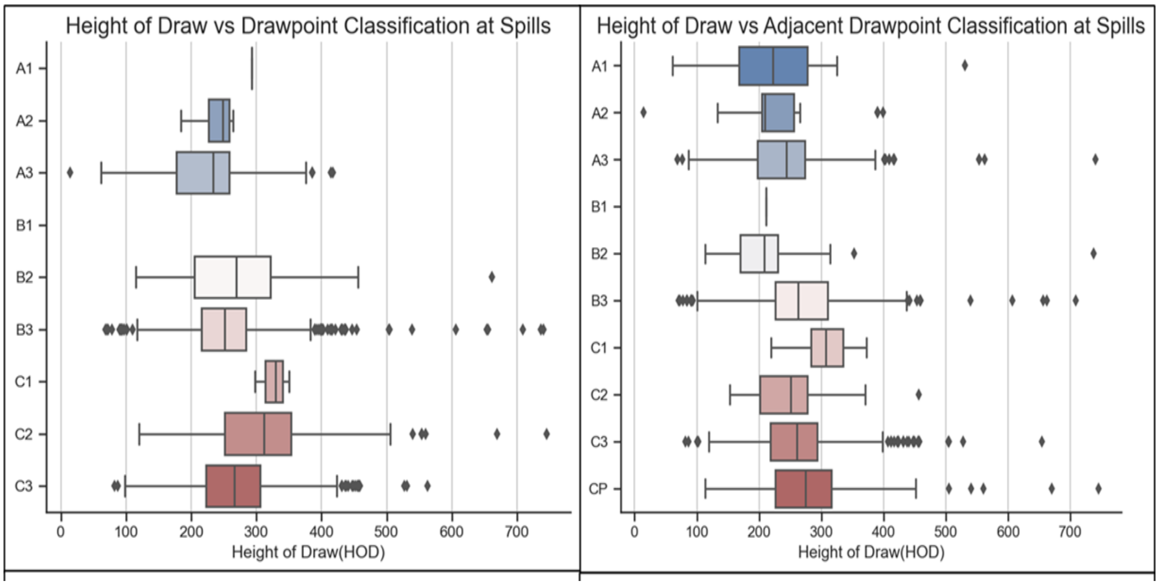

Figure B.1. Height of draw (left) and adjacent height of draw (right) distribution at each drawpoint class.

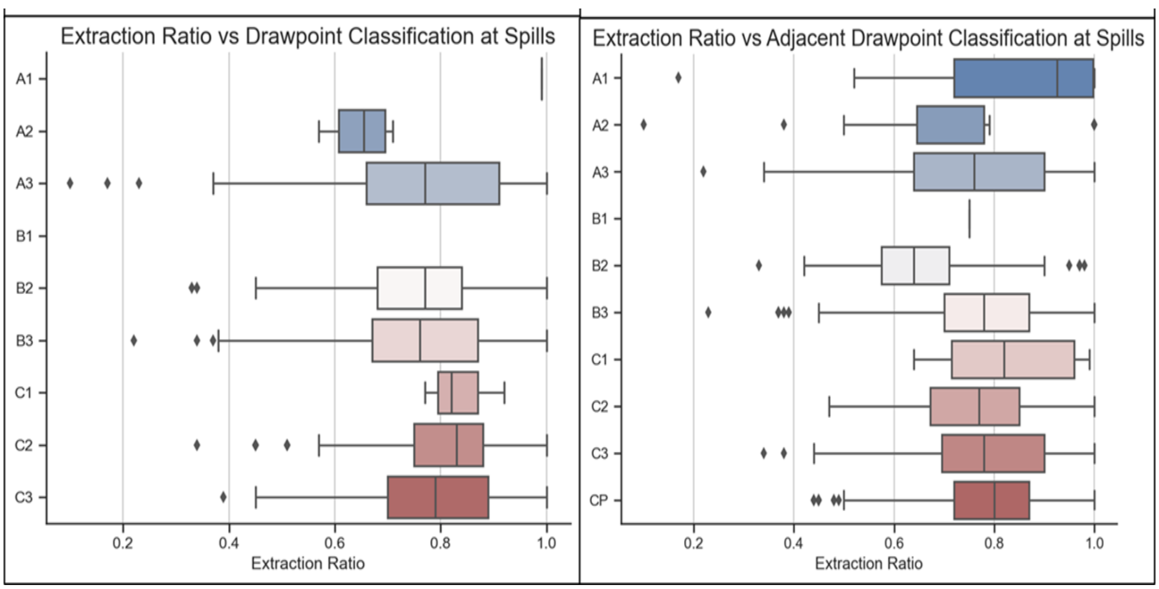

Figure B.2. Extraction ratio (left) and adjacent extraction ratio (right) distribution at each drawpoint class.

B.2 Uniformity of Draw Distributions

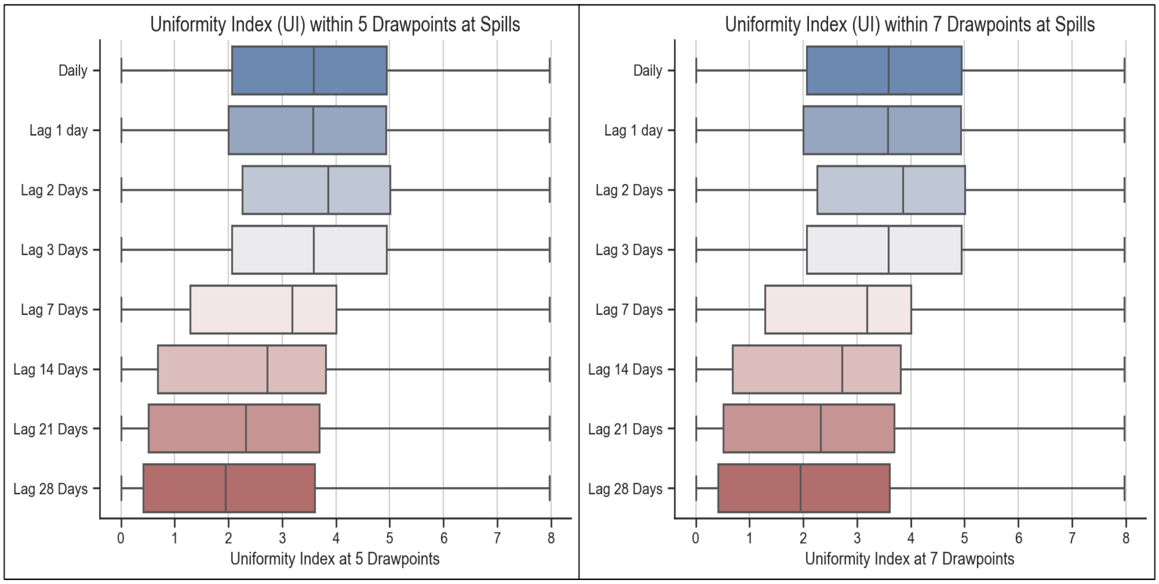

Figure B.3. Distribution of wet muck spills with uniformity index within five nearest drawpoints (left) and uniformity index within seven nearest drawpoints (right).

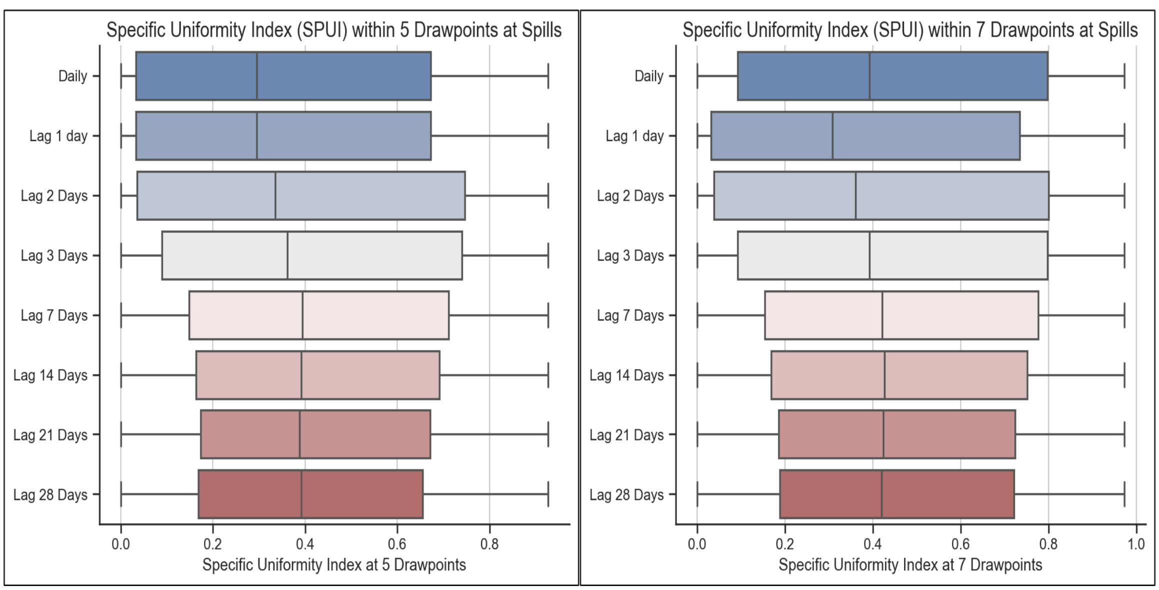

Figure B.4. Distribution of wet muck spills with specific index of uniformity within five nearest drawpoints (left) and specific index of uniformity within seven nearest drawpoints (right).

3

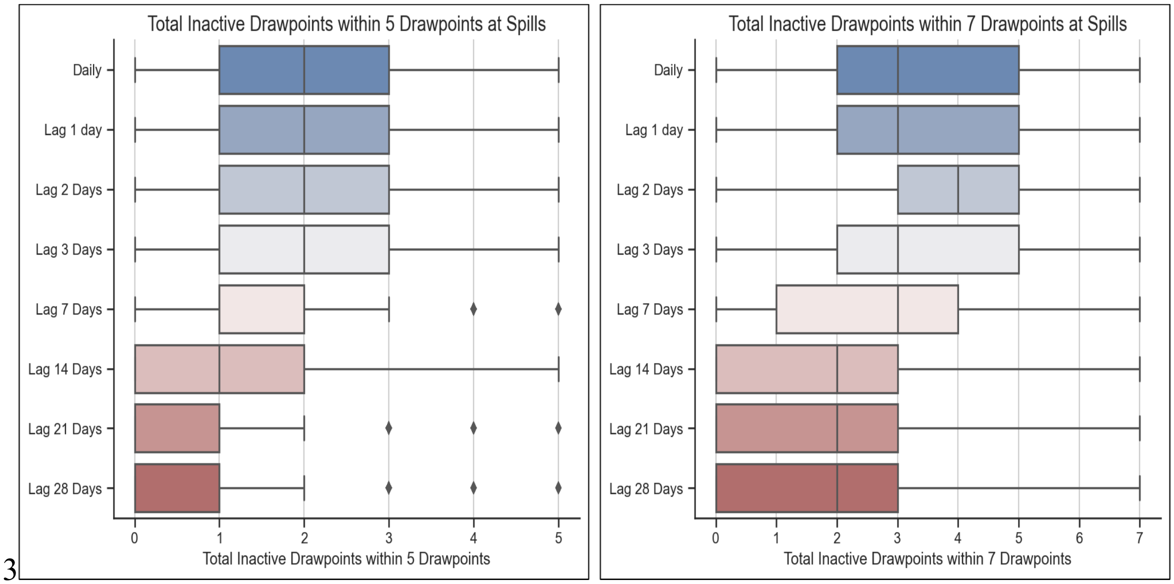

Figure B.5. Distribution of wet muck spills with total inactive drawpoints within five nearest drawpoints (left) and total inactive drawpoints within seven nearest drawpoints (right).

B.3 Tonnages Dataset Distributions

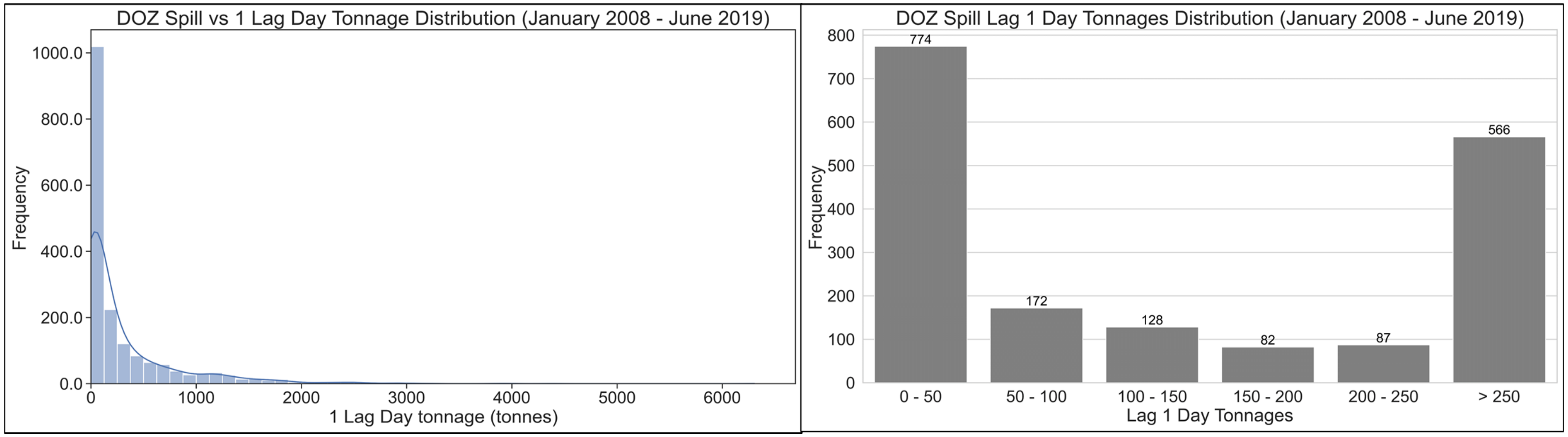

Figure B.6. Distribution of wet muck spills at lag one-day drawpoint tonnages.

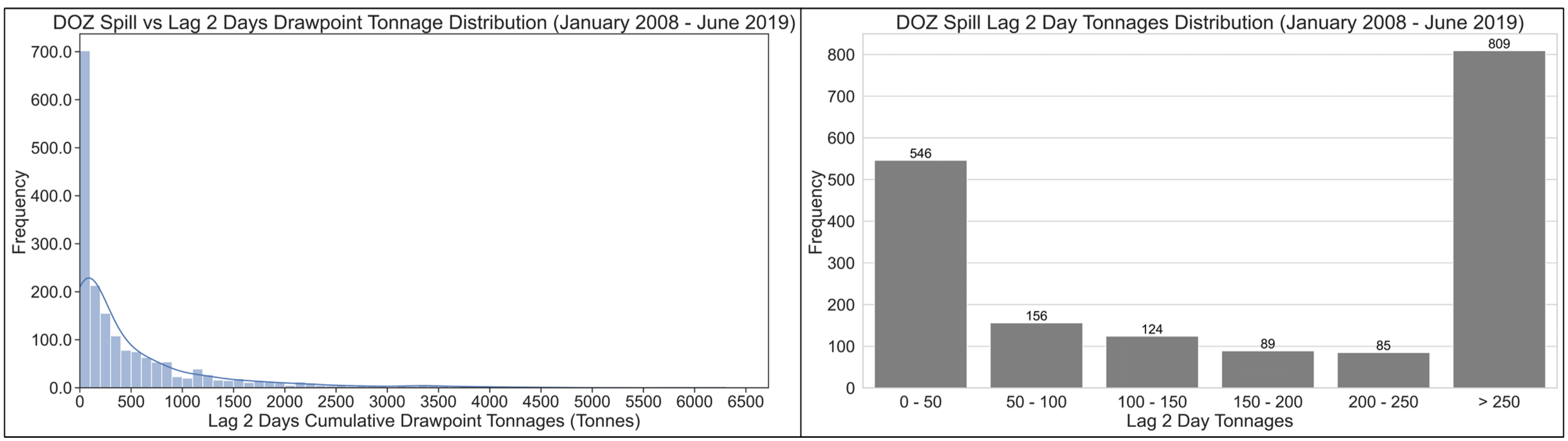

Figure B.7. Distribution of wet muck spills at cumulative lag two days drawpoint tonnages.

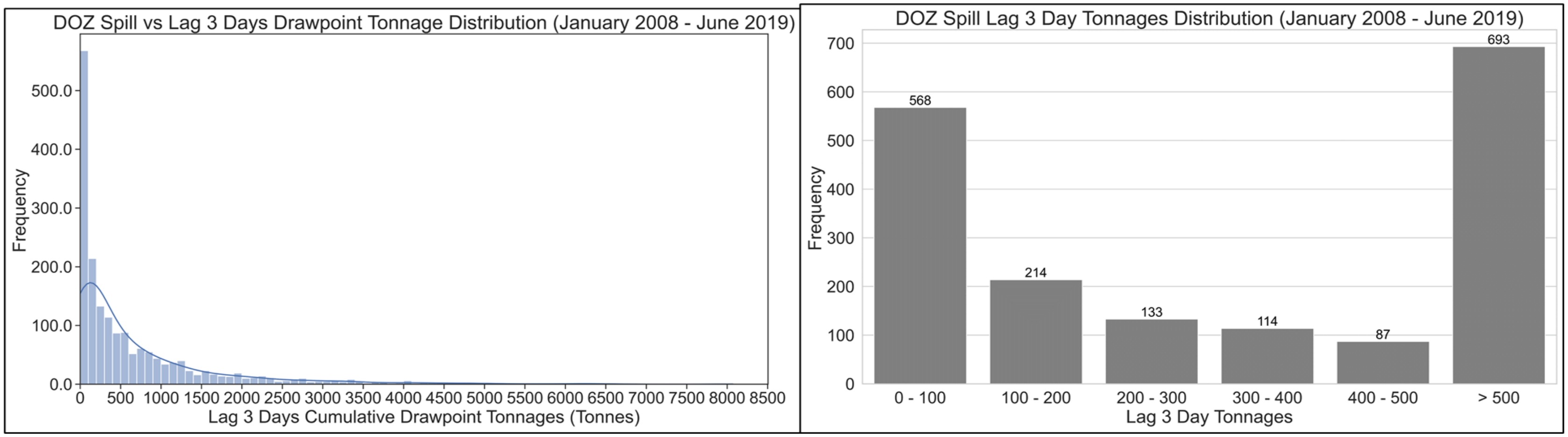

Figure B.8. Distribution of wet muck spills at cumulative lag three days drawpoint tonnages.

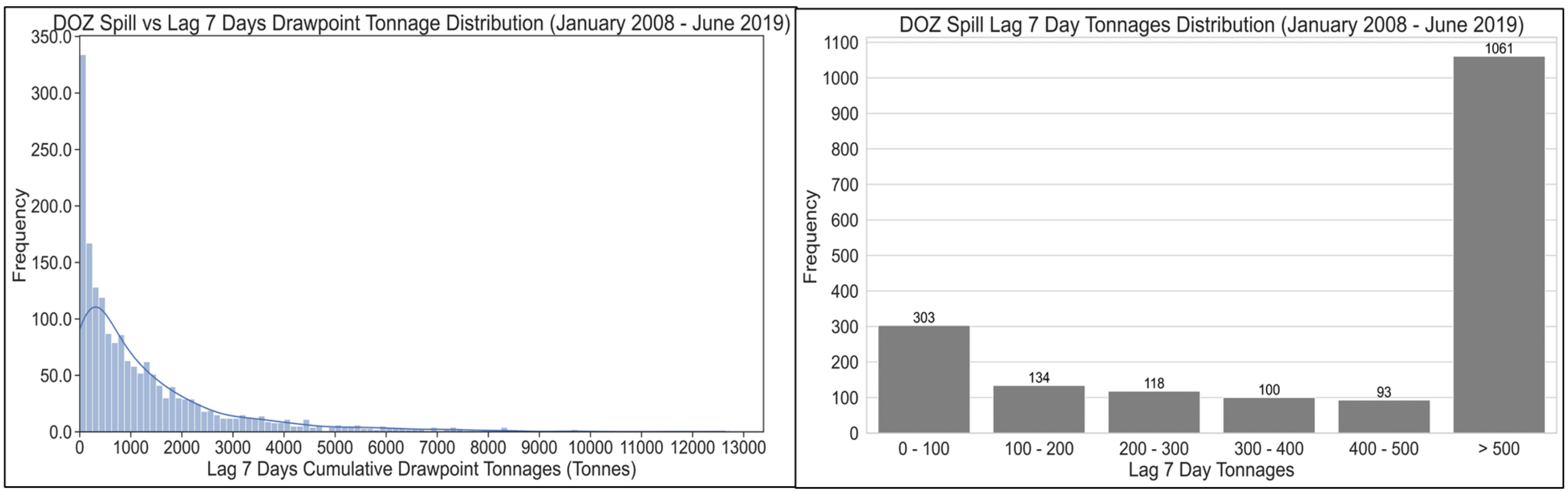

Figure B.9. Distribution of wet muck spills at cumulative lag seven days drawpoint tonnages.

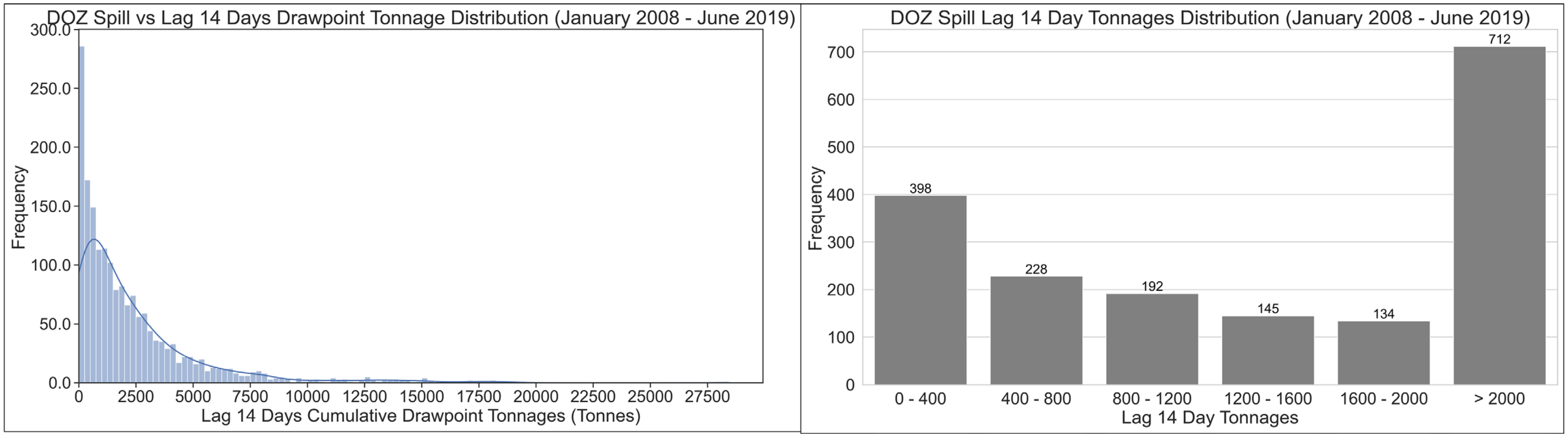

Figure B.10. Distribution of wet muck spills at cumulative lag fourteen days drawpoint tonnages.

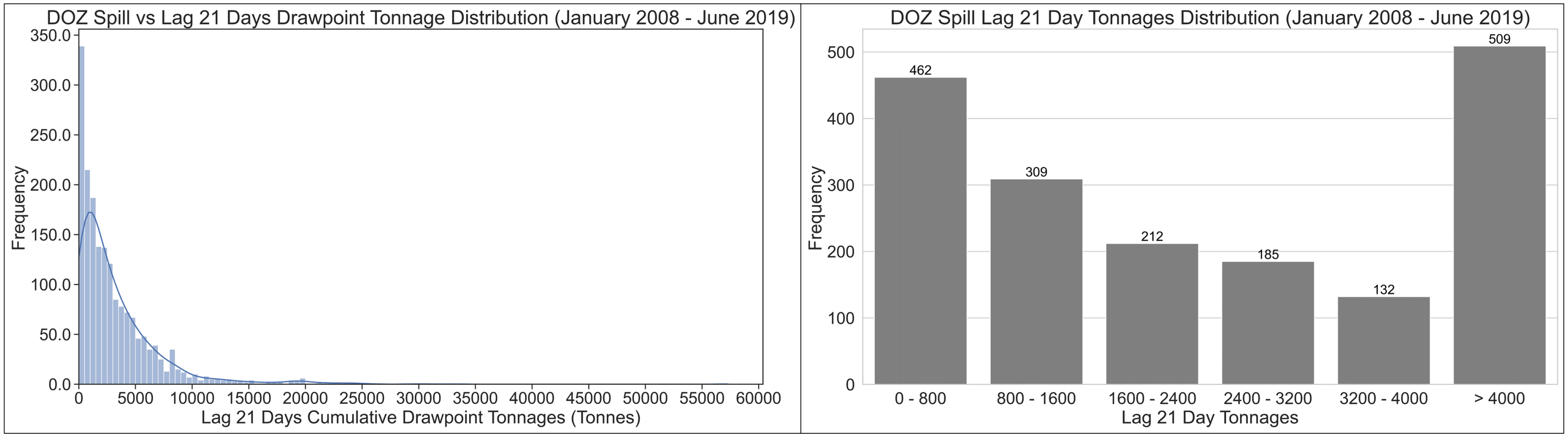

Figure B.11. Distribution of wet muck spills at cumulative lag twenty-one days drawpoint tonnages.

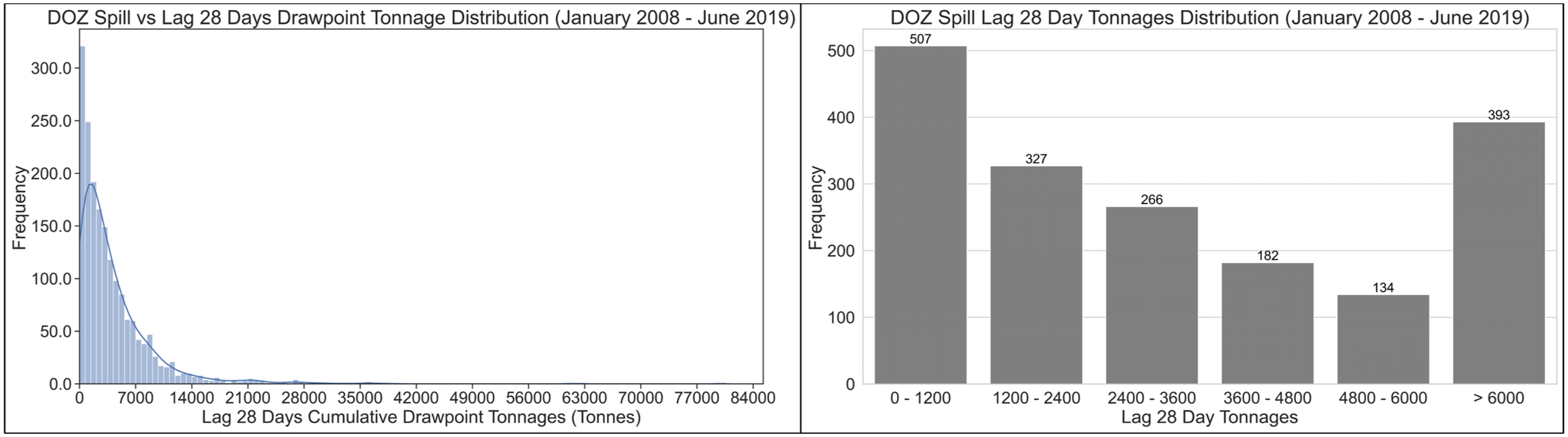

Figure B.12. Distribution of wet muck spills at cumulative lag twenty-eight days drawpoint tonnages.

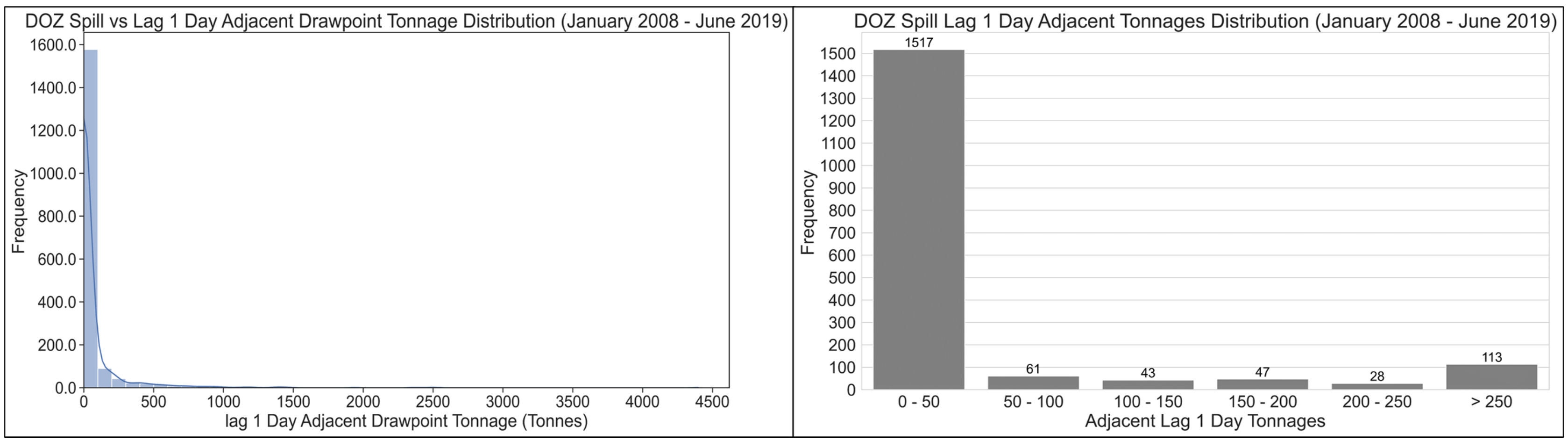

Figure B.13. Distribution of wet muck spills at lag one-day adjacent drawpoint tonnages.

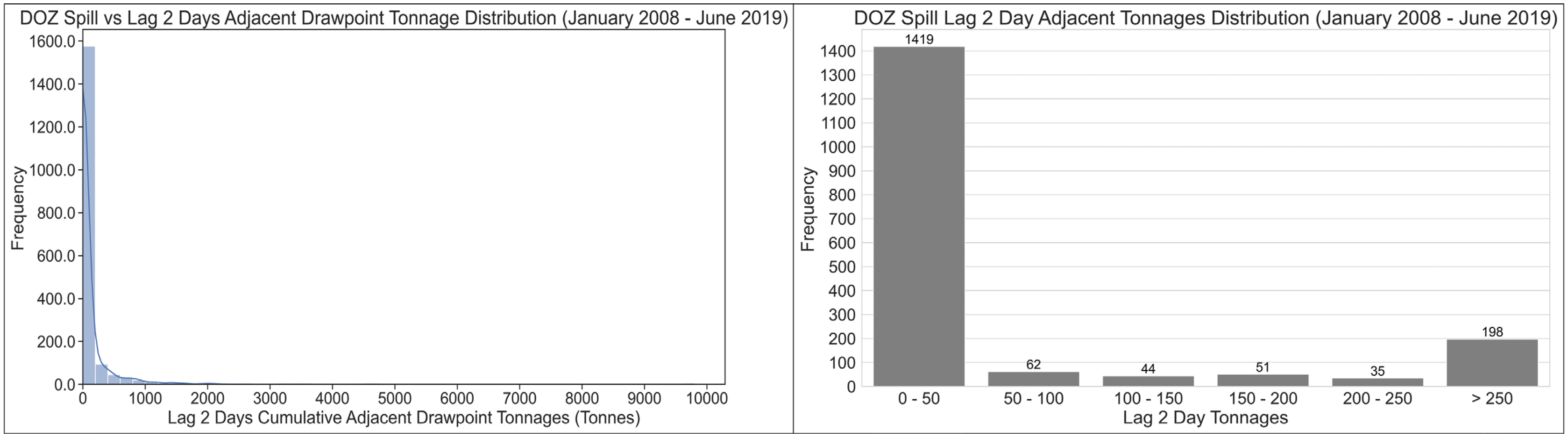

Figure B.14. Distribution of wet muck spills at cumulative lag two days adjacent drawpoint tonnages.

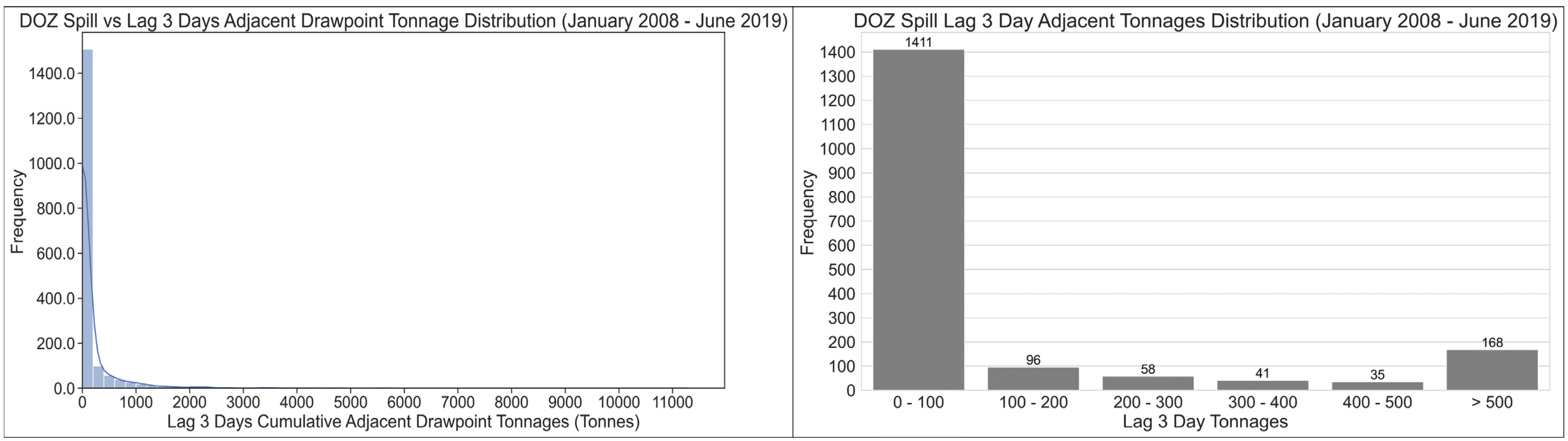

Figure B.15. Distribution of wet muck spills at cumulative lag two days adjacent drawpoint tonnages.

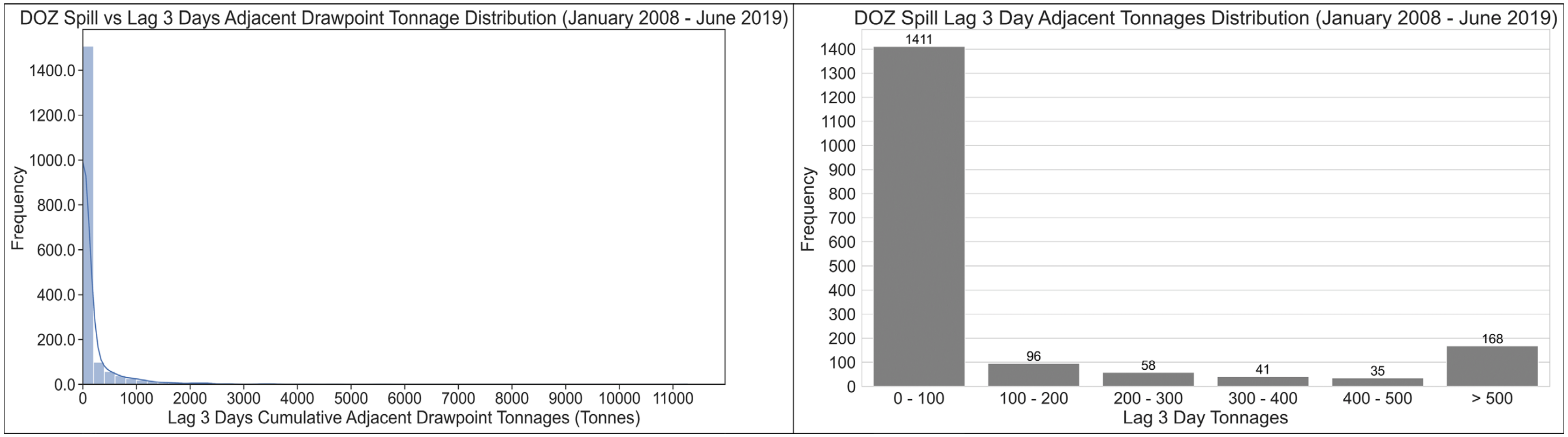

Figure B.16. Distribution of wet muck spills at cumulative lag three days adjacent drawpoint tonnages.

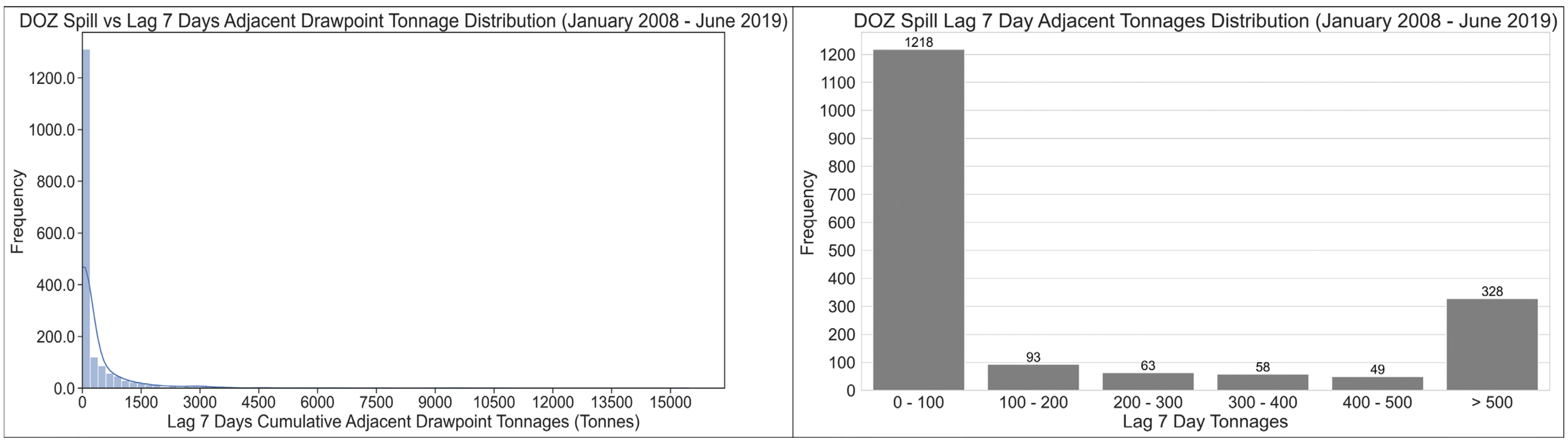

Figure B.17. Distribution of wet muck spills at cumulative lag seven days adjacent drawpoint tonnages.

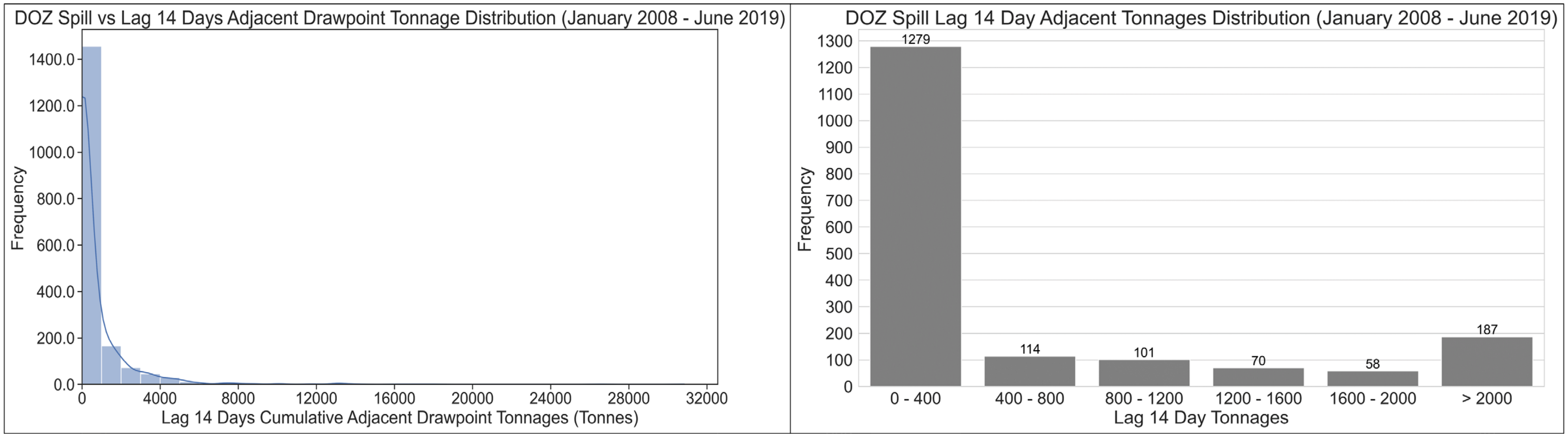

Figure B.18. Distribution of wet muck spills at cumulative lag fourteen days adjacent drawpoint tonnages.

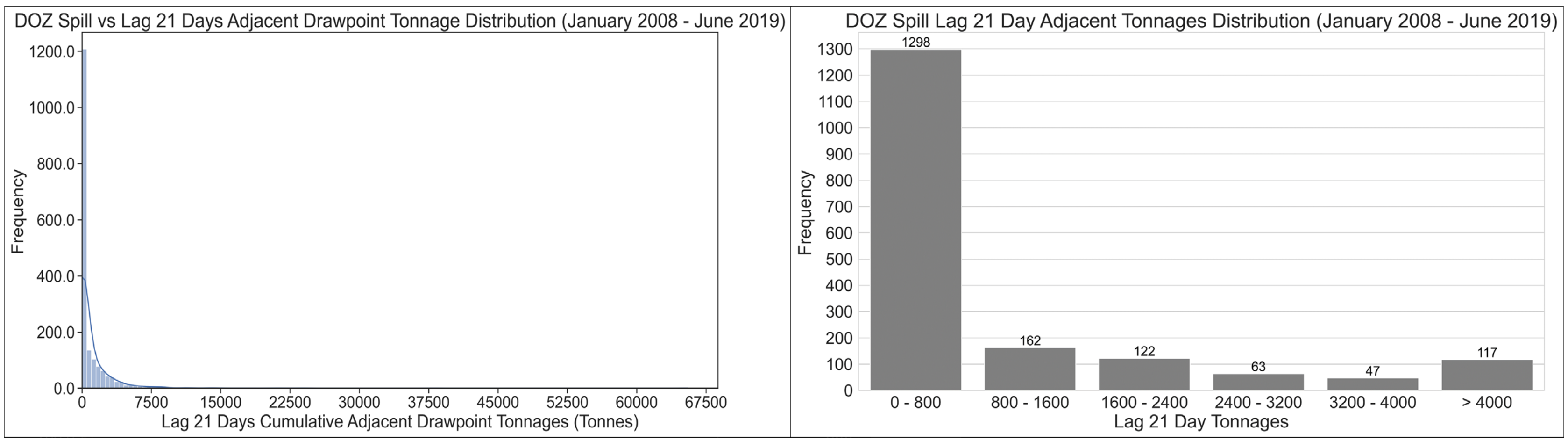

Figure B.19. Distribution of wet muck spills at cumulative lag twenty-one days adjacent drawpoint tonnages.

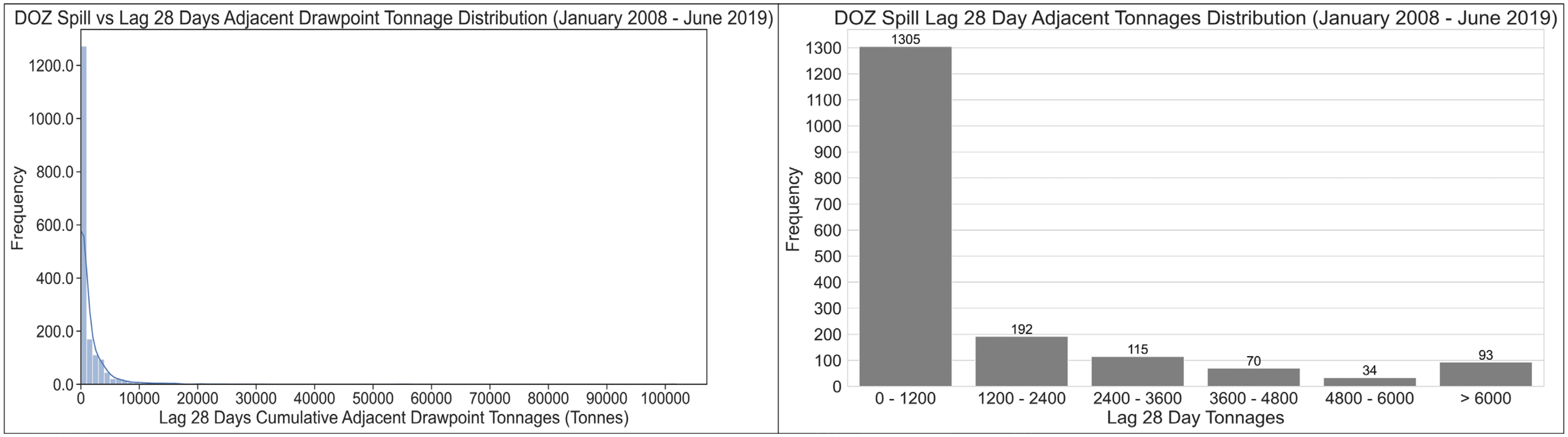

Figure B.20. Distribution of wet muck spills at cumulative lag twenty-eight days adjacent drawpoint tonnages.

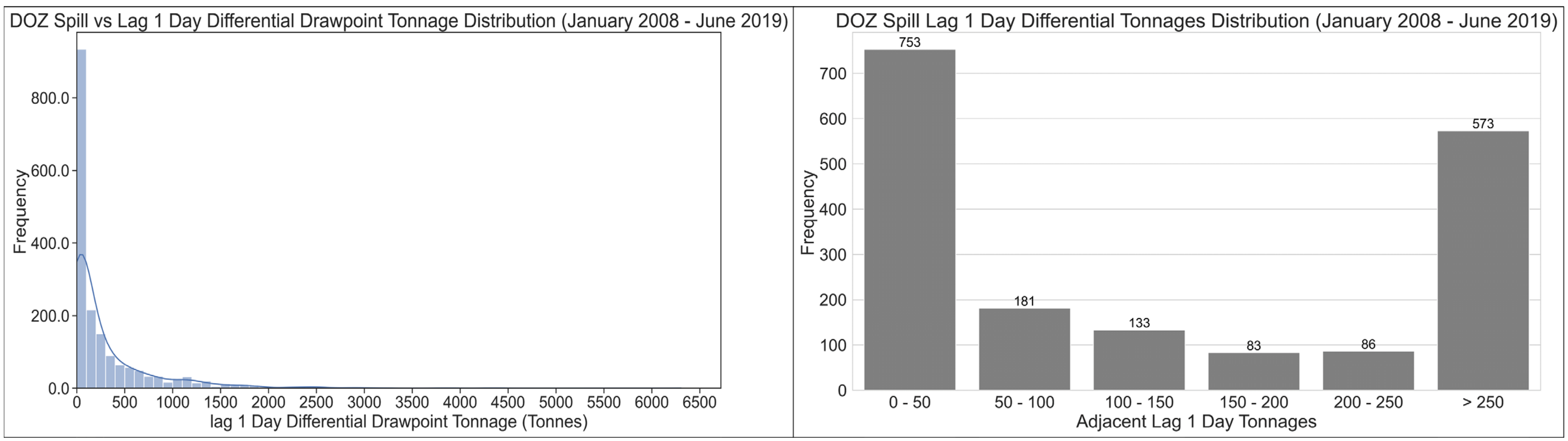

Figure B.21. Distribution of wet muck spills at lag one-day differential drawpoint tonnages.

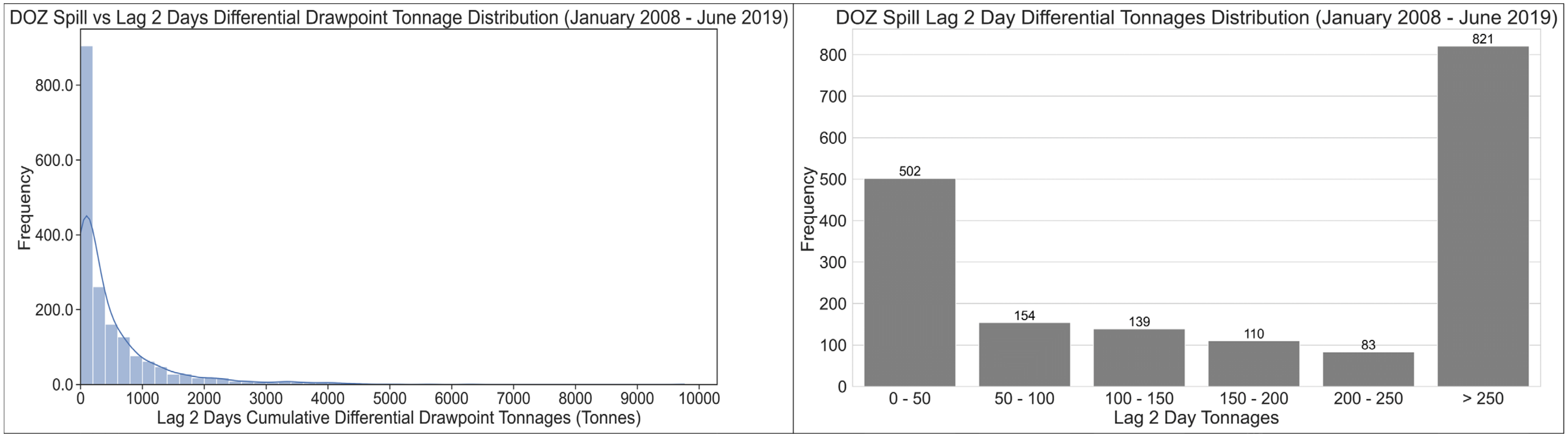

Figure B.22. Distribution of wet muck spills at cumulative lag two days differential drawpoint tonnages.

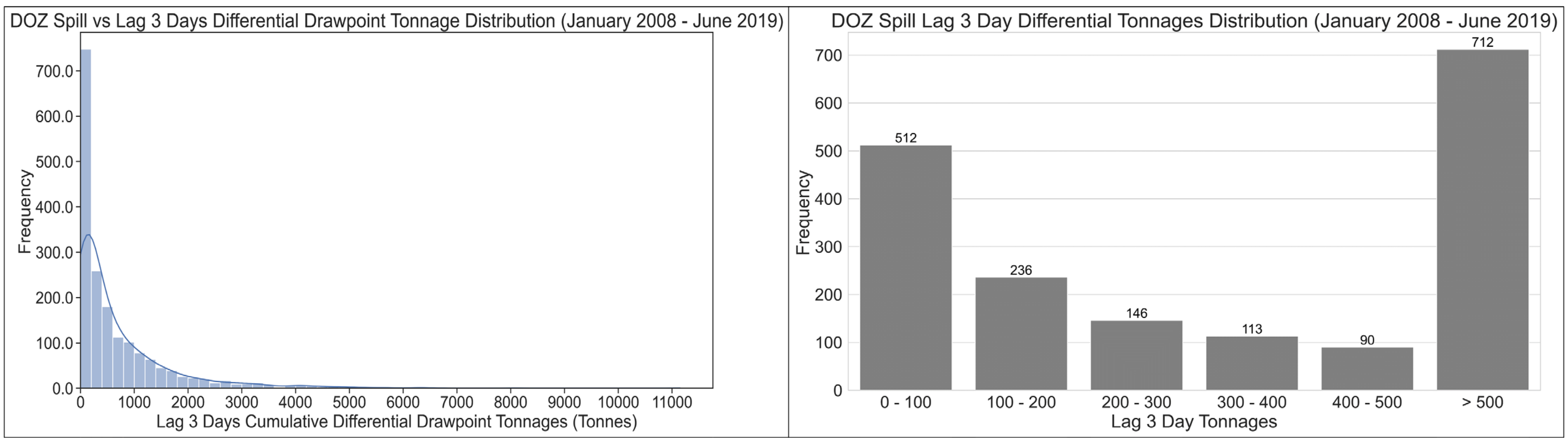

Figure B.23. Distribution of wet muck spills at cumulative lag three days differential drawpoint tonnages.

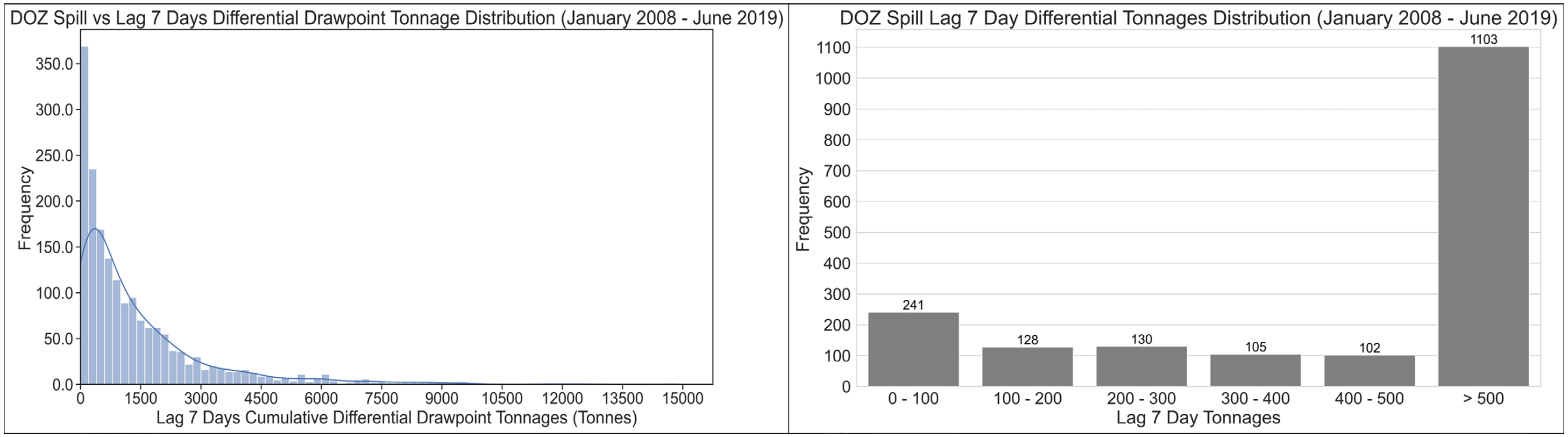

Figure B.24. Distribution of wet muck spills at cumulative lag seven days differential drawpoint tonnages.

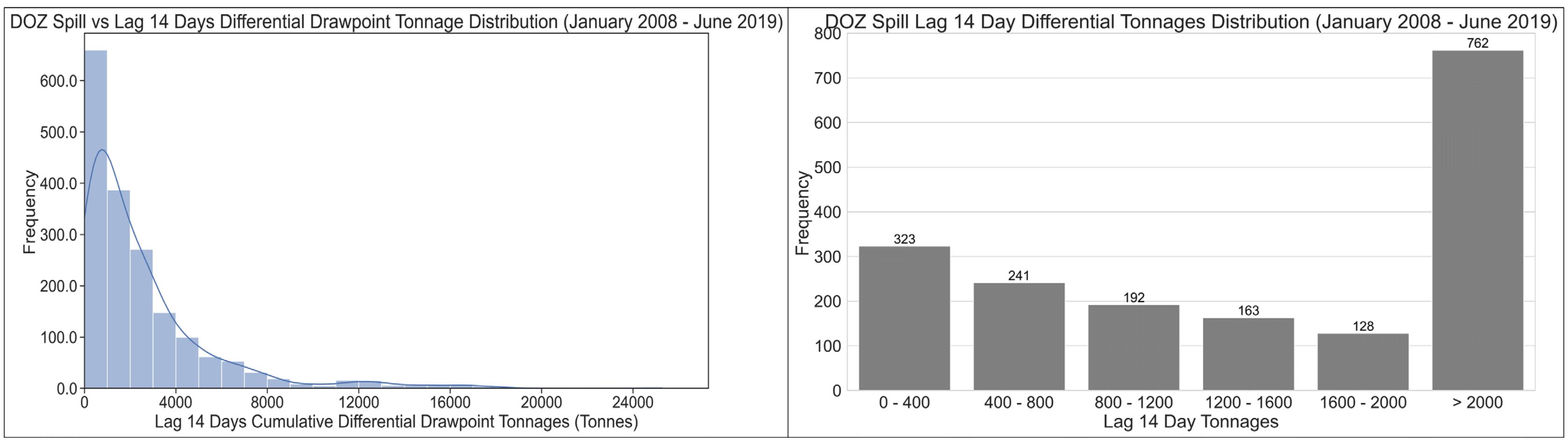

Figure B.25. Distribution of wet muck spills at cumulative lag fourteen days differential drawpoint tonnages.

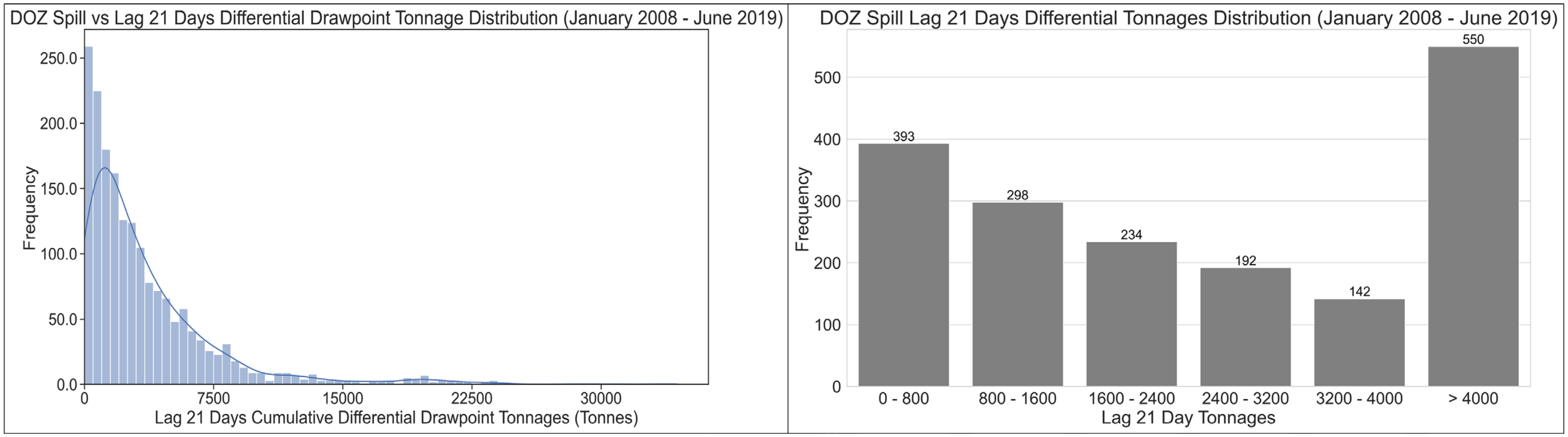

Figure B.26. Distribution of wet muck spills at cumulative lag twenty-one days differential drawpoint tonnages.

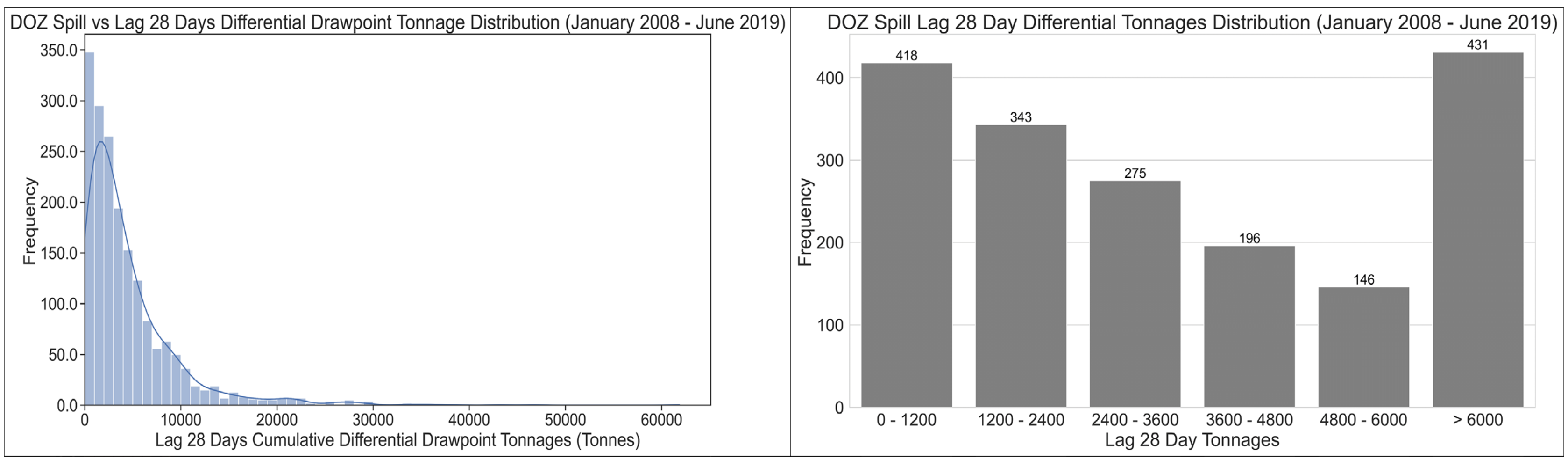

Figure B.27. Distribution of wet muck spills at cumulative lag twenty-eight days differential drawpoint tonnages.

B.4 Rainfall Dataset Distributions

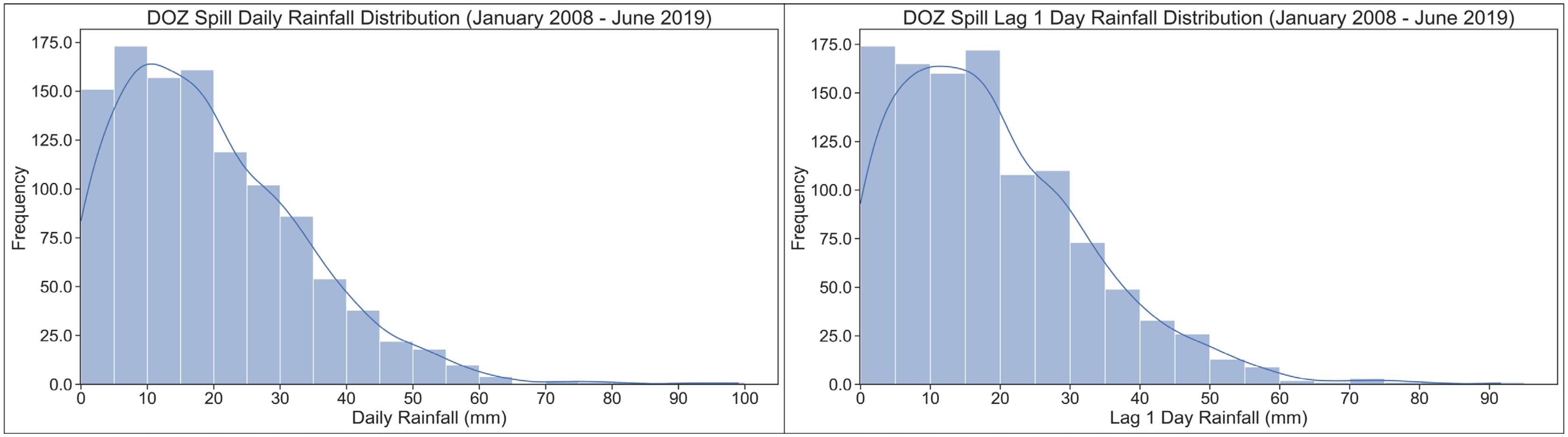

Figure B.28. Distribution of daily rainfall (left) and lag one-day rainfall (right) with wet muck spills occurrences.

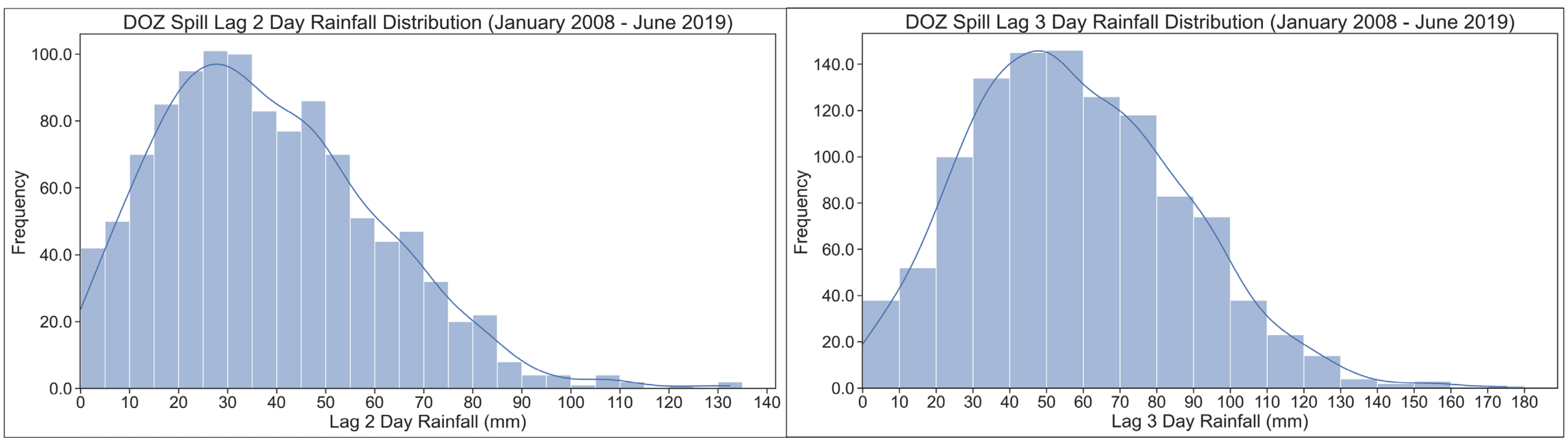

Figure B.29. Distribution of cumulative two days rainfall (left) and three days rainfall (right) with wet muck spills occurrences.

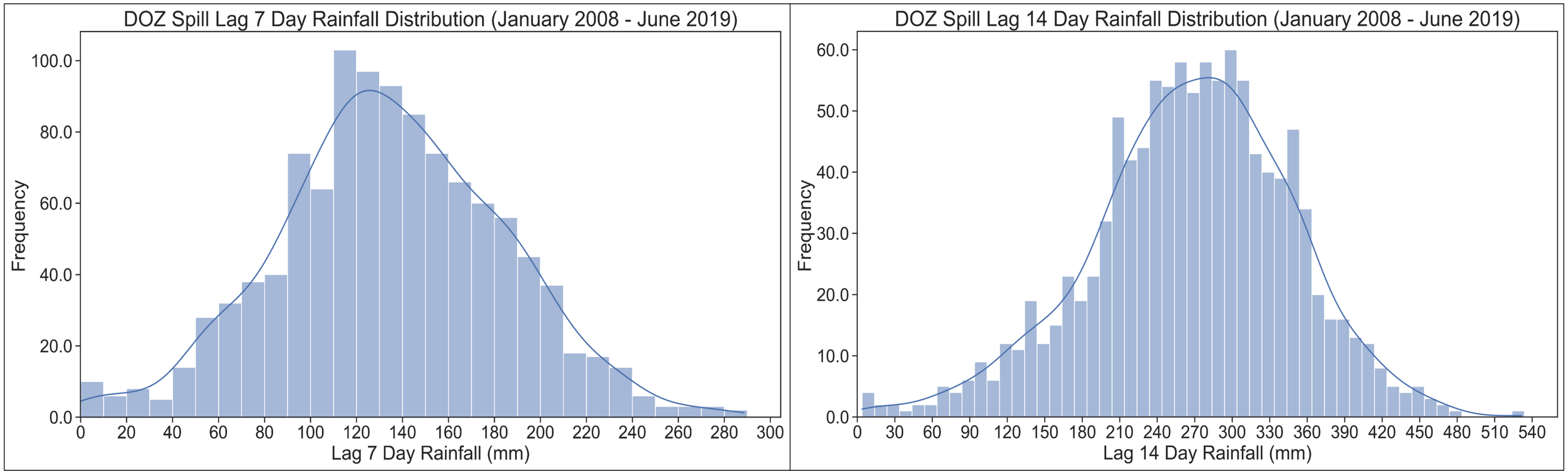

Figure B.30. Distribution of cumulative seven days rainfall (left) and fourteen days rainfall (right) with wet muck spills occurrences.

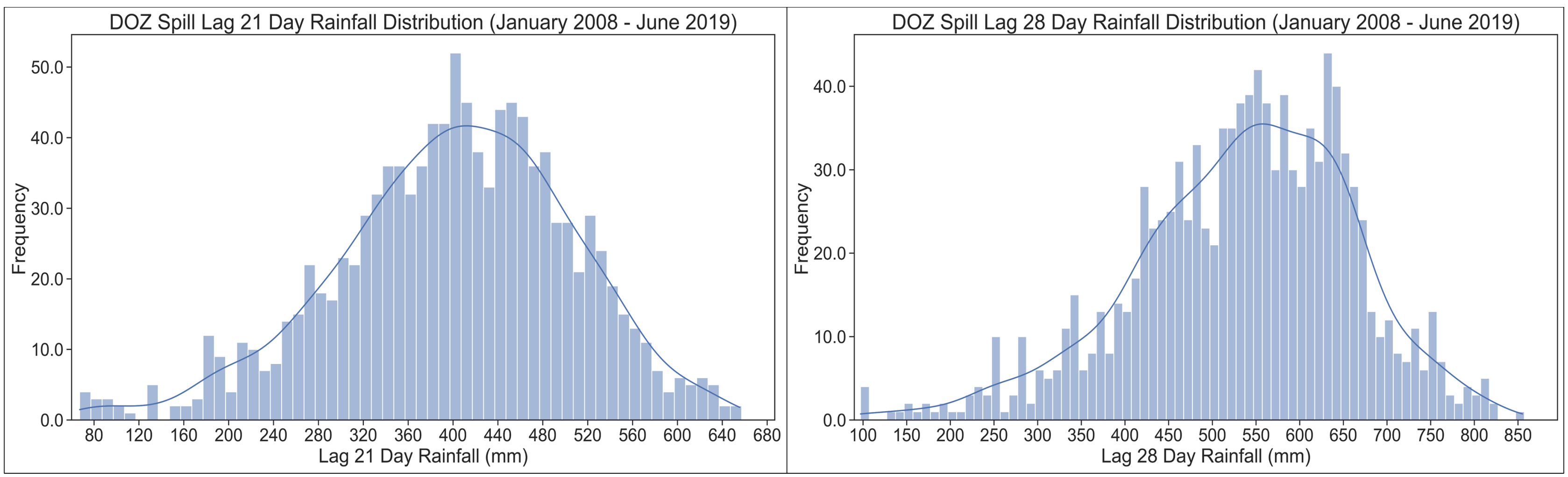

Figure B.31.Distribution of cumulative twenty-one days rainfall (left) and twenty-eight days rainfall (right) with wet muck spills occurrences.

B.5 Mucking Activities Distribution

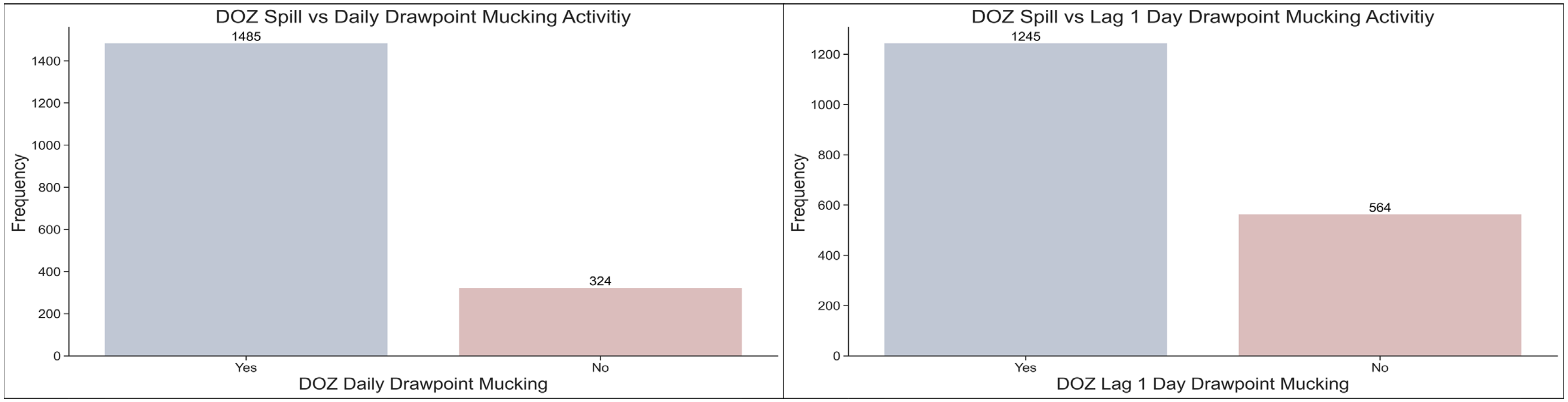

Figure B.32. Distribution of wet muck spills with the presence or absence of daily mucking activity (left) and lag one-day mucking activity (right).

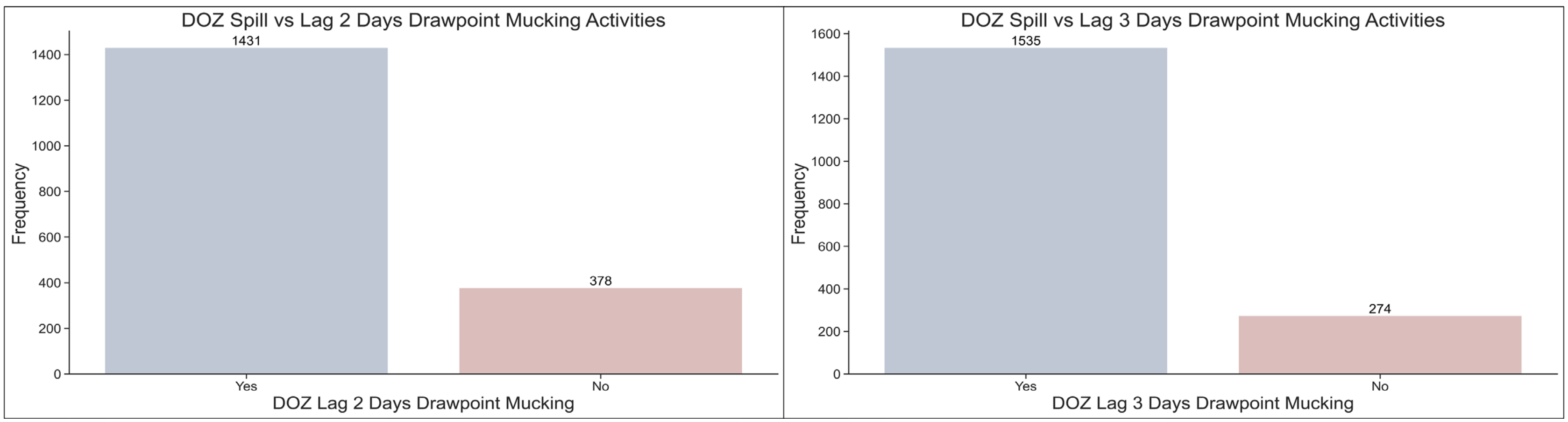

Figure B.33. Distribution of wet muck spills with the presence or absence of cumulative lag two days mucking activity (left) and cumulative lag three-day mucking activity (right).

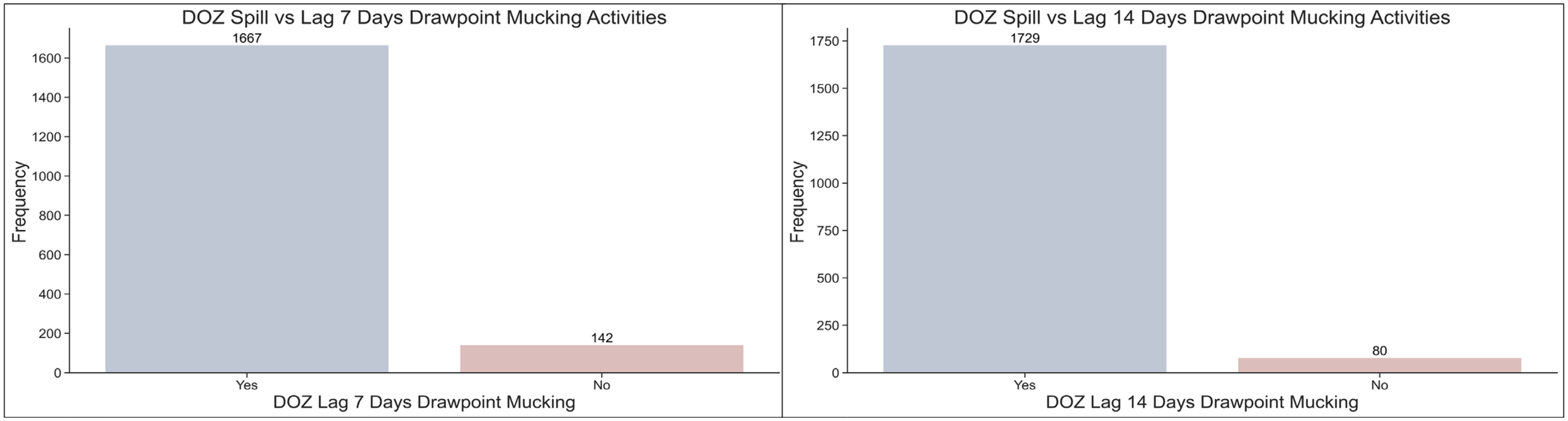

Figure B.34.Distribution of wet muck spills with the presence or absence of cumulative lag two days mucking activity (left) and cumulative lag three-day mucking activity (right).

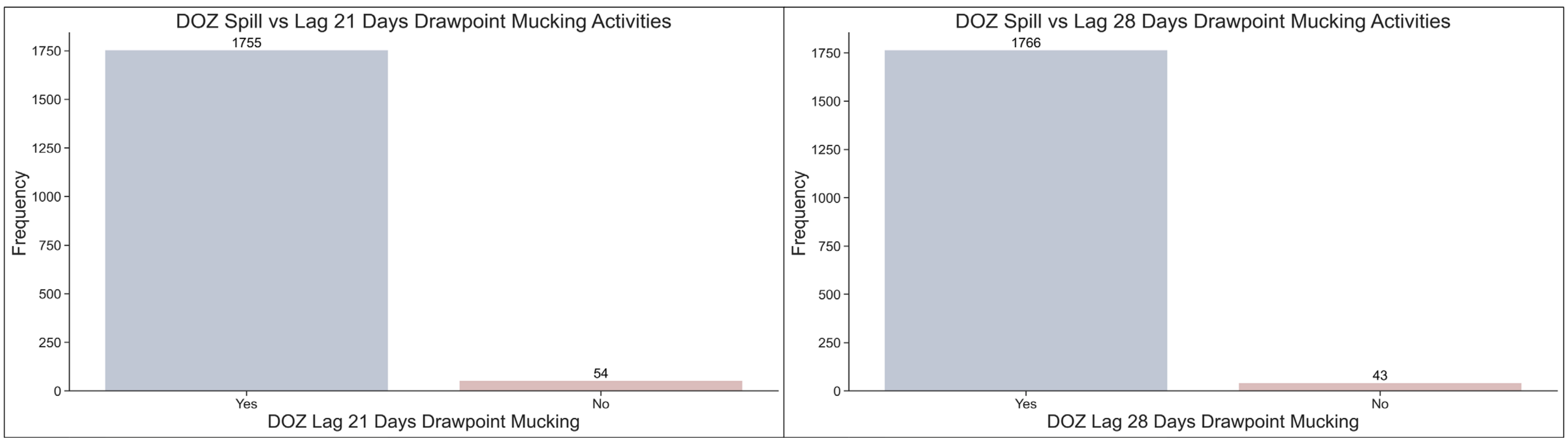

Figure B.35. Distribution of wet muck spills with the presence or absence of cumulative lag two days mucking activity (left) and cumulative lag three-day mucking activity (right).

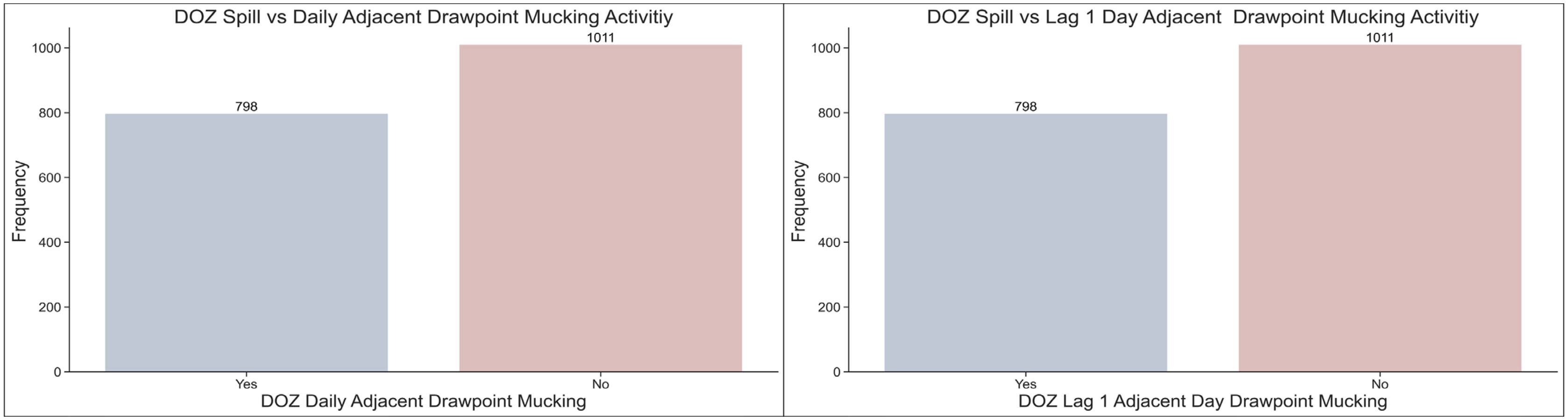

Figure B.36. Distribution of wet muck spills with the presence or absence of daily adjacent mucking activity (left) and lag one-day adjacent mucking activity (right).

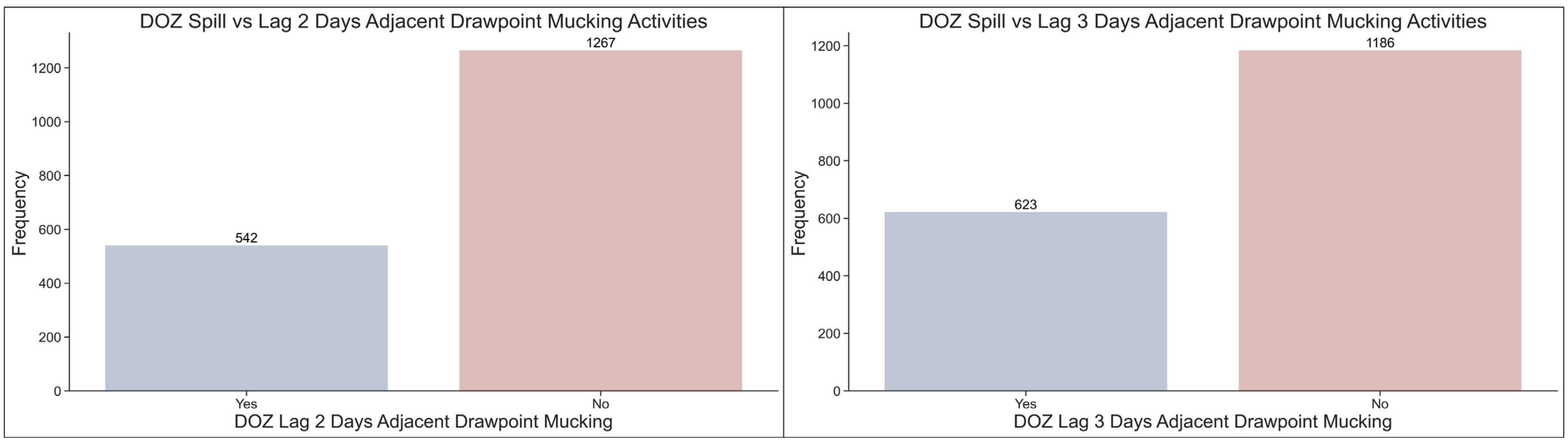

Figure B.37. Distribution of wet muck spills with the presence or absence of lag two days adjacent mucking activity (left) and lag three days adjacent mucking activity (right).

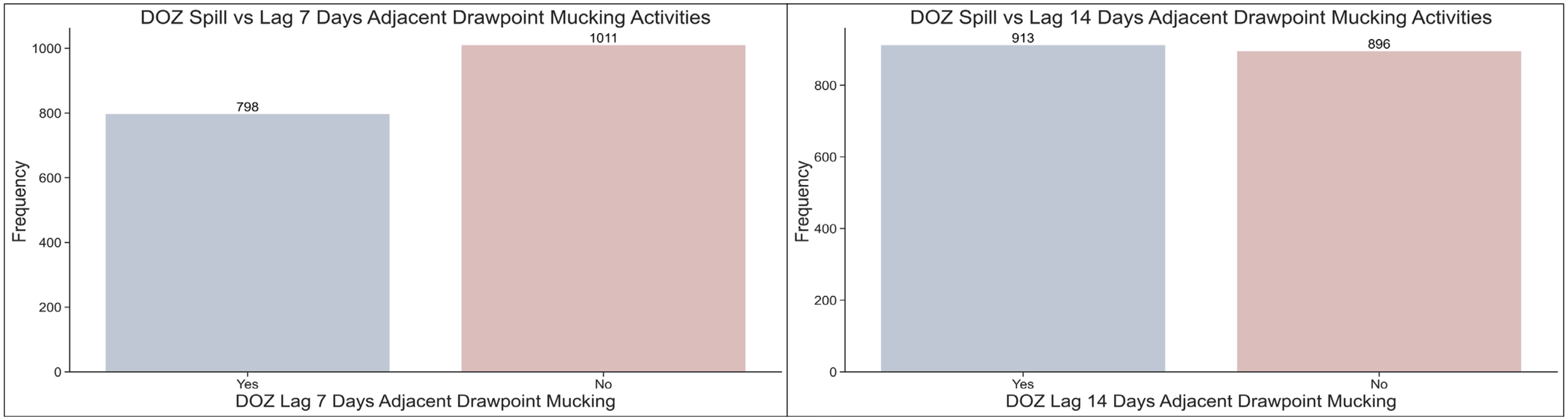

Figure B.38. Distribution of wet muck spills with the presence or absence of lag seven days adjacent mucking activity (left) and lag fourteen days adjacent mucking activity (right).

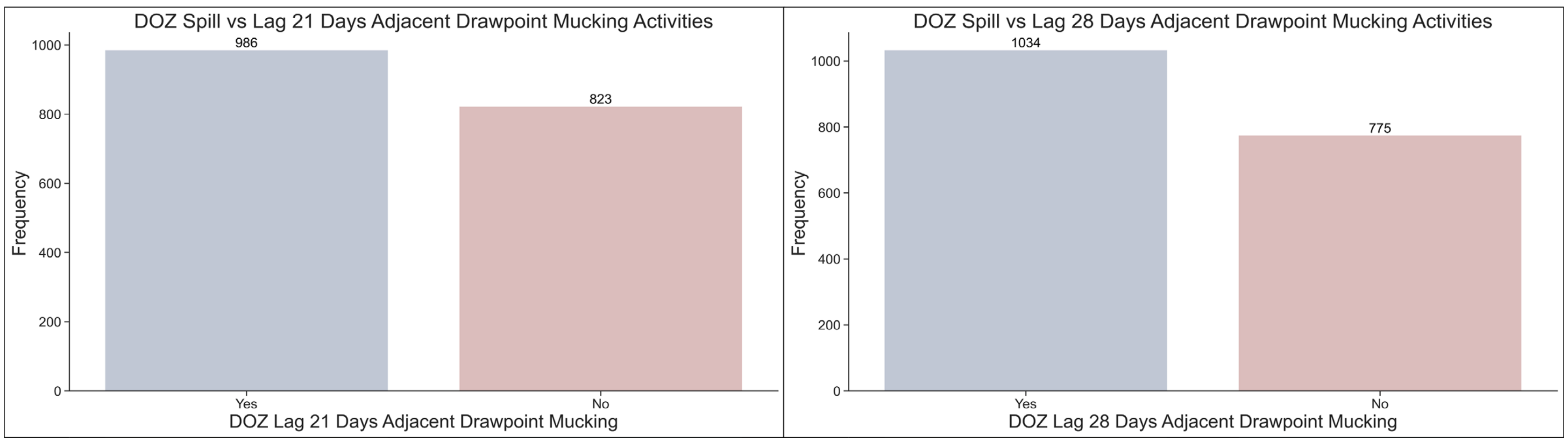

Figure B.39. Distribution of wet muck spills with the presence or absence of lag twenty-one days adjacent mucking activity (left) and lag twenty-eight days adjacent mucking activity (right).

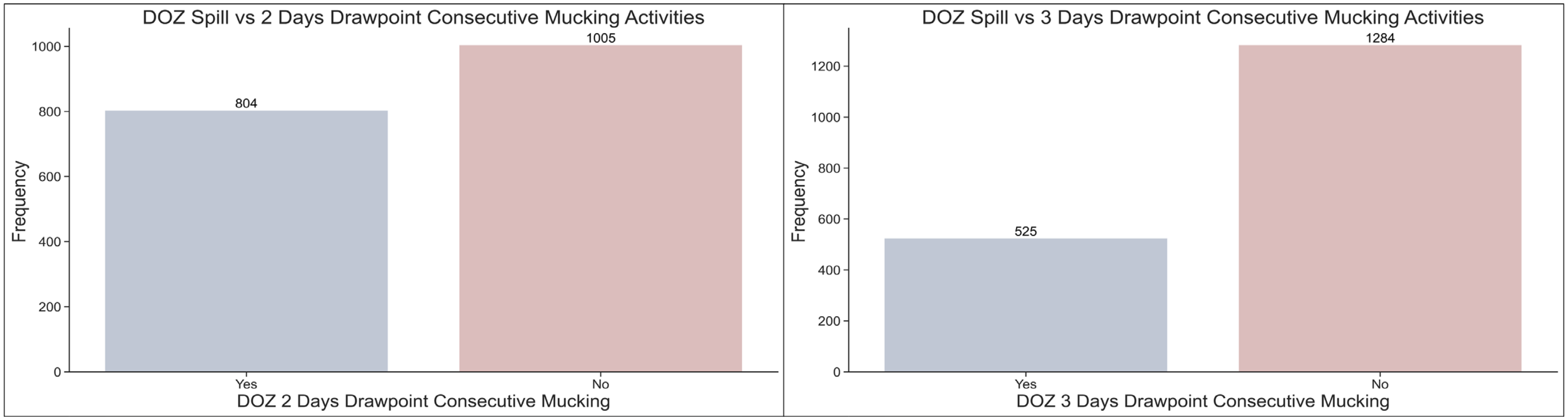

Figure B.40. Distribution of wet muck spills with the presence or absence of two days consecutive mucking activities (left) and three days consecutive mucking activities (right).

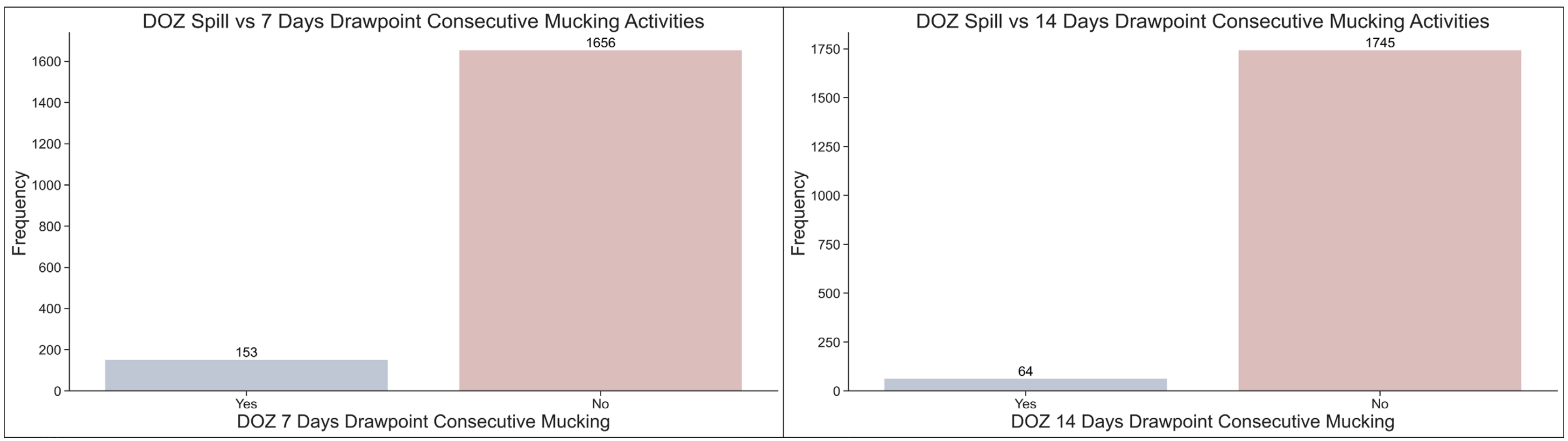

Figure B.41. Distribution of wet muck spills with the presence or absence of seven days consecutive mucking activities (left) and fourteen days consecutive mucking activities (right).

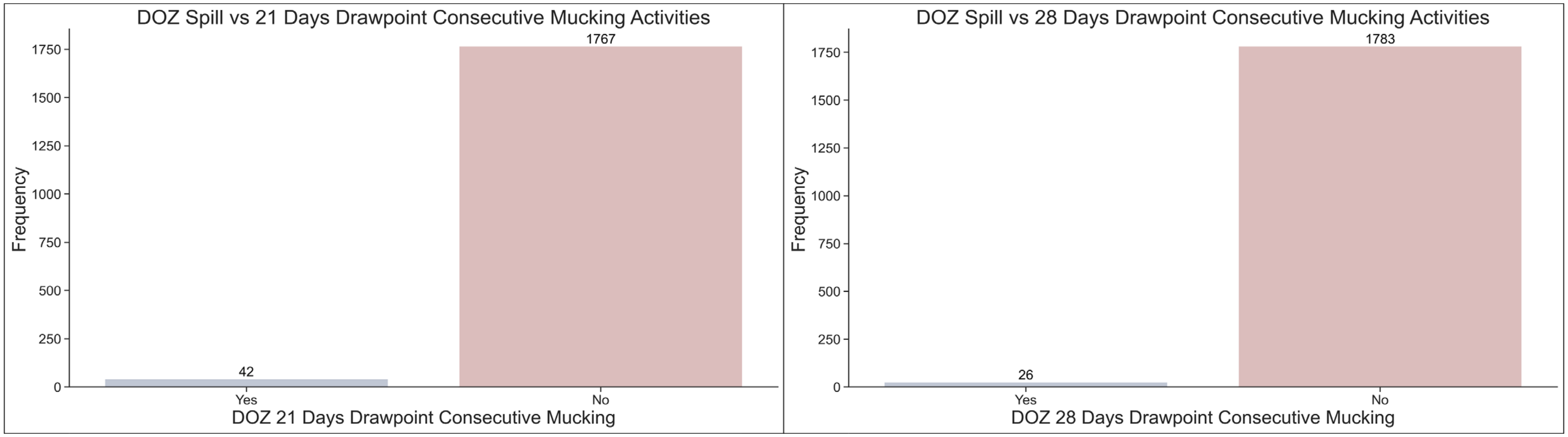

Figure B.42. Distribution of wet muck spills with the presence or absence of twenty-one days consecutive mucking activities (left) and twenty-eight days consecutive mucking activities (right).

Appendix C - Univariate Logistic Regression Coefficient and Performance Metric Results

Table C.1.Summary of univariate logistic regression results assigned to each hypothesized variable.

No	Variable	Coefficient	Precision	Recall	True Positive	True Negative	False Positive	False Negative
1	Height of Draw	1.1	0	0.44	345	227049	97346	431
2	Adjacent Height of Draw	0.82	0	0.43	330	212105	112290	446
3	Differential Height of Draw	0.21	0	0.45	349	190568	133827	427
4	Extraction Ratio	0.94	0	0.44	338	194754	129641	438
5	Adjacent Extraction Ratio	1.18	0	0.47	414	196456	127939	414
6	Differential Extraction Ratio	-0.34	0	0.46	354	195861	128534	422
7	Drawpoint Class	Varies	0	0.97	752	127062	197333	24
8	Adjacent Drawpoint Class	Varies	0	0.87	678	109397	214998	98
9	Wet Muck Neighbour 24m	0.57	0	0.94	732	83699	240696	44
10	Wet Muck Neighbour 36m	0.29	0	0.91	706	89020	235375	70
11	Wet Muck Neighbour 48m	0.17	0	0.9	701	86494	237901	75
12	Daily Tonnage	0.56	0.03	0.77	597	301,899	22,496	179
13	1 Day Tonnage	0.28	0.02	0.6	463	296,946	27,449	313
14	2 Days Tonnage	0.27	0.01	0.65	501	290,774	33,621	275

No	Variable	Coefficient	Precision	Recall	True Positive	True Negative	False Positive	False Negative
15	3 Days Tonnage	0.24	0.01	0.67	519	286,546	37,849	257
16	7 Days Tonnage	0.19	0.01	0.73	567	278,619	45,776	209
17	14 Days Tonnage	0.12	0.01	0.78	605	271,231	53,164	171
18	21 Days Tonnage	0.09	0.01	0.78	609	267,192	57,203	167
19	28 Days Tonnage	0.07	0.01	0.79	610	264,472	59,923	166
20	Daily Adjacent Tonnage	-0.55	0	0.77	598	47,320	277,075	178
21	1 Day Adjacent Tonnage	-0.36	0	0.78	604	44,093	280,302	172
22	2 Days Adjacent Tonnage	-0.46	0	0.74	576	56,207	268,188	200
23	3 Days Adjacent Tonnage	-0.5	0	0.7	543	62,952	261,443	233
24	7 Days Adjacent Tonnage	-0.6	0	0.63	492	78,413	245,982	284
25	14 Days Adjacent Tonnage	-0.7	0	0.59	455	91,397	232,998	321
26	21 Days Adjacent Tonnage	-0.72	0	0.57	441	97,023	227,372	335
27	28 Days Adjacent Tonnage	-0.71	0	0.55	428	100,564	223,831	348
28	Daily Differential Tonnage	0.57	0.02	0.76	586	294,179	30,216	190
29	1 Day Differential Tonnage	0.29	0.01	0.58	451	288,452	35,943	325
30	2 Days Differential Tonnage	0.28	0.01	0.63	491	280,059	44,336	285
31	3 Days Differential Tonnage	0.25	0.01	0.66	515	274,610	49,785	261
32	7 Days Differential Tonnage	0.2	0.01	0.72	556	265,424	58,971	221
33	14 Days Differential Tonnage	0.15	0.01	0.77	596	256,238	68,157	180

No	Variable	Coefficient	Precision	Recall	True Positive	True Negative	False Positive	False Negative
34	21 Days Differential Tonnage	0.12	0.01	0.77	601	252,122	72,273	175
35	28 Days Differential Tonnage	0.12	0.01	0.78	604	249,933	74,462	172
36	Daily UI at 5 DP	0.47	0	0.69	539	186,539	137,856	237
37	1 Day UI at 5 DP	0.47	0	0.69	539	186,539	137,856	237
38	2 Days UI at 5 DP	0.52	0	0.73	570	196,846	127,549	206
39	3 Days UI at 5 DP	0.49	0	0.72	556	186,688	137,707	220
40	7 Days UI at 5 DP	0.35	0	0.67	517	173,602	150,793	259
41	14 Days UI at 5 DP	0.25	0	0.59	457	167,628	156,767	319
42	21 Days UI at 5 DP	0.2	0	0.54	421	166,356	158,039	355
43	28 Days UI at 5 DP	0.18	0	0.52	400	166,941	157,454	376
44	Daily SPUI at 5 DP	0.58	0.01	0.61	476	273,813	50,582	300
45	1 Day SPUI at 5 DP	0.58	0.01	0.61	476	273,813	50,582	300
46	2 Days SPUI at 5 DP	0.59	0.01	0.67	522	280,775	43,620	254
47	3 Days SPUI at 5 DP	0.64	0.01	0.71	549	275,024	49,371	227
48	7 Days SPUI at 5 DP	0.72	0.01	0.74	572	263,332	61,063	204
49	14 Days SPUI at 5 DP	0.74	0.01	0.76	593	252,900	71,495	183
50	21 Days SPUI at 5 DP	0.74	0.01	0.77	598	246,170	78,225	178

No	Variable	Coefficient	Precision	Recall	True Positive	True Negative	False Positive	False Negative
51	28 Days SPUI at 5 DP	0.76	0.01	0.78	605	242,053	82,342	171
52	Daily Total Inactive Drawpoint at 5 DP	-0.1	0.01	0.57	444	241,170	83,225	332
53	1 Day Total Inactive Drawpoint at 5 DP	-0.1	0.01	0.57	444	241,170	83,225	332
54	2 Days Total Inactive Drawpoint at 5 DP	-0.08	0.01	0.51	398	258,857	65,538	378
55	3 Days Total Inactive Drawpoint at 5 DP	-0.13	0.01	0.62	482	241,257	83,138	294
56	7 Days Total Inactive Drawpoint at 5 DP	-0.2	0.01	0.57	444	244,083	80,312	332
57	14 Days Total Inactive Drawpoint at 5 DP	-0.22	0	0.72	558	210,303	114,092	218
58	21 Days Total Inactive Drawpoint at 5 DP	-0.23	0	0.79	616	187,283	137,112	160
59	28 Days Total Inactive Drawpoint at 5 DP	-0.22	0	0.83	645	169,832	154,563	131
60	Daily UI at 7 DP	0.63	0	0.74	573	171,747	152,648	203
61	1 Day UI at 7 DP	0.6	0	0.72	561	171,526	152,869	215
62	2 Days UI at 7 DP	0.64	0	0.76	587	182,591	141,804	189
63	3 Days UI at 7 DP	0.63	0	0.74	573	171,747	152,648	203
64	7 Days UI at 7 DP	0.51	0	0.66	511	156,465	167,930	265
65	14 Days UI at 7 DP	0.41	0	0.57	441	147,560	176,935	335
66	21 Days UI at 7 DP	0.38	0	0.52	303	136,701	197,694	372
67	28 Days UI at 7 DP	0.4	0	0.49	384	140,884	183,511	392
68	Daily SPUI at 7 DP	0.62	0.01	0.69	536	278,382	46,013	240
69	1 Day SPUI at 7 DP	0.55	0.01	0.58	453	277,321	47,074	323

No	Variable	Coefficient	Precision	Recall	True Positive	True Negative	False Positive	False Negative
70	2 Days SPUI at 7 DP	0.57	0.01	0.66	513	283,562	40,833	263
71	3 Days SPUI at 7 DP	0.62	0.01	0.69	536	278,382	46,013	240
72	7 Days SPUI at 7 DP	0.7	0.01	0.71	553	268,471	55,924	223
73	14 Days SPUI at 7 DP	0.73	0.01	0.74	577	259,396	64,999	199
74	21 Days SPUI at 7 DP	0.74	0.01	0.77	598	253,460	70,935	178
75	28 Days SPUI at 7 DP	0.76	0.01	0.78	605	250,009	74,386	171
76	Daily Total Inactive Drawpoint at 7 DP	-0.01	0.01	0.51	396	252,070	72,325	380
77	1 Day Total Inactive Drawpoint at 7 DP	0.01	0	0.52	405	72,401	251,994	371
78	2 Days Total Inactive Drawpoint at 7 DP	0.02	0	0.59	460	56,401	267,994	316
79	3 Days Total Inactive Drawpoint at 7 DP	-0.01	0.01	0.51	396	252,070	72,325	380
80	7 Days Total Inactive Drawpoint at 7 DP	-0.04	0	0.44	342	250,145	74,250	434
81	14 Days Total Inactive Drawpoint at 7 DP	-0.04	0	0.55	430	222,260	102,135	346
82	21 Days Total Inactive Drawpoint at 7 DP	-0.04	0	0.59	460	202,811	121,584	316
83	28 Days Total Inactive Drawpoint at 7 DP	-0.02	0	0.54	418	217,356	107,039	358
84	Daily UI at 24m	0.68	0.01	0.81	625	218,652	105,743	151
85	1 Day UI at 24m	0.54	0.01	0.74	573	217,610	106,785	203
86	2 Days UI at 24m	0.69	0	0.76	590	197,407	126,988	186
87	3 Days UI at 24m	0.67	0	0.75	581	186,933	137,462	195
88	7 Days UI at 24m	0.56	0	0.67	522	170,812	153,583	254

No	Variable	Coefficient	Precision	Recall	True Positive	True Negative	False Positive	False Negative
89	14 Days UI at 24m	0.46	0	0.57	442	148,912	175,483	334
90	21 Days UI at 24m	0.43	0	0.53	414	149,810	174,585	362
91	28 Days UI at 24m	0.42	0	0.5	391	153,447	170,948	385
92	Daily SPUI at 24m	0.66	0.02	0.78	608	295,415	28,980	168
93	1 Day SPUI at 24m	0.46	0.01	0.61	471	292,218	32,177	305
94	2 Days SPUI at 24m	0.58	0.01	0.66	513	283,160	41,235	263
95	3 Days SPUI at 24m	0.63	0.01	0.69	537	277,830	46,565	239
96	7 Days SPUI at 24m	0.71	0.01	0.71	553	267,729	56,666	223
97	14 Days SPUI at 24m	0.74	0.01	0.74	578	258,255	66,140	198
98	21 Days SPUI at 24m	0.75	0.01	0.77	598	252,320	72,075	178
99	28 Days SPUI at 24m	0.77	0.01	0.78	606	248,898	75,497	170
100	Daily Total Inactive Drawpoint at 24m	0.27	0.01	0.78	604	219,056	105,339	172
101	1 Day Total Inactive Drawpoint at 24m	0.23	0.01	0.7	543	219,190	105,205	233
102	2 Days Total Inactive Drawpoint at 24m	0.05	0	0.57	440	77,246	247,149	336
103	3 Days Total Inactive Drawpoint at 24m	0.02	0	0.46	360	93,846	230,549	416
104	7 Days Total Inactive Drawpoint at 24m	-0.02	0	0.48	361	235,944	88,451	415
105	14 Days Total Inactive Drawpoint at 24m	-0.02	0	0.58	452	205,911	118,484	324
106	21 Days Total Inactive Drawpoint at 24m	-0.02	0	0.51	394	221,481	102,914	382
107	28 Days Total Inactive Drawpoint at 24m	-0.002	0	0.56	433	206,869	117,526	343

No	Variable	Coefficient	Precision	Recall	True Positive	True Negative	False Positive	False Negative
108	Daily UI at 36m	0.69	0	0.85	662	181,509	142,886	114
109	1 Day UI at 36m	0.59	0	0.77	596	180,969	143,426	180
110	2 Days UI at 36m	0.6	0	0.81	631	150,053	174,342	145
111	3 Days UI at 36m	0.57	0	0.78	603	140,667	183,728	173
112	7 Days UI at 36m	0.43	0	0.7	540	120,116	204,279	236
113	14 Days UI at 36m	0.34	0	0.6	465	122,239	202,156	311
114	21 Days UI at 36m	0.31	0	0.56	433	126,728	197,667	343
115	28 Days UI at 36m	0.3	0	0.54	422	123,896	200,499	354
116	Daily SPUI at 36m	0.64	0.02	0.75	584	299,985	24,410	192
117	1 Day SPUI at 36m	0.41	0.02	0.58	449	296,293	28,102	327
118	2 Days SPUI at 36m	0.5	0.01	0.62	483	289,445	34,950	293
119	3 Days SPUI at 36m	0.54	0.01	0.65	504	285,627	38,768	272
120	7 Days SPUI at 36m	0.61	0.01	0.68	531	278,633	45,762	245
121	14 Days SPUI at 36m	0.65	0.01	0.69	536	272,172	52,223	240
122	21 Days SPUI at 36m	0.67	0.01	0.71	554	268,360	56,035	222
123	28 Days SPUI at 36m	0.71	0.01	0.71	552	266,081	58,314	224
124	Daily Total Inactive Drawpoint at 36m	0.12	0.01	0.34	293	271,251	53,144	483
125	1 Day Total Inactive Drawpoint at 36m	0.11	0	0.34	266	267,692	56,703	510
126	2 Days Total Inactive Drawpoint at 36m	0.03	0	0.68	525	70,518	253,877	251

No	Variable	Coefficient	Precision	Recall	True Positive	True Negative	False Positive	False Negative
127	3 Days Total Inactive Drawpoint at 36m	0.02	0	0.69	534	67,915	256,480	242
128	7 Days Total Inactive Drawpoint at 36m	0.003	0	0.58	453	83,012	241,383	323
129	14 Days Total Inactive Drawpoint at 36m	0.004	0	0.55	427	92,360	232,035	349
130	21 Days Total Inactive Drawpoint at 36m	0.01	0	0.49	382	113,134	211,261	394
131	28 Days Total Inactive Drawpoint at 36m	0.02	0	0.52	401	108,501	215,894	375
132	Daily UI at 48m	0.72	0	0.85	664	163,649	160,746	113
133	1 Day UI at 48m	0.61	0	0.82	635	161,955	162,440	141
134	2 Days UI at 48m	0.59	0	0.78	604	138,108	186,287	172
135	3 Days UI at 48m	0.56	0	0.74	572	129,439	194,956	204
136	7 Days UI at 48m	0.43	0	0.66	513	115,763	208,632	263
137	14 Days UI at 48m	0.34	0	0.58	449	110,512	213,883	327
138	21 Days UI at 48m	0.32	0	0.54	416	118,420	205,975	360
139	28 Days UI at 48m	0.39	0	0.51	394	116,205	208,190	382
140	Daily SPUI at 48m	0.6	0.03	0.74	573	302,073	22,322	203
141	1 Day SPUI at 48m	0.38	0.02	0.56	434	298,440	25,955	342
142	2 Days SPUI at 48m	0.48	0.01	0.6	468	29,1294	33,101	308
143	3 Days SPUI at 48m	0.52	0.01	0.63	490	287,816	36,579	286
144	7 Days SPUI at 48m	0.59	0.01	0.67	518	281,129	43,266	258
145	14 Days SPUI at 48m	0.63	0.01	0.68	530	275,294	49,101	246

No	Variable	Coefficient	Precision	Recall	True Positive	True Negative	False Positive	False Negative
146	21 Days SPUI at 48m	0.65	0.01	0.7	546	272,007	52,388	230
147	28 Days SPUI at 48m	0.69	0.01	0.7	540	270,067	54,328	236
148	Daily Total Inactive Drawpoint at 48m	-0.05	0	0.59	454	109,522	214,873	322
149	1 Day Total Inactive Drawpoint at 48m	-0.05	0	0.59	457	109,480	214,915	319
150	2 Days Total Inactive Drawpoint at 48m	0.03	0	0.65	504	63,274	261,121	272
151	3 Days Total Inactive Drawpoint at 48m	0.02	0	0.65	504	65,279	259,116	272
152	7 Days Total Inactive Drawpoint at 48m	0.01	0	0.62	478	69,873	254,522	298
153	14 Days Total Inactive Drawpoint at 48m	0.01	0	0.54	421	84,775	239,620	355
154	21 Days Total Inactive Drawpoint at 48m	0.01	0	0.48	372	104,591	219,804	404
155	28 Days Total Inactive Drawpoint at 48m	0.02	0	0.43	334	120,143	204,252	442
156	Daily Mucking	1.22	0.01	0.86	668	274,110	50,285	108
157	1 Day Mucking	0.81	0.01	0.74	576	269,672	54,723	200
158	2 Days Mucking	1.01	0.01	0.82	637	250,633	73,762	139
159	3 Days Mucking	1.22	0.01	0.88	682	234,754	89,641	94
160	7 Days Mucking	1.47	0.01	0.93	720	199,924	124,472	56
161	14 Days Mucking	1.71	0	0.98	758	165,093	159,302	18
162	21 Days Mucking	1.96	0	0.98	761	143,278	181,117	15
163	28 Days Mucking	1.97	0	0.99	766	127,347	197,048	10
164	Daily Adjacent Mucking	-0.69	0	0.54	421	110,375	214,020	355

No	Variable	Coefficient	Precision	Recall	True Positive	True Negative	False Positive	False Negative
165	1 Day Adjacent Mucking	-0.97	0	0.78	605	43,806	280,589	171
166	2 Days Adjacent Mucking	-0.88	0	0.72	557	63,229	261,166	219
167	3 Days Adjacent Mucking	-0.82	0	0.67	517	76,074	248,321	259
168	7 Days Adjacent Mucking	-0.75	0	0.58	449	103,319	221,077	327
169	14 Days Adjacent Mucking	-0.68	0	0.49	381	130,563	193,832	395
170	21 Days Adjacent Mucking	-0.7	0	0.44	339	147,560	176,835	437
171	28 Days Adjacent Mucking	-0.73	0	0.41	318	160,092	164,303	458
172	2 Days Consecutive Mucking	0.32	0.01	0.44	343	296,932	27,463	433
173	3 Days Consecutive Mucking	-0.08	0	0.73	568	16,515	307,880	208
174	7 Days Consecutive Mucking	-0.89	0	1	761	1,539	322,856	15
175	14 Days Consecutive Mucking	-0.9	0	1	774	1,351	323,044	2
176	21 Days Consecutive Mucking	-0.86	0	1	776	667	323,728	0
177	28 Days Consecutive Mucking	-0.97	0	1	776	339	324,056	0

Appendix D - Sensitivity of Variable Input Values to Wet Muck Susceptibility Prediction

For each explanatory variable, the sensitivity of wet muck spill susceptibility was generated across the range of values in the data or each category member. In the plots below, the predicted wet muck susceptibilities are compared to the proportion of spill drawpoints. Other model variables were held at a constant value, typically at the mean or median value. The illustration in Appendix D uses the constant values in Table D.1.

Table D.1. The constant values used for the wet muck spill susceptibility variable sensitivity.

Variable	Condition
Drawpoint Class	B3
Adjacent Drawpoint Class	B3
Wet Muck Neighboring Drawpoint within 36m	7
Height of Draw	250
3 Days Uniformity Index at 7 nearest DP	3.50
14 Days Mucking Activities	1
14 Days Adjacent Mucking Activities	1
2 Days Consecutive Mucking Activities	1

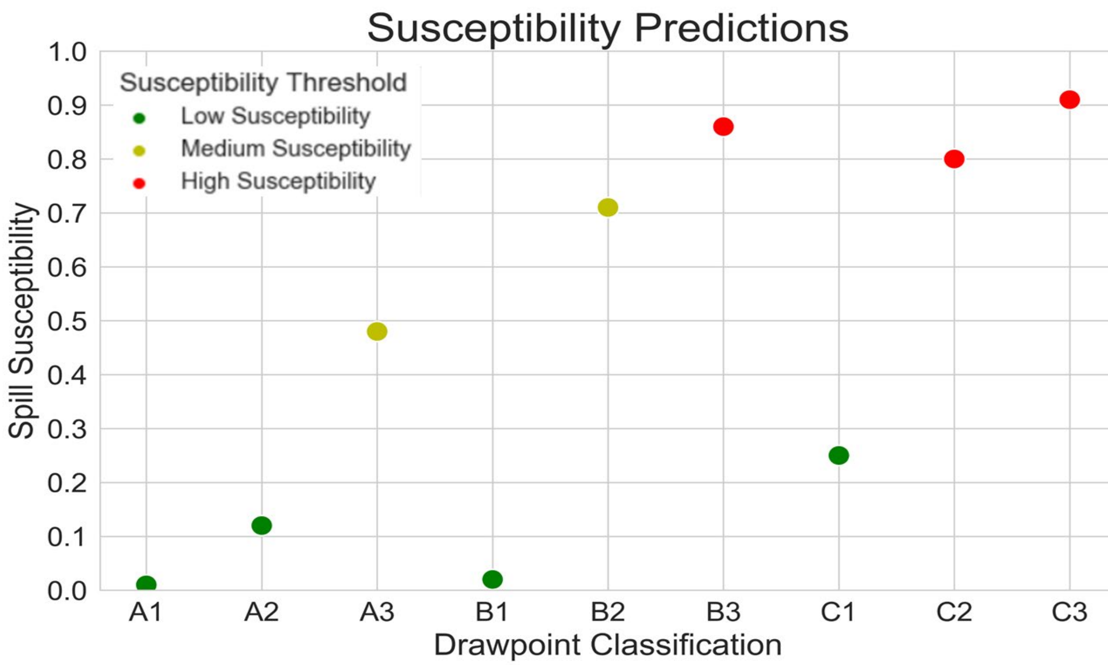

Figure D.1. Wet muck spill susceptibility predictions based on each change in drawpoint classification.

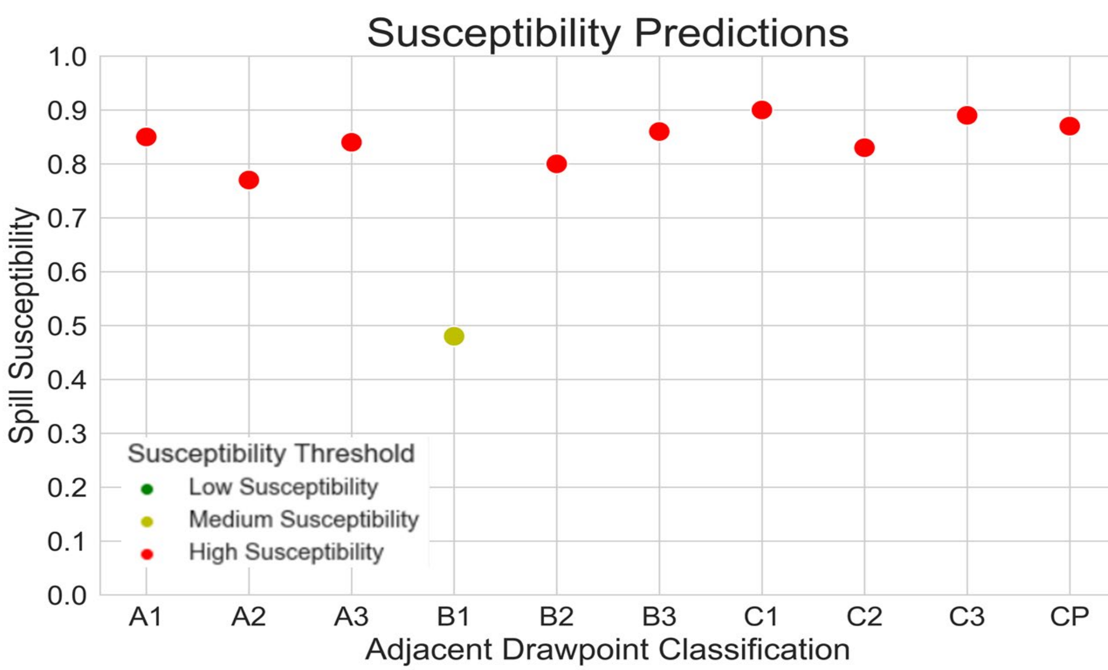

Figure D.2. Wet muck spill susceptibility predictions based on each change in adjacent drawpoint classification.

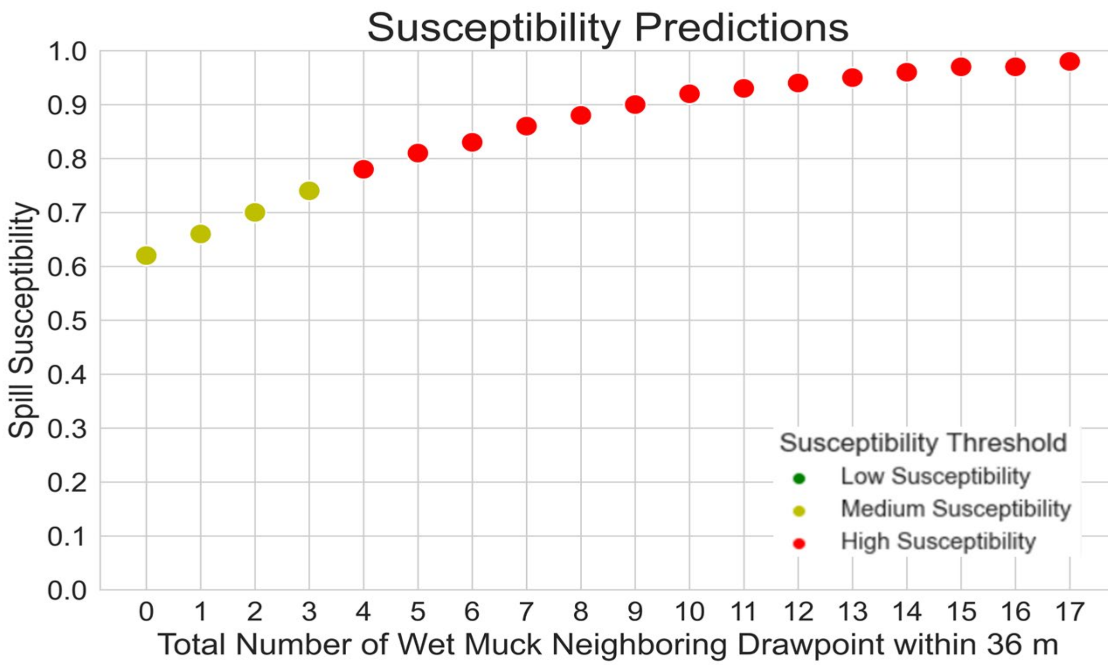

Figure D.3. Wet muck spill susceptibility predictions based on each increase of the number of wet muck neighboring drawpoint within 36 m.

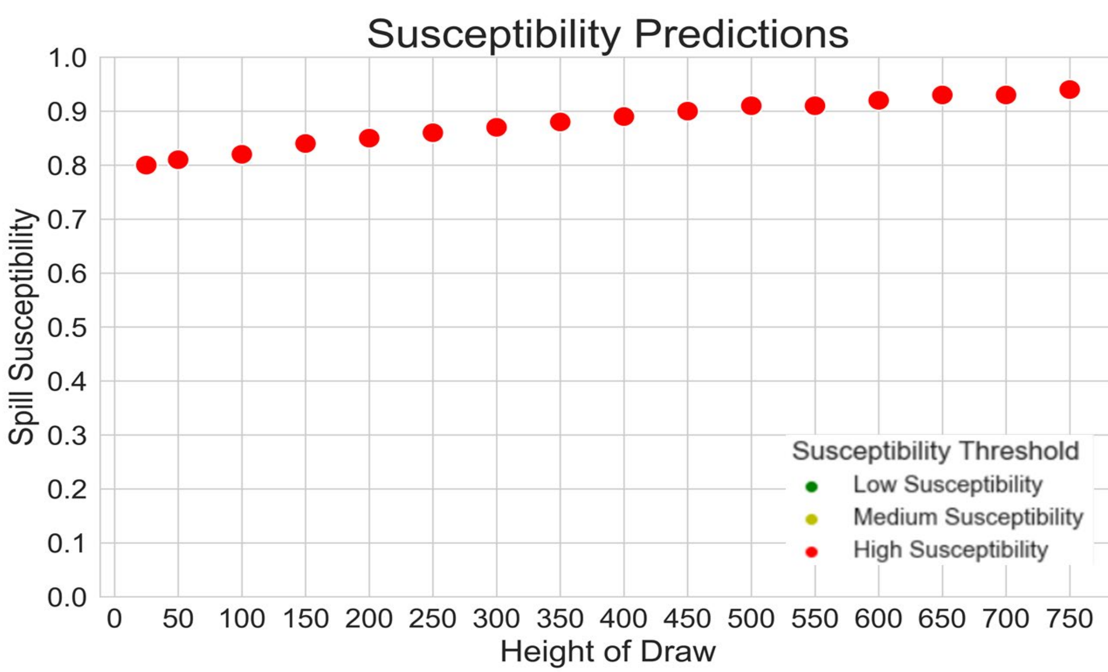

Figure D.4. Wet muck spill susceptibility predictions based on each increase of HoD per 50m.

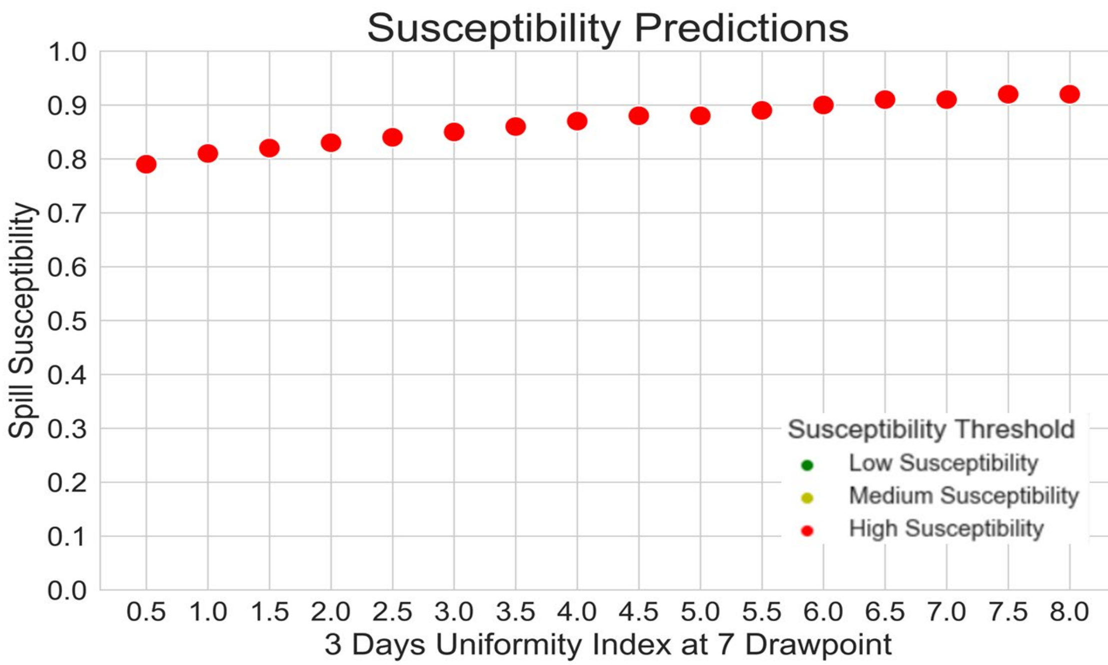

Figure D.5. Wet muck spill susceptibility predictions based on each increase of three days uniformity index at seven drawpoint per 0.5.

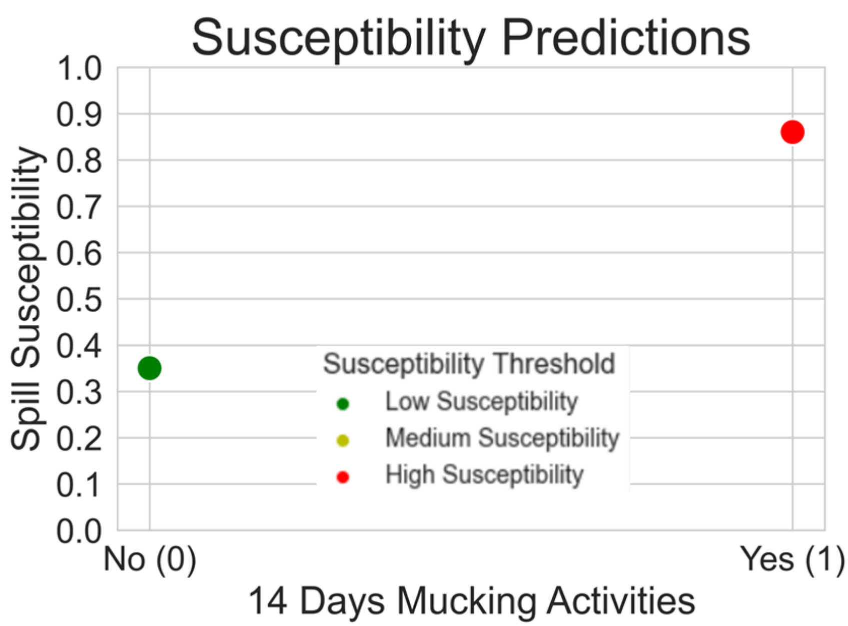

Figure D.6. Wet muck spill susceptibility predictions based on the presence or absence of 14 days of drawpoint mucking activities.

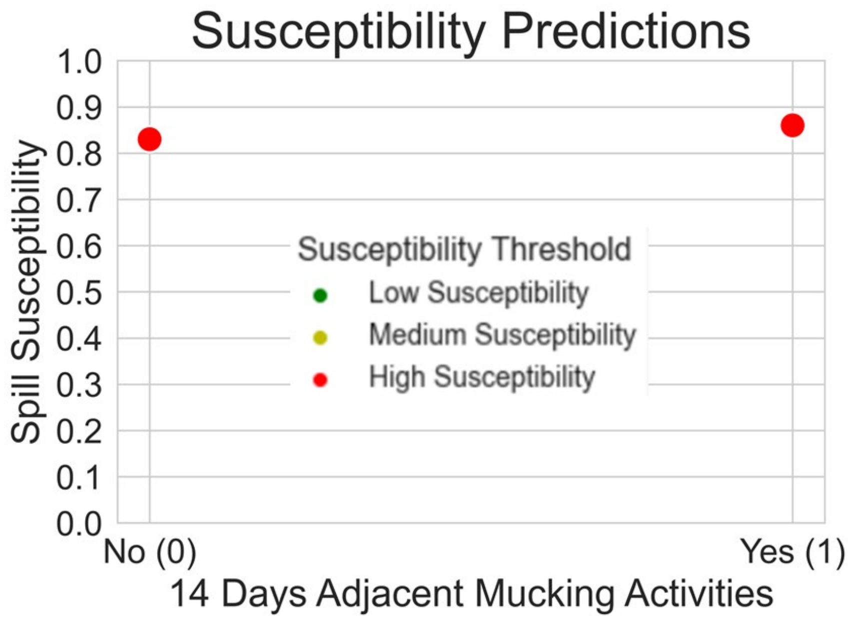

Figure D.7. Wet muck spill susceptibility predictions based on the presence or absence of 14 days adjacent drawpoint mucking activities.

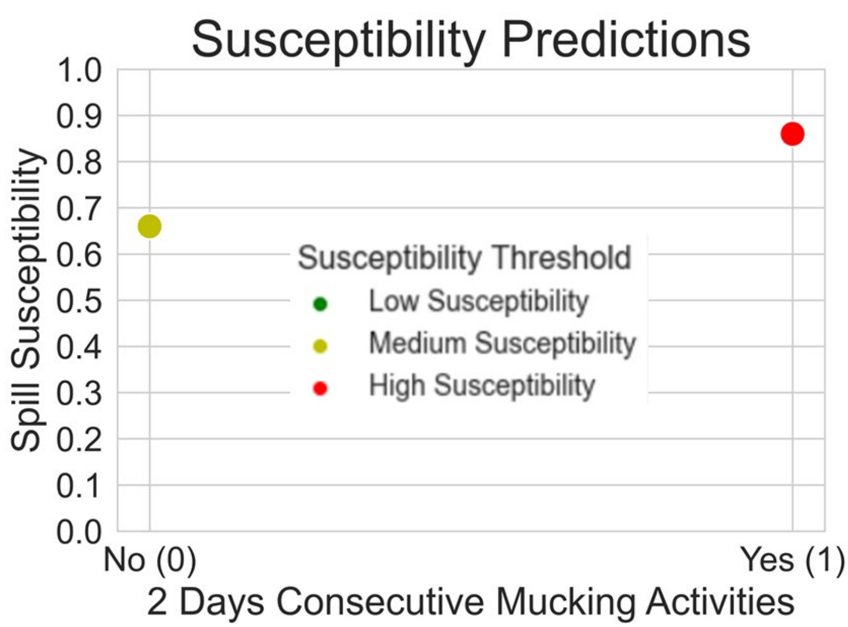

Figure D.8. Wet muck spill susceptibility predictions based on the presence or absence of 2 days of consecutive drawpoint mucking activities.